US Army Corps
of Engineers
Construction Engineering
Research Laboratories

USACERL Technical Report 95/22
August 1995

Structural Control of Buildings Response Using Shape-Memory Alloys

by
Andrew S. Whittaker
Robert Krumme
Steven C. Sweeney
John R. Hayes, Jr.

This study developed the technical base for the design of shape-memory alloy energy dissipation devices for building structures by: (1) characterization of the basic materials behavior for the design of prototype shape-memory alloy (SMA or SMM) energy dissipators; (2) development of conceptual designs for SMA structural damping devices; (3) detailed analysis of the seismic response of a preselected nonductile concrete building with and without SMM energy dissipators under moderate earthquake shaking, and (4) parametric analyses of a reduced-order model of the pre-selected building upgraded with SMM energy dissipators possessing different hysteretic characteristics from that used for the detailed analysis.

SMAs can be configured to provide a shape-memory effect (SME) or a superelastic effect (SEE); energy dissipation devices based on both SME and SEE were shown to be technically viable. Several prototype SMA energy dissipators were designed and one energy dissipator was fabricated. The vulnerability of one building typical of many in the DOD inventory was mitigated by adding SMA energy dissipators.

The contents of this report are not to be used for advertising, publication, or promotional purposes. Citation of trade names does not constitute an official endorsement or approval of the use of such commercial products. The findings of this report are not to be construed as an official Department of the Army position, unless so designated by other authorized documents.

DESTROY THIS REPORT WHEN IT IS NO LONGER NEEDED

DO NOT RETURN IT TO THE ORIGINATOR

DISCLAIMER NOTICE

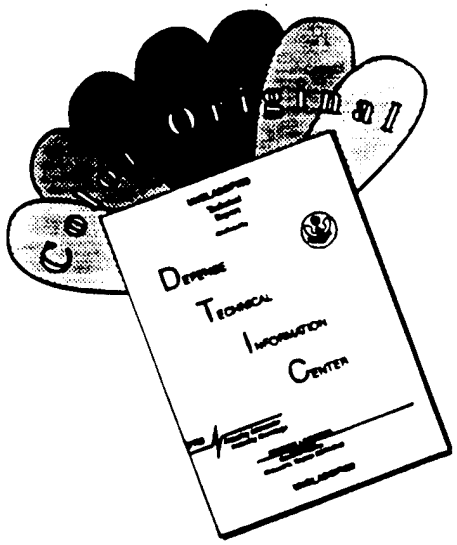

THIS DOCUMENT IS BEST QUALITY AVAILABLE. THE COPY FURNISHED TO DTIC CONTAINED A SIGNIFICANT NUMBER OF COLOR PAGES WHICH DO NOT REPRODUCE LEGIBLY ON BLACK AND WHITE MICROFICHE.

USER EVALUATION OF REPORT

REFERENCE: USACERL Technical Report 95/22, *Structural Control of Building Response Using Shape-Memory Alloys*

Please take a few minutes to answer the questions below, tear out this sheet, and return it to USACERL. As user of this report, your customer comments will provide USACERL with information essential for improving future reports.

1. Does this report satisfy a need? (Comment on purpose, related project, or other area of interest for which report will be used.)

_____

_____

_____

2. How, specifically, is the report being used? (Information source, design data or procedure, management procedure, source of ideas, etc.)

_____

_____

3. Has the information in this report led to any quantitative savings as far as manhours/contract dollars saved, operating costs avoided, efficiencies achieved, etc.? If so, please elaborate.

_____

_____

4. What is your evaluation of this report in the following areas?

a. Presentation: _____

b. Completeness: _____

c. Easy to Understand: _____

d. Easy to Implement: _____

e. Adequate Reference Material: _____

f. Relates to Area of Interest: _____

g. Did the report meet your expectations? _____

h. Does the report raise unanswered questions? _____

i. General Comments. (Indicate what you think should be changed to make this report and future reports of this type more responsive to your needs, more usable, improve readability, etc.)

_____

_____

_____

_____

_____

_____

5. If you would like to be contacted by the personnel who prepared this report to raise specific questions or discuss the topic, please fill in the following information.

Name: _____

Telephone Number: _____

Organization Address: _____

_____

_____

6. Please mail the completed form to:

Department of the Army
CONSTRUCTION ENGINEERING RESEARCH LABORATORIES
ATTN: CECER-TR-I
P.O. Box 9005
Champaign, IL 61826-9005

REPORT DOCUMENTATION PAGE

Form Approved
OMB No. 0704-0188

1. AGENCY USE ONLY *(Leave Blank)*	2. REPORT DATE	3. REPORT TYPE AND DATES COVERED
	August 1995	Final

4. TITLE AND SUBTITLE
Structural Control of Building Response Using Shape-Memory Alloys

5. FUNDING NUMBERS
FAD
95-080026
19 January 1995

6. AUTHOR(S)
Andrew S. Whittaker, Robert Krumme, and John R. Hayes, Jr.

7. PERFORMING ORGANIZATION NAME(S) AND ADDRESS(ES)
U.S. Army Construction Engineering Research Laboratories (USACERL)
P.O. Box 9005
Champaign, IL 61826-9005

8. PERFORMING ORGANIZATION REPORT NUMBER
TR 95/22

9. SPONSORING / MONITORING AGENCY NAME(S) AND ADDRESS(ES)
Headquarters, U.S. Army Corps of Engineers (HQUSACE)
ATTN: CERD-M
20 Massachussetts Ave., NW.
Washington, DC 20314-1000

10. SPONSORING / MONITORING AGENCY REPORT NUMBER

11. SUPPLEMENTARY NOTES
Copies are available from the National Technical Information Service, 5285 Port Royal Road, Springfield, VA 22161.

12a. DISTRIBUTION / AVAILABILITY STATEMENT
Approved for public release; distribution is unlimited.

12b. DISTRIBUTION CODE

13. ABSTRACT (Maximum 200 words)

This study developed the technical base for the design of shape-memory alloy energy dissipation devices for building structures by: (1) characterization of the basic materials behavior for the design of prototype shape-memory alloy (SMA or SMM) energy dissipators; (2) development of conceptual designs for SMA structural damping devices; (3) detailed analysis of the seismic response of a preselected nonductile concrete building with and without SMM energy dissipators under moderate earthquake shaking, and (4) parametric analyses of a reduced-order model of the pre-selected building upgraded with SMM energy dissipators possessing different hysteretic characteristics from that used for the detailed analysis.

SMAs can be configured to provide a shape-memory effect (SME) or a superelastic effect (SEE); energy dissipation devices based on both SME and SEE were shown to be technically viable. Several prototype SMA energy dissipators were designed and one energy dissipator was fabricated. The vulnerability of one building typical of many in the DOD inventory was mitigated by adding SMA energy dissipators.

14. SUBJECT TERMS
shape-memory alloys
structural design
seismic vulnerability

15. NUMBER OF PAGES
238

16. PRICE CODE

17. SECURITY CLASSIFICATION OF REPORT	18. SECURITY CLASSIFICATION OF THIS PAGE	19. SECURITY CLASSIFICATION OF ABSTRACT	20. LIMITATION OF ABSTRACT
Unclassified	Unclassified	Unclassified	SAR

EXECUTIVE SUMMARY

The objective of the Phase I SBIR research effort was to develop the technical base required for the design of shape-memory alloy (SMA or SMM) energy dissipation devices for building structures. Although much of the information presented in this report has direct application to other civil, mechanical, and aerospace structures, only applications relevant to the retrofit of existing buildings and the construction of new buildings in regions of low, moderate, and high seismic risk are considered here.

The research effort was composed of four main tasks: characterization of the basic materials behavior for the design of prototype SMA energy dissipators; development of conceptual designs for SMA structural damping devices; detailed analysis of the seismic response of a pre-selected non-ductile concrete building with and without SMM energy dissipators under moderate earthquake shaking, and parametric analyses of a reduced-order model of the pre-selected building upgraded with SMM energy dissipators possessing different hysteretic characteristics from that used for the detailed analysis.

Active and semi-active control strategies using SMA alloys were not reviewed in detail in this report because the results of this Phase I research effort are intended to partly form the basis of retrofitting strategies for the DOD's large inventory of seismically hazardous buildings in the near future. A detailed evaluation of active control using shape-memory alloys will be conducted as part of the Phase II research effort.

The Phase I research program has established the technical basis for the development, design and construction of passive energy dissipation devices for the earthquake-resistant design and construction/retrofit of building structures. The mechanical characteristics of different shape-memory alloys were thoroughly investigated in a detailed testing program. SMAs can be configured to provide a shape-memory effect (SME) or a superelastic effect (SEE); energy dissipation devices based on both SME and SEE were shown to be technically viable. Passive energy dissipation devices incorporating shape-memory alloys, in particular NiTi alloys, possess many desirable structural characteristics that include:

1. hysteretic (rate-independent) damping
2. variety of hysteretic characteristics
3. highly reliable energy dissipation based on a precisely repeatable solid state phase transformation
4. very high energy dissipation per unit mass and per unit volume of SMA material
5. negligible creep over the range of operating temperatures encountered in nearly all civil engineering applications
6. temperature independence of the hysteretic response

7. excellent low- and high-cycle fatigue properties
8. excellent corrosion resistance

Characteristics 6, 7, and 8 are unavailable with most other rate-independent supplemental damping systems currently in the marketplace.

Several prototype SMA energy dissipators were designed as part of the Phase I research effort. One energy dissipator was fabricated towards the end of the Phase I research program. Although preliminary testing of the device has been undertaken already, the results are currently unavailable. Detailed testing of this device is proposed as part of the Phase II SBIR research program.

Detailed analysis of one non-ductile reinforced concrete building in Washington State (typical of many in the DOD inventory) found the building to be vulnerable to collapse in the event of moderate or severe earthquake shaking. This assessment was based on the nonlinear time-history analysis of the building using three recorded earthquake ground motions consistent with moderate earthquake shaking at the building site. Two upgrade schemes developed for the building, based on the use of SMA energy dissipators installed in TS brace elements, were found to effectively mitigate the seismic hazard for the moderate level of earthquake shaking considered appropriate for the Fort Lewis site. The most cost-effective upgrade scheme for this particular building involved the addition of 6, 4, and 2 energy dissipators in each frame of the wing of the building considered, in the first, second, and third stories of the building, respectively. The use of 12 - 22 kip dissipators per building frame reduced the displacements in the building to a level whereby the frame suffered no damage when subjected to three moderate earthquake ground motions.

As noted above, SMA energy dissipators can be configured to provide a variety of force-deformation profiles. Two of these profiles (rectangular flag and triangular flag) were programmed in the MATLAB environment and exported to a newly-developed nonlinear program, INADEL. The results of these analyses demonstrated the attributes of these hysteretic shapes, namely substantial reductions in the response of the existing building. A large number of plausible hysteretic shapes make it possible to optimize the design of a supplemental damping system; such an optimization is impossible with most energy dissipation systems. Further development of the MATLAB:INADEL environment is planned for the Phase II research effort.

In summary, the materials characterization and device development reported in this report clearly demonstrate the technical viability of SMAs as passive energy dissipation devices for earthquake-resistant design applications in the building industry. The advantages of SMA-based energy dissipators over other hysteretic systems are outlined above. The vulnerability of one building typical of many in the DOD inventory was mitigated through the addition of SMA energy dissipators, thereby demonstrating some of the attributes of SMA passive energy dissipation technology.

FOREWORD

This study was conducted for Headquarters, U.S. Army Corps of Engineers (HQUSACE) under a Department of Defense (DOD) Phase I Small Business Innovative Research (SBIR) contract issued under the 1991 DOD Phase I SBIR Solicitation and funded under Funding Acquisition Document (FAD) No. 95-080026, dated 19 January 1995. The technical monitor was Dr. Clemens Meyer, CERD-M.

The work was performed by the Engineering Division (FL-E) of the Facilities Technology Laboratory (FL), U.S. Army Construction Engineering Research Laboratories (USACERL). The USACERL project monitors for this contract were John Hayes and Steven Sweeney. The research was done by E-Sorb Systems, Champaign, IL under Contract DACA-88-92-C-0015. Andrew Whittaker and Robert Krumme are associated with E-Sorb Systems. Special acknowledgement is given to the contributions of Dr. Ian Aiken and Dr. Jose Inaudi, of E-Sorb Systems, for substantial contributions to the testing and analysis presented in the report; Dr. Aiken also reviewed the report for theoretical content and technical merit. Carol Cameron, also of E-Sorb Systems, carefully reviewed and edited the manuscript. Larry M. Windingland is Acting Chief, CECER-FL-E, Donald F. Fornier, Jr. is Acting Operations Chief, and Alvin Smith is Acting Chief, CECER-FL.

COL James T. Scott is Commander and Acting Director of USACERL, and Dr. Michael J. O'Connor is Technical Director.

TABLE OF CONTENTS

LIST OF FIGURES

LIST OF TABLES

1.0 INTRODUCTION

1.1 Background

Over the past 20 years, rigorous dynamic performance specifications in the aerospace, mechanical, chemical, electrical, automotive, military, and nuclear engineering industries have necessitated the design and development of passive, semi-active, and active control systems. In almost every case, the principal objective associated with the implementation of the control devices to reduce dynamic response to an *acceptable* level.

For example, aerospace systems such as the NASA space shuttle and the USAF fighter and bomber fleet both take advantage of passive energy dissipation technology to reduce the high-g (impact) forces imposed on certain aircraft components. Similarly, the US Army has long used passive energy dissipators to mitigate recoil effects in rifles, machine-guns, and artillery pieces and to reduce vibration effects in armored vehicles, battle tanks, and so on. The US Navy's surface and submarine fleets likewise make extensive use of passive energy dissipators to protect lifeline systems and isolate on-board launch platforms.

Suppression of machine-induced vibration in mechanical components, wind-induced vibration in building and lifeline structures, and road surface-induced vibration in automotive vehicles is now routine practice. In essential public facilities such as nuclear power plants, vibration isolation devices in the form of passive energy dissipators, also known as passive/supplemental dampers or snubbers, have been used to mitigate the effects of a variety of dynamic loads that include thermal shock, impact loads, and seismic excitation. A wide variety of rate-dependent (viscous) and rate-independent (friction-slip and steel-yielding among others) energy dissipators have been implemented for this purpose.

The use of energy dissipation devices for civil building applications, either new construction or retrofit of existing construction, is extremely limited in comparison with the other engineering disciplines. This is due in part to technology that is unfamiliar (and therefore uninviting) to structural engineers.

Structural and mechanical engineers have several techniques for reducing dynamic response in structural and mechanical components. These include passive, active, and semi-active control. This research focuses on an energy dissipation technology based on exploiting the unique properties of shape-memory materials (SMMs). SMMs are a family of materials displaying a characteristic thermoelastic phase transformation which is the basis of two mechanical hystereses: shape-memory (SME) and superelasticity (SEE). Passive energy dissipators, also known as *passive* or *supplemental* dampers, use either SME or SEE characteristics. Both provide an

energy dissipation mechanism with attractive properties for structural damping applications that include:

- hysteretic (rate-independent) damping
- a variety of hysteretic characteristics
- highly reliable energy dissipation based on a precisely repeatable solid state phase transformation
- very high energy dissipation per unit mass and per unit volume of SMA material
- negligible creep over the range of operating temperatures encountered in nearly all civil engineering applications
- a wide range of design operating temperatures
- excellent low-cycle and high-cycle fatigue properties
- excellent corrosion resistance.

1.2 Objective

The objective of this Phase I Small Business Innovative Research (SBIR) project was to develop the technical base required for the design of prototype energy dissipation/ damping devices for building structures.

1.3 Approach

The following steps were taken to achieve the stated objectives:

Task 1. Characterization of basic material behavior in sufficient detail to provide a basis for the design of prototype energy dissipators.

Task 2. Development of a basic set of conceptual designs for structural damping devices and the characterization of their mechanical behavior.

Task 3. Detailed analysis of the seismic response of a pre-selected non-ductile concrete building, with and without SMM energy dissipators, under moderate earthquake shaking, to demonstrate the attributes of hysteretic damping.

Task 4. Parametric analyses of a reduced-order model of the pre-selected building (*Task 3*) upgraded with SMM energy dissipators possessing different hystereses.

1.4 Scope

The scope of the Phase I SBIR effort was focused on developing a sound technological base for the design of structural damping devices using the nickel-titanium (NiTi) family of shape-memory alloys (SMAs). Because NiTi alloys currently dominate the SMM marketplace for damping applications, this restriction on alloy-selection does not compromise the objective outlined earlier, nor the wide-ranging applicability of the results presented in this report. Although much of the information presented in this report has direct application to other civil, mechanical, and aerospace structures and components, the focus of this study was structural control by passive means. Although active control is the subject of much current theoretical research both in the United States, Europe, and Japan, active control technology lags well behind that of passive control. As the results of this Phase I research effort are intended to form, in part, the basis of retrofitting strategies for the DOD's large inventory of seismically hazardous buildings, the scope of this study was limited to passive control of structural response. A detailed evaluation of active control using shape-memory alloys will be conducted as part of the Phase II research effort.

In addition to passive damping applications, SMMs have other important applications for the control of dynamic structural response, including semi-active and active control of environmental and impact loads. These applications of SMMs are not directly addressed in this study.

1.5 Report Organization

The Phase I SBIR report is composed of seven chapters, a detailed bibliography on energy dissipation for building structures, and five appendices.

Chapter 2 provides an introduction to the seismic response of building structures, the mechanisms by which seismic energy is dissipated in conventional buildings, the advantages of supplemental damping devices, and the passive and active means by which these devices can be implemented.

The characterization of the mechanical behavior of NiTi SMMs (Task 1) is presented in Chapter 3.

Conceptual structural damping device designs (Task 2) are discussed in Chapter 4.

Chapter 5 presents the results of a detailed analysis of a non-ductile reinforced concrete building typical of many buildings in the DOD inventory (Task 3). The building analyzed for this study was selected by USACERL and is sited in Fort Lewis, Washington. The building was constructed in 1956 using then-current seismic design procedures. The analyses presented in this report include eigen analysis, static load-

to-collapse and nonlinear time history analysis of the existing building, and two upgrading schemes that make use of SMM energy dissipators. The analysis results presented in Chapter 5 are based on the use of rectangular hysteresis.

In Chapter 6, a reduced-order model of the building analyzed in Chapter 5, upgraded with SMM energy dissipators exhibiting hysteresis shapes markedly different than those assumed in Chapter 5, is analyzed (Task 4). This effort was undertaken to demonstrate the differences in response that can be achieved with different SMM energy dissipators.

The research work conducted for the Phase I SBIR is summarized in Chapter 7. Conclusions drawn from the research results and recommendations for future research and development efforts are also presented in this chapter.

Appendix A.1 contains materials test data in tabular and graphical formats. Appendix A.2 includes a photocopy of the design calculations performed in this study. Appendix A.3 includes a copy of the Structural Engineers Association of Northern California's (draft) *Seismic Design Requirements for Passive Energy Dissipation Systems.*

2.0 SEISMIC ENERGY DISSIPATION SYSTEMS

2.1 Seismic Response of Building Structures

The design of a conventional building structure, that is, a building neither seismically isolated nor incorporating energy dissipation devices, is routinely based on seismic forces calculated using an elastic response spectrum divided by a response modification factor, denoted as R_w in the Uniform Building Code [57], that typically ranges between 8 and 12. The rationale, although flawed, behind the reduction factors embodied in the UBC is that lateral force-resisting systems exhibit both stable nonlinear behavior (ductility) and a lateral strength in excess of that for which it was designed.

Nonlinear behavior in conventional structural systems is generally associated with structural damage. For example, energy dissipation in a reinforced concrete ductile moment-resisting frame is provided by the formation of plastic hinges in the beams adjacent to the columns. The formation of plastic hinges in confined reinforced concrete beams is accompanied by spalling of the concrete cover and degradation of the strength and stiffness of the plastic hinge zone. In most instances, this damage should be repairable, but the repair may necessitate closure of the building for an extended period. In a worst case scenario, assuming that collapse is prevented, the lateral force resisting system may be so badly damaged that the building must be demolished.

One major problem with conventional buildings is that the gravity and lateral load-resisting systems share many common members, that is, if the lateral load-resisting system is damaged during an earthquake, so is the gravity load-resisting system. Significant damage to the gravity system in a building will generally result in its evacuation and the relocation of the occupants. The nonconstruction-related costs of the repair of an earthquake-damaged building may be appreciably higher than the construction costs. Protection of a building's gravity load-resisting system through the use of supplemental damping devices would appear to be cost-effective in many cases.

2.2 Energy Dissipation Using Supplemental Damping Devices

The use of supplemental damping elements to dissipate the earthquake-induced energy in a building is attractive for the following reasons:

- the distribution of energy dissipation in the building can be controlled by constraining it to occur in the supplemental dampers

- damage to the building can be limited to elements (supplemental dampers) that can be simply replaced after an earthquake

- the replacement of the supplemental dampers, should it be necessary, will not affect the gravity load-resisting system.

The use of supplemental dampers affords the designer with an opportunity to essentially uncouple the gravity and lateral load-resisting systems in a building.

2.3 Overview of Passive Energy Dissipation Systems

2.3.1 Friction Systems

A variety of friction devices have been proposed for structural energy dissipation. All of the friction systems except one (the Fluor-Daniel EDR) generate rectangular hysteresis loops characteristic of Coulomb friction (Figure 2.1). Typically these devices have very good performance characteristics, and their behavior is not significantly affected by load amplitude, frequency, or the number of applied load cycles. The devices differ in their mechanical complexity and in the materials used for the sliding surfaces.

Friction dampers made by Sumitomo Metal Industries, Ltd. (Figure 2.2), have been used in two buildings in Japan [3], and a friction device manufactured by Pall Dynamics, Ltd., has been used in one retrofit and two new buildings in Canada [100,101,146]. The Pall device (Figure 2.3) is intended to be mounted in X-bracing. Several earthquake simulator studies of multi-story steel frames incorporating Pall devices have been performed [1,34], and a design methodology has been developed for friction-damped structures [35]. The design of the Sumitomo devices for the two building applications was with the primary objective of reducing the response of the structures to ground-borne vibrations and small-to-moderate earthquakes. Response control under large earthquake shaking was not a primary design consideration. The Sumitomo device is an evolution of a friction damper used for railway cars. The frictional resistance is generated by copper alloy pads with graphite plug inserts sliding against the inner surface of the steel barrel of the device.

Fluor Daniel, Inc., has developed and tested a unique type of friction device called the Energy Dissipating Restraint (EDR) [113]. The EDR has self-centering capabilities, and the slip load is proportional to the displacement. Several hysteresis behaviors are possible (Figure 2.4). The friction surfaces in this device are bronze wedges sliding on a steel barrel. A detailed description of the EDR and its behavior is provided elsewhere in these proceedings [95].

Simpler devices with Coulomb behavior include those which use a brake pad material

on a steel friction interface [42, 142]. Other friction schemes that involve no special devices, but rather allow slip in bolted connections, have also been developed [38,115]. A promising refinement of the slotted bolted concept has recently been made using a brass on steel friction couple [46]. Earthquake simulator tests of a three-story steel building model with these slotted bolted connection (SBC) energy dissipators have recently been completed.

Issues of importance with friction devices are long-term reliability and maintenance; the potential for introduction of higher frequencies as the devices undergo stick-slip behavior; and possible permanent offsets after an earthquake. The maintenance and protection from deterioration of a device in which the sliding surfaces are required to slip at a specific load during an earthquake, even after decades of nonuse, are essential.

2.3.2 Metallic Systems

These energy dissipation systems take advantage of the hysteretic behavior of metals deformed into their post-elastic range. A wide variety of different types of devices have been developed that utilize flexural, shear, or extensional deformation modes into the plastic range. A particularly desirable feature of these systems is their stable behavior, long-term reliability, and generally good resistance to environmental and temperature factors.

Yielding Steel Systems

The ability of mild steel to sustain many cycles of stable yielding behavior has led to the development of a wide variety of devices which utilize this behavior to dissipate seismic energy [69,126]. Many of these devices use mild steel plates with triangular or hourglass shapes [130,140] so that the yielding is spread almost uniformly throughout the material. The result is a device which is able to sustain repeated inelastic deformations in a stable manner, avoiding concentrations of yielding and premature failure.

One such device that uses X-shaped steel plates is the Bechtel Added Damping and Stiffness (ADAS) device. ADAS elements are an evolution of an earlier use of X-plates as damping supports for piping systems [132]. Extensive experimental studies have investigated the behavior of individual ADAS elements and structural systems incorporating ADAS elements [13,149]. The tests showed stable hysteretic performance (Figure 2.5). ADAS devices have been installed in a two-story, non-ductile reinforced-concrete building in San Francisco as part of a seismic retrofit [32], and in two buildings in Mexico City. The principal characteristics that affect the behavior of an ADAS device are its elastic stiffness, yield strength, and yield displacement. ADAS devices are usually mounted as part of a bracing system, which must be substantially stiffer than the surrounding structure. The introduction of such a

heavy bracing system into a structure may be prohibitive.

Triangular-plate energy dissipators were originally developed and used as the damping elements in several base isolation applications [16]. The triangular plate concept has been extended to building dampers in the form of the triangular ADAS, or T-ADAS, element [138]. Component tests of T-ADAS elements and pseudodynamic tests of a two-story steel frame have shown very good results (Figure 2.6). The T-ADAS device embodies a number of desirable features; no rotational restraint is required at the top of the brace connection assemblage and there is no potential for instability of the triangular plate due to excessive axial load in the device.

An energy dissipator for cross-braced structures, which uses mild steel round bars or flat plates as the energy absorbing element, has been developed [142]. This concept has been applied to several industrial warehouses in New Zealand. A number of variations on the steel cross-bracing dissipator concept have been developed in Italy [22]. In Naples, Italy, a 29-story steel suspension building with floors "hung" from the central tower utilizes tapered steel devices as dissipators between the core and the suspended floors.

A six-story government building in Wanganui, New Zealand, uses steel-tube energy-absorbing devices in precast concrete cross-braced panels [85]. The devices were designed to yield axially at a given force level. Recent studies have experimentally and analytically investigated a number of different cladding connection concepts [25].

Several types of mild steel energy dissipators have been developed in Japan [65,73]. So-called honeycomb dampers have been incorporated in 15-story and 29-story buildings in Tokyo. Honeycomb dampers are X-plates (either single plates or multiple plates connected side by side) that are loaded in the plane of the X. (This is orthogonal to the loading direction for triangular or ADAS X-plates). Kajima Corporation has also developed two types of omni-directional steel dampers called "Bell" dampers and "Tsudumi" dampers [73]. The Bell damper is a single-tapered steel tube, and the Tsudumi damper is a double-tapered tube intended to deform in the same manner as an ADAS X-plate but in multiple directions. Bell dampers have been used as part of an atrium roof system connecting a 5-story and a 9-story building. Tsudumi dampers have been used in a massive 1600-ft long ski-slope structure to permit differential movement between four dissimilar parts of the structure under seismic loading while dissipating energy. Both of these applications are located in the Tokyo area.

Another type of joint damper for application between two buildings has been developed [119]. This device is a short lead tube that is loaded to deform in shear (Figure 2.7). Experimental investigations and an analytical study have been undertaken.

Particular issues of importance with metallic devices are the appropriate post-yield deformation range, such that a sufficient number of cycles of deformation can be sustained without premature fatigue, and the stability of the hysteretic behavior under repeated post-elastic deformations.

Lead Extrusion Devices (LEDs)

The extrusion of lead was identified as an effective mechanism for energy dissipation in the 1970s [113]. LED hysteretic behavior is very similar to that of many friction devices, being essentially rectangular (Figure 2.8). LEDs have been applied to a number of structures both for damping in seismic isolation systems and as energy dissipators in multi-story buildings. In Wellington, New Zealand, a 10-story, cross-braced, concrete police station is base isolated with sleeved-pile flexible elements and LED damping elements [21]. Several seismically isolated bridges in New Zealand also utilize LEDs [126]. In Japan, LEDs have been incorporated in 17-story and 8-story steel frame buildings [96]. The devices are connected between precast concrete wall panels and the surrounding structural frame.

LEDs have a number of particularly desirable features: their load-deformation relationship is stable and repeatable, being largely unaffected by the number of loading cycles; they are insensitive to environmental factors; and tests have demonstrated insignificant aging effects [114] (Figure 2.8).

Shape Memory Alloys (SMAs)

Shape memory alloys have the ability to "yield" repeatedly without sustaining any permanent deformation. This is because the material undergoes a reversible phase transformation as it deforms rather than intergranular dislocation, which is typical of steel. Thus, the applied load induces a crystal phase transformation, which is reversed when the load is removed (Figure 2.9). This provides the potential for the development of simple devices which are self-centering and which perform repeatedly for a large number of cycles.

Several earthquake simulator studies of structures with SMA energy dissipators have been carried out. At the Earthquake Engineering Research Center of the University of California [4], a 3-story steel model was tested with Nitinol tension devices as part of a cross-bracing system, and at the National Center for Earthquake Engineering Research [153], a 5-story steel model was tested with copper-zinc-aluminum SMA devices. In this second study, devices with torsion, bending, and axial deformation modes were investigated. Typical hysteresis loops from these tests are shown in Figure 2.10. Results showed that the SMA dissipators were effective in reducing the seismic responses of the models.

Shape memory devices must be designed such that the device deformations do not

occur beyond the elastic limit strain (into the plastic range), resulting in permanent yield in the material. The elastic limit strain varies by SMA, but is typically on the order of 5%. Some members of the SMA family also exhibit excellent fatigue resistance. Nitinol has outstanding corrosion resistance, superior even to that of stainless steels and other corrosion-resistant alloys.

2.3.3 Viscous and Viscoelastic Systems

Viscoelastic materials have been in use in structural engineering for vibration control for more than 20 years. Mahmoodi described the characteristics of a double-layer, constrained-layer, viscoelastic (VE) shear damper in 1969 [80]. Viscoelastic copolymers developed by 3M Company have been used in a number of structural applications. Double-layer shear dampers using a 3M material were used in the 110-story, twin towers of the World Trade Center in New York City, where a total of 10,000 dampers were installed in each tower to damp wind-induced dynamic response [81]. VE damping systems have since been adopted in several other tall buildings for the same purpose [68,83].

The extension of VE shear dampers to the seismic domain has occurred more recently. Wind vibration control applications have typically provided buildings with only about 2% of critical damping. The level of damping required for a feasible seismic energy dissipation system is significantly higher than this; in experimental studies, damping ratios on the order of 10 to 20% have been targeted. To obtain a feasible design for a VE damper system, a number of factors that affect material properties must be taken into account. The stiffness and damping properties of VE polymers are influenced by the level of shear deformation in the material, temperature, and frequency of loading. Practical materials have been fully characterized for a wide range of these factors. Several earthquake simulator studies of large-scale, steel frame models with VE dampers have been conducted [3,77]. In each study, the VE dampers were found to significantly improve the response of the test models, reducing drifts and story shears (compared to those of the models without VE dampers). More recently, tests of VE dampers applied to a 1/3-scale, non-ductile reinforced-concrete model have been performed, and a full-sized steel frame has been constructed in China as a test structure for VE dampers. One study subjected a VE-damped model to earthquake shaking under different levels of ambient temperature [77], and several experiments have monitored the internal temperature in the VE layers of a shear damper during earthquake shaking. Observed transient temperature increases have not been very significant (typically less than 10° F). A number of analytical studies have also been undertaken, and an effective modal design method developed [19].

Several companies in Japan have developed damping systems based on different VE materials. Shimizu Corporation has developed a bitumen rubber compound (BRC) VE damper which has been used in a one 24-story steel building of a twin-tower complex. Both buildings are instrumented to provide seismic response data for comparison

between VE-damped and undamped responses [159]. Bridgestone Corporation has developed a visco-plastic rubber shear damper, which has been shake table tested in a 5-story steel frame model [40].

A viscous-damping (VD) wall system has been developed by Oiles and Sumitomo Construction (Figure 2.11). Earthquake simulator tests of a full-scale, 4-story steel frame with and without VD walls showed very large response reductions - up to 60% to 75% - with the walls [7]. A 4-story, reinforced-concrete test building with VD walls was constructed in Tsukuba, Japan, in 1987. It has since been monitored for earthquake response; observed accelerations are 25% to 70% lower than those of the building without VD walls [7]. A VD wall system in a 15-story building now under construction in Shizuoka City, Japan, will provide 20% to 32% damping to the building, and achieve response reductions of the order of 75% to 80% [87]. Another type of wall damping system has been developed and tested by Kumagai-Gumi Corporation. It is a super-plastic and silicone rubber VE shear damper that is included at the top connection between a wall panel and the surrounding frame [145]. Earthquake simulator tests of a 1/2-scale, 3-story steel frame showed significant response reductions in the VE damped model; as large as 50% in story accelerations and 60% in story displacements.

Fluid viscous dampers, which for many years have been used in the military and aerospace fields, are beginning to emerge in structural engineering. These dampers possess linear viscous behavior, are relatively insensitive to temperature changes, and can be very compact in size considering their force capacity and stroke. Experimental and analytical studies of building and bridge structures incorporating fluid viscous dampers (Figure 2.12) made by Taylor Devices, Inc., have recently been performed [24]. Very large response reductions were achieved by using these devices. In a pure viscous damper, the damping force is out-of-phase with the displacement. This can be a particularly desirable attribute for passive damping applications to buildings. If dampers are included in the structure in such a way that there is a column axial force component to the damper force (i.e., with a diagonal brace), then the out-of-phase peak damper force means that the peak-induced column moments are less than if the peak damper force occurred at peak displacement.

2.4 Design Provisions for Energy Dissipation Systems

The interest of the engineering profession in passive energy dissipation has resulted in the development of tentative requirements for the design and implementation of passive energy dissipation (PED) devices in the USA.

The *Tentative Seismic Design Requirements for Passive Energy Dissipation Systems* [124] (hereafter known as the document) was prepared by the Energy Dissipation Working Group (EDWG) of the Base Isolation Subcommittee of the Seismology

Committee of the Structural Engineers Association of Northern California. It was the intent to supplement the Uniform Building Code (UBC) [57] with additional design requirements developed specifically for buildings incorporating discrete passive energy dissipation devices. The format and nomenclature in the document is consistent with that in the UBC to facilitate formal integration into the UBC in the event that the requirements are adopted.

The general philosophy of the document is to confine the inelastic activity in a structure primarily to the energy dissipators and for the gravity load-resisting system to remain elastic for the design-basis earthquake. Since the dissipators do not form part of the gravity load-resisting system, they are replaceable after an earthquake. As such, this type of innovative structural system is fundamentally different from a conventional seismic lateral load-resisting system.

The document provides general design requirements applicable to a wide range of possible systems. In remaining general, the document relies on the testing of system hardware to confirm the engineering parameters used in the design and to verify the overall adequacy of the EDUs and EDS. In general, acceptable systems will:

- remain stable for required design displacements,
- provide non-decreasing resistance with increasing displacement (for rate-independent systems),
- not degrade under repeated cyclic load at the design displacement, and
- have quantifiable engineering parameters (e.g., force-deflection and energy-dissipation characteristics).

There are two types of energy-dissipation devices recognized in the document: rate-dependent and rate-independent devices. Guidelines for the design of tuned mass or liquid dampers are not provided in the document. The only rate-dependent devices explicitly recognized in the document are viscous and viscoelastic PED devices. The rate-independent PED devices implicitly recognized in document are: friction-slip, steel yielding, and shape-memory devices.

A hierarchial nomenclature is used in the document. Passive energy dissipation devices are known as energy dissipation units (EDUs). EDUs form an integral part of an energy dissipation assembly (EDA); the EDA is a one-bay, one-story assembly composed of the EDUs and the elements that provide lateral and vertical stability to the EDUs. An illustration of the relationship between an EDU and an EDA is presented in Figure 2.13. The energy dissipation system (EDS) is the three-dimensional collection of all of the EDAs.

The document prescribes the use of dynamic analysis procedures to determine maximum responses. Dynamic analysis procedures include both response spectrum analysis and linear and nonlinear time history analysis. Linear procedures can be used for the earthquake-resistant design of structures incorporating viscous or viscoelastic energy dissipators. Nonlinear time history analysis is mandatory for non-compliant rate-dependent EDSs and for all rate-independent EDSs.

The seismic demands are described by the spectral demands of the design-basis earthquake (DBE). These spectral demands correspond to a level of ground motion that has a 10% probability of being exceeded in a 50-year time period. For building designs not using a site-specific hazard analysis, the design-basis spectra are defined by the ground motion spectra specified by the UBC for dynamic analysis of conventional buildings. The seismic design actions and deformations in the EDS are based on the DBE analysis.

The UBC places a lower bound on the design actions and deformations computed using dynamic analysis. Similarly, minimum base shear coefficients at the ultimate (strength) level are specified for EDSs. The minimum base shear coefficient is calculated as ZC/R_w using the method specified in the UBC, and scaled to the ultimate (strength) level via a material-dependent conversion factor, for comparison with the results of the dynamic analysis. The minimum base shear coefficient is dependent on the type of lateral load-resisting system: for EDSs with no supplemental moment frame (non-dual system), the minimum base shear coefficient is computed using an R_w of 10; for dual system EDSs, the minimum base shear coefficient is computed using an R_w of 12.

The document will be supplemented with a commentary in the near future and then issued as a "Green-Book" that will supplement the Structural Engineers Association of California's "Tentative Lateral Force Requirements" [133]. A copy of the draft document (as of April 15, 1993) is presented in Appendix A.3.

2.5 Active Control of Building Response

The active control of building response involves modification or control of the building's motion by the implementation of a control system. In general, the control system is powered by an external source, although Inaudi has proposed extracting the elastic strain energy from the structure to power the active control system.

Soong [128] listed a number of factors that have arisen in recent years that highlight the need to develop structural systems ". . . with some degree of adaptability or responsiveness. . ." as follows:

- *increased building flexibility* resulting from the construction of taller, more flexible structures

- *increased reliability requirements* for critical structures (off-shore platforms, defense-related installations, nuclear power plants) and essential facilities (hospitals, 911 centers, emergency operation centers, etc.)

- *enhanced performance requirements* for important civil engineering structures such as off-shore oil and gas platforms and buildings that house sensitive national security-related equipment or expensive irreplaceable computational or industrial hardware

- *improved utilization of materials*, especially for applications to lightweight structures such as space-based platforms.

Active control of building response under external dynamic excitations was first proposed more than 30 years ago. Soong [128] notes that Freyssinet first proposed to use pre-stressing cables to stabilize the dynamic response of tall structures in 1960. The world-renown structural engineer, Lev Zetlin, independently devised a strategy for the design of tall buildings that incorporated cables attached to both the structural frame and hydraulic actuators, and a closed-loop control system that controlled the response of the actuators based on the response of sensors or transducers mounted at the top of the building.

In 1972, Yao [158] published a paper on structural control intended to "...stimulate interest among structural engineers in the application of control theory to the design of civil engineering structures...." Yao and Soong both schematically depicted, in block diagram form, the general structure of most active control systems; the block diagram form [127] is reproduced in Figure 2.14. (The block diagram presented in Figure 2.14 is that of an open-closed loop control system.) The control system presented in this figure is composed of the following three components:

1. Externally or internally powered actuators to impose the control forces

2. Data acquisition and analysis computational hardware to process the transducer output and compute the appropriate control forces (based on pre-determined control algorithms and an a-priori knowledge of the dynamic characteristics of the building)

3. Transducers measuring structural response *(closed-loop control)* or external excitation *(open-loop control)* or both *(open-closed loop control)*

Numerous control algorithms have been developed for the active control of buildings subjected to random dynamic excitation. Soong [128] provides detailed information on this subject.

The principles of active control have been demonstrated in the laboratory [55,128] and in the field. Soong et al. have tested an active tendon system (similar in principal to that proposed by Zetlin) in scale models of single-, three-, and six-story buildings on an earthquake simulator at the State University of New York at Buffalo. The responses of the actively controlled structures were appreciably less than those of the "uncontrolled" structures, indicating that relatively simple control systems can effectively reduce the seismic response of structures.

Experimental studies of model structures incorporating tuned active mass dampers (AMDs) have been conducted by Takenaka Corporation and Kajima Corporation [74] in Japan. These studies have shown that AMDs can be effective in reducing seismically-induced building motion. A full-scale AMD system has been installed in the top story of the 11-story Kyobashi Seiwa building in Tokyo. This AMD system, developed by Kajima Corporation, is a pendulum-type dual mass system capable of mitigating torsional and lateral building response.

Researchers at the Kajima Kobori Research Complex [75,76] have developed, tested, and implemented an active control system that reduces a building's response by actively controlling its lateral stiffness. A three-story, one-span, two-frame steel structure with active braces was tested on an earthquake simulator. The primary result of this testing program was that the acceleration response of the controlled system (with the active braces) was significantly less than that of the uncontrolled system. In 1990, the active variable stiffness (AVS) system was implemented in the earthquake simulator control building at Kajima Corporation's Institute of Construction Technology in Tokyo. At the time of writing, this building had not yet been subjected to either moderate or severe earthquake shaking.

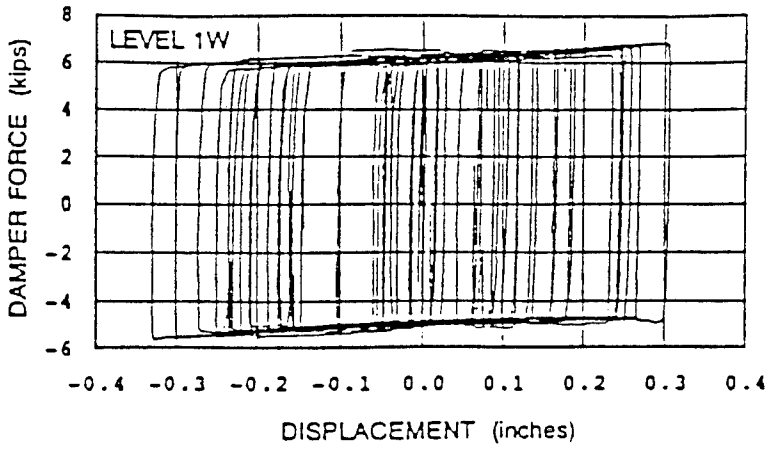

Figure 2.1 Sumitomo Friction Device Hysteresis [3]

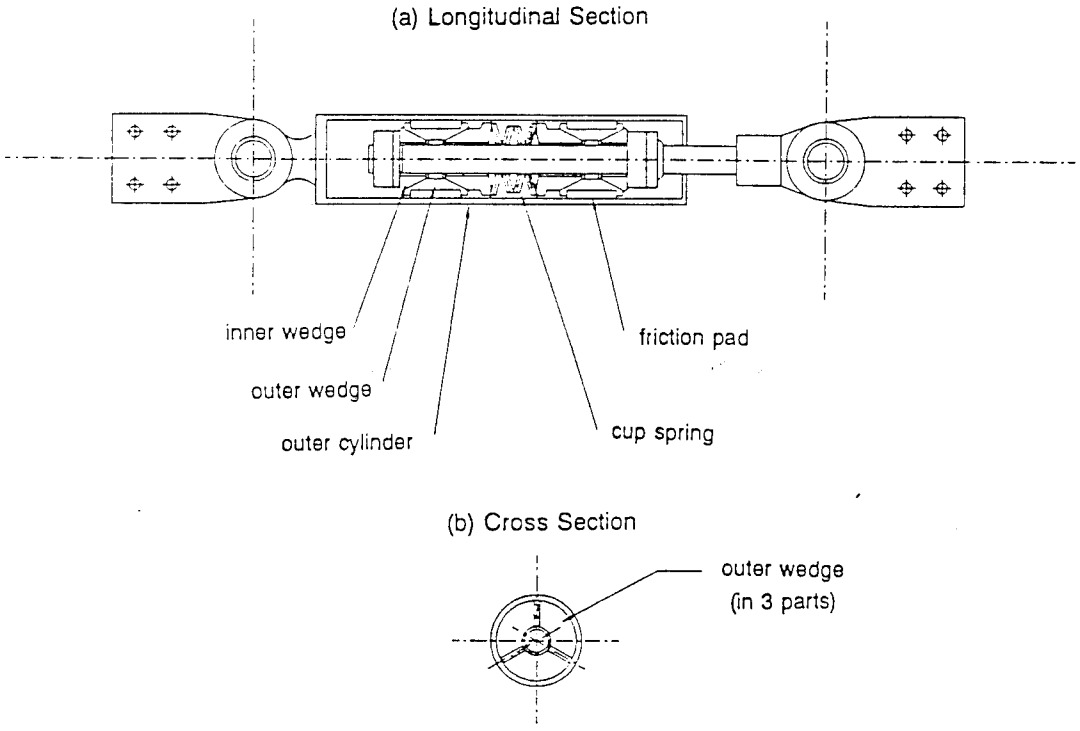

Figure 2.2 Sumitomo Friction Device Cross Sections [3]

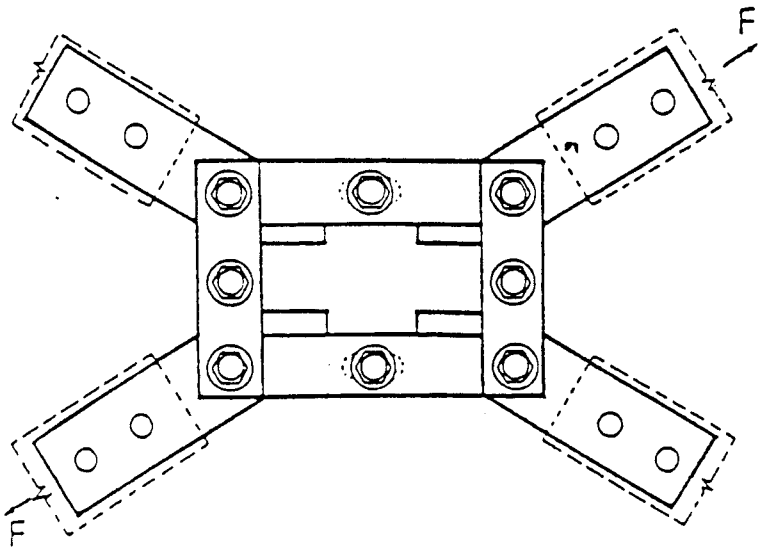

Figure 2.3 Pall Friction Device [146]

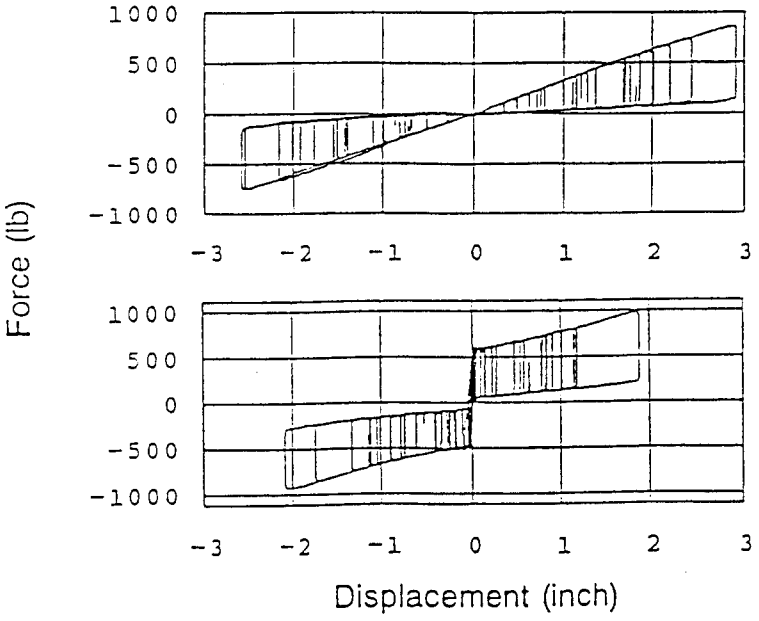

Figure 2.4 Fluor-Daniel Device EDR Hysteresis Loops [113]

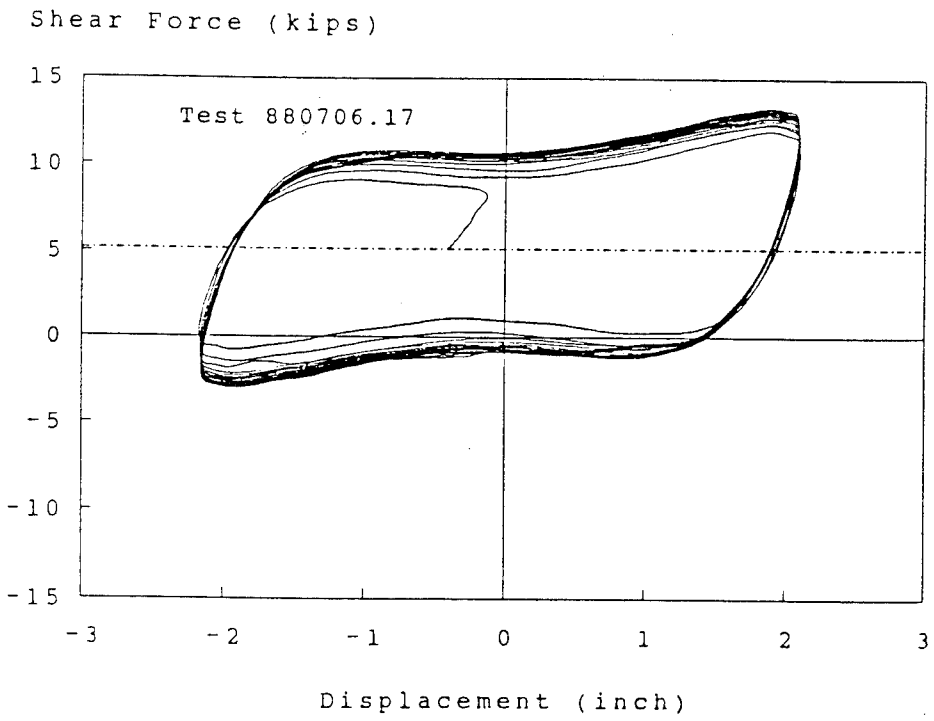

Figure 2.5 ADAS Device Hysteresis Loops [149]

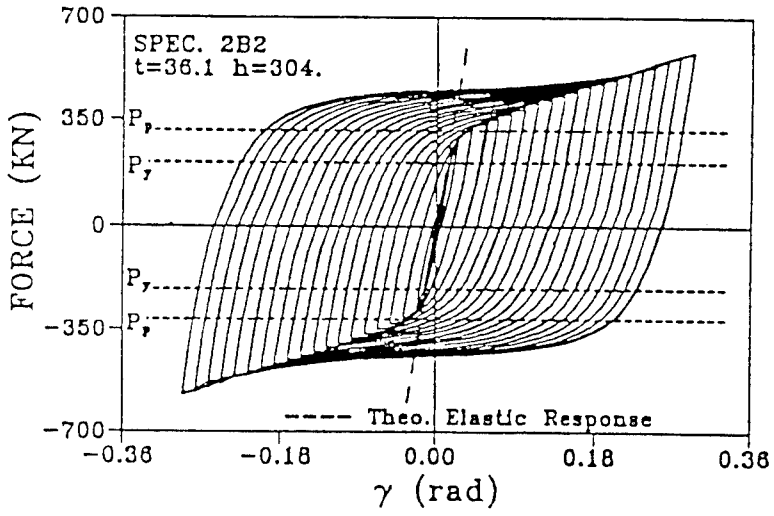

Figure 2.6 T-ADAS Device Hysteresis Loops [138]

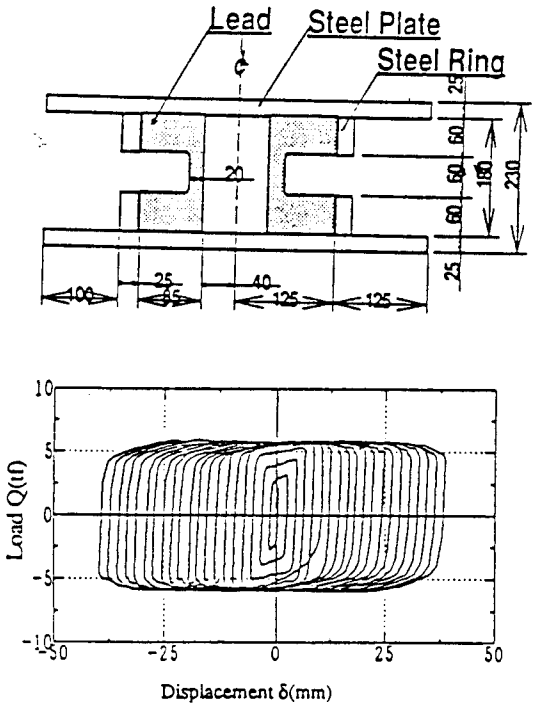

Figure 2.7 Lead Joint Damper and Hysteresis Loops [119]

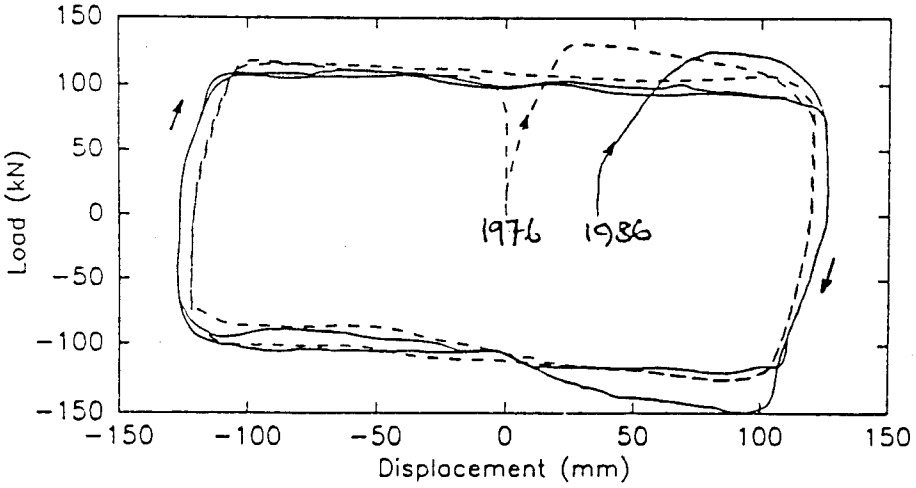

Figure 2.8 LED Hysteresis Loops [114]

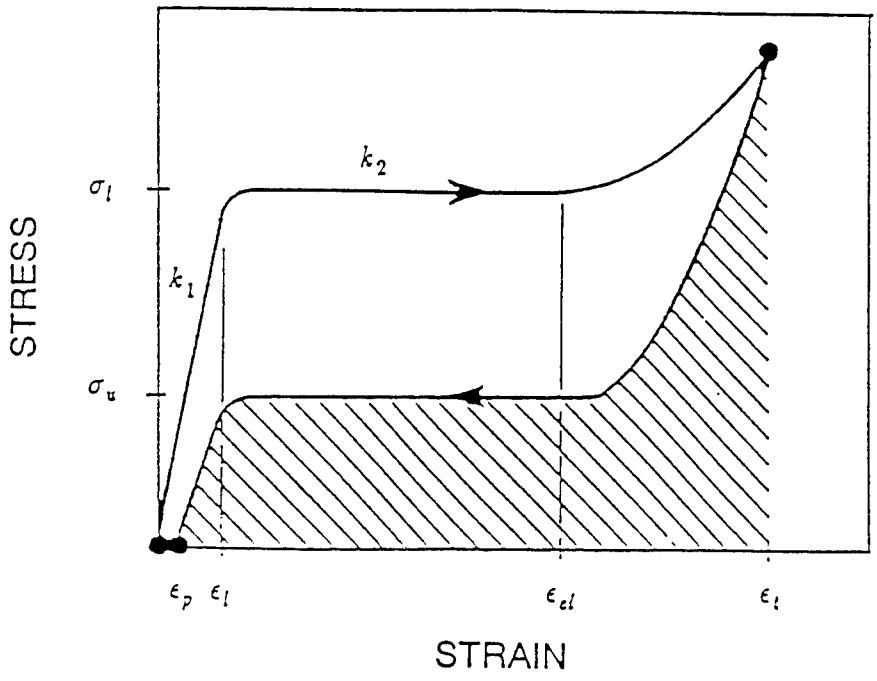

Figure 2.9 SMA Superelastic Hysteresis

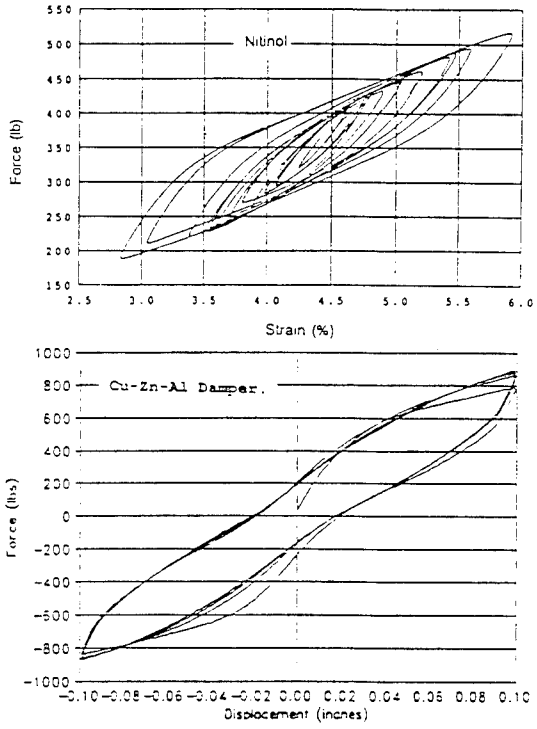

Figure 2.10 NiTi and CuZnAl SMA Hysteresis Loops [153]

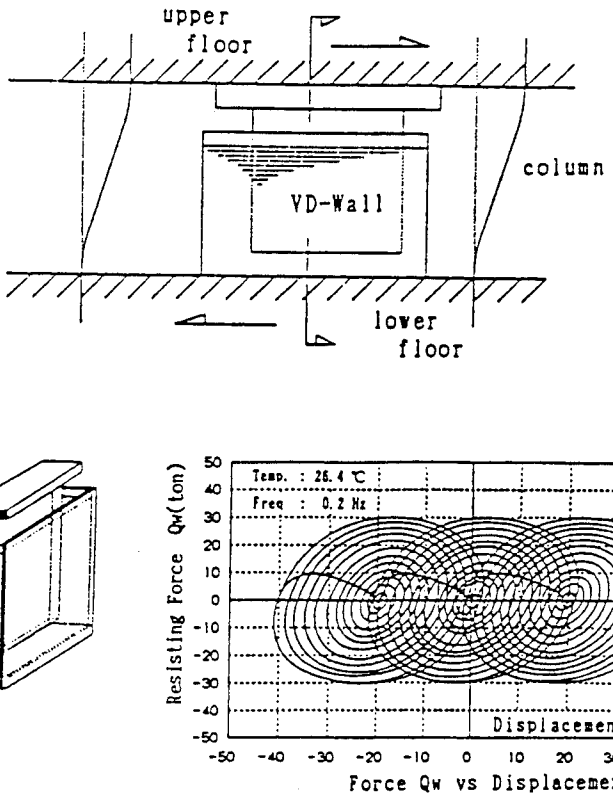

Figure 2.11 VD Wall and Hysteresis Loops [7]

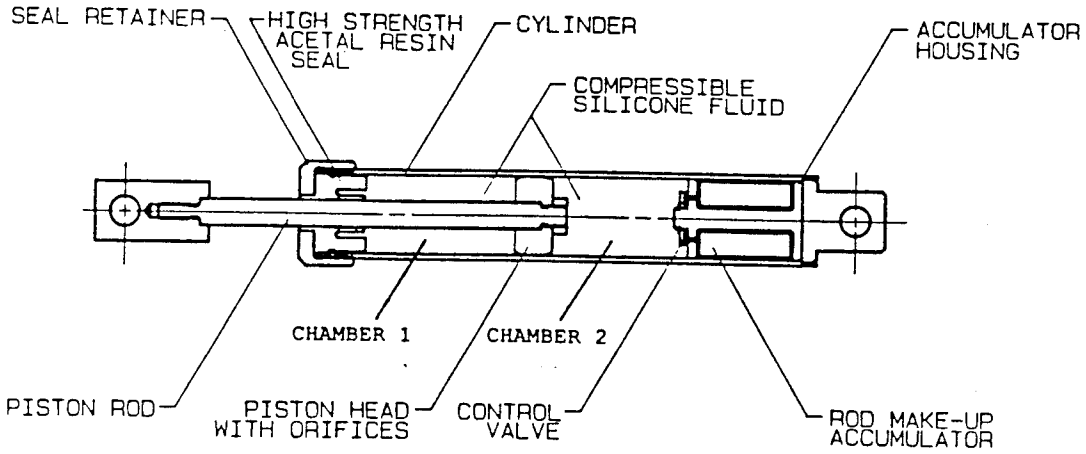

Figure 2.12 Fluid Viscous Damper [24]

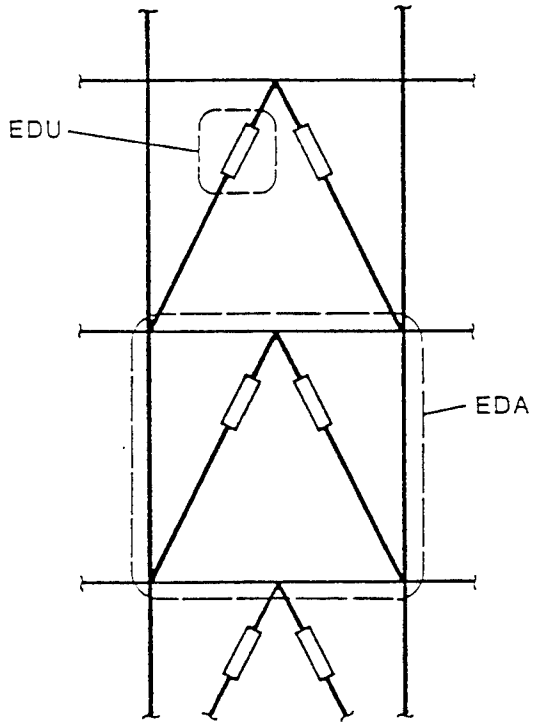

Figure 2.13 Nomenclature for Code Requirements [124]

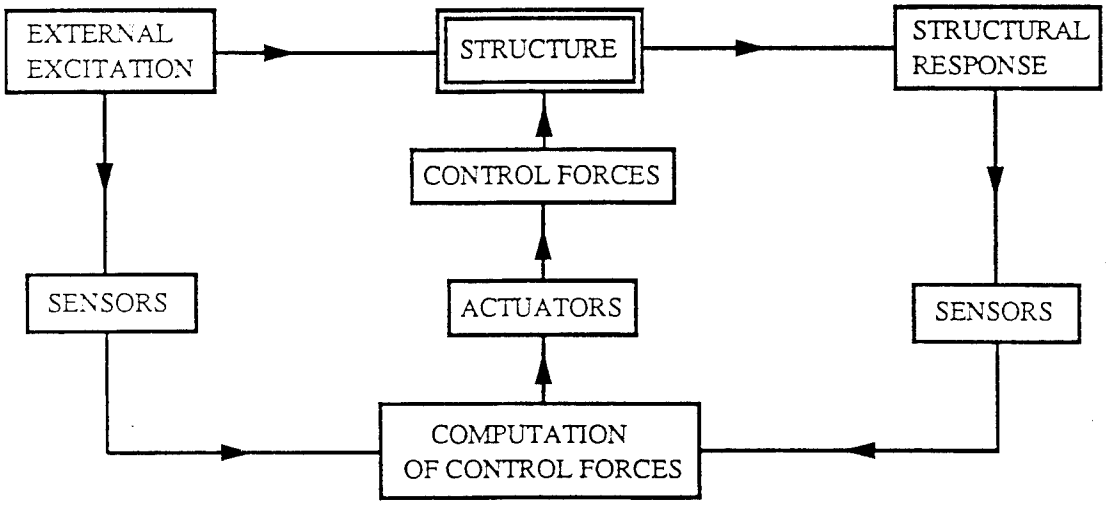

Figure 2.14 Active Control Block Diagram [127]

3.0 SMM MATERIALS CHARACTERIZATION

3.1 Objectives

The two objectives of the shape-memory alloy materials characterization program were:

1. to validate the use of SMMs as an energy dissipation mechanism for structural damping devices by constructing a descriptive knowledge base of the material characteristics relevant to damping applications, including hysteretic behavior, thermal sensitivity, and durability-related attributes,

2. to construct a catalog of material property data for a specific alloy in sufficient detail to facilitate the design of prototype damping devices.

3.2 Approach and Methods

3.2.1 General

The approach to accomplishing the objective outlined above was the following:

1. to analyze all commercially-available shape-memory alloys to select the best candidate alloy,

2. to compile a database on the candidate alloy from the literature and our extensive in-house data base,

3. to design and conduct a materials testing program consistent with the program objectives,

4. to present the results of the testing program and provide an annotated bibliography on relevant materials properties, a compilation of materials tests results, and a summary of results and conclusions.

3.2.2 Detailed Methods

The bibliography was constructed through a conventional literature search supplemented by extensive informal consulting with experts in the field. The focus was confined to material directly relevant to the damping application of SMMs. The material testing program was conducted in a conventional test machine equipped with a thermally controlled environment with a temperature range of 0° C to 80° C.

TEST	MATERIAL	DIAMETER (in)	LOOPS	FREQUENCY (Hz)	TEMP. (°C)
1A	F4904-2-2	0.015	14	0.2	22
1B	F4903-2B	0.009	22	0.2	22
1C	F00642-1B	0.162	14	0.2	22
1D	F2234-2-2A	0.014	19	0.2	22
2A	F4904-2-2	0.015	14	0.3	22
2B	F4904-2-2	0.015	14	0.3	23
2C	F4904-2-2	0.015	14	1.0	23
2D	F4904-2-2	0.015	14	3.0	23
2E	F4904-2-2	0.015	14	10.0	23
2F	F4903-1B	0.035	5	3.0	23[a]
2G	F4903-1B	0.035	5	3.0	23
3A	F4904-2-2	0.015	14	0.2	40
3B	F4904-2-2	0.015	14	0.2	60
3C	F4904-2-2	0.015	14	0.2	80
3D	F4904-2-2	0.015	14	0.2	0
4A	F00642-1B	0.016	18	0.2	22[b]
4B	F00642-1B	0.016	18	0.1	23
4C	F4903-1B	0.035	6	0.1	23
5A	F4903-2B	0.009	15	0.2	23
6A	F4904-2-2	0.015	14[c]	0.2	23
6B	F4904-2-2	0.015	14[c]	0.2	22[b]
6C	F4904-2B	0.0091	16[d]	0.2	23
6D	F4904-2B	0.0091	16[d]	0.2	23

a. Sample came loose during testing
b. Servo gain too low
c. 6 of 14 loops slack to 2% strain
d. 7 of 14 wires slack to 4% strain
e. 8 of 16 loops slack to 4% strain

Table 3.1 Details of the Testing Program

The testing program was developed to investigate strain rate, temperature, and thermomechanical processing dependence for NiTi alloys over the relevant strain

range for this alloy. Table 3.1 summarizes the parameters considered in the test program. Test samples consisted of multiple loops of NiTi wires tested in tension. Testing was limited to tension because devices can be constructed using tension loops alone. Testing was restricted to superelastic materials on the basis that purely martensitic (SME) behaviors of NiTi are sufficiently well discussed in the literature. Two additional tests of specific configurations of tension loops were also conducted. In the first, a NiTi sample was pre-strained to approximately 4% and then cycled between 2% and 6% strain. The result is the hysteresis loop shown in Figure 3.1. The second test used successively engaged loops of NiTi to create piece-wise linear hysteresis as shown in Figures 3.2 (Test 6C) and 3.3 (Test 6D).

3.2.3 Phase II Results

3.2.3.1 SMM Descriptive Summary

Shape-Memory Alloys (SMAs or SMMs) are a class of alloys that display a characteristic thermoelastic martensitic phase transformation above a Transformation Temperature Range (TTR), which is specific to each alloy (Figure 3.4). As these alloys are cooled through their TTR, they transform from the higher temperature austenite phase to the lower temperature martensite phase. Over a dozen alloy families have been shown to exhibit this transformation, and each of these families has many specific compositions, each of which possesses unique mechanical and transformation properties. Most of the alloys have a long-range ordered atomic structure, and some are clearly intermetallic compounds with extremely narrow compositional ranges. For the purposes of this study, there are five primary alloy systems of significant interest. These are the Nickel-Titanium family (often called Nitinol); two copper-based systems, CuZnAl and CuAlNi; FeMnSi alloys; and some special stainless steel compositions.

In each of the SMAs, the austenitic form is a relatively simple cubic lattice at the molecular level. If deformed, the austenitic alloy strains by standard dislocation mechanisms in a permanent manner. In the martensitic state, however, the material assumes a more complex crystal structure, such as monoclinic or orthorhombic, and tends to exist in alternate twin bands of opposite crystal tilt if cooled under zero stress.

There are two primary features of SMAs of interest, irrespective of alloy type. The first of these is called the Shape Memory Effect (SME), which occurs if the alloy is strained in shear at a temperature below its TTR. As long as the shear strain is less than a critical strain for the particular alloy, the strain can be accommodated in the alloy by a twin re-orientation process: no dislocation motion or permanent damage occurs at the atomic level. Upon heating the strained structure, each of the twinned elements reverts to the original austenitic crystal structure, and any imposed strain is lost: the material reverts to its pre-strained shape and the shape memory effect is observed. The reversion of the martensite to the austenite is a first-order phase change with a

strong driving force. For this reason, the shape recovery occurs with a large mechanical force, and only a restraining force large enough to create permanent deformation in the austenitic parent will hinder shape recovery.

The second feature of the SMAs is called the Superelastic Effect (SEE). This effect is observed when a strain is imposed on an SMA material at a temperature slightly above its TTR. The alloy system can relieve the stress imposed on it by transforming to the thermally unstable martensite and allowing that martensite to strain as it is formed, thus creating a stress-induced martensite. Since this martensite is not thermally stable, as soon as the stress is lowered below the stress level required to create the martensitic form, the material may revert to the austenite and thus eliminate the strain in the stress-induced martensite. The stress at which the martensite undergoes a phase change to austenite is termed the reversion stress.

Both of the above features of SMAs are illustrated schematically in Figures 3.5 and 3.6, which show typical stress strain curves for a NiTi alloy. In Figure 3.5, the alloy was tested at a temperature slightly below that at which it changes to martensite upon cooling. The force-deformation response takes the form of a low flow stress, a long horizontal yield plateau, followed by a significant increase in stiffness. Merely heating the material through its TTR will remove all accumulated strain and return the material to its original form. This is the classical shape memory effect. Figure 3.6 shows the curve for an alloy tested at a temperature slightly above its TTR, where the alloy exhibits the superelastic effect. The same plateau is seen as in Figure 3.5, but at a much higher stress. Reduction of the stress at the end of the plateau results in a lower stress at which the material will lose the imposed strain. Different families of SMAs show widely different levels of shape memory strain, have different ultimate ductilities, and show very different responses to cyclic deformation. The candidate alloy systems mentioned above are of interest for reasons of cost, fabricability, or optimum mechanical properties. This Phase I study focuses exclusively on the NiTi family of alloys because of their superior mechanical properties.

Each of the alloy systems noted above will be assessed in the Phase II program. Within each system, several specific compositions will be investigated if the alloy system is promising. The copper-based alloys will be investigated in Phase II because they are potentially less expensive than NiTi; can be fabricated differently than NiTi; and, in specialized forms, have shown larger SEE strains than NiTi. The FeMnSi and stainless steel alloys are potentially more economical than the other SMMs. Although the cyclic properties of their thermoelastic martensite is comparatively poor, they will be examined in the Phase II program to determine in what type of damping application they might prove to be useful.

3.2.3.2 Annotated bibliography

To provide USACERL and structural engineers in general with information regarding NiTi material properties relevant to damping device design, an annotated bibliography was organized by major properties and processes. Each annotation refers to the best source of information on that topic.

1. *Material Science of Shape-Memory and Superelasticity [28,4,60]*

An overview of basic material science of materials displaying a thermoelastic martensitic phase transformation, including their crystallography and thermodynamics.

2. *R-phase transitions [88]*

Some SMMs display a distinct phase transformation referred to as an R-phase transition, which is also thermoelastic and produces both a shape-memory and a superelastic effect.

3. *General Mechanical Properties and Physical Metallurgy [58]*

A compilation of data on NiTi and its physical metallurgy, including thermal and electrical conductivity, density, specific heats, hardness, effects of alloying corrosion resistance, and machinability.

4. *Creep and Stress Relaxation [107]*

There are no specific references on the creep behavior of NiTi. At temperatures below 300° C, no stress relaxation occurred in NiTi samples subjected to high imposed stresses.

5. *Temperature Effects on Superelasticity in SMMs [28]*

The formation of martensite is a thermoelastic process, meaning that a decrease in temperature is equivalent to an increase in stress. The variation in stress required to induce martensite as a function of temperature is given by a Clausius-Clapeyron equation. The engineering implication of this is that at higher temperatures, higher stresses are required to induce martensite formation: superelastic materials stiffen with an increase in temperature (Figure 3.7). However, as a first-order approximation, the energy dissipation characteristics for superelastic alloys remains constant. Loading and reversion stresses vary in the same manner with temperature.

6. *Parametric Models of SMM Behavior [43,79]*

Parametric models of the constitutive behavior of SMMs are important both for development of finite element modeling capability as well as for engineering design.

7. *Temperature Control Related Properties [58]*

Temperature control of SMMs can be easily accomplished through resistive heating; properties related to temperature control (electrical resistivity, thermal conductivity, specific heat) are all available for NiTi [58] and from commercial materials suppliers.

8. *Engineering Applications [153]*

Information and an extensive bibliography on general applications of SMMs is given [29]. There is very little written on the subject of structural damping with either SME or the SEE [153].

9. *Thermomechanical Processing [31,52]*

Properties of NiTi can be significantly enhanced and altered through appropriate thermomechanical processing.

3.2.3.3 Materials Testing Results

As stated above, the objective of the testing program was to experimentally verify the important characteristics of the superelastic hysteresis of NiTi in tension. As summarized in Table 3.1, the test program consisted of more than 20 tests that evaluated the effects of temperature, strain-rate or frequency, and thermomechanical processing. Tests 6A, 6B, 6C, and 6D demonstrated the response of a device composed of successively engaging NiTi loops to provide successive stages of softening and hardening. The results of the materials testing program are discussed below in terms of the implications to the design of structural dampers.

1. *Hysteretic Energy Dissipation*

The results of Test 4C (Figure 3.8) demonstrate the high level of energy dissipation available with superelastic hysteresis: more than 2500 in-lb/cubic inch in its elastic range at strains less than 10%.

2. *Hardening at Large Strains*

Another useful characteristic of superelastic NiTi is that it hardens after its

conversion to stress-induced martensite. For the NiTi sample in Test 4C, this effect occurred at approximately 9.5% strain. In Test 4C, strains of up to 10% were recovered; the residual strain of 2% was a result of the preconditioning work treatment of the alloy.

3. *Thermomechanical Processing*

The influence of thermomechanical processing on the hysteretic response of a NiTi alloy can be seen by comparing the results of Test 2A (Figure 3.9) and Test 4C (Figure 3.8). The process for producing the sample for Test 2A was designed to increase the yield, or load stress level, of the alloy. Tests 2A and 4C were conducted at approximately the same temperature. Although the area of the hysteresis loops is similar for both tests, the loading and reversion stresses clearly are influenced by the thermomechanical processes used to produce the alloy.

4. *Temperature Effects*

Figure 3.7 illustrates the effects of temperature on superelastic hysteresis: an increase in temperature above the superelastic temperature range (A_f - M_d as shown in Figure 3.4) produces an increase in both the yield and reversion stresses as well as a reduction in the area of the hysteresis loop. It should be noted that the increase in the yield stress can be useful both for active control purposes and as a complementary effect to viscoelastic behavior in passive composite damping devices and that the total energy dissipated per cycle over a significant range of temperatures remains large.

5. *Use of Prestressed Superelastic Material*

One option for the construction of NiTi structural damping devices is to use superelastic components prestressed to operate about the midpoint of their hysteresis. The results of Test 5A presented in (Figure 3.1) show the rhomboidal hysteretic response that results from cycling a prestressed superelastic NiTi alloy in both directions about a midpoint strain of approximately 4%.

6. *Progressive Engagement*

Test 6A (Figure 3.10) demonstrates the response of a damping device composed of progressively engaged or staged NiTi superelastic elements. The test sample consisted of two groups of NiTi wire loops: the first group of wires was fully engaged over the entire strain range; the second group of wires engaged at 2% strain in the first group of wires. The resulting hysteresis is the sum of the hystereses of the two wire groups; the mechanism of staged

engagement provides a useful means of controlling the force-deformation hysteresis of a passive damping device.

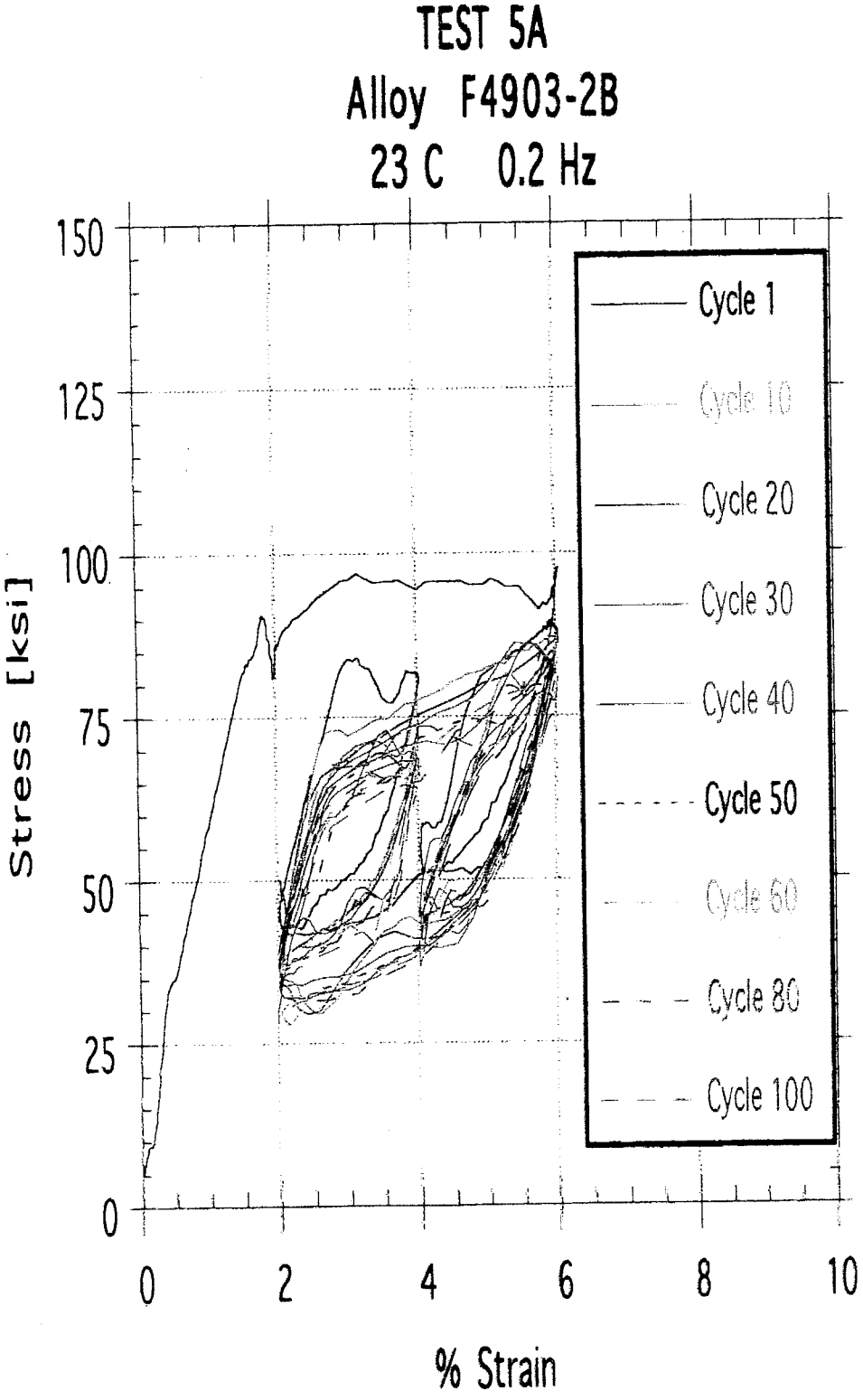

Figure 3.1 Hysteretic Response: Test 5A

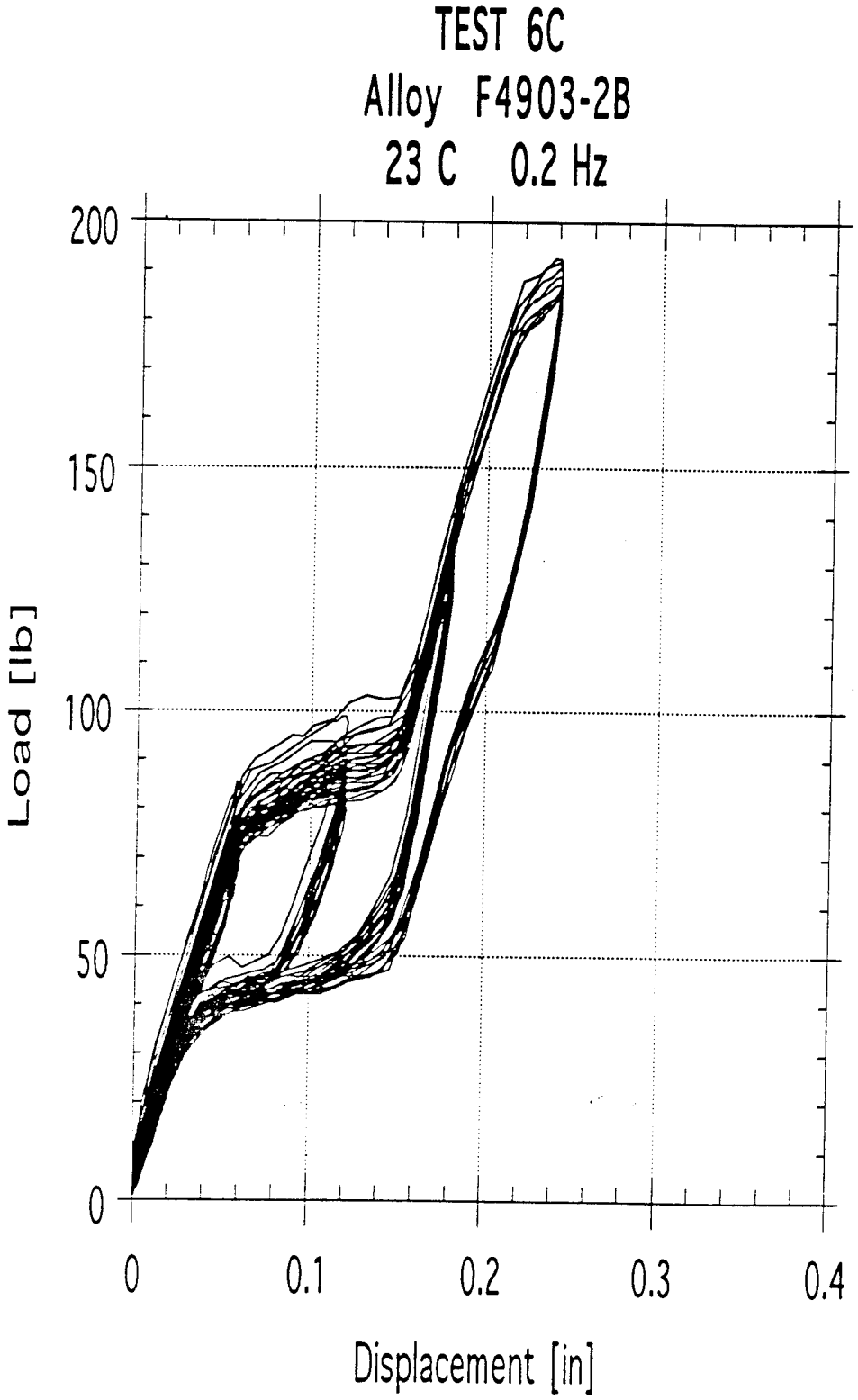

Figure 3.2 Hysteretic Response: Test 6C

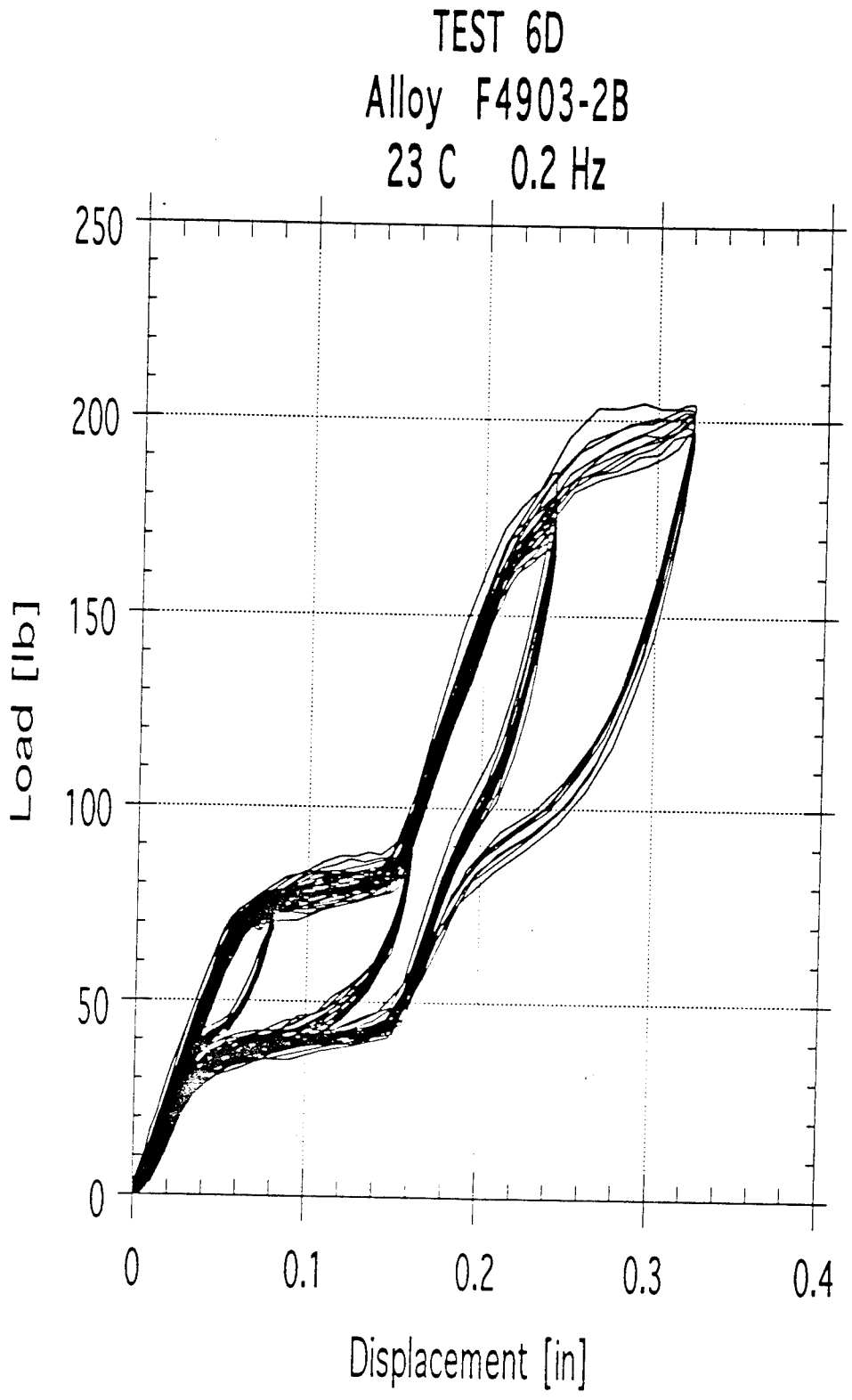

Figure 3.3 Hysteretic Response: Test 6D

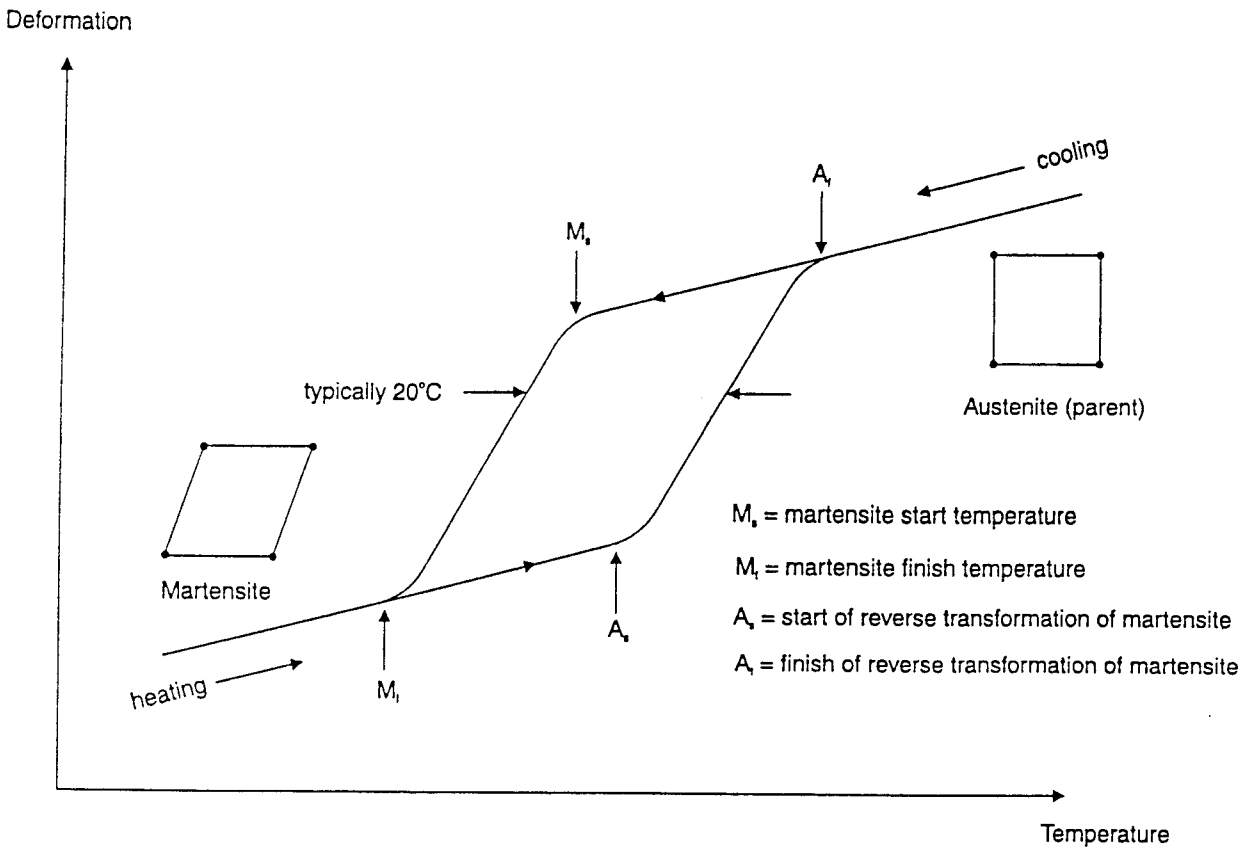

Figure 3.4 SMA Deformation-Temperature Relationship

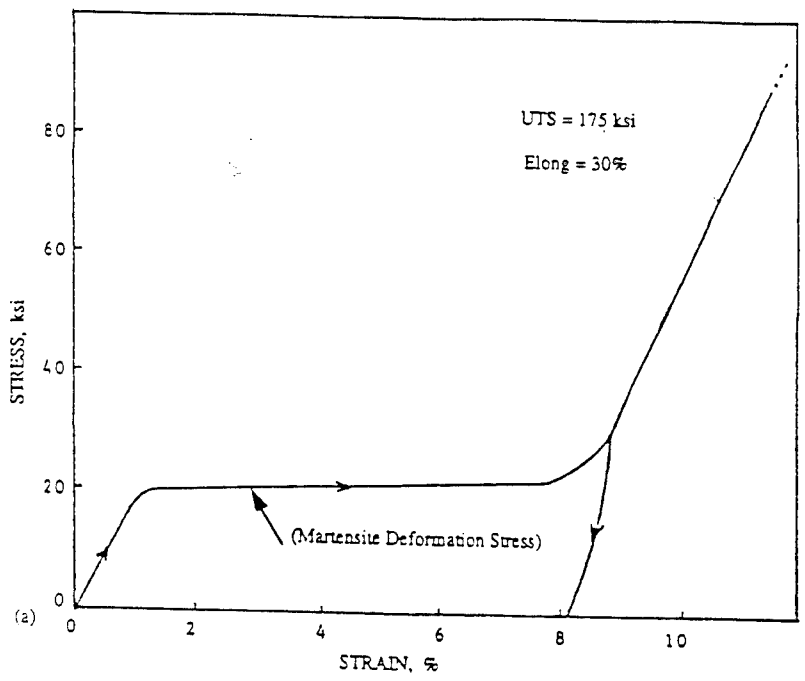

Figure 3.5 Shape Memory Hysteresis

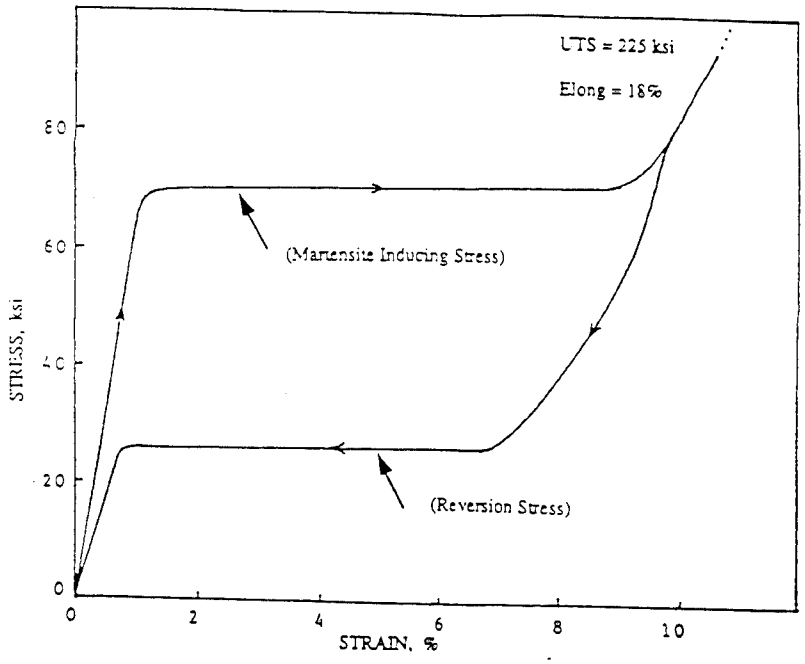

Figure 3.6 Superelastic Hysteresis

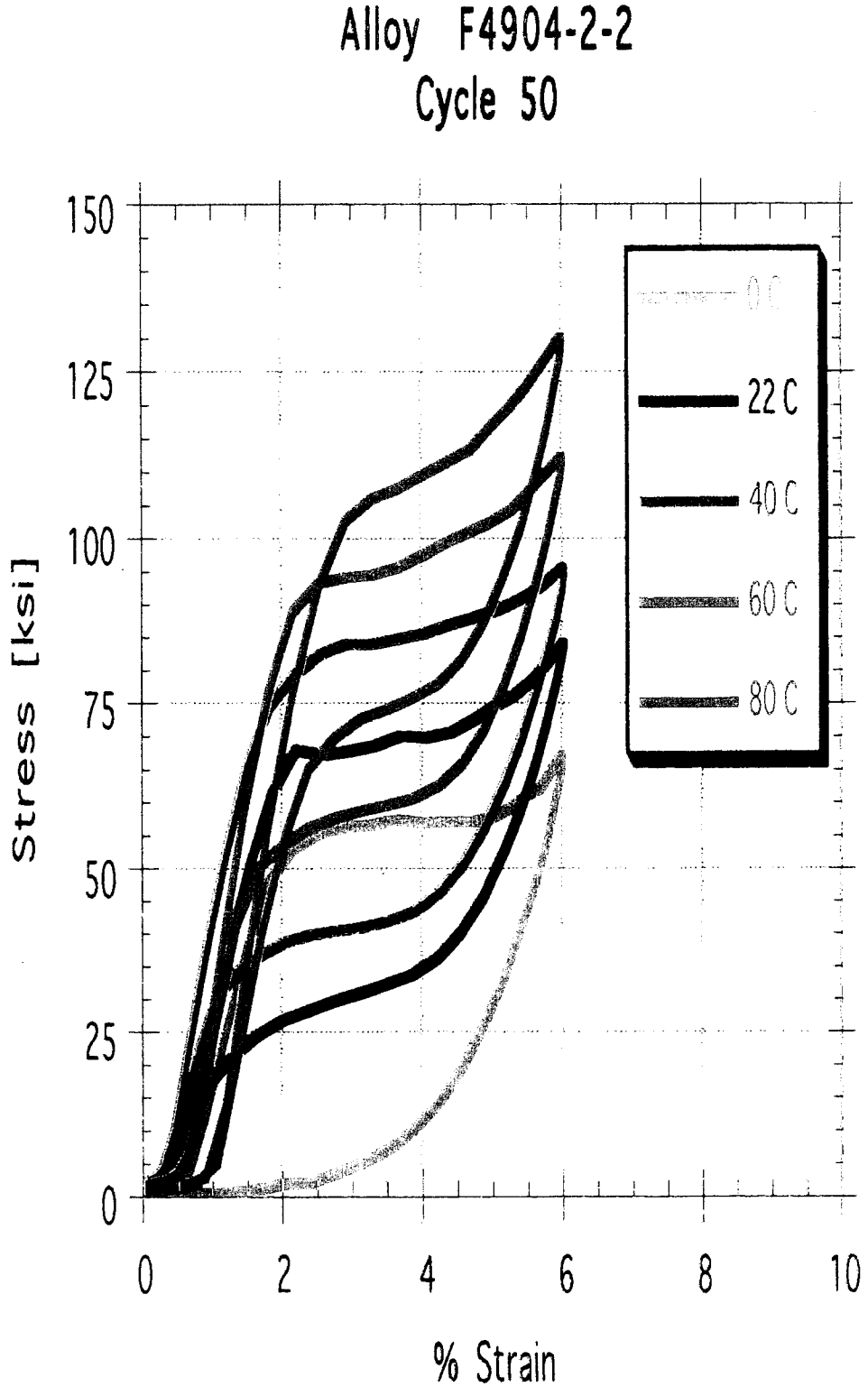

Figure 3.7 Temperature Dependence of SMA Hysteretic Response

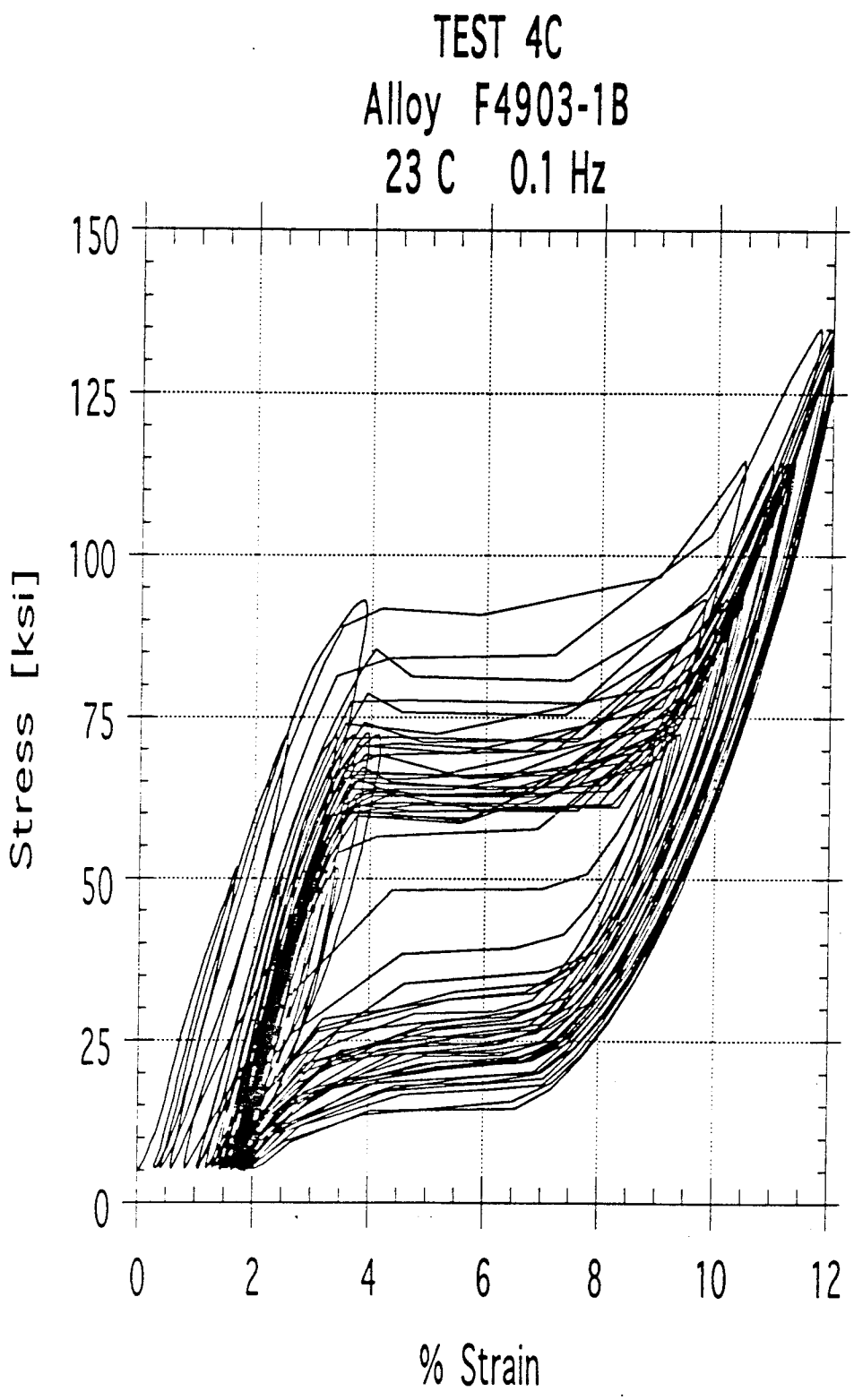

Figure 3.8 Hysteretic Response: Test 4C

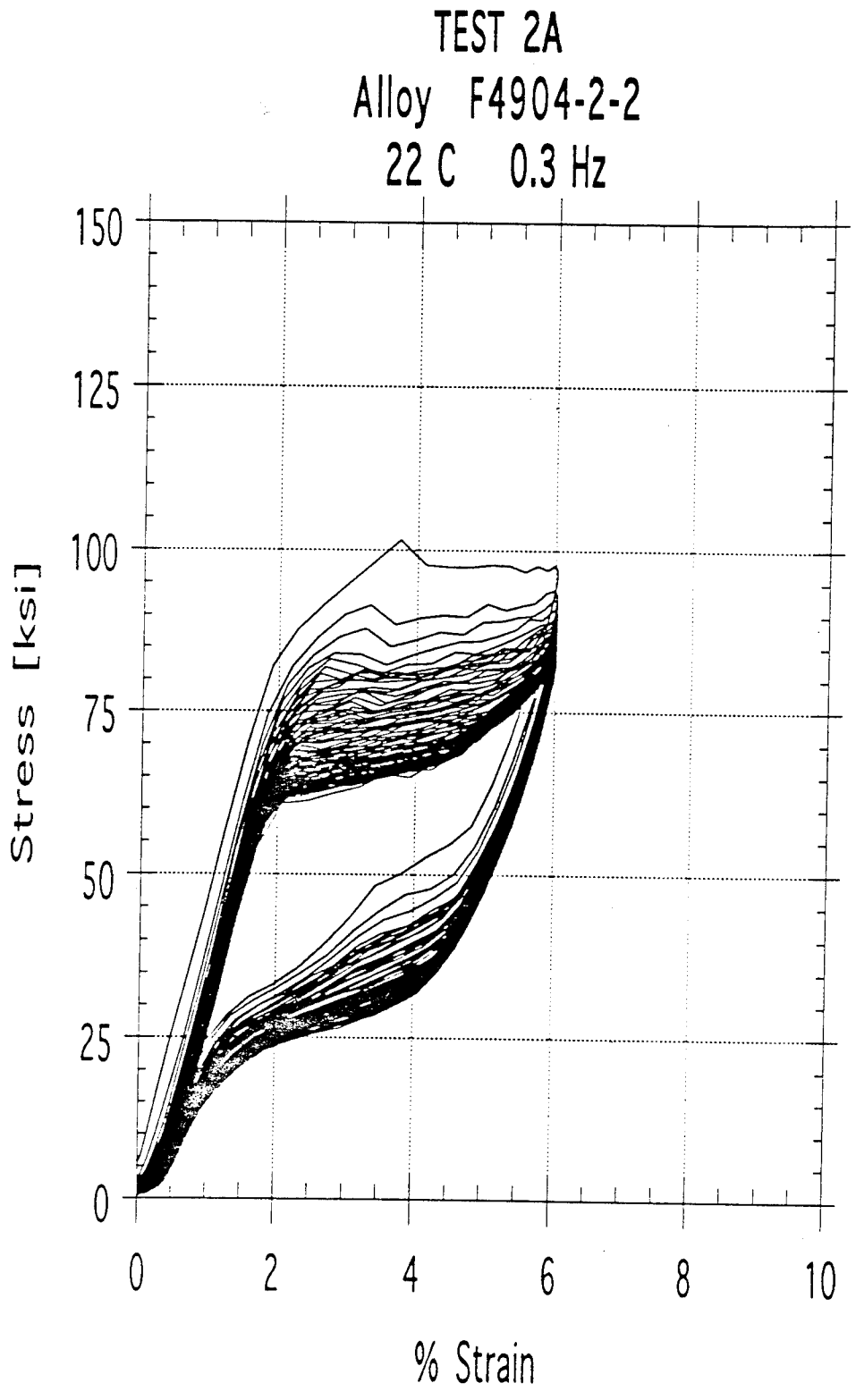

Figure 3.9 Hysteretic Response: Test 2A

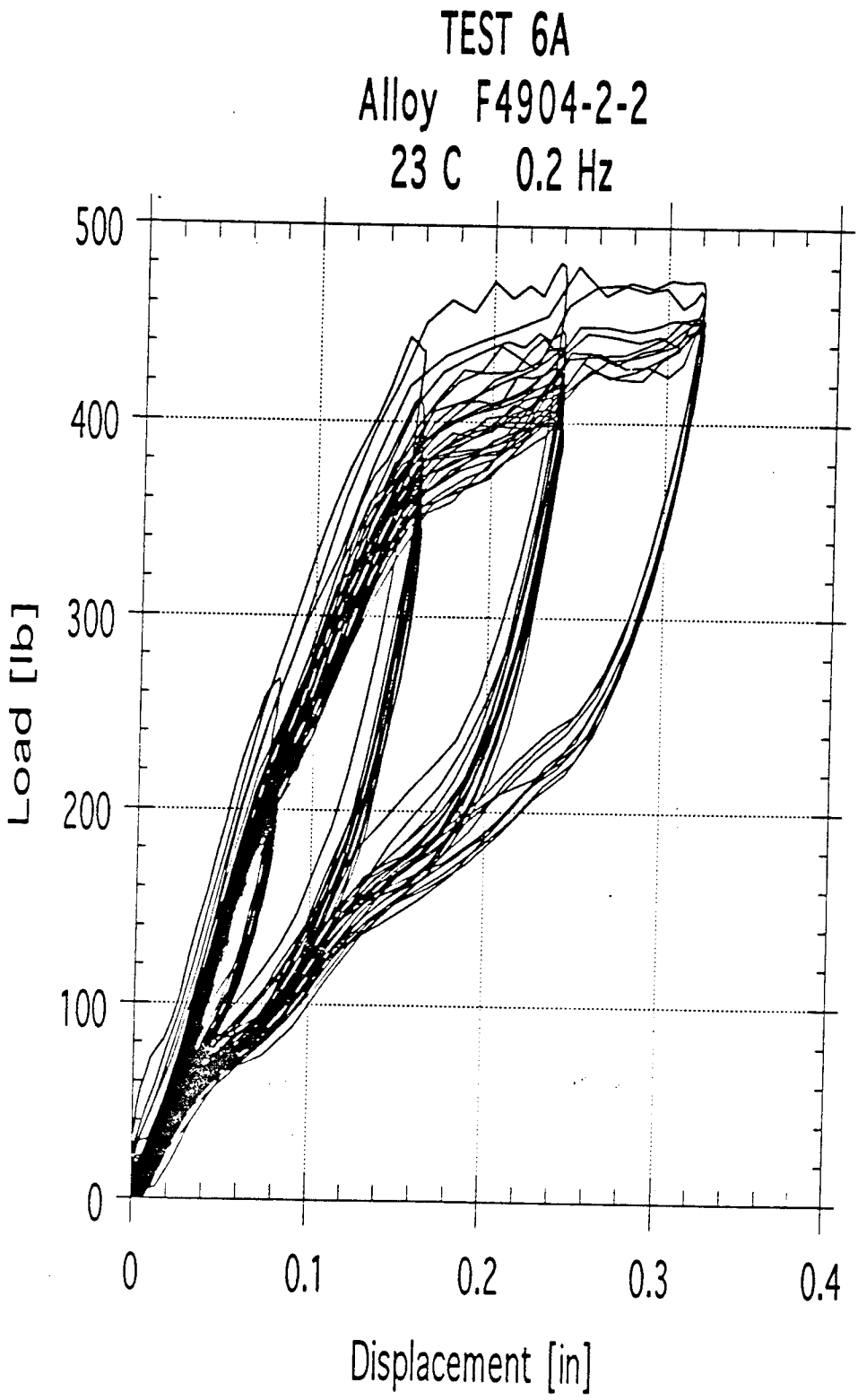

Figure 3.10 Hysteretic Response: Test 6A

4.0 SMA DEVICE DEVELOPMENT

4.1 Objectives and Scope

The objective of this component of the Phase I program is the characterization of both passive and active SMA vibration control device technology. The scope of the device technology considered herein is limited to devices incorporating commercially available SMA materials. Despite their considerable potential for active control applications, structural damping devices based on the R-phase transition behavior of SMAs are not discussed further.

4.2 Approach and Method

Device types, both passive and active, are generally characterized by force-deformation response (hysteretic shape) and stability of the hysteresis loops. This information is presented in the following section. The development of passive SMA structural dampers is presented in Section 4.4, and basic actuation mechanisms for active devices are briefly described in Section 4.5. A prototype device constructed to demonstrate both passive and active damping control is described in Section 4.6. Although configured as a passive damper, this device can be configured to provide active control through electrical actuation of the NiTi.

4.3 Hysteretic Shapes

Shape-memory effect (SME) and superelastic effect (SEE) hystereses can be used for the design of linkage, joint, constrained layer, and mass damping devices to obtain a variety of hystereses. Figure 4.1 shows several of the force-deformation responses (hystereses) that can be achieved with SMA devices exploiting different kinematic mechanisms.

For example, the rectangular hysteresis shown schematically in Figure 4.1c is produced by exploiting pre-stressed superelastic SMM. Figure 4.2 illustrates the loading cycle of a simple spring element displaying rectangular hysteresis. Upward motion of the crossbar (C) in Figure 4.2 is assisted by spring A as shown in the schematic stress/strain diagram. Concurrently, this motion is resisted by spring B. Downward motion is entirely symmetric with the role of the two springs reversed. Thus, the effect of these two prestressed superelastic elements working in opposition to one another is to provide a constant resisting force which is the difference in their respective loading and reversion force levels. Operationally, this schematic device provides a constant resistance force damping element with approximately zero (static) stiffness.

Figure 4.3 provides a schematic representation of a mechanism which produces the triangular flag hysteresis shown in Figure 4.1b. Figure 4.3a shows a prestressed wire W spanning between fixed supports. The displacement of the wire from its initial position at A to B is resisted at a stress SI, that is, the stress at which the phase transformation is induced. Upon reversal of the motion, the wire assists the motion at a stress Sr, the stress at which reversion to parent phase occurs. Thus the device applies both a constant resisting and a constant assisting force over the full range of motion. The triangular force-deformation response shown in Figure 4.3c is the hysteresis that results from the deformation of this device.

The bowtie hysteresis (Figure 4.1b) can be achieved as the sum of two triangular hystereses, that is, through the use of two devices.

The force and deformation capacities for all of the hysteretic shapes shown in Figure 4.1 are essentially unlimited. Higher force levels can be achieved by the addition of more SMA material. Large deformation can be accommodated in relatively compact SMA devices due to the large strain range of the transformation plateau over which stress remains approximately constant.

4.4 Passive Device Technology

4.4.1 General

A suite of passive damping devices spanning all major device categories including truss link, joint, constrained layer, mass damping, and shear link types have been developed. Schematic designs for two device types, all based on simple NiTi wire or tubular components, are presented below:

1. Truss Link Device (TLD)

2. Truss Joint Device (TJD)

Each of these devices can display several types of force-deflection hysteresis, depending on the phase state of the NiTi alloy: including the rectangular flag and rectangular hysteresis (Figure 4.1c). For the purposes of this discussion, the devices are assumed to be configured to produce the pure rectangular force-deformation response. On the basis of the material testing results presented both in Chapter 3 for NiTi wire, and in the literature for other SMAs, the stability and fatigue characteristics of these devices should be excellent.

4.4.2 Truss Link Device (TLD)

Figure 4.4 shows a longitudinal section of a truss link device. The device is comprised

of a tubular element sliding within another tubular element. The other tube is slotted to permit the insertion of a pin fixed to the inner tube and sliding in the slot. NiTi wire loop elements connect this sliding pin to two pins fixed in the outer tube as shown.

For the SMA TLD, there is a constant axial resistance in the device in both extension and compression. This results in the pure rectangular hysteresis. The device can be designed to protect against excessive deflection by exploiting the material stiffening which occurs in NiTi at strains in excess of 10%. At strains exceeding 10%, the NiTi device will stiffen and recover excess strain elastically.

4.4.3 Truss Joint Device (TJD)

Figure 4.5 shows a section view of a schematic truss joint damping element. This device is composed of a simple bolted connection: the bolt is surrounded by two NiTi annular rings or washers. For this device, the mode of action provides a rectangular flag-shaped force-deformation hysteresis in any direction. This action is the result of the unprestressed superelastic element resisting initially in an elastic manner. At levels of force sufficient to stress-induce martensitic yield, the device will yield and dissipate energy as it cycles through the superelastic hysteresis.

4.5 Active Device Technology

The material characteristics of SMAs offer a variety of means by which to actively control structural response to dynamic excitation including:

1. direct actuation based on the shape-memory effect,

2. modulation of friction based on the shape-memory effect, and

3. modulation of stiffness through control of the yield plateau of a superelastic alloy by manipulating the temperature of the SMA.

Schematic models illustrating each of these approaches are presented below.

4.5.1 Direct Actuation

Schematic models for a variety of SME-actuated devices providing added stiffness and/or supplemental damping were outlined above. However, for civil engineering applications, the most promising device types are those described in Sections 4.5.2 and 4.5.3. Although the problem of heat transfer, both in and out of the alloy, can be mitigated using parallel SMA elements and counter-acting elements, it is preferable to use SMAs to modulate other damping and stiffening mechanisms (as will be described).

Figure 4.6 illustrates schematically a direct actuation device developed and tested by the research team. This device produces linear motion by peristaltic action. A piston (P) is driven along a tube by the constriction of the tube created by heating, in the proper sequence, rings of SME material. As a ring on one side of the tapered piston is heated above its TTR, it contracts, thus driving the piston along the tube. The force from the driving ring is sufficient to both move the opposing load and deform (and thus reset) the SME rings in its path. This device can provide both supplemental damping and added stiffness.

4.5.2 Modulation of Friction

Figure 4.7 illustrates schematically a device which uses the shape-memory effect to provide a high-force actuator with very good dynamic response (on the order of 0.1 second). In this device, a four-bar mechanism is actuated by opposing pairs of SME wires. Actuation of the horizontal wires, that is, heating the wires through their TTR, provides work along the vertical axis. Correspondingly, actuation of the vertical wires provides work along the horizontal axis. The force provided by a wire set must be sufficient to both overcome the applied load and to reset the opposing wires.

To achieve reasonable response times requires the use of multiple wires and a switching mechanism, which switches the electrical power used to resistively heat the wires.

Response time can also be minimized by using this device to modulate a friction damper. This approach uses very small amounts of SMA material and thus permits acceptable heating and, more importantly, cooling times. By modulating the normal force of a conventional friction device, this approach can provide a fast stiffness and damping control capability.

4.5.3 Stiffness Control Through Temperature Modulation of SEE

In Chapter 2, a distinction was made between the shape-memory effect and the superelastic effect. Both effects are in fact based on the same phase transformation and represent two related stress/strain/temperature behaviors in a complete phase space.

Below an SMA's transformation temperature range (TTR), the system is fully martensitic and only the shape-memory effect is observed. Above the TTR, the superelastic effects are possible because sufficient stress can be applied to overcome the thermomechanically stable form of the alloy, that is, to stress-induce martensite. The stress required to induce martensite increases with increasing temperature. The stress increase over the TTR is given by a Clausius-Clopeyron relationship. The temperature sensitivity of the SEE alloy is moderate, and full superelastic behavior can be obtained over a useful temperature range for several SMAs. For passive damping

devices, this means that consistent damping levels are possible over a wide temperature range.

For active control, temperature dependence of NiTi yields many potential applications because it is possible to control the yield force of a structural component containing an SEE element by controlling the temperature of the NiTi. Increasing the temperature of the NiTi will increase its relative stiffness. Such a device would provide constant damping and variable stiffness. The demonstration device developed for the Phase I research effort can be controlled actively to provide variable axial stiffness (a concept already implemented by Kajima Corporation in Tokyo, Japan). This device will be tested as part of the Phase II program.

4.6 Construction of a Passive/Active SMA Device

Figure 4.8 is a photograph of the device configured with NiTi wire to act as a passive energy dissipator. With the SMA wires configured as shown, the device acts as a passive damper providing bowtie hysteresis (Figure 4.1b). The behavior of the device has been confirmed by simple test procedures; comprehensive testing of this device will form part of the Phase II research effort.

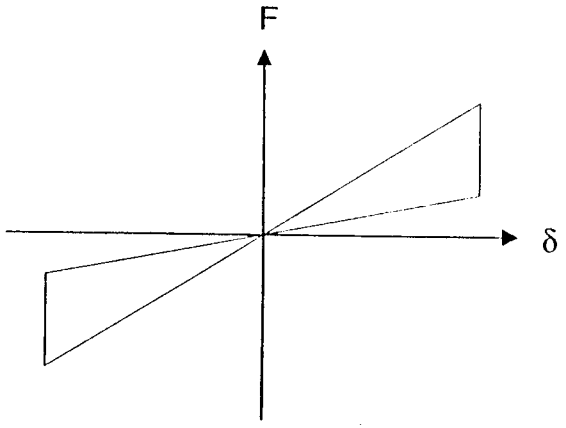

(a) Triangular Flag

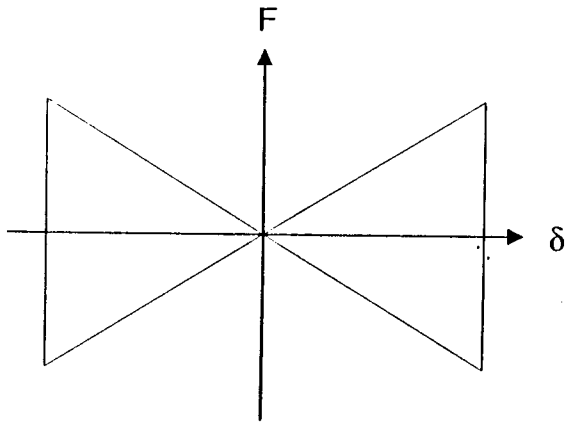

(b) Triangular Bowtie

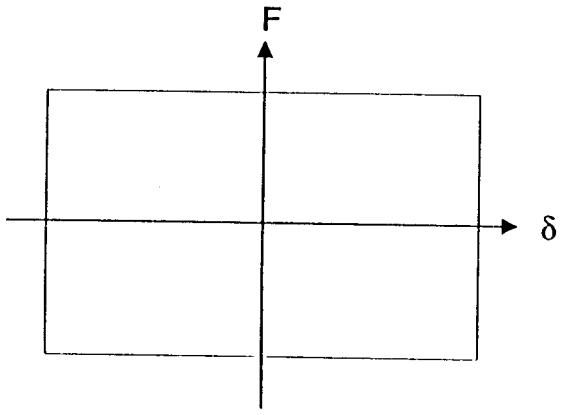

(c) Rectangular

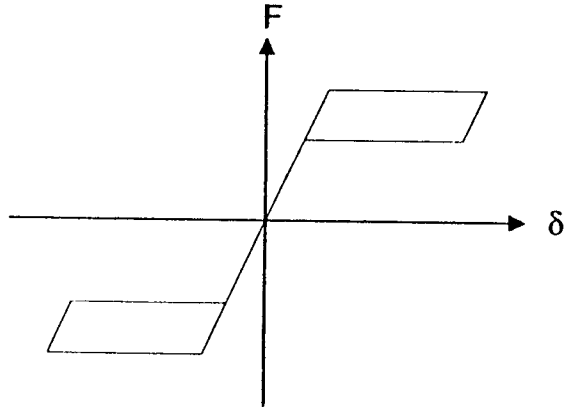

(d) Rectangular Flag

Figure 4.1 SMA Hysteresis Types

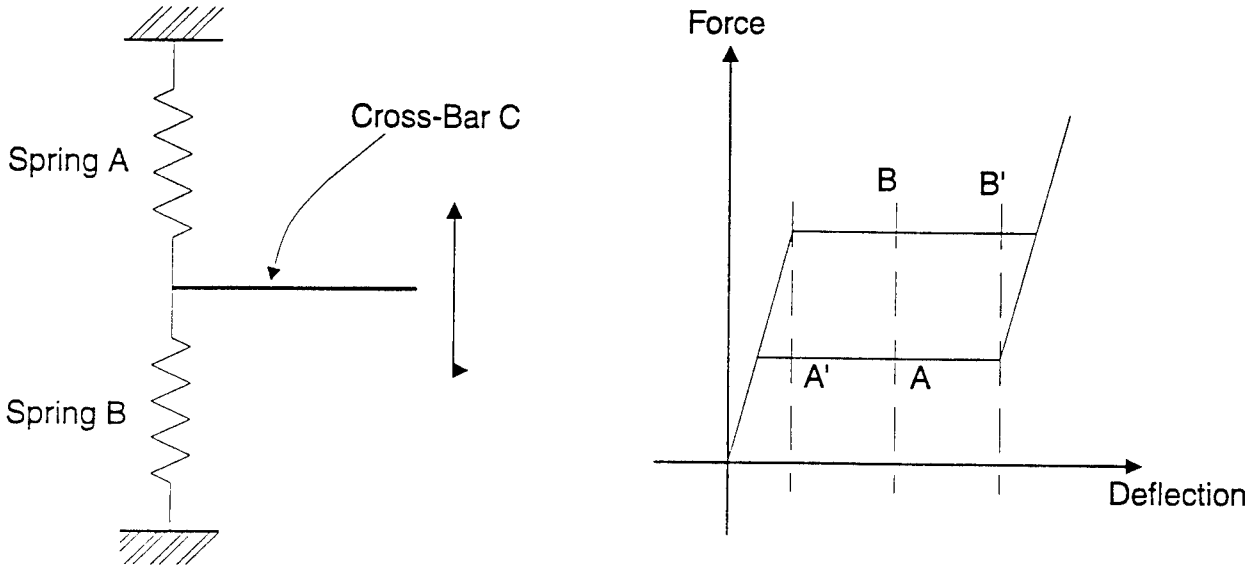

(a) Device Schematic

(b) Device Hysteresis

Figure 4.2 Rectangular SMA Hysteresis

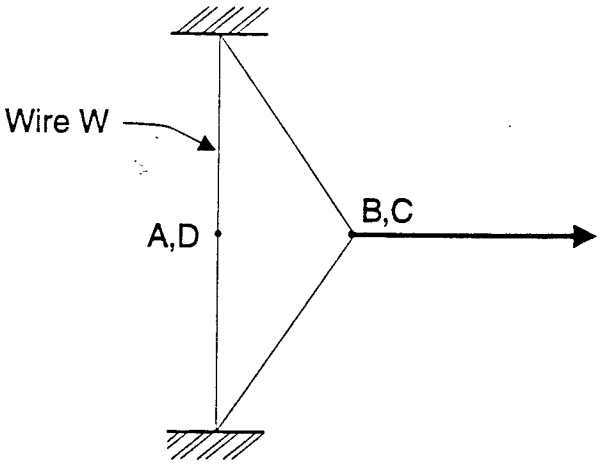

(a) Device Schematic

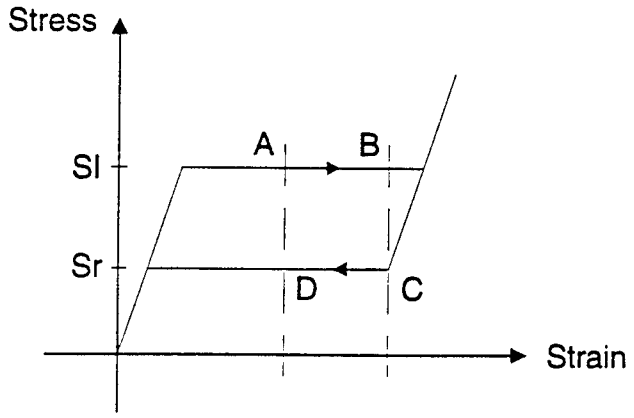

(b) Stress-Strain Response of NiTi Wire

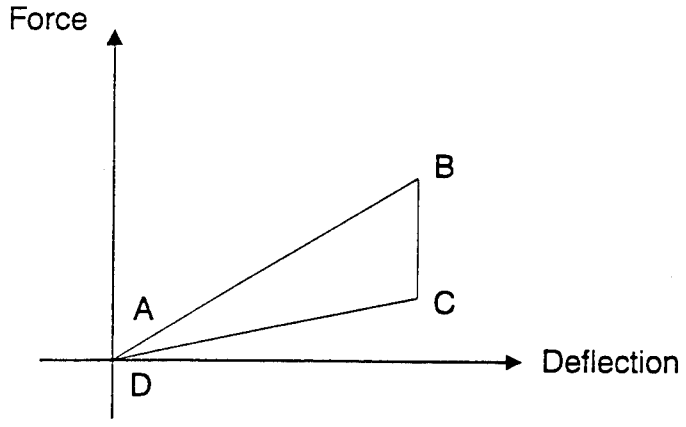

(c) Device Hysteresis

Figure 4.3 Triangular Flag Hysteresis

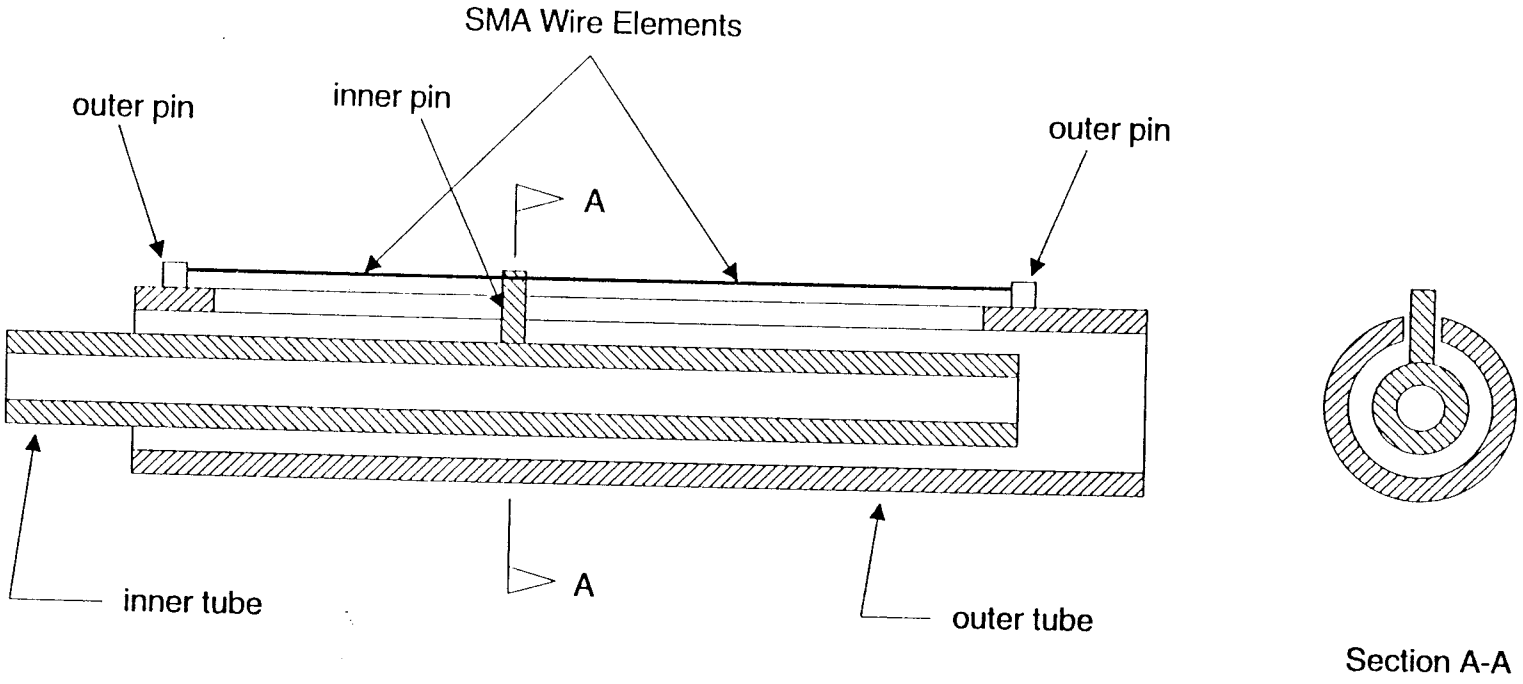

Figure 4.4 SMA Truss Link Device

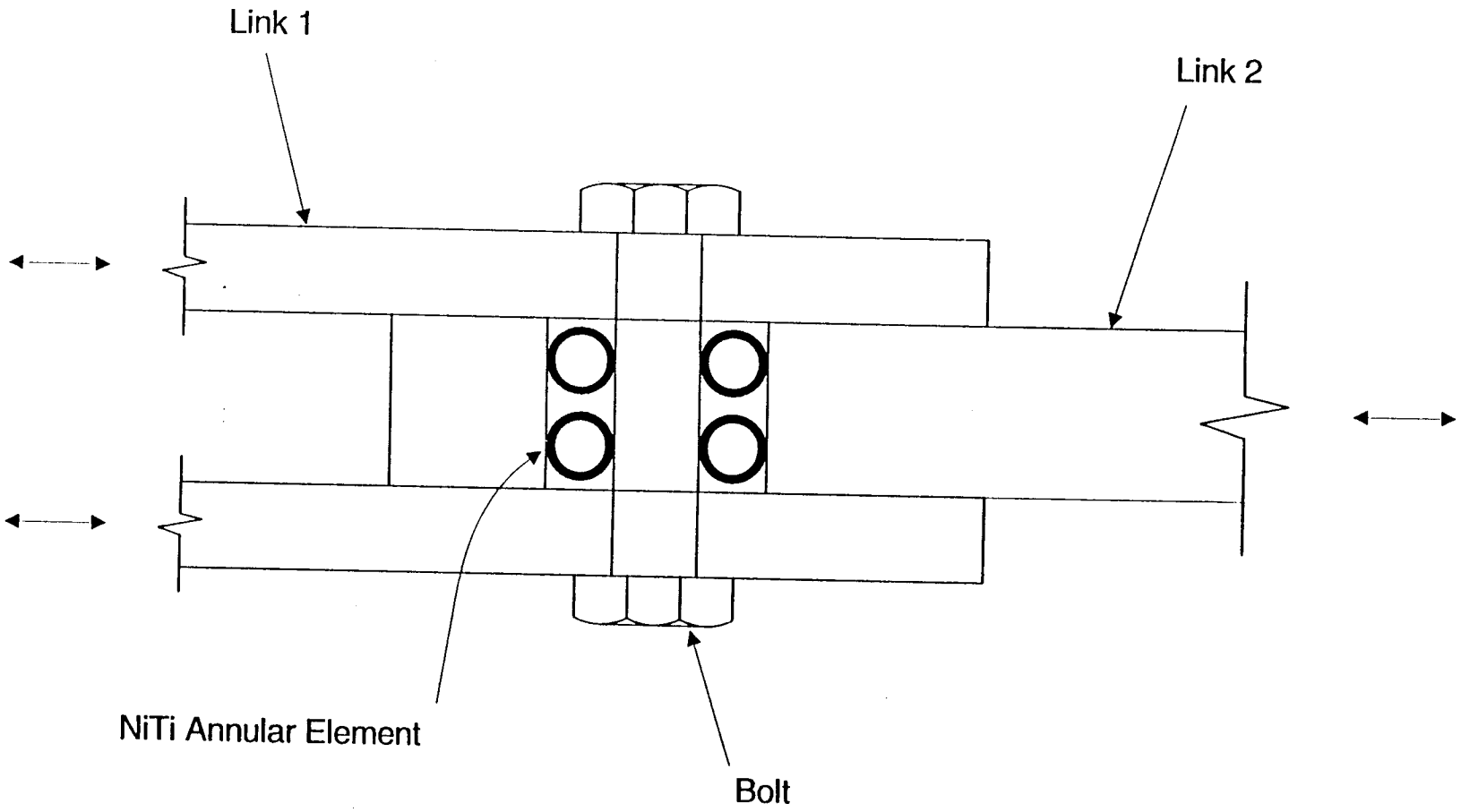

Figure 4.5 SMA Truss Joint Device

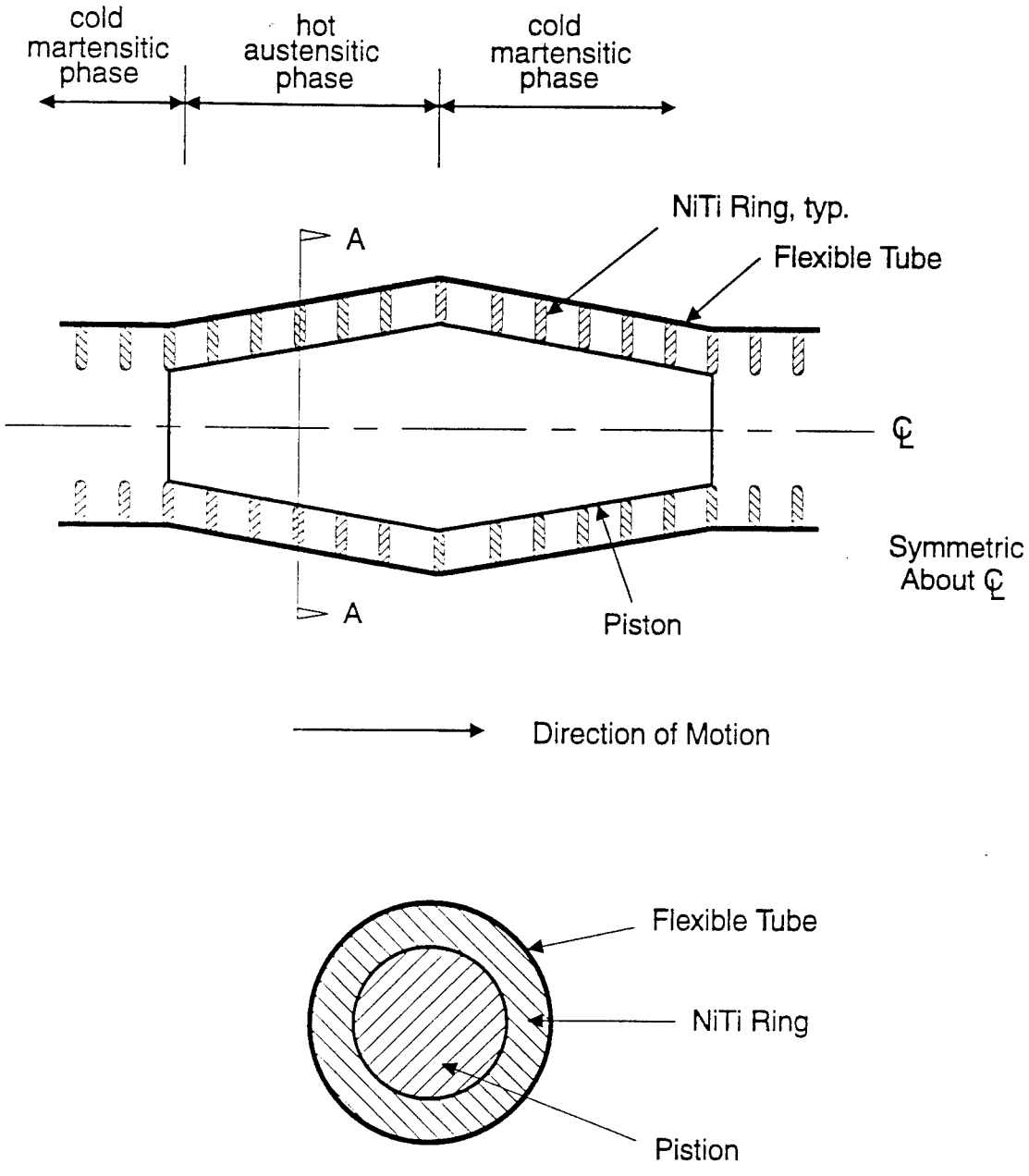

Figure 4.6 SMA Direct Actuation Device

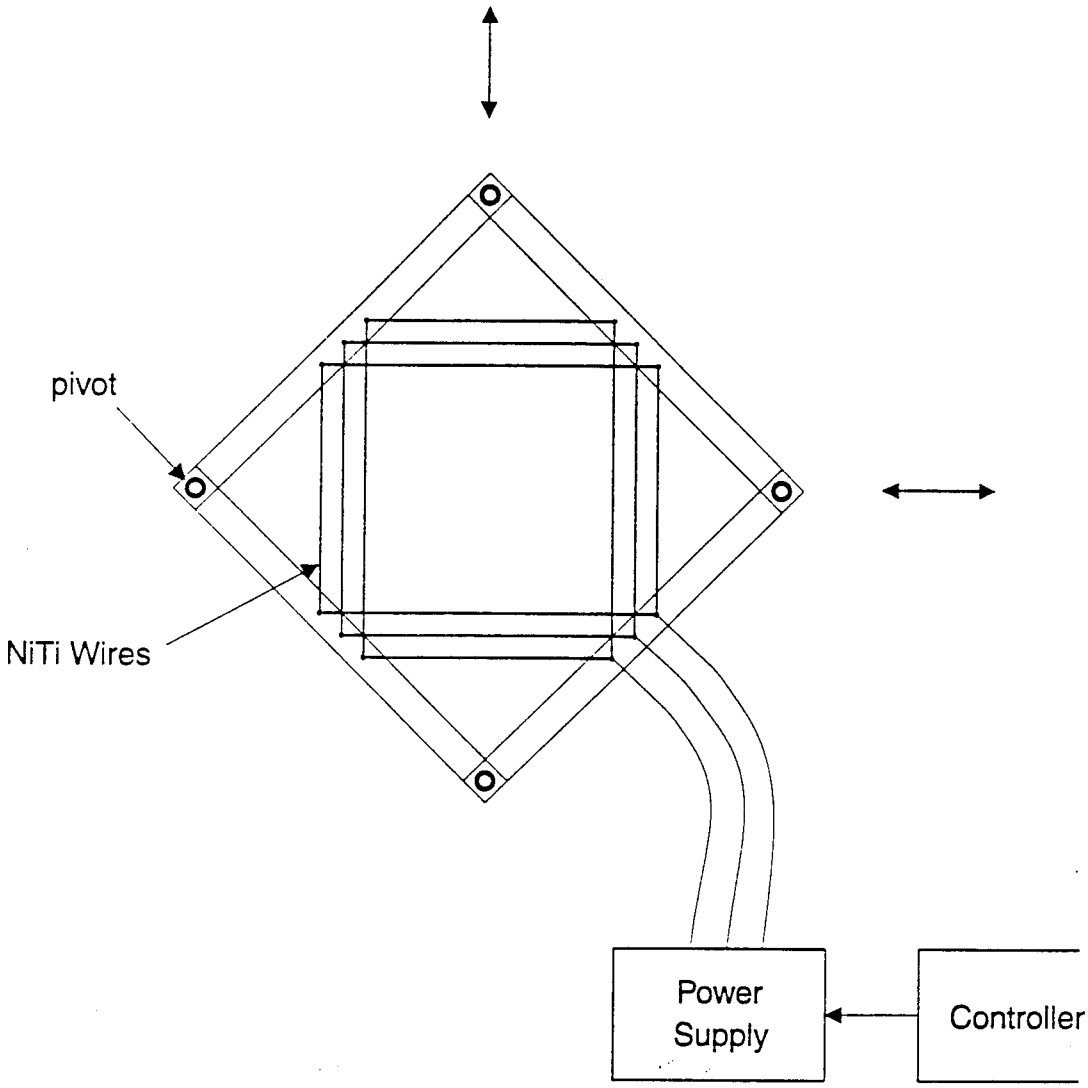

Figure 4.7 SMA Friction Modulation Device

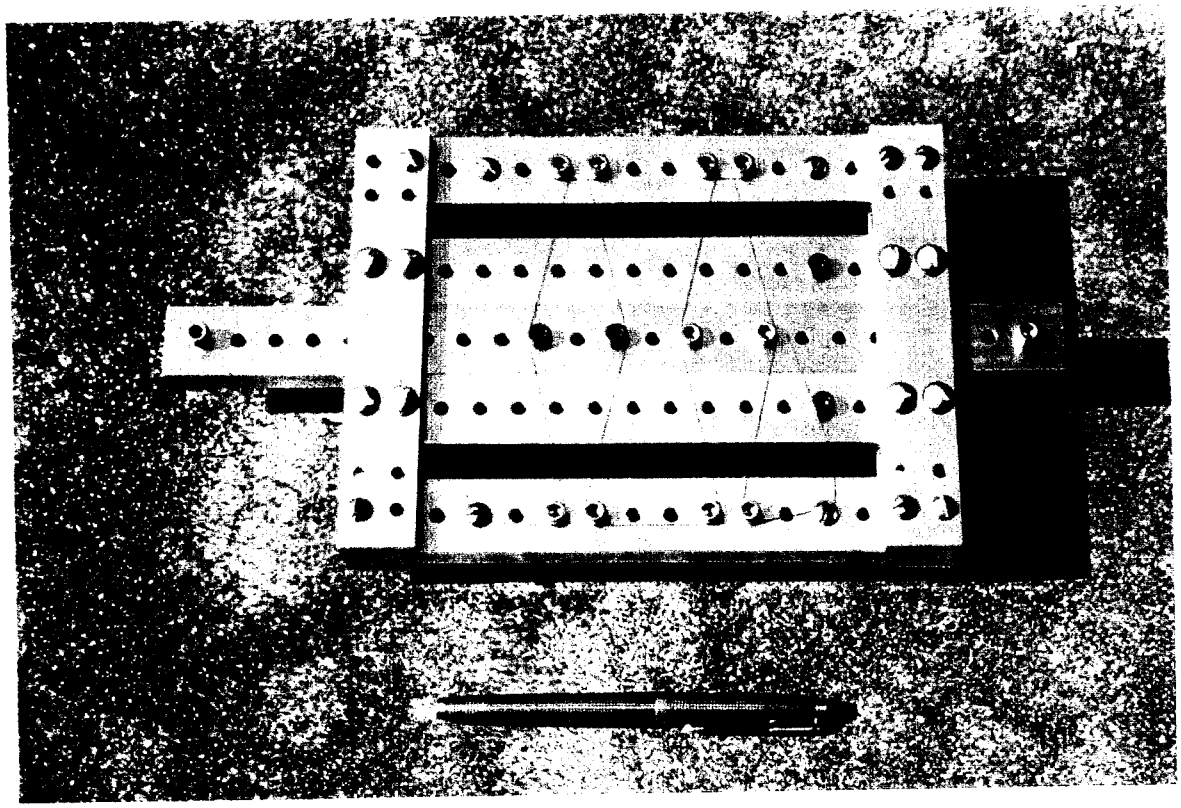

Figure 4.8 Demonstration Device Photograph

5.0 ENERGY DISSIPATION DEVICES FOR SEISMIC RETROFIT

5.1 Objectives of the Case Study

In order to demonstrate that upgrading non-ductile concrete frames with hysteretic energy dissipators is viable, a sample building was selected by USACERL from the U.S. Army's inventory of pre-1970 concrete frame buildings. The building chosen is sited in Fort Lewis, Washington, and is representative of many of the older buildings owned and maintained by the U.S. Army.

It is not the objective of this case study to develop seismic retrofit details for the building, but rather to demonstrate that the use of passive, active, or semi-active shape-memory alloy (SMA) energy dissipators results in significant improvements in the seismic response of buildings and structures considered inadequate by current seismic standards [UBC, 1991]. As such, limited attention is paid to the cyclic response of the non-ductile elements at the local level. Rather, attention is focussed on global improvements in structural response that can be achieved with hysteretic energy dissipators.

5.2 Earthquake Ground Motion Description

The seismic response of the sample building (hereafter known as the building) was evaluated using nonlinear time-history analysis and recorded earthquake acceleration records.

The nonlinear computer program used for the analysis work was DRAIN-2DX. A description of DRAIN-2DX is provided in the following section.

Three recorded acceleration time-history records were used to study the response of the building:

Caleta de Campos
The Caleta de Campos records were recovered following the September 19, 1985, Michoacan subduction zone earthquake in Mexico. The recording site was approximately 21 km (13 miles) from the epicenter of the M_L 8.1 event. Two orthogonal components of horizontal acceleration were recorded: 000 and 090. The 000 component had peak maximum and minimum accelerations of +0.141g and -0.130g, respectively. The 090 component had peak maximum and minimum accelerations of +0.140g and -0.100g, respectively. The 000 component was chosen for the analysis of the building. The 5% damped acceleration response spectrum of this component is presented in Figure 5.01; the corresponding Fourier spectrum is

presented in Figure 5.02.

Joshua Tree Fire Station
The Joshua Tree Fire Station is situated on the backward azimuth, 9 km (6 miles) from the epicenter of the M_L 7.6 Landers earthquake of June 28, 1992. The faulting mechanism for the Landers event was predominately strike-slip. Two orthogonal components of horizontal acceleration were recorded: 090 and 360. The 090 component had peak maximum and minimum accelerations of +0.273g and -0.176g, respectively. The 360 component had peak maximum and minimum accelerations of +0.284g and -0.255g, respectively. The 360 component was chosen for the analysis of the building. The 5% damped acceleration response spectrum of this component is presented in Figure 5.03; the corresponding Fourier spectrum is presented in Figure 5.04.

Desert Hot Springs
The Desert Hot Springs earthquake records were recovered after the M_L 5.9 Palm Springs earthquake of July 8, 1986. The recording station was situated 12 km (8 miles) from the epicenter. Two orthogonal components of horizontal acceleration were recorded: 000 and 090. The 000 component had peak maximum and minimum accelerations of +0.300g and -0.286g, respectively. The 090 component had peak maximum and minimum accelerations of +0.269g and -0.247g, respectively. The 000 component was chosen for the analysis of the building. The 5% damped acceleration response spectrum of this component is presented in Figure 5.05; the corresponding Fourier spectrum is presented in Figure 5.06.

These three earthquake records are representative of moderate earthquake shaking resulting from two different source mechanisms. Although these two mechanisms may not be representative of intra-plate events on, for instance, the New Madrid fault, the absence of such U.S. records prevented the inclusion of an intra-plate ground motion in the suite of time-histories used for the analysis of the building.

5.3 Nonlinear Analysis Using DRAIN-2DX

The computer program DRAIN-2DX [Prakash, 1992] was developed for the nonlinear analysis of buildings and other two-dimensional structures. It consists of a main program that controls the analysis and manages data and data transfer, and a series of subroutines for the different element types.

The element types currently available in DRAIN-2DX are: truss bar; beam-column; zero-length connection; gap; and rectangular panel. The rectangular panel element is an elastic element; the other four are nonlinear elements.

A stiffness-degrading model, for example the Takeda model, is more suitable to the modeling of non-ductile concrete than the beam-column element. However, a stiffness -degrading model has not yet been implemented in DRAIN-2DX. As noted in Section 5.5, the beam-column (Type 2) element was used for the analysis of the existing building frame.

DRAIN-2DX can be used to undertake nonlinear static and dynamic analysis. Possible forms of dynamic excitation include in-phase ground acceleration, out-of-phase support displacement excitation, nodal dynamic loading, and nodal velocity loading (to simulate impulse loading). Modal analysis and response spectrum analysis can also be undertaken with DRAIN-2DX. For this study, the following analysis options were used: static gravity analysis, modal analysis, static load-to-collapse analysis, and nonlinear time-history analysis.

5.4 Building Description

The sample building, a three-story, non-ductile concrete structure with a partial basement, was designed in 1956. The building's footprint is similar to the letter **H**, with a gross floor area of approximately 51,400 sq. ft. The **H**-shape is articulated into three separate buildings (wings) by two 2"-wide expansion joints.

The gravity load-resisting system in the building is typically composed of 7-inch reinforced concrete flat plates with shearheads, 18-inch-deep perimeter beams, and reinforced concrete columns.

Wind and seismic lateral loads are resisted by reinforced concrete, structural walls, and reinforced concrete, non-ductile, moment frames.

The structure was designed in accordance with the Pacific Coast Uniform Building Code and the ACI Building Code. The design live, wind, and seismic loads specified by the engineers of record, Miller & Ahlson of Seattle, Washington, were:

- live loads: 40psf to 60psf typical; 100psf for stairs
- wind loads: 20psf on the projected area
- seismic loads: Seismic Zone 3 (1956)

The typical column and beam rebar ratios are approximately 1% and 1.25%, respectively, and are substantially less than normal practice in the 1980s and 1990s. Shear reinforcement is typically #3 ties @ 12 inches on center in both the columns and the beams. Shear reinforcement is not provided in the beam-column joints.

5.5 Seismic Deficiencies of the Existing Building

The detailing of the concrete elements in the building is consistent with normative engineering practice in the 1950s but is inadequate by current standards. The seismic deficiencies in the existing building include:

- no beam-column joint reinforcement
- minimal or non-existent splices in column and beam reinforcement
- insufficient beam and slab rebar anchorage in perimeter columns and beams

In a moderate or severe seismic event, these shortcomings will prevent the formation of ductile plastic hinges in the beams and may result in the bottom rebar in the beams pulling out of the beam-column joint as a result of bond failure; buckling of the beam rebar adjacent to the column face due to insufficient lateral restraint; shear fracture of the beam-column joint; or the partial collapse of the building.

5.6 Dynamic Analysis of the Existing Building

In order to satisfy the objectives stated in Section 5.1, the building analysis was simplified by modeling the mechanical characteristics of one line of framing in one wing of the building. A plan sketch of this wing is presented in Figure 5.07. For the wing that was modeled in this study, there are two different orthogonal lateral load-resisting systems: structural walls (Grids A and L) and non-ductile concrete frames (Grids 1 and 3).

A two-dimensional model of the moment frame on Grid 1 was developed for analysis using DRAIN-2DX. The frame geometry and nodal layout are presented in Figure 5.08.

Beam-columns (DRAIN-2DX Type 2 element) were used to model the beams and columns in the building. The post-yield behavior of the Type 2 element assumes stable ductile response. As such, the Type 2 element does not accurately capture the post-yield behavior of the frame. However, since reliable constitutive models for non-ductile response have not been implemented into DRAIN-2DX, the Type 2 elements were used in this study to model the cyclic response of the existing framing.

Using the information provided in the architectural and mechanical drawings, an accurate estimate of the tributary reactive weight to the frame on Grid 1 was prepared. After lumping the mass at the building nodes at each level, an eigen analysis was performed to compute the modal characteristics of the frame. The modal periods and the effective modal mass, as a fraction of the total mass, are listed in Table 5.1 below.

MODE	PERIOD (sec.)	EFFECTIVE MASS
1	1.55	96.0%
2	0.39	3.5%
3	0.18	0.5%

Table 5.1 Modal Periods and Effective Modal Masses

The corresponding mode shapes are presented in Table 5.2.

MODE	LVL 1	LVL 2	LVL 3
1	0.60	0.86	1.00
2	-0.99	-0.29	1.00
3	-0.72	1.00	-0.50

Table 5.2 Mode Shapes

5.7 Strength of the Existing Building

In order to estimate the strength of the building, a series of static load-to-collapse analyses were undertaken. Collapse analyses using the upper bound kinematic method predicted:

Triangular Force Distribution: $V_{max} < 84$ kips (=0.074W)

Rectangular Force Distribution: $V_{max} < 98$ kips (=0.087W),

where W is the reactive weight associated with the moment frame on Grid 1 (=1129 kips). These results assume that material behavior is rigid-perfectly plastic, hinge rotation capacity is unlimited, and that gravity load effects can be ignored: none of these assumptions are valid for non-ductile structures.

DRAIN-2DX was used to compute the strength of the frame by means of a series of static load-to-collapse analyses. Gravity load effects were included in these analyses.

In order to estimate the deformation capacity of the existing concrete frame, the ultimate rotation capacities of the beam and column cross-sections were calculated

using a method developed by Corley. On the basis of an ultimate concrete strain of 0.004 and a plastic hinge length of 12 inches, the ultimate rotation capacities of both the beams and columns were calculated to be 0.01 radian. The ultimate lateral strength of the frame was assumed to be equal to the lateral resistance at which the plastic hinge rotation at one or more cross-sections exceeded 0.01 radians. The results from the DRAIN-2DX analyses can be summarized as follows:

Triangular Force Distribution: $V_{max} < 68$ kips (=0.060W)

Rectangular Force Distribution: $V_{max} < 68$ kips (=0.060W)

The collapse loads for both lateral load distributions are identical as a result of the frame forming a soft first story under both the triangular and rectangular load patterns.

The base shear force versus first-floor and roof displacement relationships for the triangular and rectangular force profiles are presented in Figures 5.09 through 5.12, respectively. The collapse load of 68 kips is an upper bound on the true strength of the existing frame. This is because the formation of ductile plastic hinges is precluded by the lack of continuous longitudinal reinforcement in the joint, the lack of confinement in the plastic hinge zones, and the lack of shear reinforcement in the beam-column joint.

The true cyclic lateral strength of the existing building is probably on the order of 0.030W to 0.050W. For comparison purposes, the nominal strength of the moment frame is assumed to be 55 kips (0.05W).

5.8 Nonlinear Time History Analysis of the Building

The existing building was analyzed using the three acceleration records described in Section 5.2: Caleta de Campos 000 component; Joshua Tree Fire Station 090 component; and Desert Hot Springs 000 component. The results of these analyses follow:

Caleta de Campos:
The maximum base shear force, first-floor displacement, and roof displacement were 79 kips, 2.1 inches, and 2.4 inches, respectively. These responses correspond to a base shear coefficient of 0.070W, a first interstory drift index of 1.8%, and a roof drift index (measured as the roof displacement divided by the building height) of 0.7%, respectively. The base shear force, first-floor displacement, and roof displacement time histories are shown in Figures 5.13, 5.14, and 5.153, respectively.

The maximum base shear force of 0.070W exceeds the nominal strength of the frame (assumed to equal 0.05W) by 40%, and the maximum interstory drift exceeds the

nominal deformation capacity of the frame by over 100%.

Joshua Tree Fire Station
The maximum base shear force, first-floor displacement, and roof displacement were 97 kips, 5.0 inches, and 6.0 inches, respectively. These responses correspond to a base shear coefficient of 0.086W, a first interstory drift index of 4.2%, and a roof drift index of 1.67%, respectively. The base shear force, first-floor displacement, and roof displacement time histories are shown in Figures 5.16, 5.17, and 5.18, respectively.

The maximum base shear force of 0.086W exceeds the nominal strength of the frame by 72%, and the maximum interstory drift exceeds the nominal deformation capacity of the frame by in excess of 400%. Total collapse of this building could result from a ground motion similar to the Joshua Tree record.

Desert Hot Springs
The maximum base shear force, first-floor displacement, and roof displacement were 72 kips, 1.0 inches, and 1.3 inches, respectively. These responses correspond to a base shear coefficient of 0.063W, a first interstory drift index of 0.83%, and a roof drift index of 0.36%, respectively. The base shear force, first-floor displacement, and roof displacement time histories are shown in Figures 5.19, 5.20, and 5.21, respectively.

The maximum base shear force of 0.063W exceeds the nominal strength of the frame by 26%.

5.9 Discussion of the Time-History Analysis Results

The results of the nonlinear analysis of the existing building have clearly demonstrated that the building is at significant risk in the event of moderate or severe earthquake shaking.

The critical earthquake ground motion for this building is the Joshua Tree record. The acceleration pulse at the 10-second mark in the earthquake record forms a soft first story in the building. In excess of 80% of the total roof drift must be accommodated in the first story of the building. This places excessive demands on the rotation capacity of the columns in the first story. Collapse of the existing building, either partial or total, is likely given the level of the deformation demand on the non-ductile columns.

The strength of the building is substantially less than that required by current codes for buildings in regions of moderate or severe seismic risk. The limited lateral strength of the building coupled with the non-ductile detailing of the critical regions clearly indicate that the existing building needs to be upgraded in order to provide life-safety protection to the occupants. The design and analysis of two such upgrade schemes are presented in Sections 5.12 and 5.13.

5.10 Extraction of Lumped Mass and Stiffness Properties

Only a limited number of hysteretic shapes are available with the elements currently implemented in DRAIN-2DX. In order to gain a better understanding of the options afforded to the designer by SMA energy dissipators, a MATLAB characterization of a reduced-order model of the existing building is analyzed in the following chapter. The stiffness and mass characteristics of this three degrees-of-freedom, lumped-mass model were computed using the DRAIN-2DX model of the existing building.

The stiffness and mass characteristics of the reduced-order model are presented in Table 5.3 below.

STORY NUMBER	LATERAL STIFFNESS (kips/inch)	WEIGHT (kips)
1	78	397
2	100	397
3	80	335

Table 5.3 Stiffness and Mass Properties of the Reduced-Order Model

A comparison between the dynamic characteristics of the complete and reduced-order systems in terms of the first three modal periods is presented in Table 5.4. For the purposes of this study, the correlation between the dynamic properties of the complete and reduced-order mathematical models is adequate.

	PERIOD (secs)		
	MODE 1	MODE 2	MODE 3
COMPLETE	1.55	0.39	0.18
REDUCED-ORDER	1.48	0.54	0.37

Table 5.4 Comparison of Dynamic Characteristics

5.11 Retrofit of Existing Building with SMA Dampers

In Section 5.9, the need to upgrade the existing building was clearly demonstrated by the results of the nonlinear time history analysis of the building using earthquake ground motion records consistent with moderate earthquake shaking.

There are many issues to be considered for the upgrade of an existing building. These include:

1. the need to protect the existing frame by reducing the lateral displacements such that the plastic hinge formation, bar pull-out, and joint shear failure in the existing frame are precluded,
2. the consequences of increasing the axial force demands in the existing columns,
3. the ease by which the upgrade scheme, including any foundation work, can be implemented,
4. the impact of the upgrade scheme on the aesthetic appeal of the building and on the existing mechanical, electrical, and plumbing services, and
5. the cost-effectiveness of the upgrade scheme.

Of these five issues (and noting that other constraints may apply), only the first will be explicitly addressed in the following sections. A complete retrofit of the building is beyond the scope of this study. The Phase II study will address both the first and second items listed above.

Two preliminary upgrade schemes were developed for the existing building. In the following sections, these two upgrade schemes are denoted as UG1 and UG2. In both instances, the two principal objectives of the retrofit design were to reduce the interstory displacements to below 0.75 inch for all three earthquake records (corresponding to a column rotation of approximately 0.006 radians) and to dissipate most of the energy absorbed in the frame in the shape-memory alloy (SMA) dissipators. The rationale used to design the energy dissipators (or supplemental dampers) for both UG1 and UG2 is outlined in the following two sections.

5.12 Design and Analysis of Upgrade Scheme UG1

The mass distribution over the height of the building is presented in Table 5.3. The relative distribution of lateral stiffness can also be ascertained from Table 5.3.

The relative stiffnesses of the first, second, and third stories in the existing building is in the ratio 1.00:1.25:1.03; the cumulative reactive weight distribution is 1.00:0.65:0.30. The relative strengths of the first, second, and third stories, as determined from static load-to-collapse analysis of the existing building, are approximately 1.00:1.83:1.47 (68:125:100).

The preliminary design of Scheme UG1 SMA energy dissipators augmented the strength of the lower two levels of the existing frame in order to approximately replicate the existing cumulative weight distribution noted above. The disposition of energy dissipation devices is presented in Figure 5.22. The SMA energy dissipators are supported by TS4x4x1/2 braces. For these analyses, the SMA dissipators are assumed to have rectangular (rigid-plastic) hysteresis with a yield force of 22.5 kips per damper. The TS4x4 braces were selected so as to ensure that:

1. at an interstory drift of 0.5%, less than 10% of the total brace/dissipator axial displacement was in the brace itself, and
2. the buckling strength of the brace was at least 1.5 times the yield force in the SMA dissipator.

The UG1 upgrade scheme included 12, 6, and 4 SMA dissipators in the first, second, and third stories, respectively. The addition of these dissipators resulted in story strengths of approximately 310 kips, 220 kips, and 150 kips in the first, second, and third stories, respectively, or story strength ratios of 1.00:0.70:0.48.

Static load-to-collapse analyses using DRAIN-2DX were performed on the UG1 upgrade of the existing building. The results of these analyses, for both triangular and rectangular load distributions, are presented in Figures 5.23 through 5.26.

The UG1 upgrade scheme was analyzed using the three acceleration records used to analyze the existing building in Section 5.8. The results of these analyses follow:

Caleta de Campos:
The maximum base shear force, first-floor displacement, and roof displacement were 250 kips, 0.07 inch, and 0.20 inch, respectively. These responses correspond to a base shear coefficient of 0.22W, a first interstory drift index of 0.06%, and a roof drift index of 0.06%, respectively. The base shear force, first-floor displacement, and roof displacement time histories are shown in Figures 5.27, 5.28, and 5.29, respectively. The strength-versus-interstory displacement relationships for the first, second, and third stories are presented in Figures 5.30, 5.31, and 5.32, respectively.

Joshua Tree Fire Station
The maximum base shear force, first-floor displacement, and roof displacement were 290 kips, 0.18 inch, and 0.37 inch, respectively. These responses correspond to a base shear coefficient of 0.26W, a first interstory drift index of 0.15%, and a roof drift index of 0.10%, respectively. The base shear force, first-floor displacement, and roof displacement time histories are shown in Figures 5.33, 5.34, and 5.35, respectively. The strength-versus-interstory displacement relationships for the first, second, and third stories are presented in Figures 5.36, 5.37, and 5.38, respectively.

Desert Hot Springs
The maximum base shear force, first-floor displacement, and roof displacement were 270 kips, 0.17 inch, and 0.4 inch, respectively. These responses correspond to a base shear coefficient of 0.24W, a first interstory drift index of 0.14%, and a roof drift index of 0.11%, respectively. The base shear force, first-floor displacement, and roof displacement time histories are shown in Figures 5.39, 5.40, and 5.41, respectively. The strength-versus-interstory displacement relationships for the first, second, and third stories are presented in Figures 5.42, 5.43, and 5.44, respectively.

The results of the nonlinear analyses, both static load-to-collapse and time-history, of the UG1 upgrade scheme building have clearly demonstrated that the addition of the SMA energy dissipators has substantially improved the seismic response of the building. This was accomplished by increasing the lateral stiffness of the frame (thereby reducing the lateral displacements in the building to below the threshold level associated with damage to the existing frame) and by adding energy dissipation capacity to the building at extremely low levels of interstory drift. This improvement is evinced in the displacement time-history results and in the strength-versus-deformation relationships.

The response of the upgraded building to the Joshua Tree earthquake record is markedly different from that of the existing building: the maximum interstory drifts were reduced by a factor exceeding 35. Furthermore, the upgraded frame did not form a soft first story, and the upper levels of the building contributed to the energy dissipation mechanism. Although less dramatic, similar results were obtained for the Caleta de Campos and Desert Hot Springs earthquake records.

The increase in building stiffness through the addition of bracing elements generally results in an increase in the axial forces in the columns attached to the braces. The brace configuration was chosen to minimize such an increase. The maximum increase in axial force in any column can be calculated on the basis of the vertical component of the yield force in the brace, which in this case is 10.3 kips. Such an axial force represents less than 2% of the compression capacity (P_o) of the columns and 10% of the tensile capacity of the columns (T_o). Accordingly, the issue of modified axial forces in the columns in the existing frame for the UG1 upgrade is not discussed further.

Given that the interstory deformation capacity of the existing frame is on the order of 0.75 inch or greater, and noting that the maximum interstory drift with the UG1 upgrade was less than 0.2 inch, another upgrade scheme (UG2) incorporating fewer SMA energy dissipators was developed. The UG2 upgrade scheme is described below.

5.13 Design and Analysis of Upgrade Scheme UG2

The preliminary design of the Scheme UG2 SMA energy dissipators made use of the results of the UG1 analyses described above. The number of the SMA dissipators for Scheme UG2 in the first, second, and third stories of the building are 6, 4, and 2 respectively, compared with 12, 6, and 4 in Scheme UG1. The layout of the UG2 SMA energy dissipation devices is presented in Figure 5.45. The UG2 SMA energy dissipators are supported by TS4x4x1/2 braces for the reasons cited above for Scheme UG1. For Scheme UG1, the SMA dissipators were assumed to have rectangular (rigid-plastic) hysteresis with a yield force of 22.5 kips per damper. The addition of these dissipators resulted in story strengths of approximately 200 kips, 150 kips, and 100 kips in the first, second, and third stories respectively, or story strength ratios of 1.00:0.75:0.50.

Static load-to-collapse analyses using DRAIN-2DX were performed on the UG2 upgrade of the existing building. The results of these analyses for both triangular and rectangular load distributions are presented in Figures 5.46 through 5.49.

The UG2 upgrade scheme was analyzed using the three acceleration records used to analyze both the existing building and the UG1 upgrade scheme. The results of these analyses follow:

Caleta de Campos:
The maximum base shear force, first-floor displacement, and roof displacement were 180 kips, 0.25 inch, and 0.41 inch, respectively. These responses correspond to a base shear coefficient of 0.16W, a first interstory drift index of 0.21%, and a roof drift index of 0.11%, respectively. The base shear force, first-floor displacement, and roof displacement time histories are shown in Figures 5.50, 5.51, and 5.52, respectively. The strength-versus-interstory displacement relationships for the first, second, and third stories are presented in Figures 5.53, 5.54, and 5.55, respectively.

Joshua Tree Fire Station
The maximum base shear force, first-floor displacement, and roof displacement were 225 kips, 0.75 inch, and 1.25 inches, respectively. These responses correspond to a base shear coefficient of 0.20W, a first interstory drift index of 0.63%, and a roof drift index of 0.35%, respectively. The base shear force, first-floor displacement, and roof displacement time histories are shown in Figures 5.56, 5.57, and 5.58, respectively. The strength-versus-interstory displacement relationships for the first, second, and third stories are presented in Figures 5.59, 5.60, and 5.61, respectively.

Desert Hot Springs
The maximum base shear force, first-floor displacement, and roof displacement were

200 kips, 0.32 inch, and 0.55 inch, respectively. These responses correspond to a base shear coefficient of 0.18W, a first interstory drift index of 0.26%, and a roof drift index of 0.15%, respectively. The base shear force, first-floor displacement, and roof displacement time histories are shown in Figures 5.62, 5.63, and 5.64, respectively. The strength-versus-interstory displacement relationships for the first, second, and third stories are presented in Figures 5.65, 5.66, and 5.67, respectively.

The results of the nonlinear analyses, both static load-to-collapse and time-history, of the UG2 upgrade scheme building have clearly demonstrated that the addition of the SMA energy dissipators has substantially improved the seismic response of the existing building.

The maximum displacement response of the UG2 upgraded building to the Joshua Tree earthquake record borders on the predetermined deformation limit of 0.75 inch. The maximum displacement responses for the other two earthquake records are significantly smaller than the 0.75-inch limit.

The maximum increase in axial force in any column in the frame can be calculated on the basis of the vertical component of the yield force in the brace, which in this case is 10.3 kips. For the brace layout shown in Figure 5.45, the maximum change in axial force in any column resulting from the addition of the SMA dissipators is 20.6 kips, or less than 4% of the compression capacity (P_0) of the columns and 20% of the tensile capacity of the columns (T_0). Accordingly, the issue of modified axial forces in the columns in the existing frame for the UG2 upgrade is not discussed further.

5.14 Summary and Conclusions of the DRAIN Analyses

The nonlinear analyses of the existing building numerically exposed the seismic deficiencies promulgated in Section 5.5. Given that this building is typical of many of the buildings in the DOD inventory, substantial reconstruction costs to the Federal Government in the event of a moderate or severe earthquake could be substantial.

Two upgrade schemes, UG1 and UG2, incorporating SMA energy dissipators were developed for the building studied in this chapter. Both upgrade schemes reduced the response of the existing building below the assumed damage threshold, measured in this chapter as an interstory displacement of 0.75 inch.

Given that both schemes satisfied the design criteria, UG2 is preferred to UG1 solely on the basis of construction cost: the cost of the supplemental dampers (braces, SMA dissipators, and connections) for Scheme UG2 is less than 55% of that for UG1.

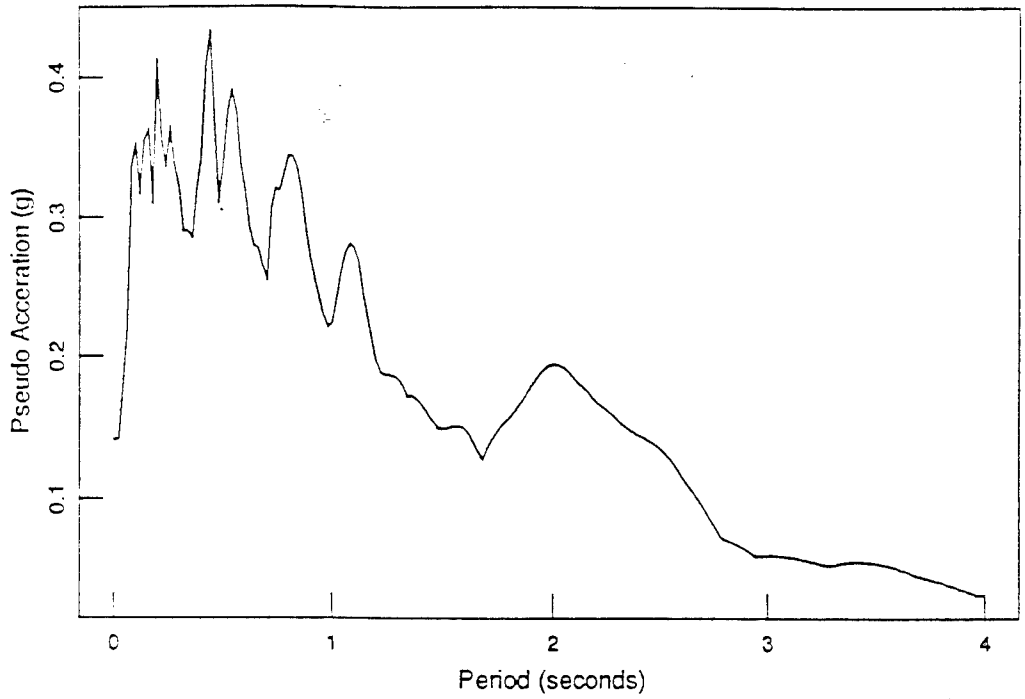

Figure 5.1 Caleta de Campos: Response Spectrum

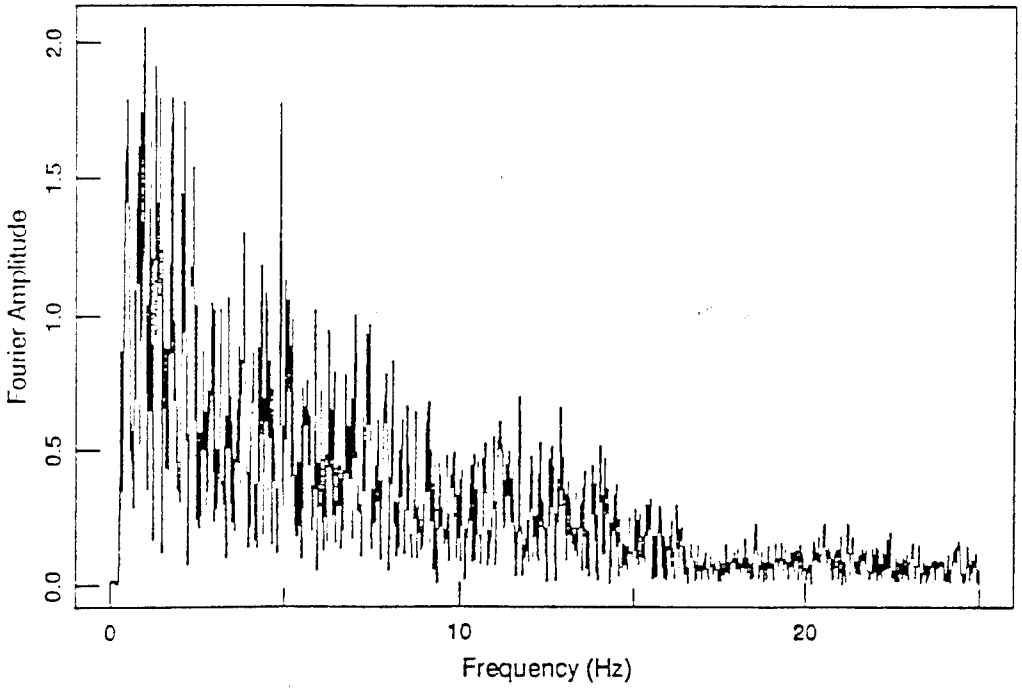

Figure 5.2 Caleta de Campos: Fourier Spectrum

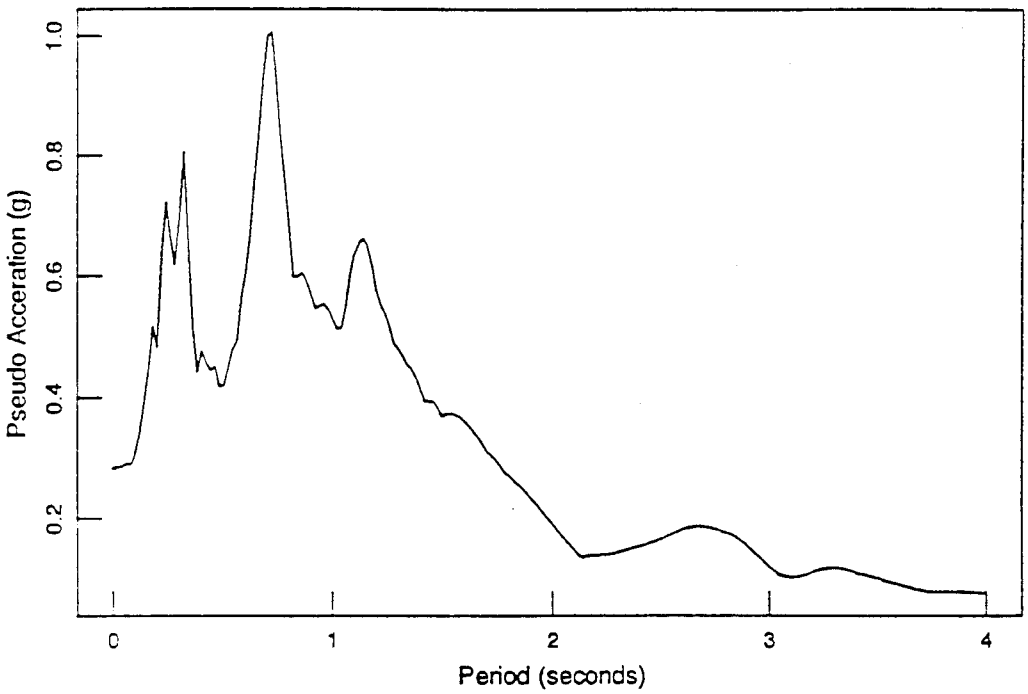

Figure 5.3 Joshua Tree Station: Response Spectrum

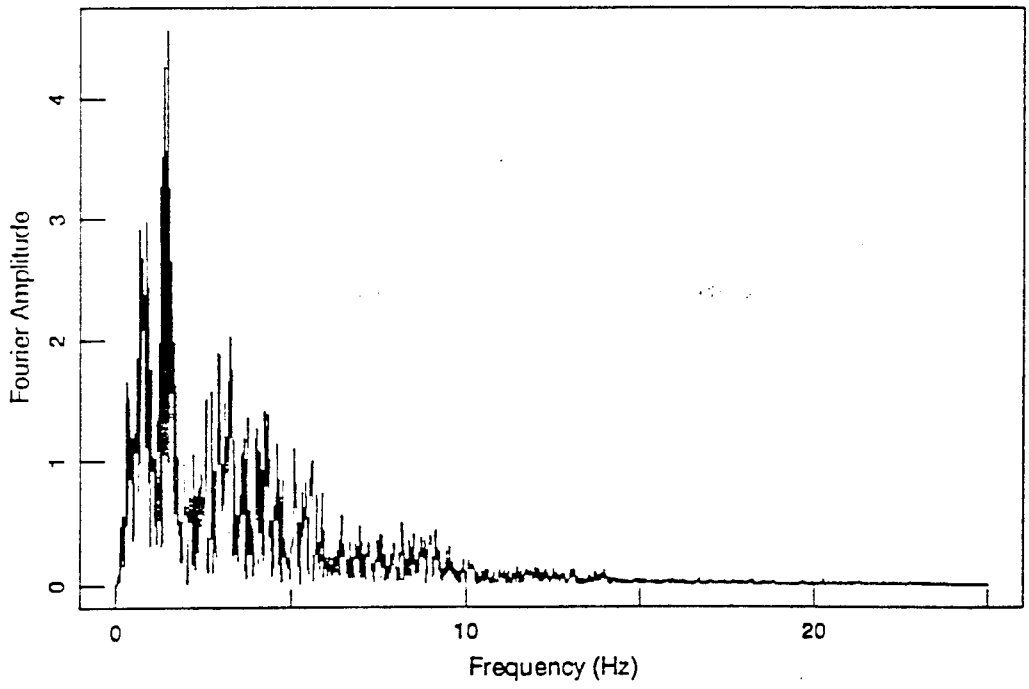

Figure 5.4 Joshua Tree Station: Fourier Spectrum

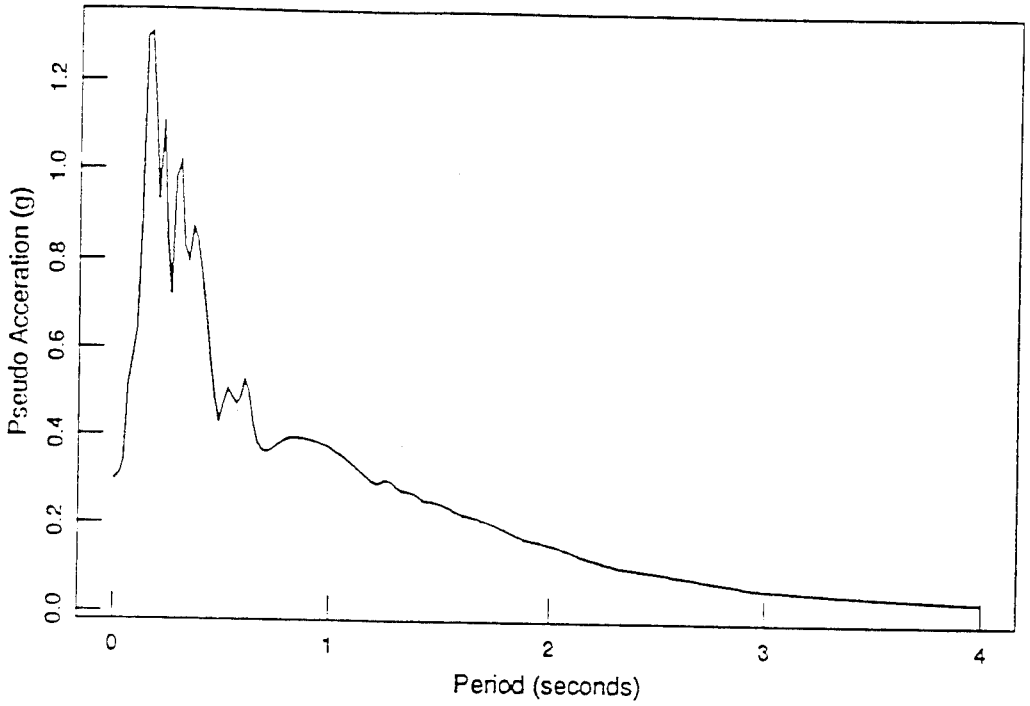

Figure 5.5 Desert Hot Springs: Response Spectrum

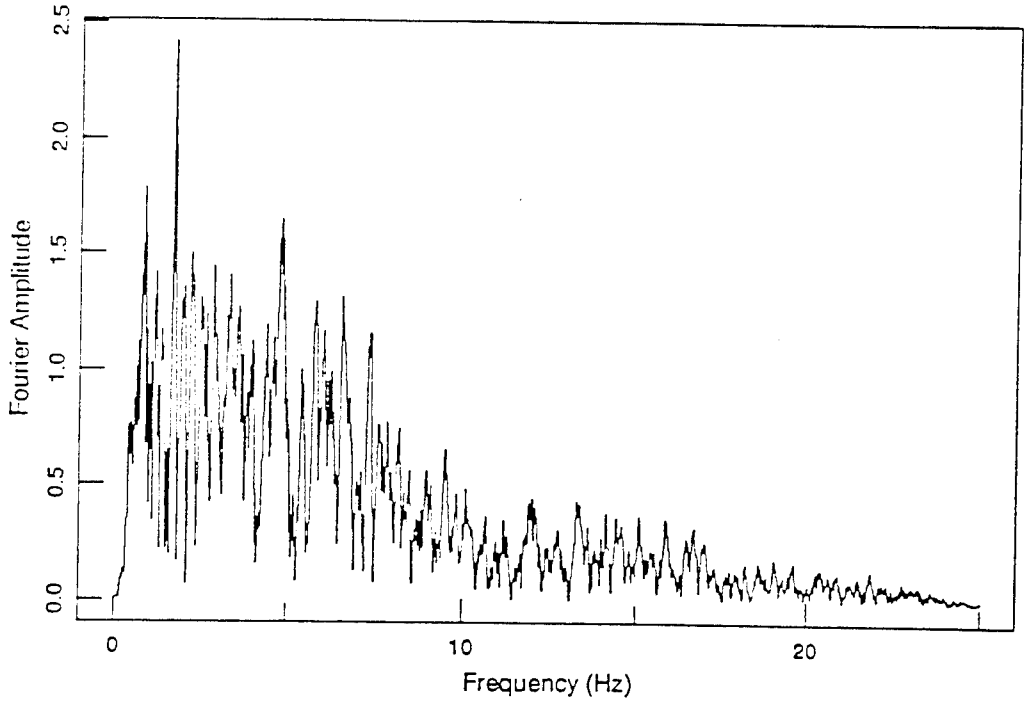

Figure 5.6 Desert Hot Springs: Fourier Spectrum

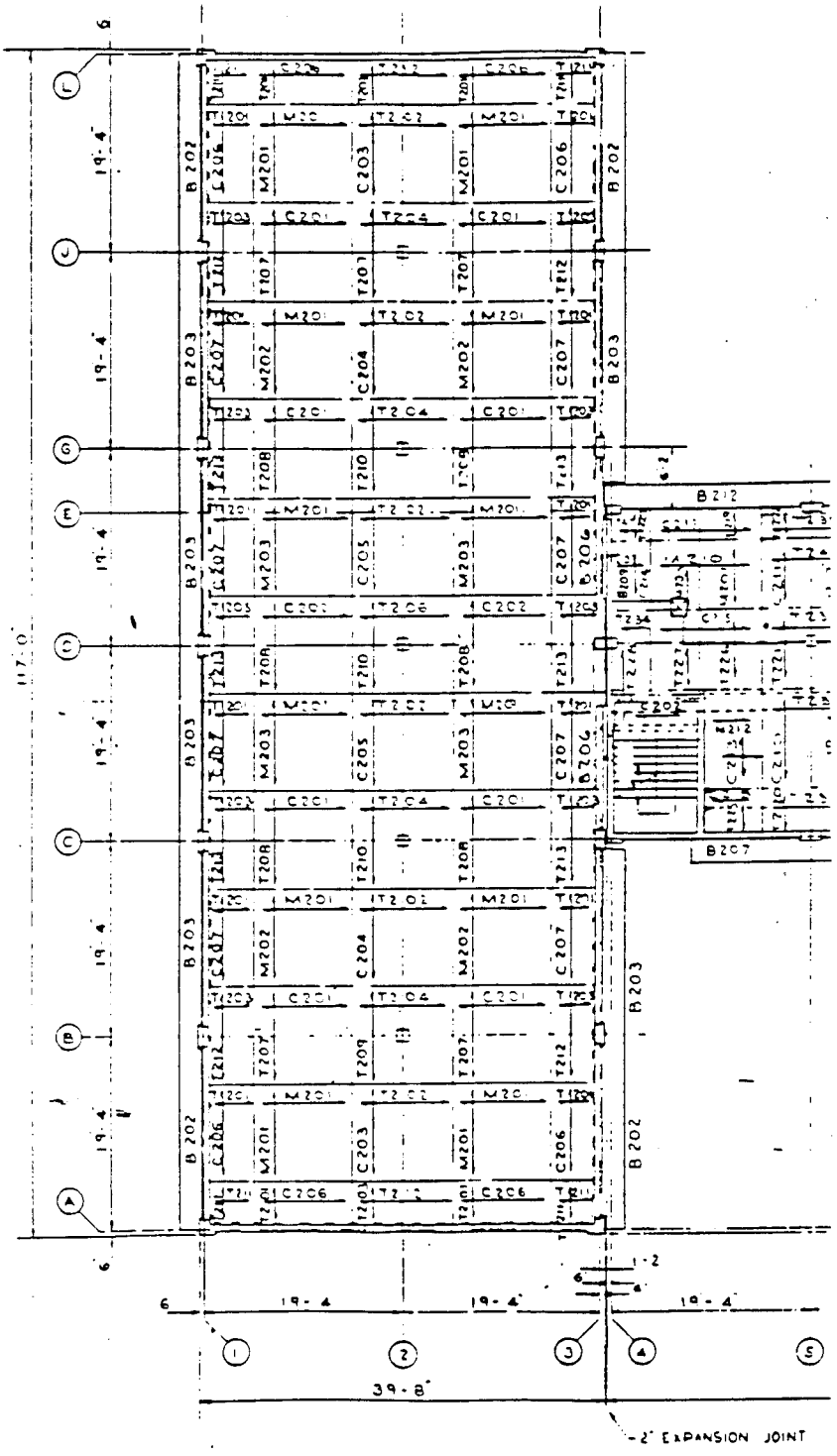

Figure 5.7 Plan Details of Analyzed Wing of Building

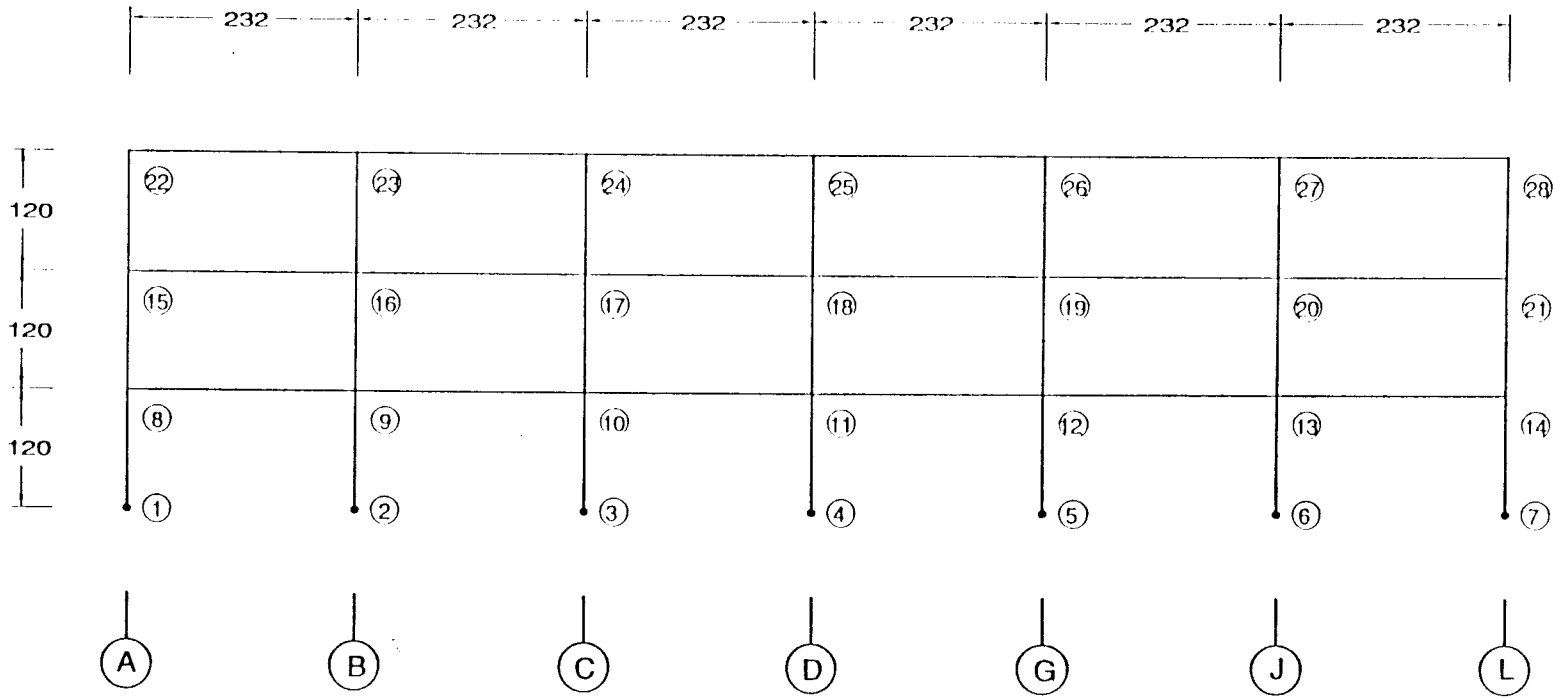

All dimensions in inches

Figure 5.8 Frame Geometry and Nodal Layout

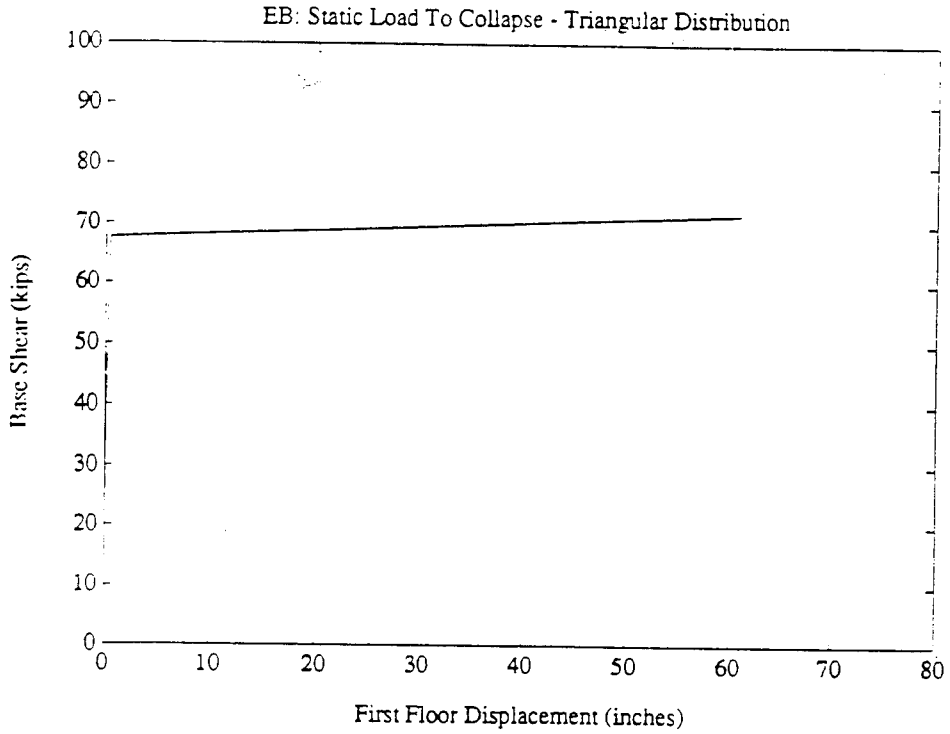

Figure 5.9 EB: Collapse Analysis Results - Triangular Load Distribution

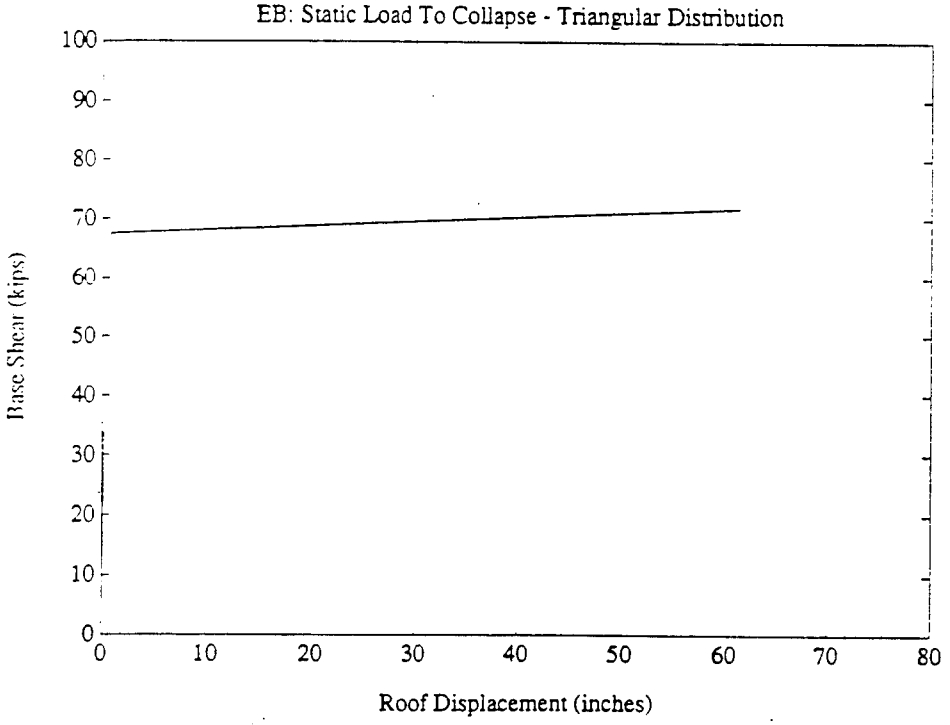

Figure 5.10 EB: Collapse Analysis Results - Triangular Load Distribution

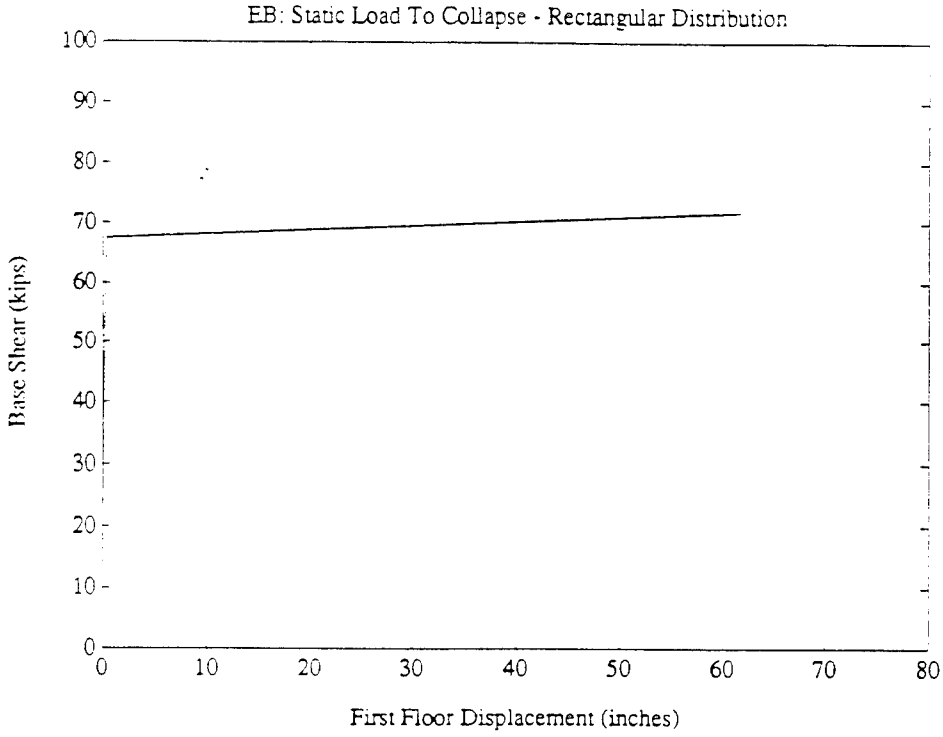

Figure 5.11 EB: Collapse Analysis Results - Rectangular Load Distribution

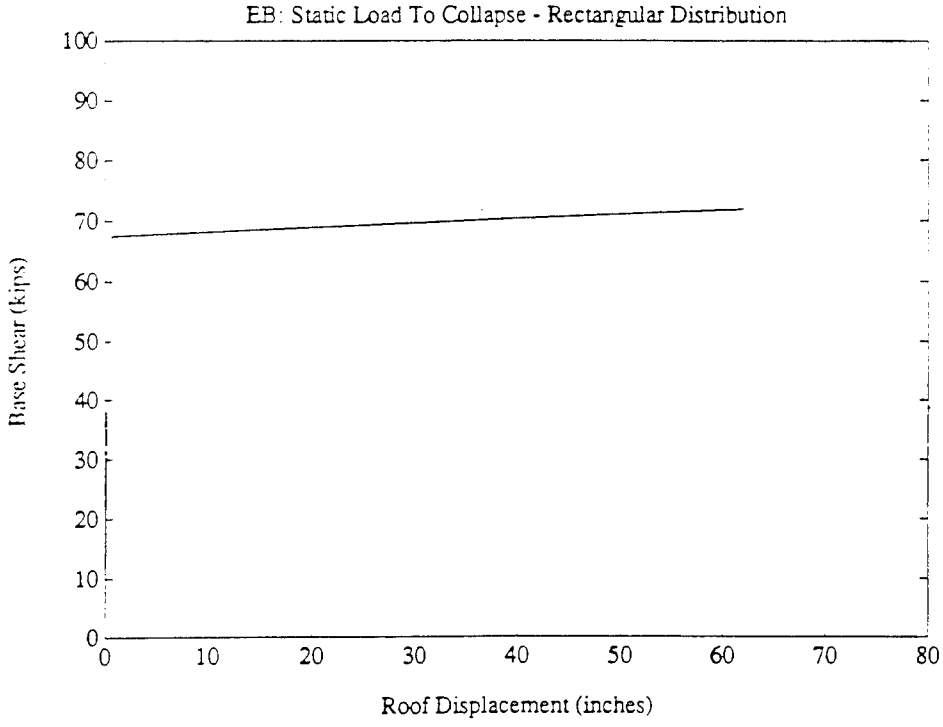

Figure 5.12 EB: Collapse Analysis Results - Rectangular Load Distribution

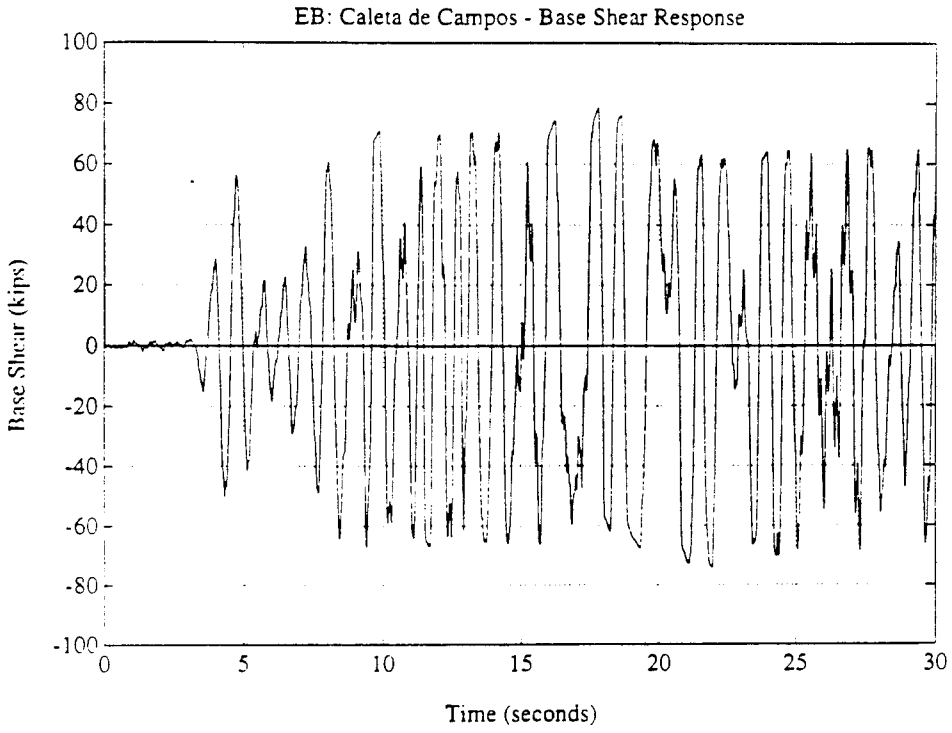

Figure 5.13 EB: Caleta de Campos - Base Shear Response

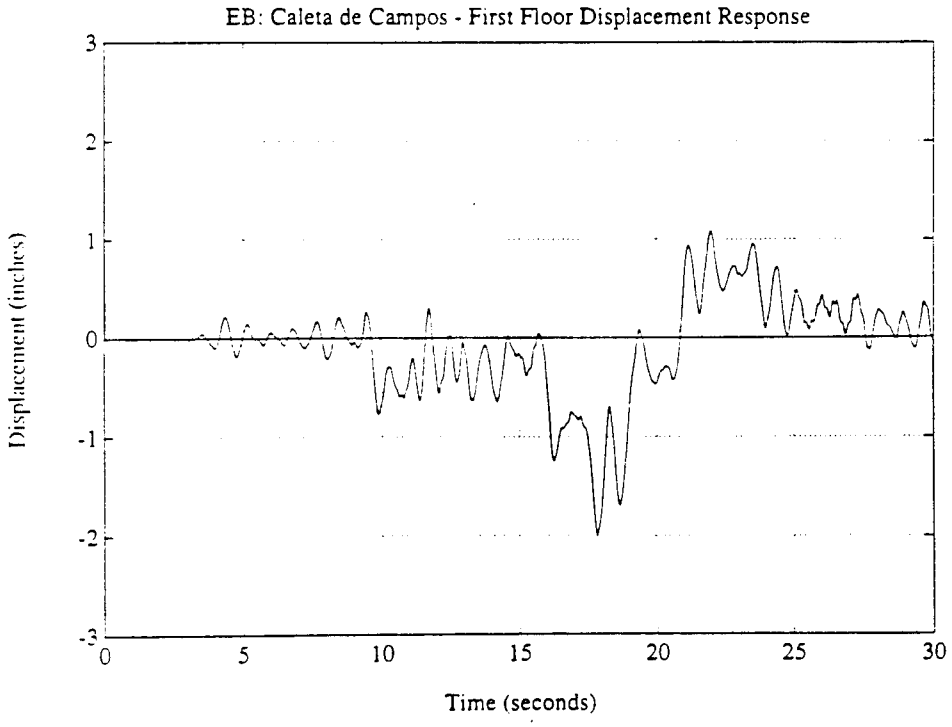

Figure 5.14 EB: Caleta de Campos - First Floor Displacement Response

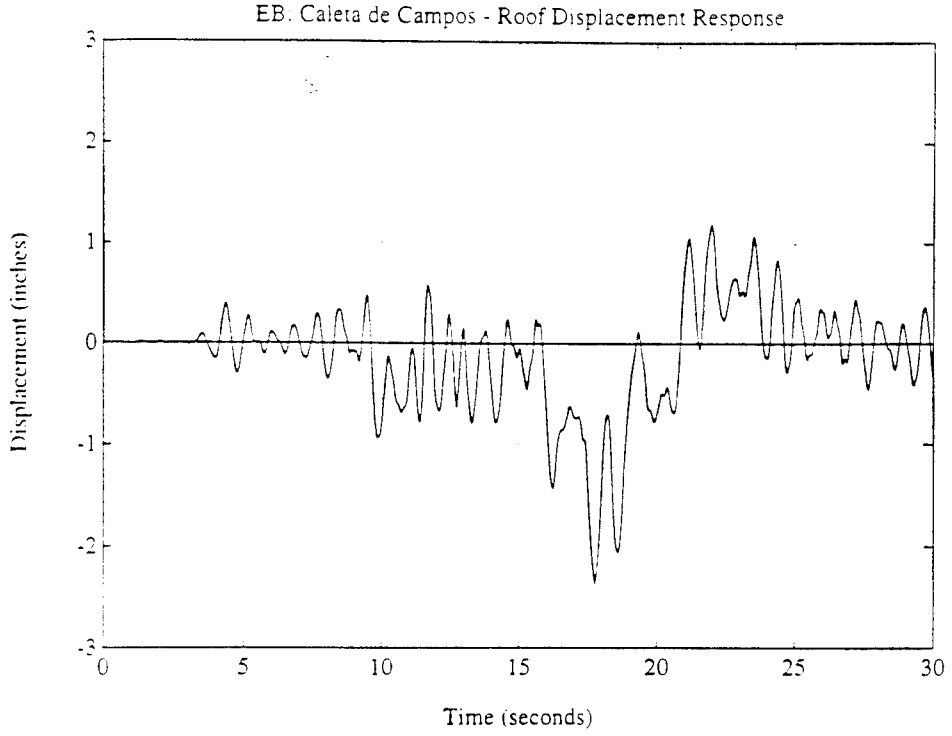

Figure 5.15 EB: Caleta de Campos - Roof Displacement Response

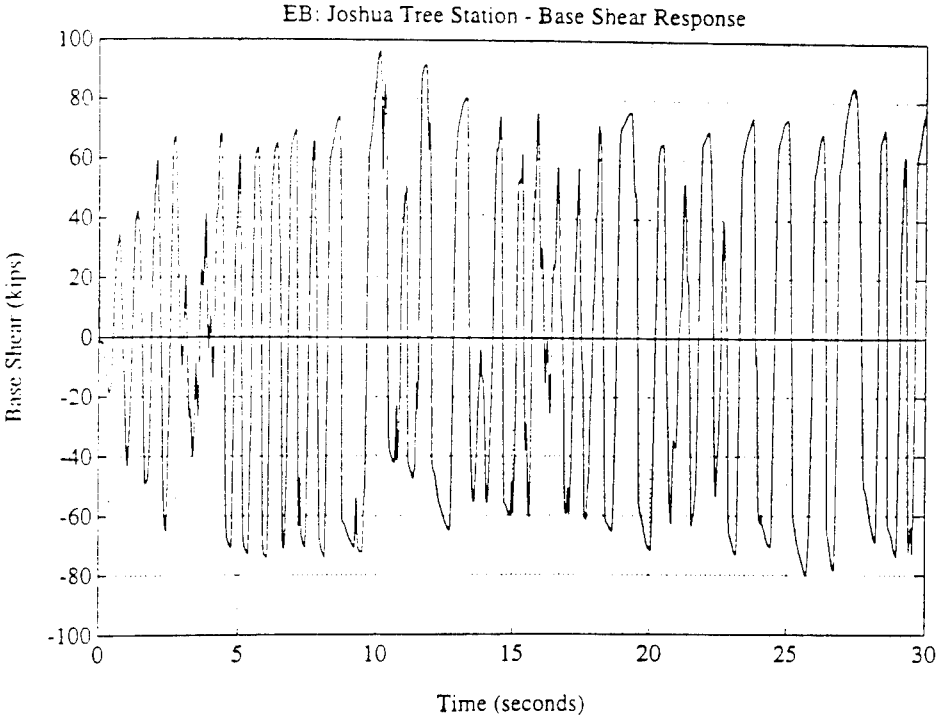

Figure 5.16 EB: Joshua Tree Station - Base Shear Response

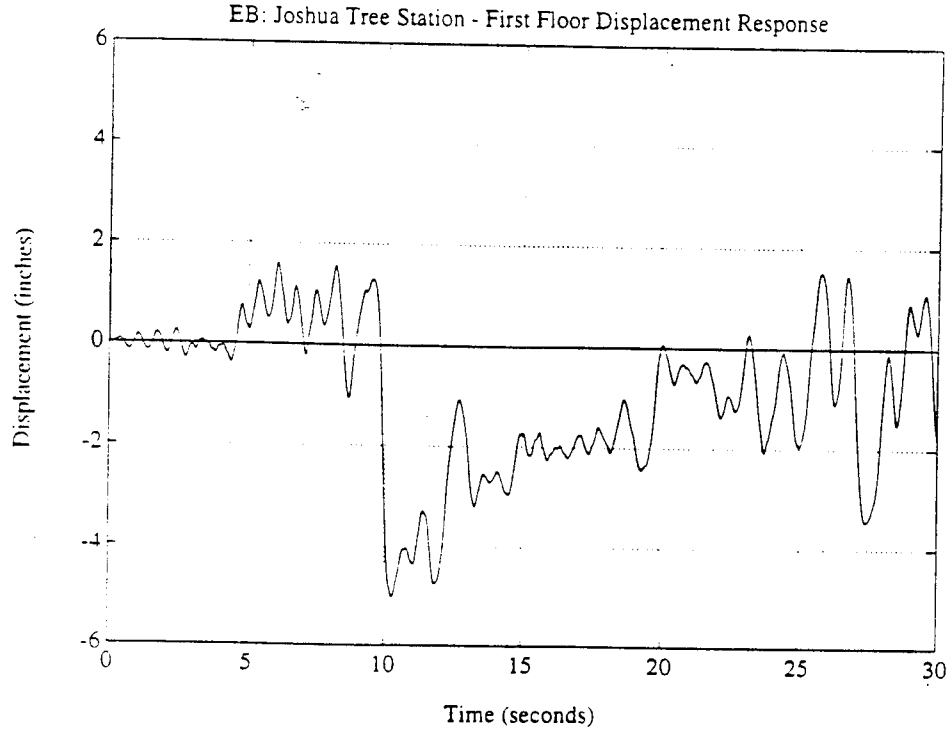

Figure 5.17 EB: Joshua Tree Station - First Floor Displacement Response

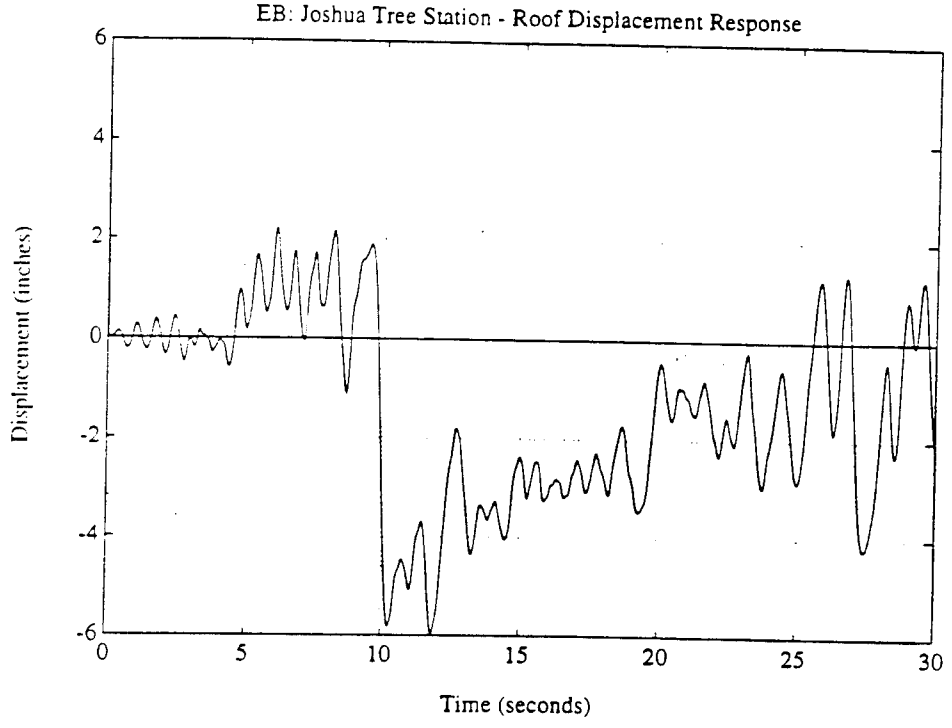

Figure 5.18 EB: Joshua Tree Station - Roof Displacement Response

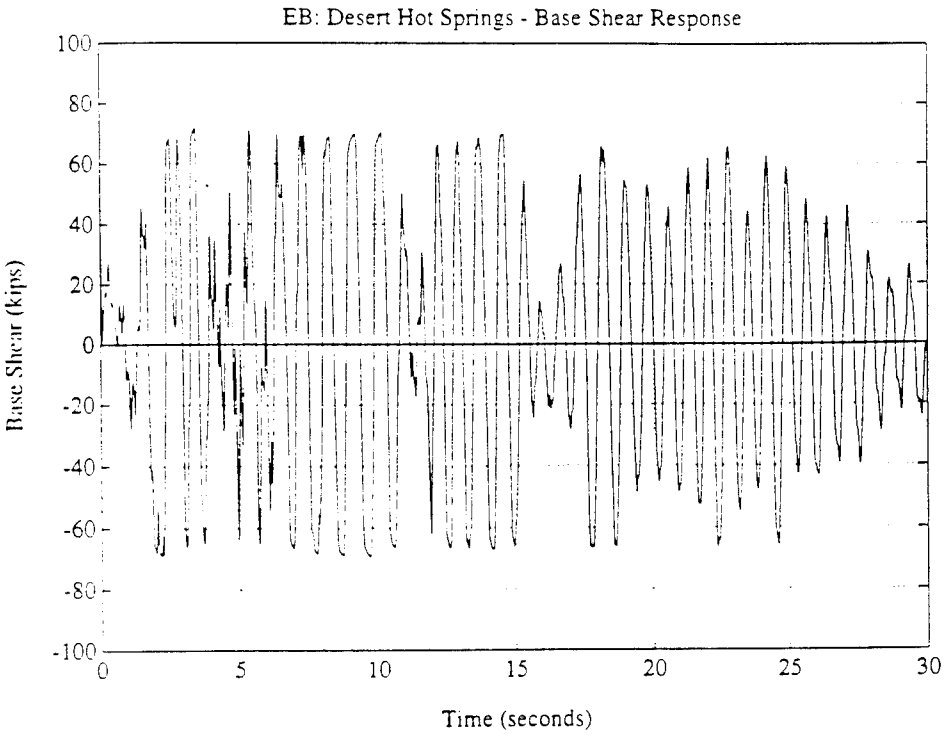

Figure 5.19 EB: Desert Hot Springs - Base Shear Response

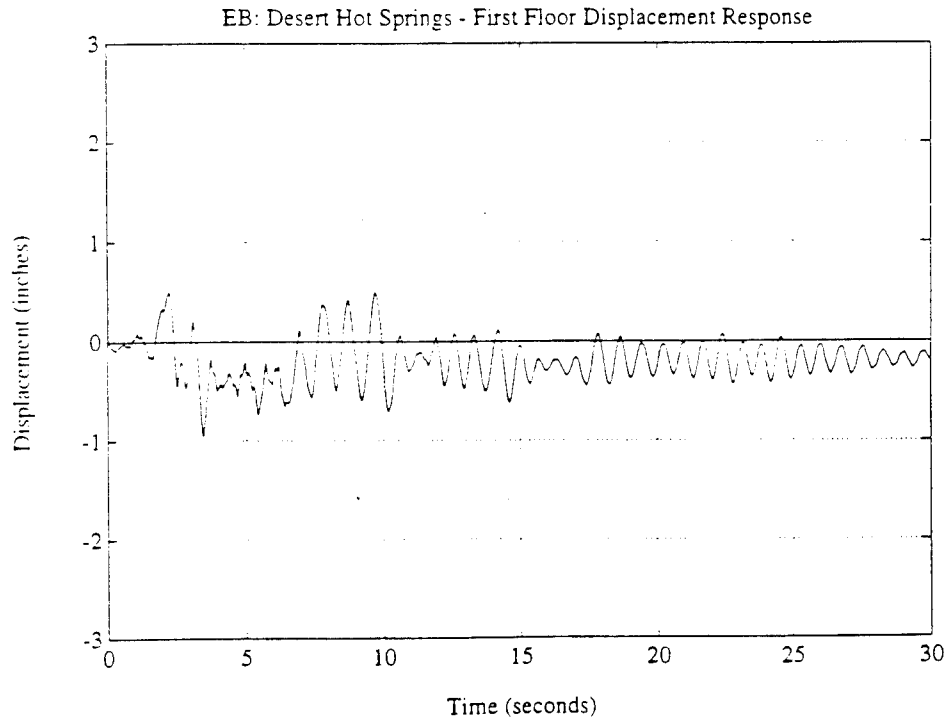

Figure 5.20 EB: Desert Hot Springs - First Floor Displacement Response

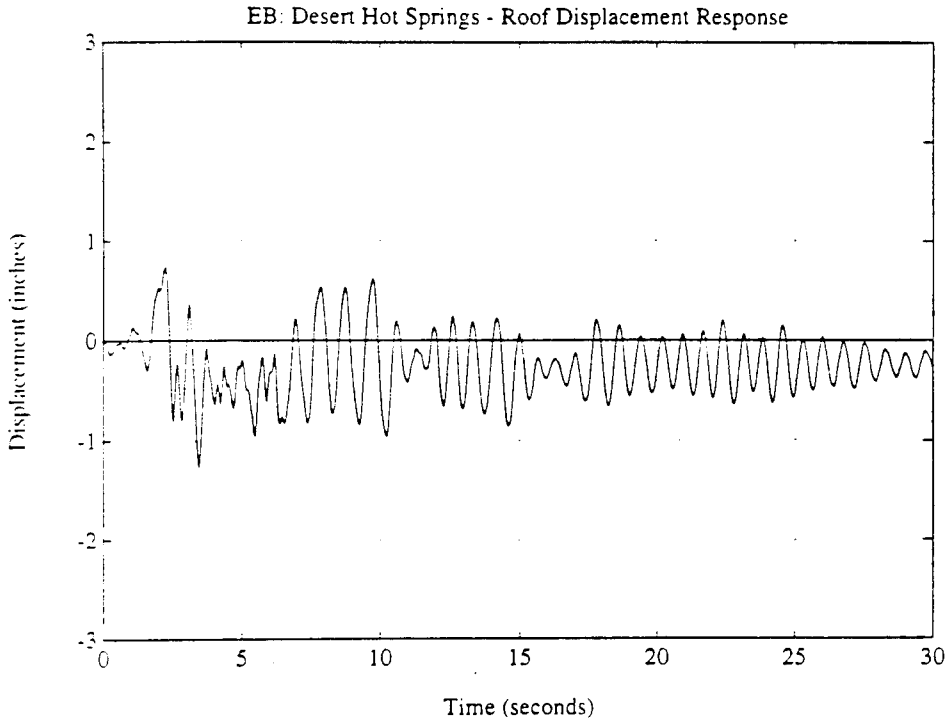

Figure 5.21 EB: Desert Hot Springs - Roof Displacement Response

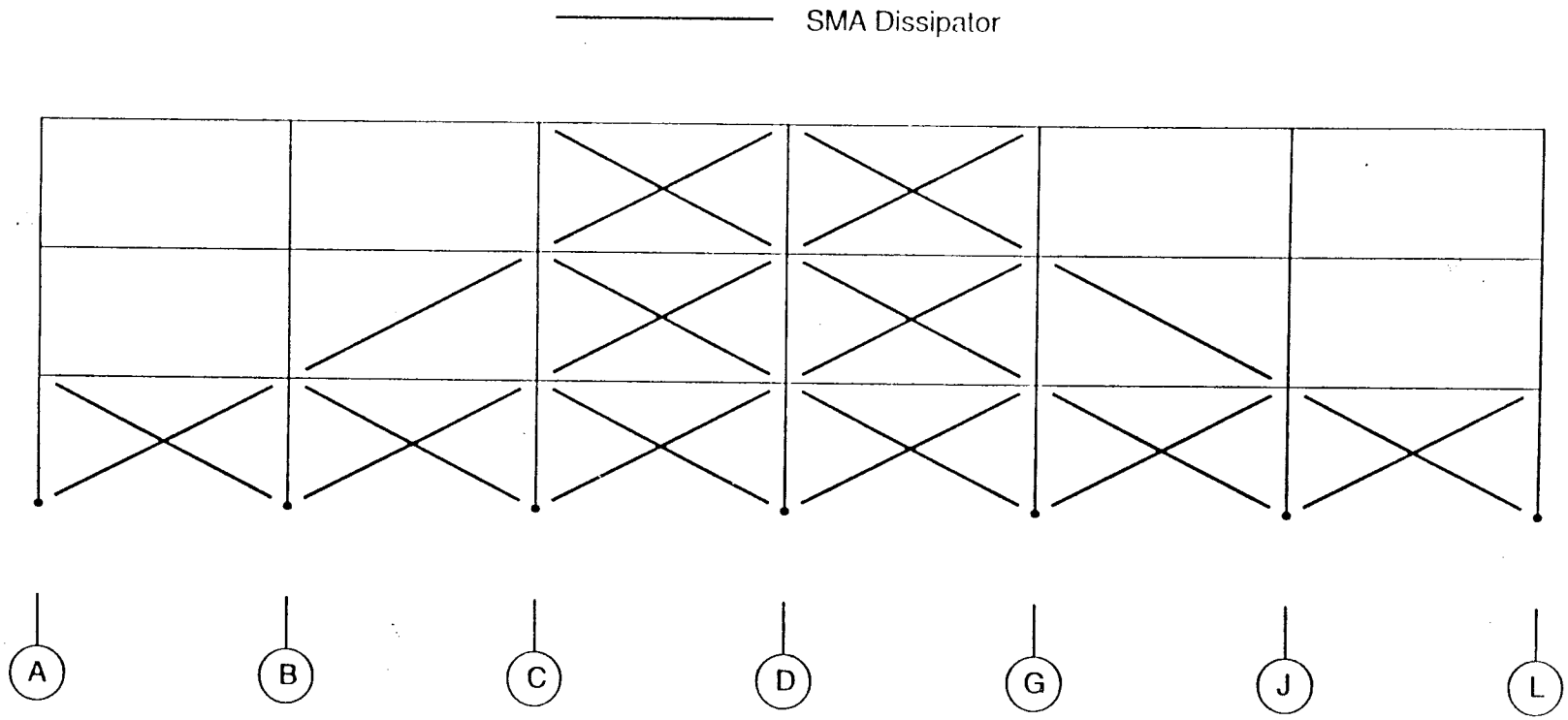

Figure 5.22 UG1: SMA Energy Dissipator Layout

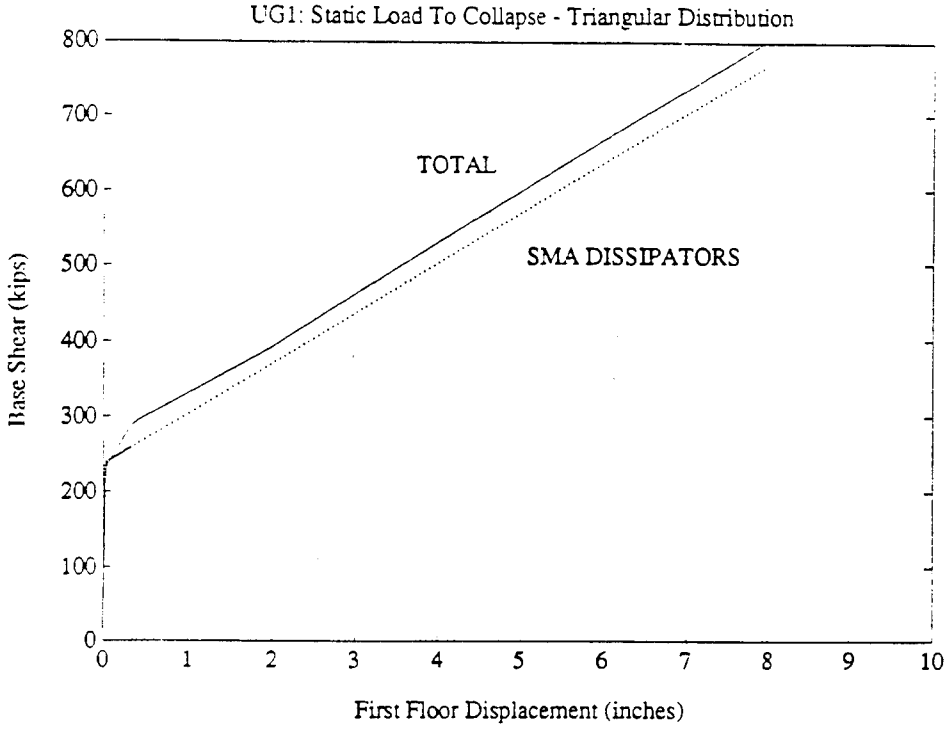

Figure 5.23 UG1: Collapse Analysis Results - Triangular Load Distribution

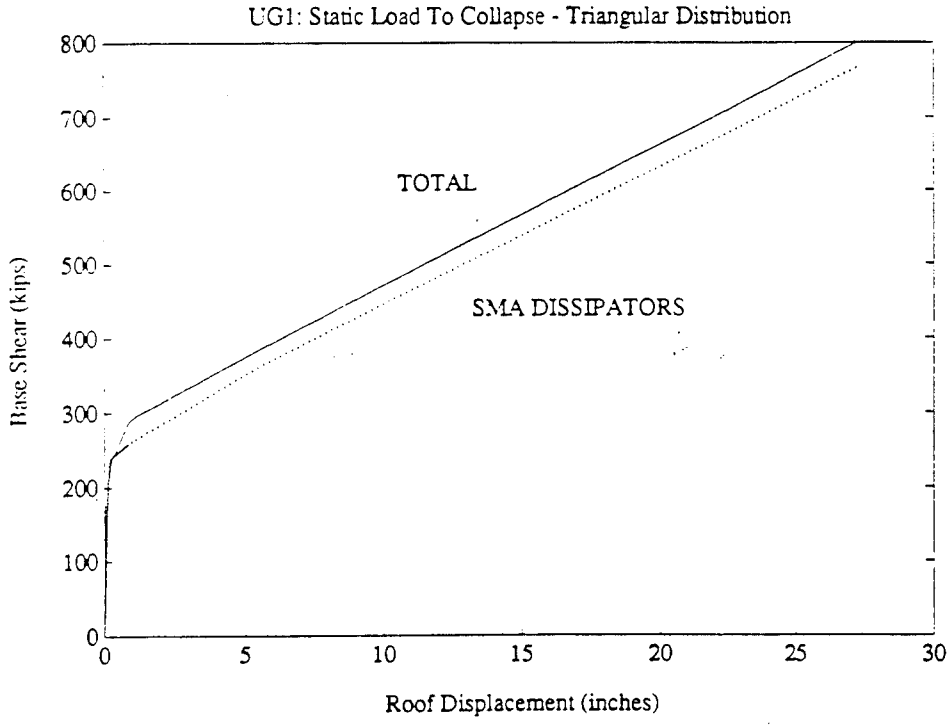

Figure 5.24 UG1: Collapse Analysis Results - Triangular Load Distribution

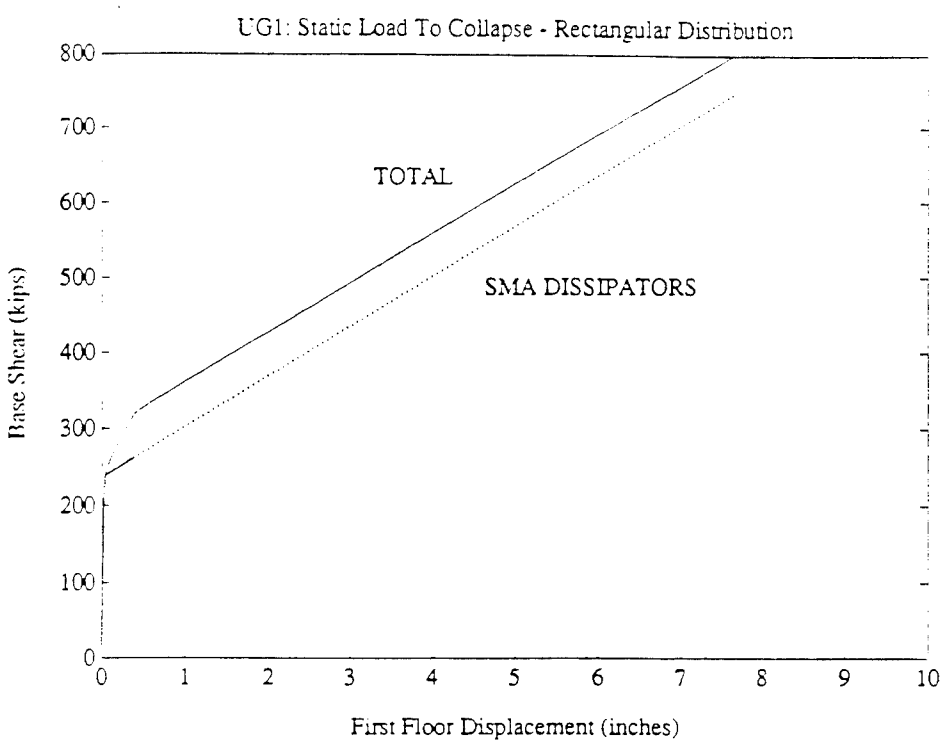

Figure 5.25 UG1: Collapse Analysis Results - Rectangular Load Distribution

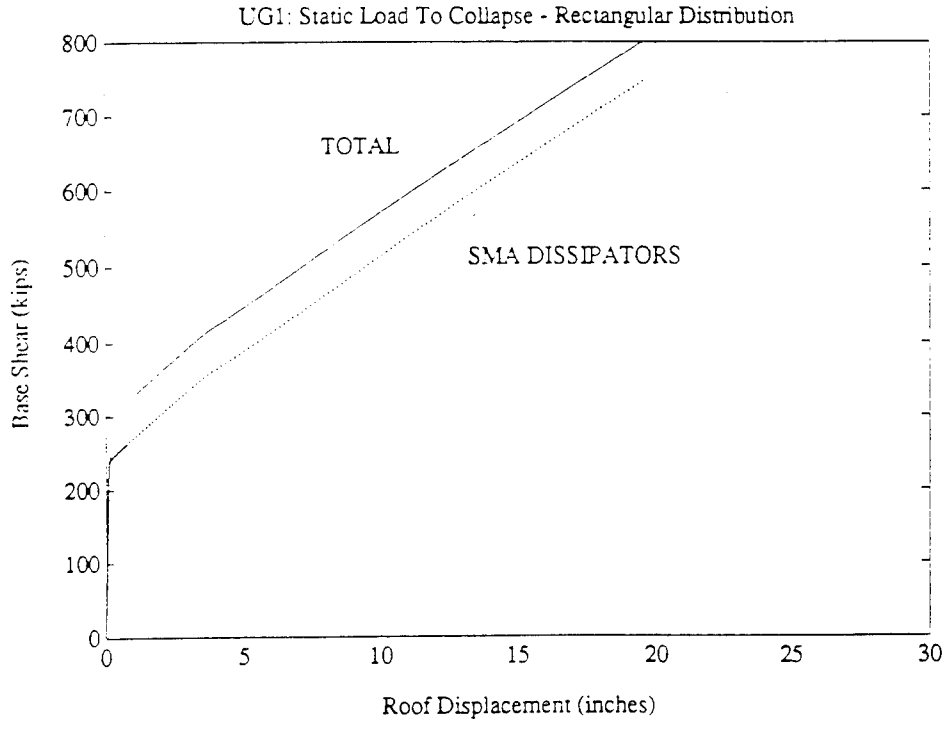

Figure 5.26 UG1: Collapse Analysis Results - Rectangular Load Distribution

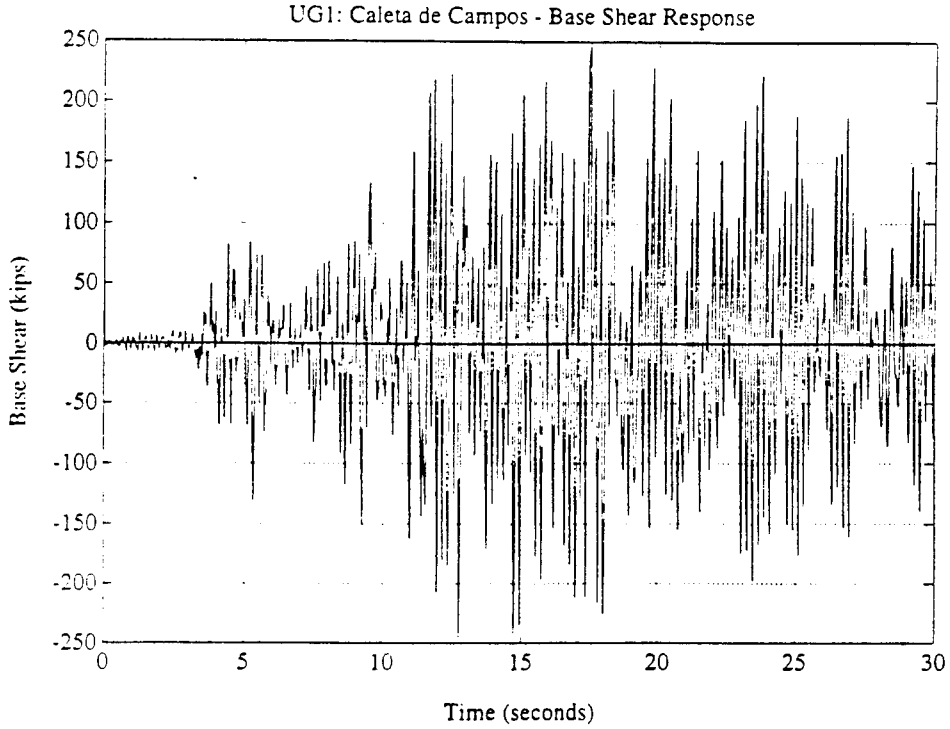

Figure 5.27 UG1: Caleta de Campos - Base Shear Response

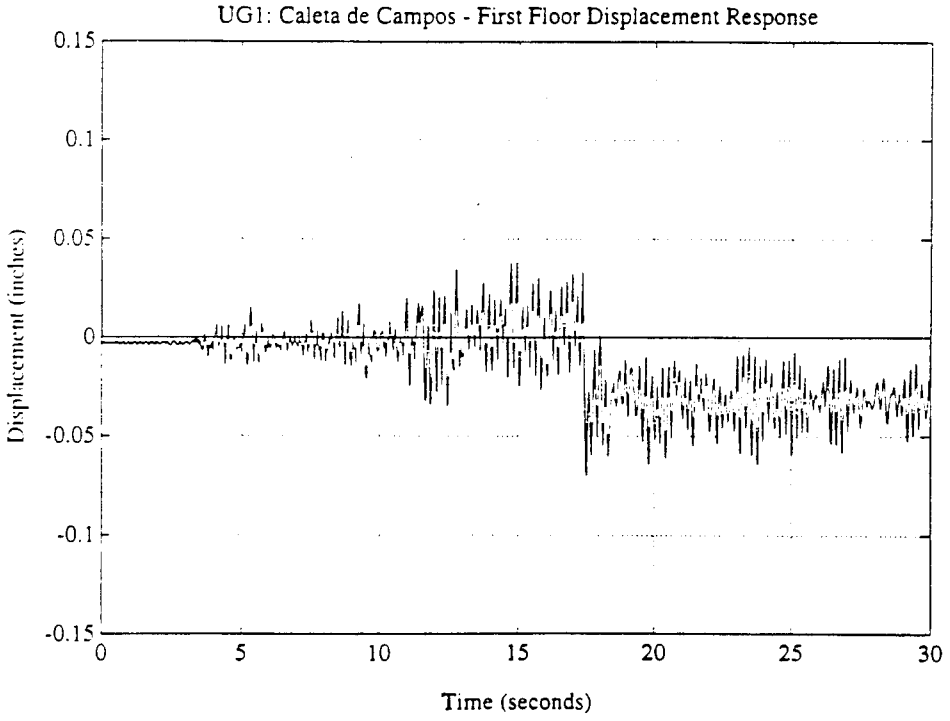

Figure 5.28 UG1: Caleta de Campos - First Floor Displacement Response

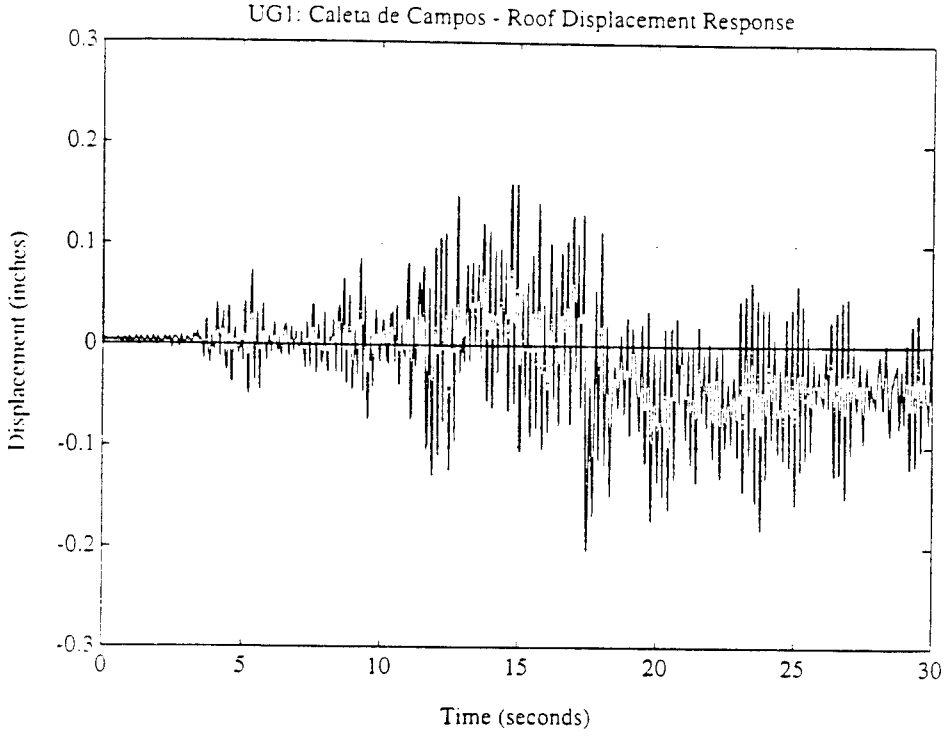

Figure 5.29 UG1: Caleta de Campos - Roof Displacement Response

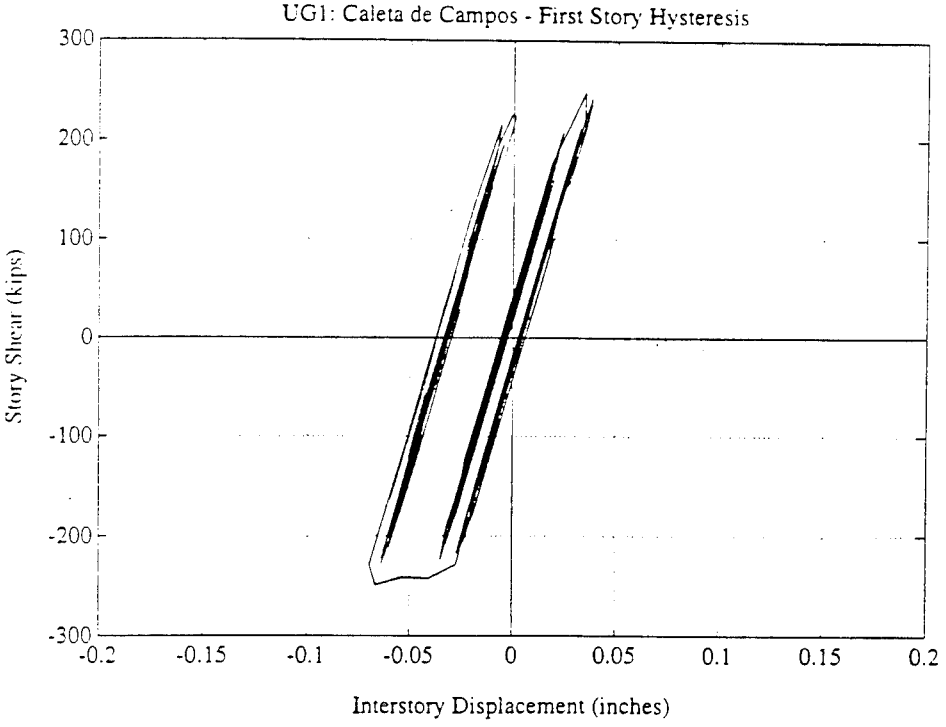

Figure 5.30 UG1: Caleta de Campos - First Story Hysteresis

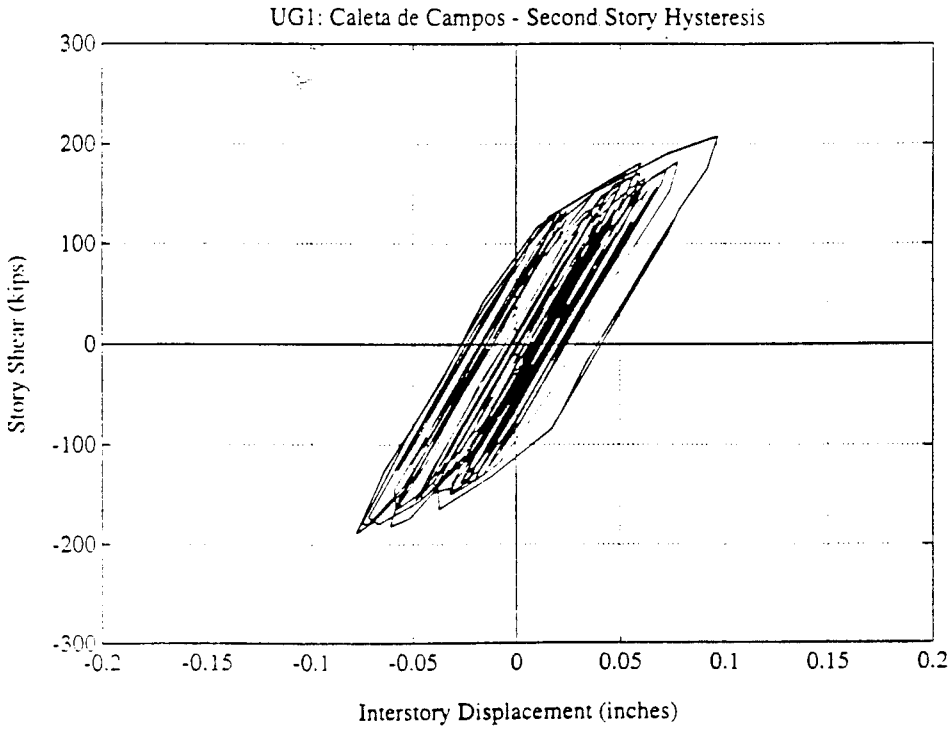

Figure 5.31 UG1: Caleta de Campos - Second Story Hysteresis

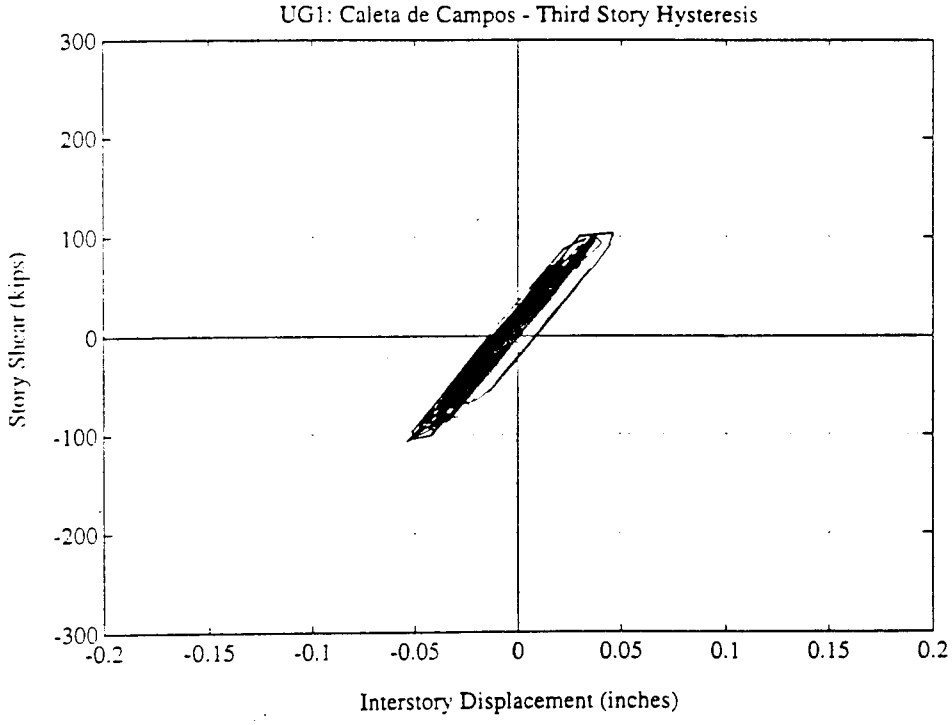

Figure 5.32 UG1: Caleta de Campos - Third Story Hysteresis

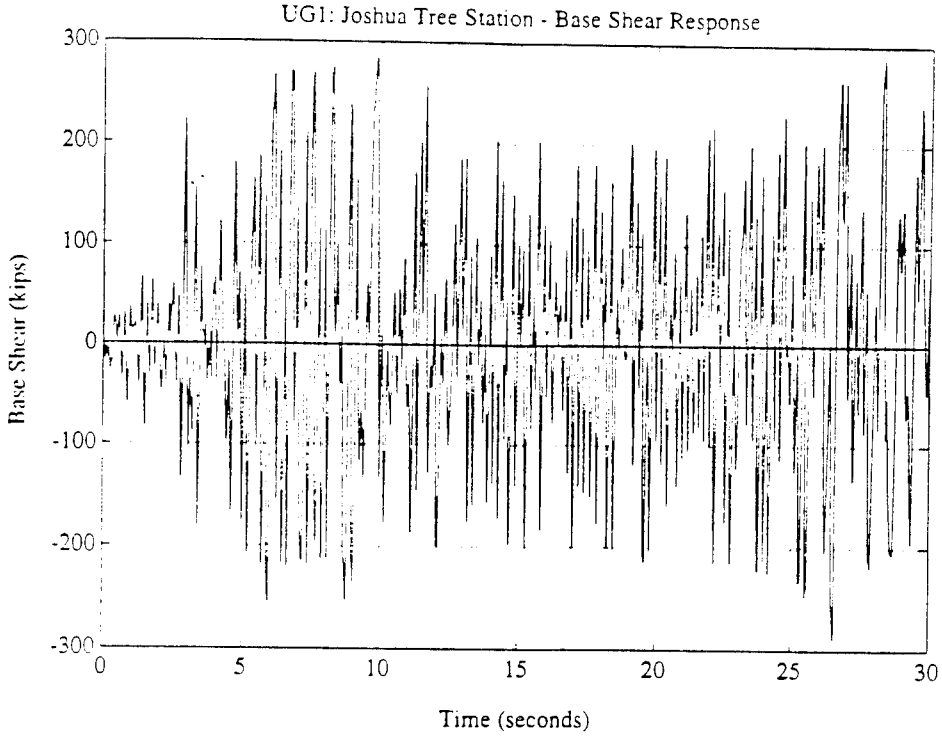

Figure 5.33 UG1: Joshua Tree Station - Base Shear Response

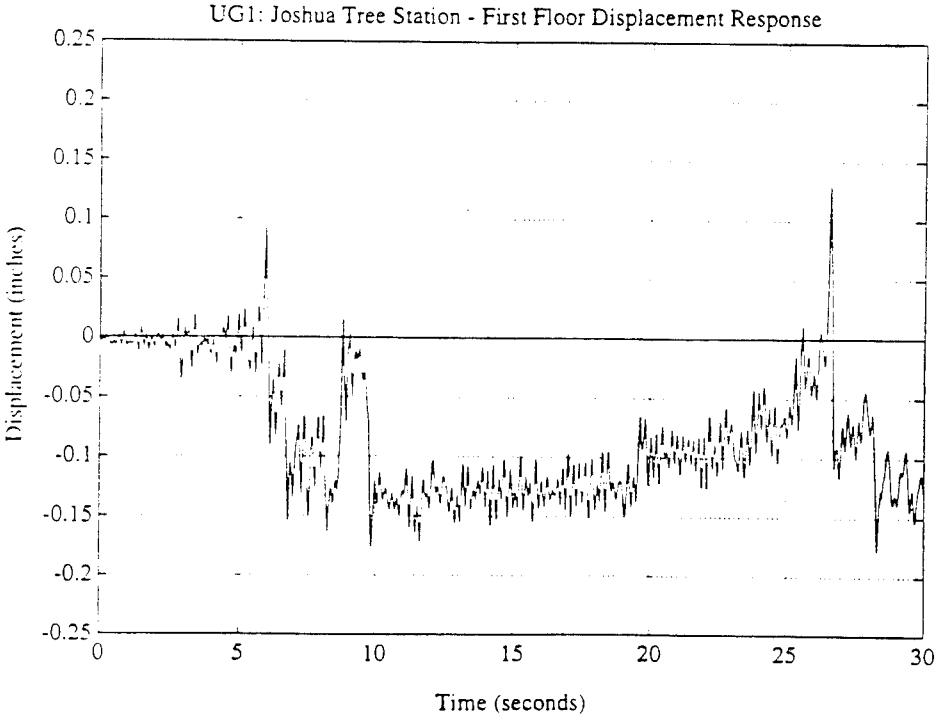

Figure 5.34 UG1: Joshua Tree Station - First Floor Displacement Response

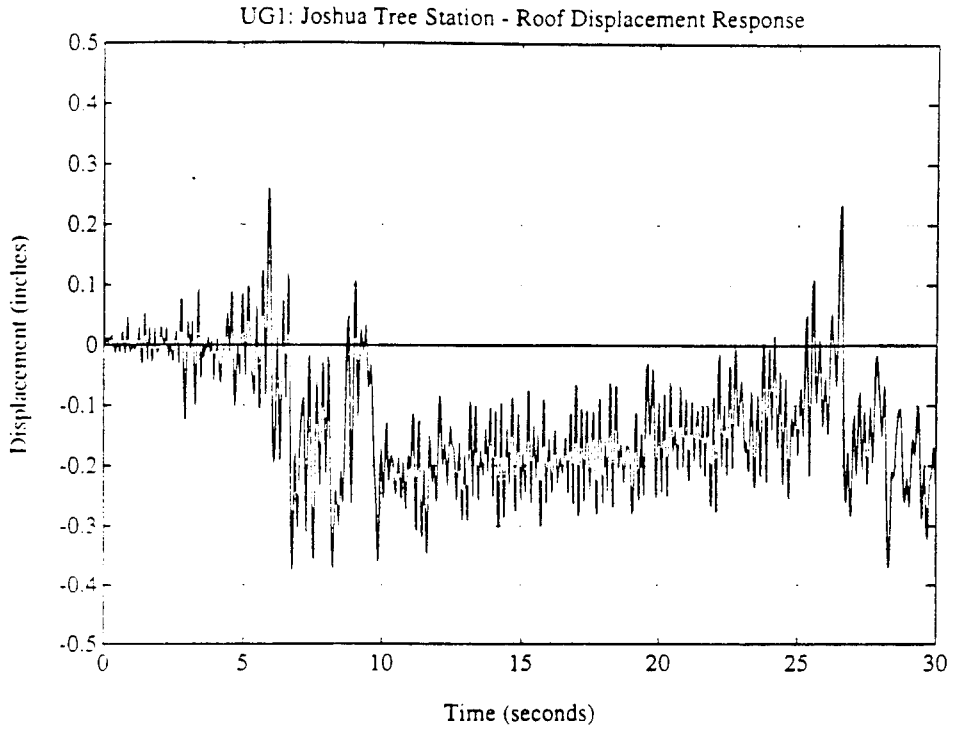

Figure 5.35 UG1: Joshua Tree Station - Roof Displacement Response

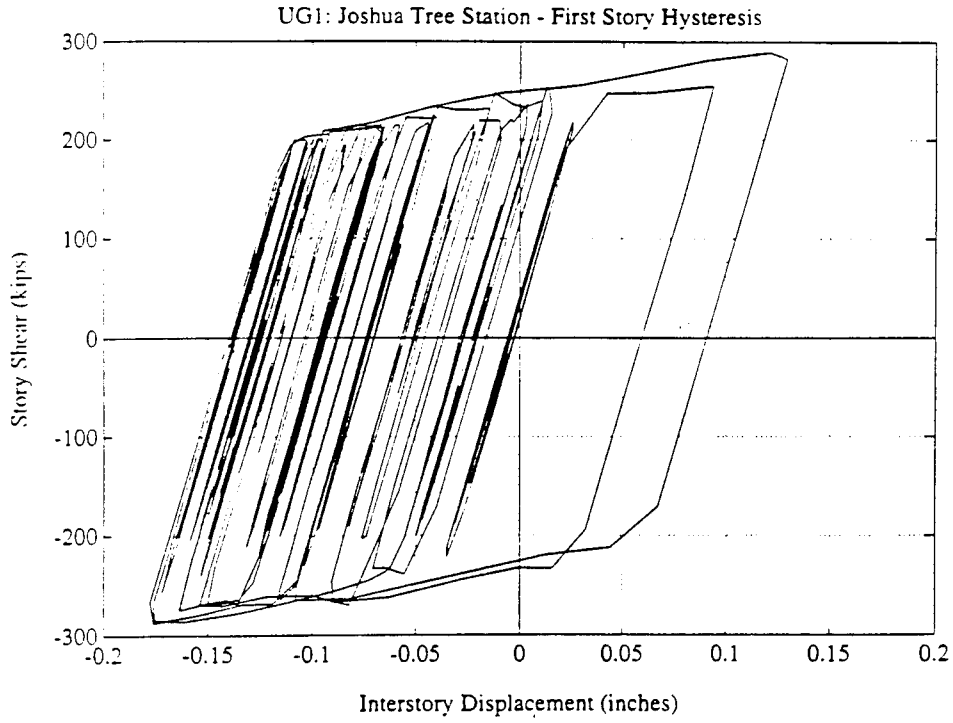

Figure 5.36 UG1: Joshua Tree Station - First Story Hysteresis

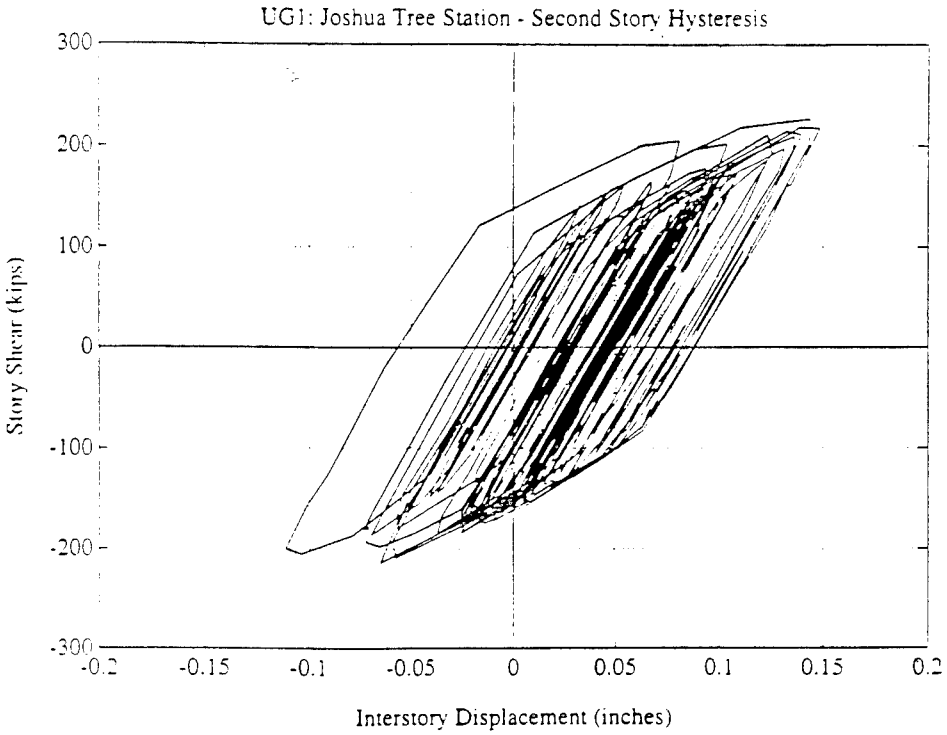

Figure 5.37 UG1: Joshua Tree Station - Second Story Hysteresis

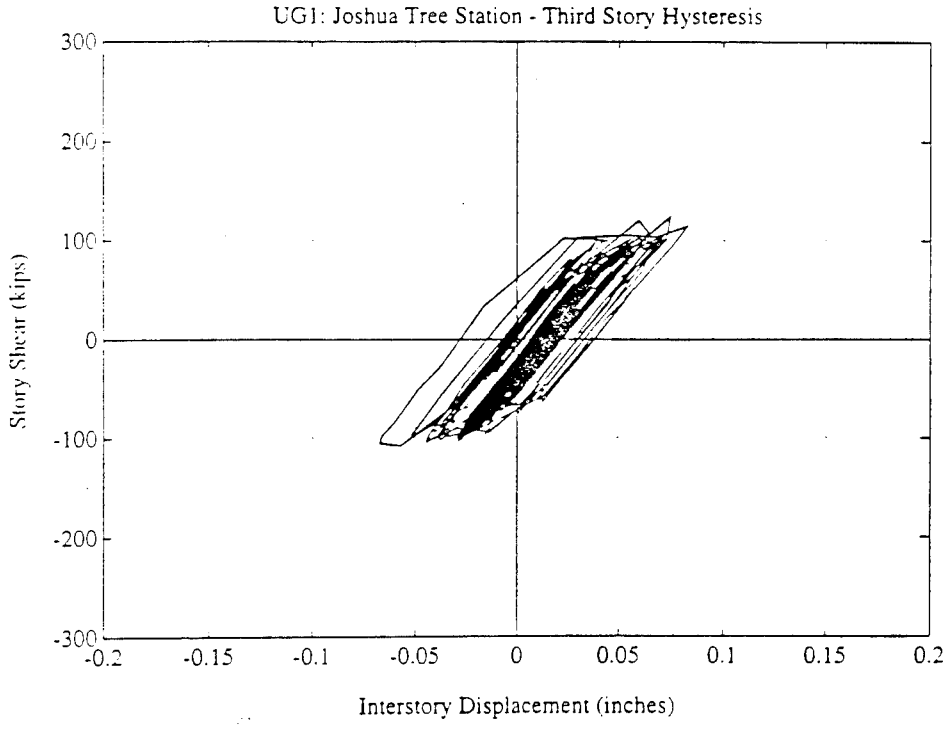

Figure 5.38 UG1: Joshua Tree Station - Third Story Hysteresis

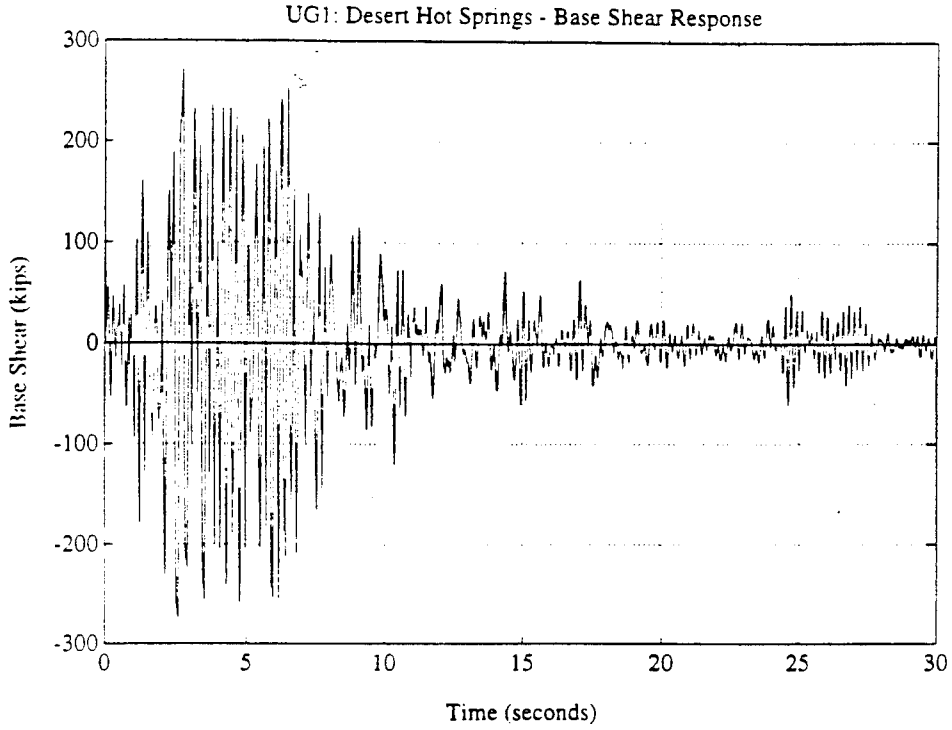

Figure 5.39 UG1: Desert Hot Springs - Base Shear Response

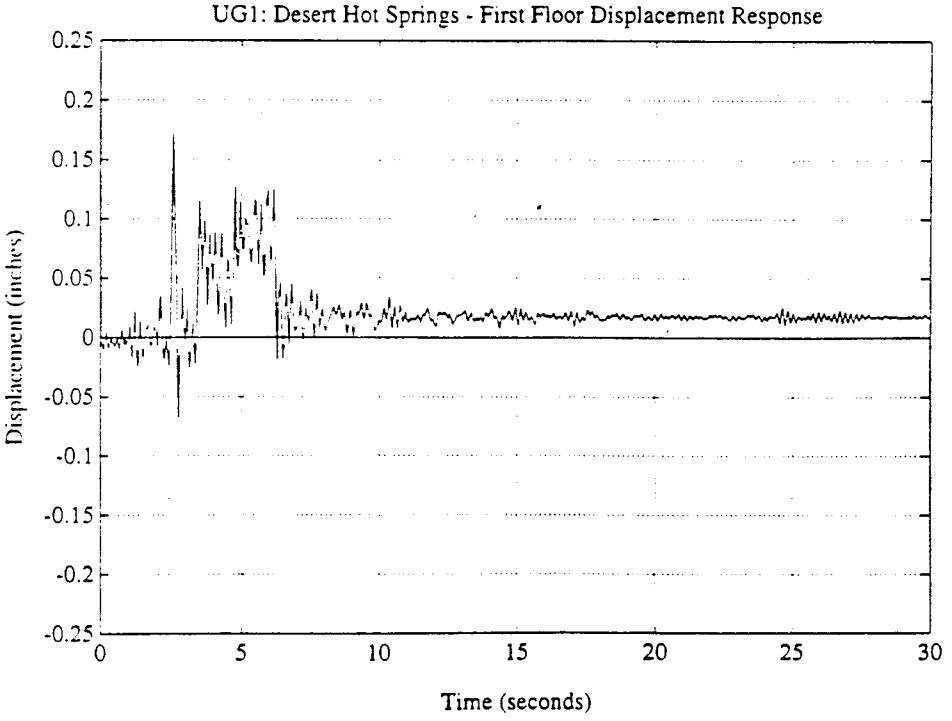

Figure 5.40 UG1: Desert Hot Springs - First Floor Displacement Response

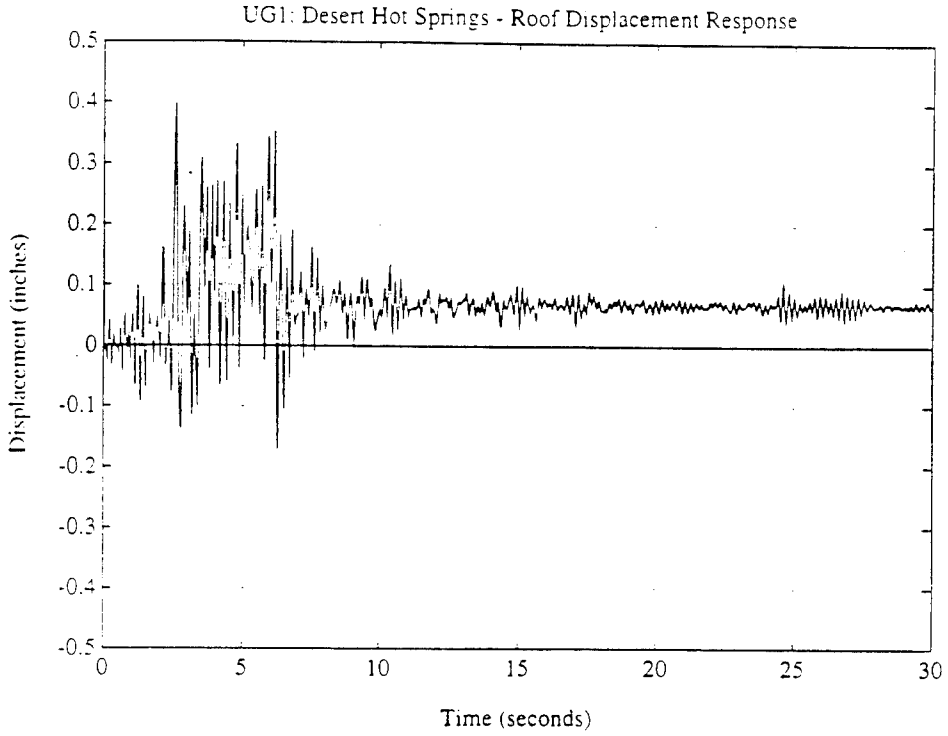

Figure 5.41 UG1: Desert Hot Springs - Roof Displacement Response

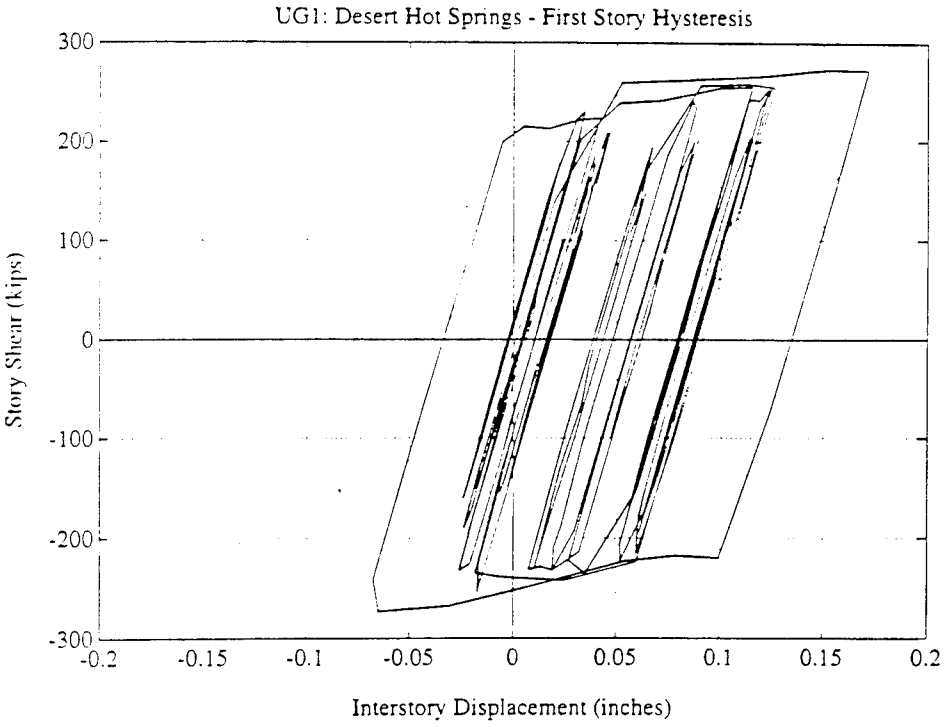

Figure 5.42 UG1: Desert Hot Springs - First Story Hysteresis

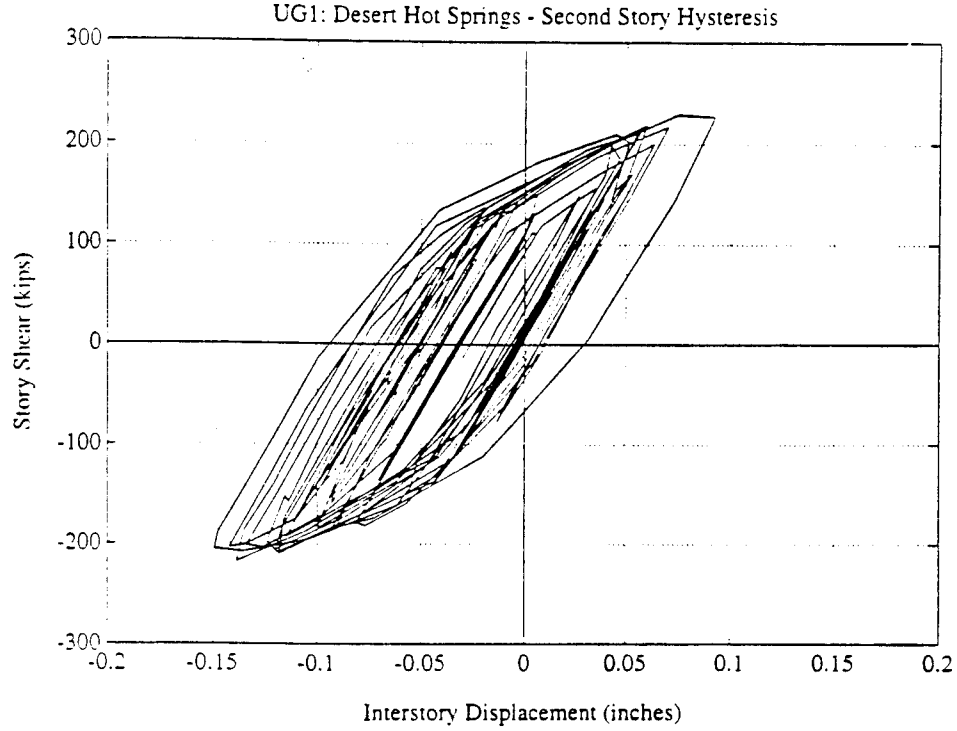

Figure 5.43 UG1: Desert Hot Springs - Second Story Hysteresis

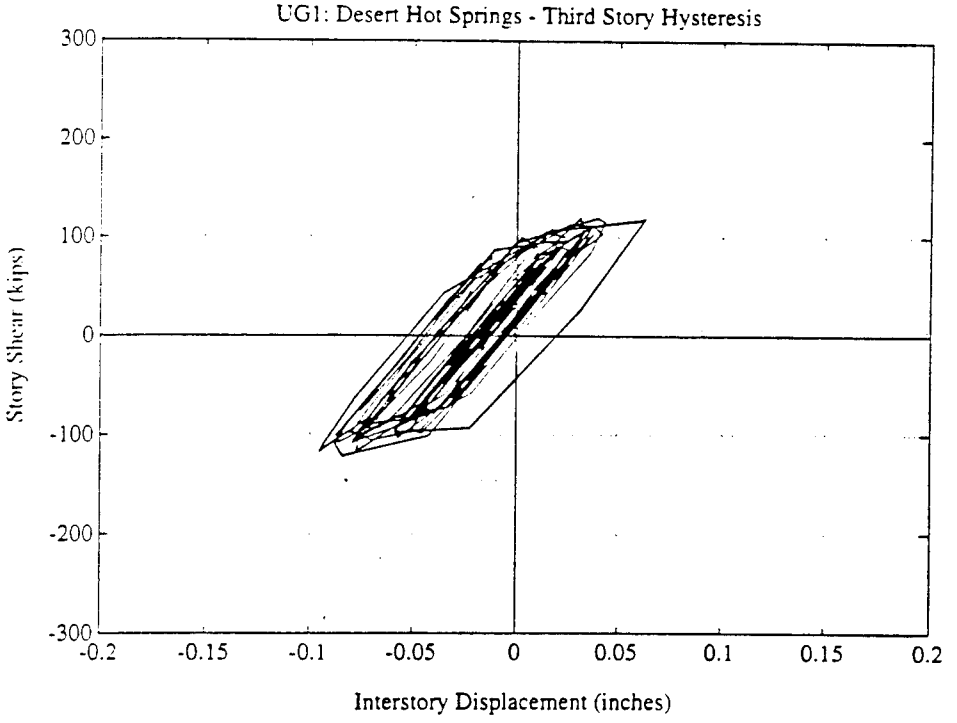

Figure 5.44 UG1: Desert Hot Springs - Third Story Hysteresis

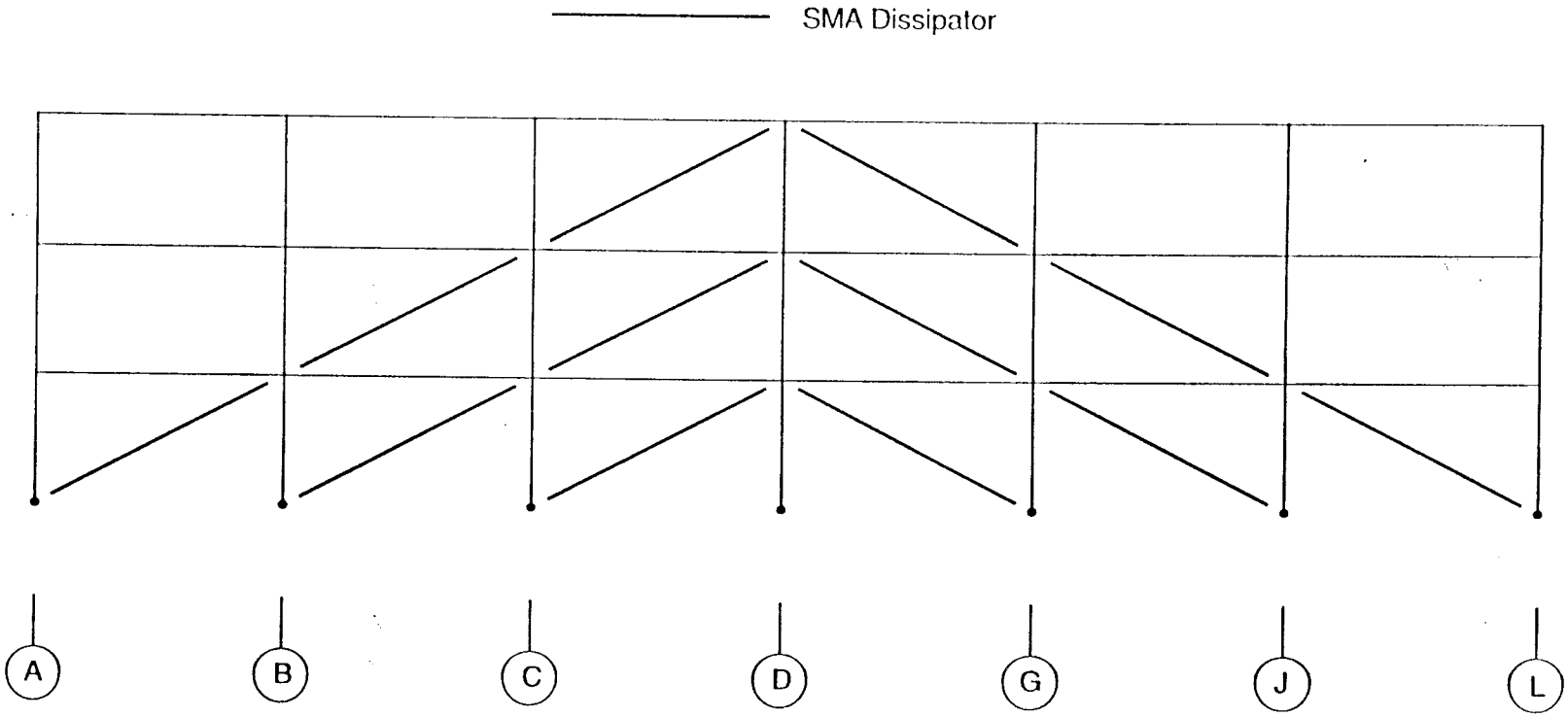

Figure 5.45 UG2: SMA Energy Dissipator Layout

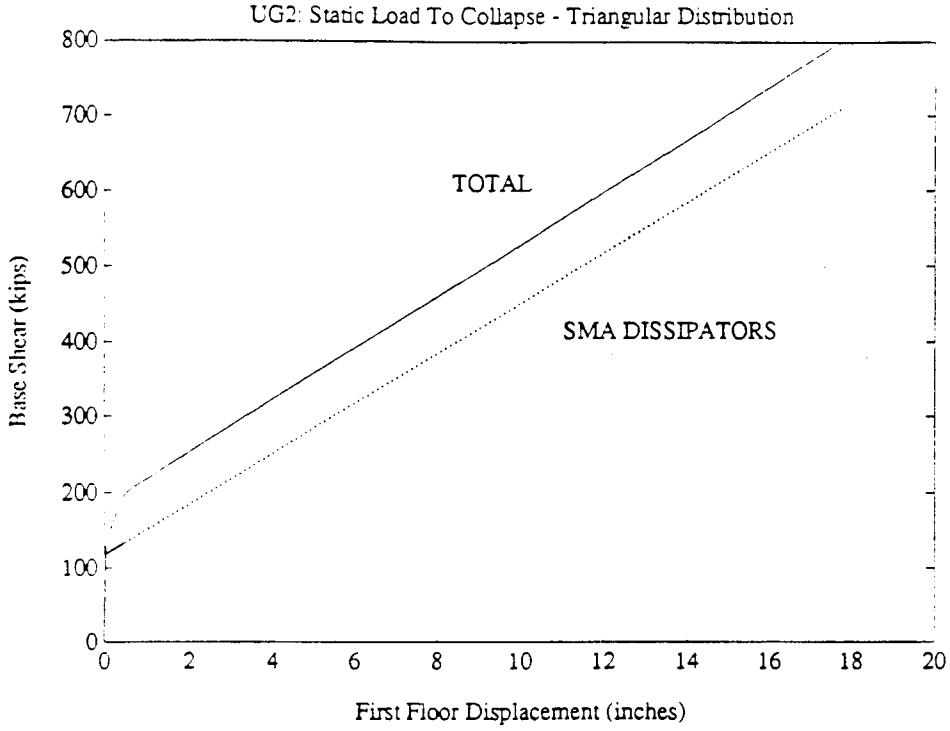

Figure 5.46 UG2: Collapse Analysis Results - Triangular Load Distribution

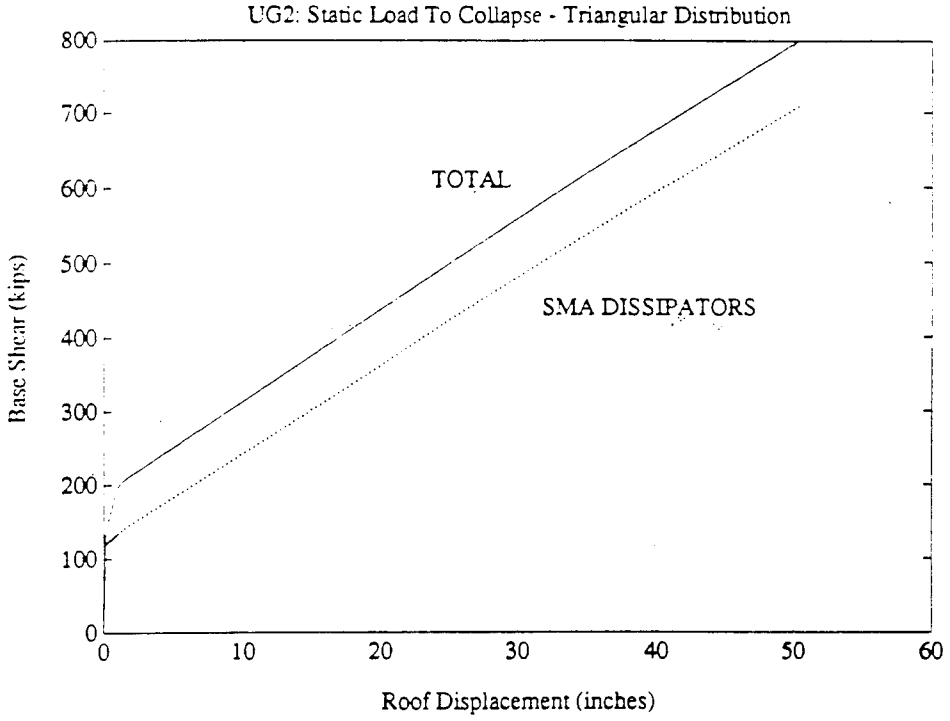

Figure 5.47 UG2: Collapse Analysis Results - Triangular Load Distribution

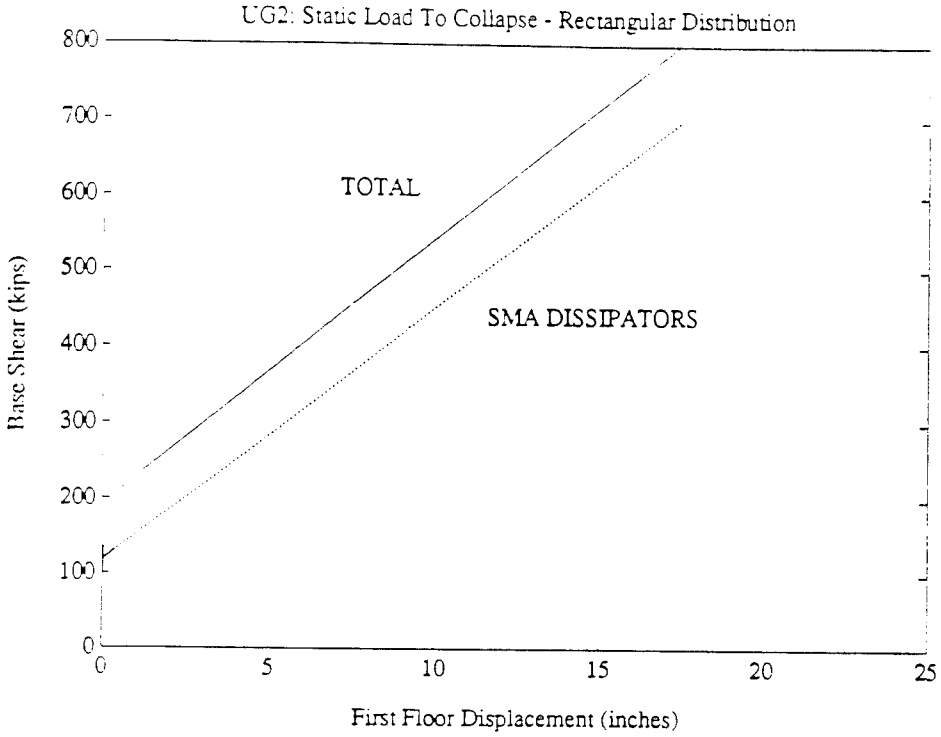

Figure 5.48 UG2: Collapse Analysis Results - Rectangular Load Distribution

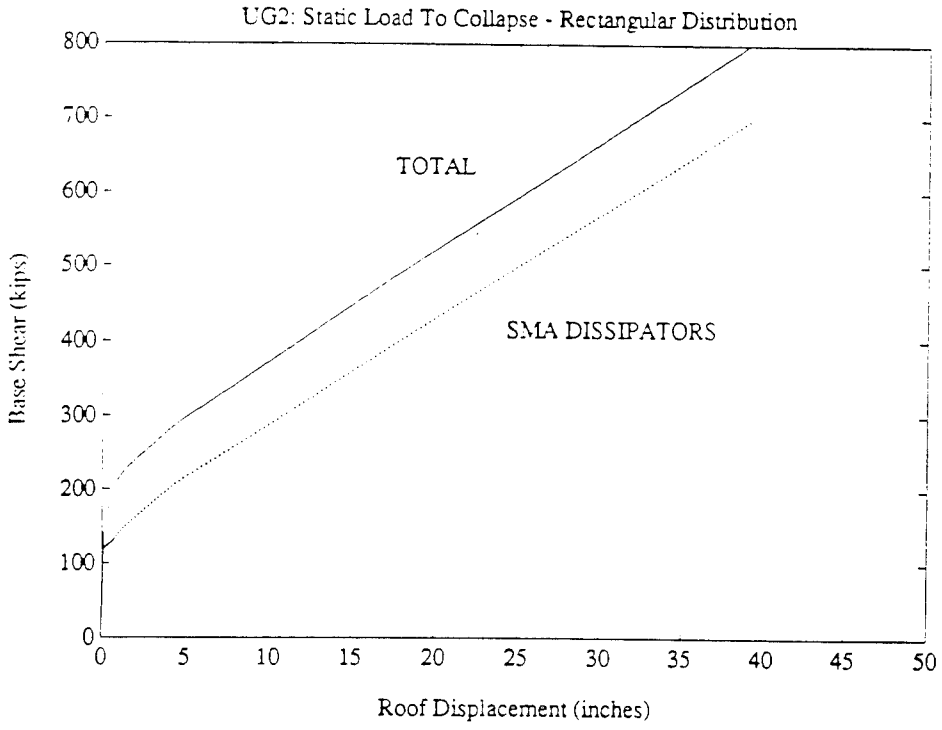

Figure 5.49 UG2: Collapse Analysis Results - Rectangular Load Distribution

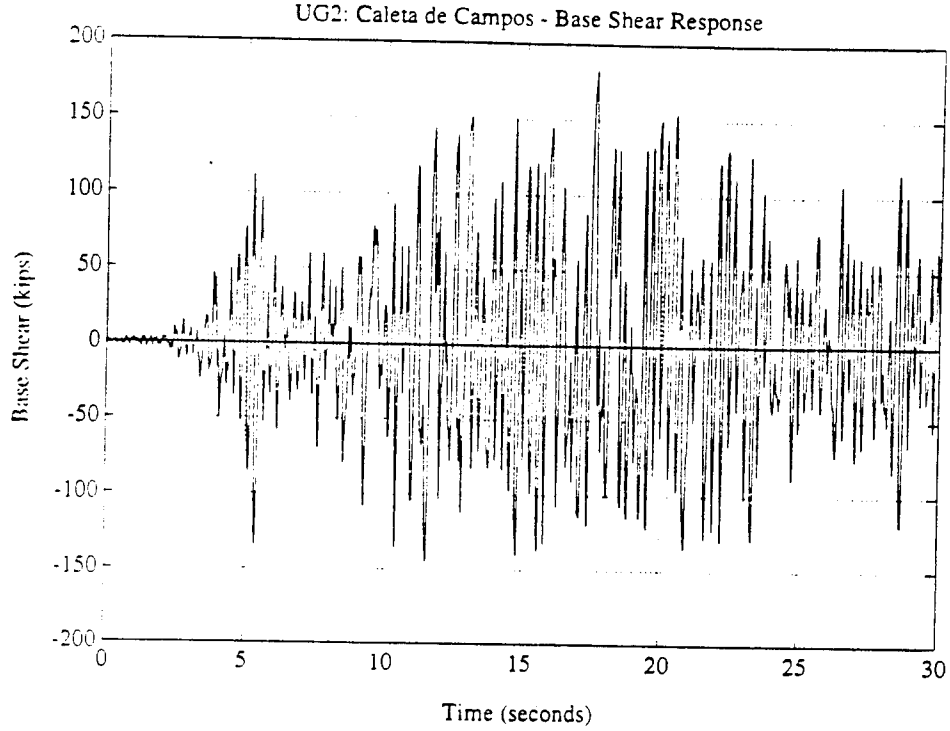

Figure 5.50 UG2: Caleta de Campos - Base Shear Response

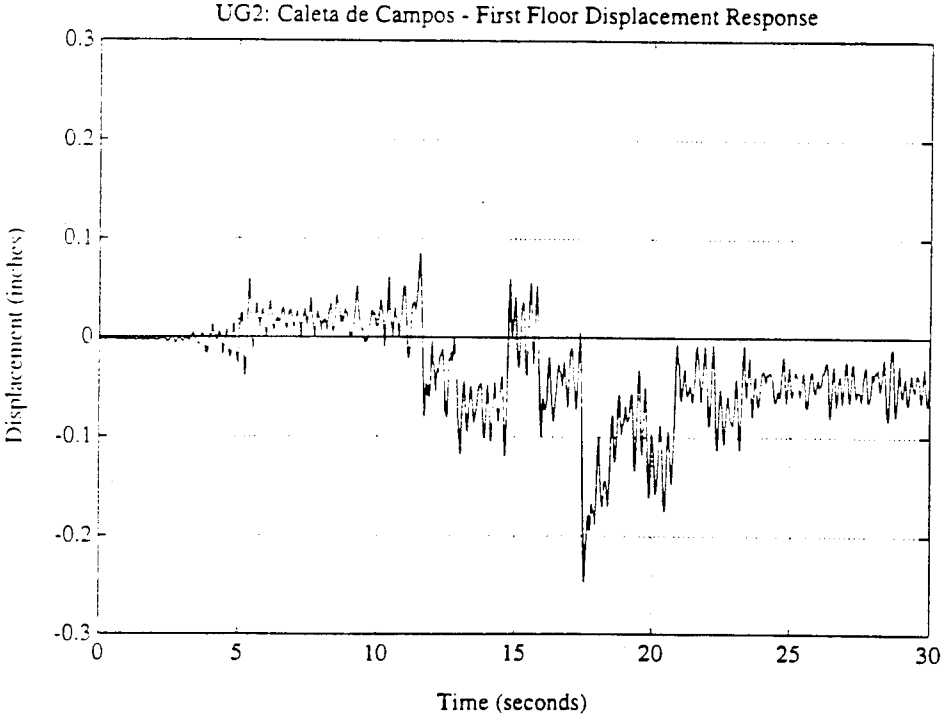

Figure 5.51 UG2: Caleta de Campos - First Floor Displacement Response

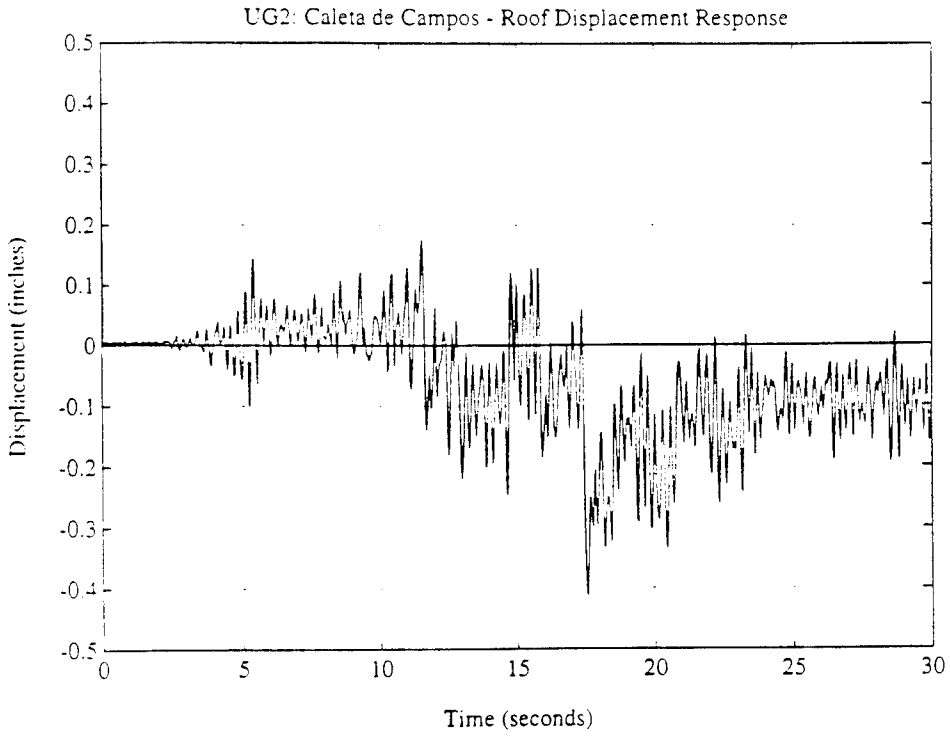

Figure 5.52 UG2: Caleta de Campos - Roof Displacement Response

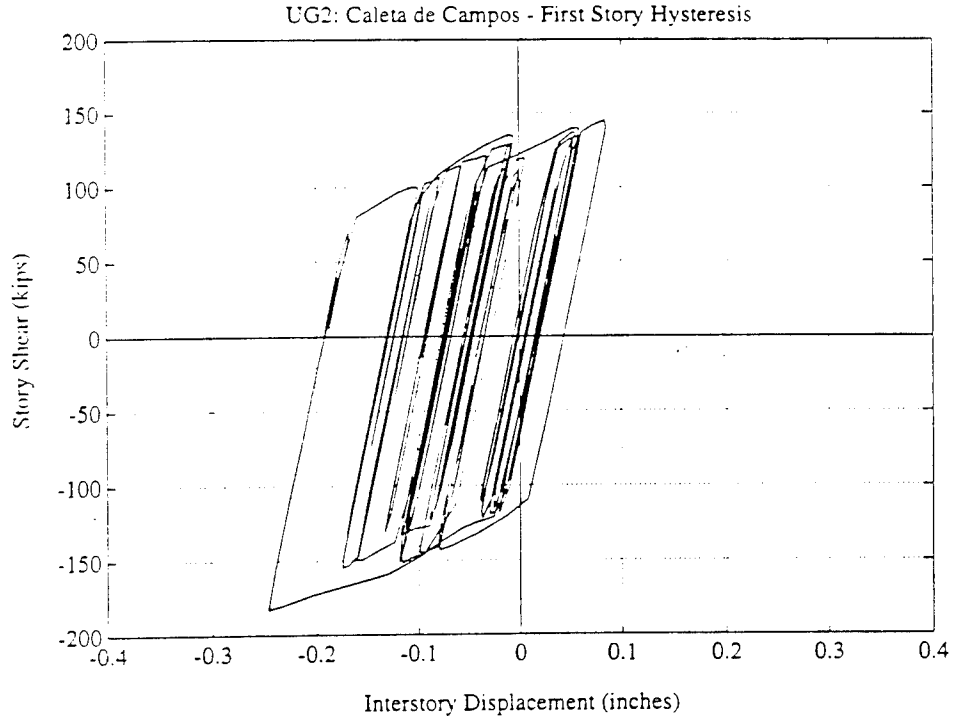

Figure 5.53 UG2: Caleta de Campos - First Story Hysteresis

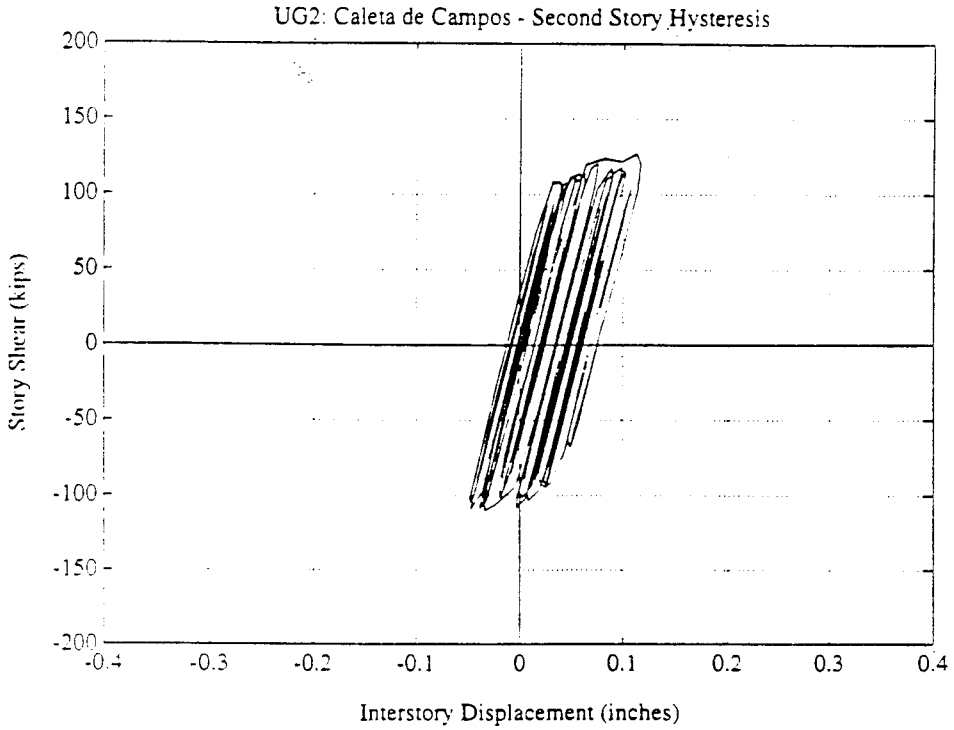

Figure 5.54 UG2: Caleta de Campos - Second Story Hysteresis

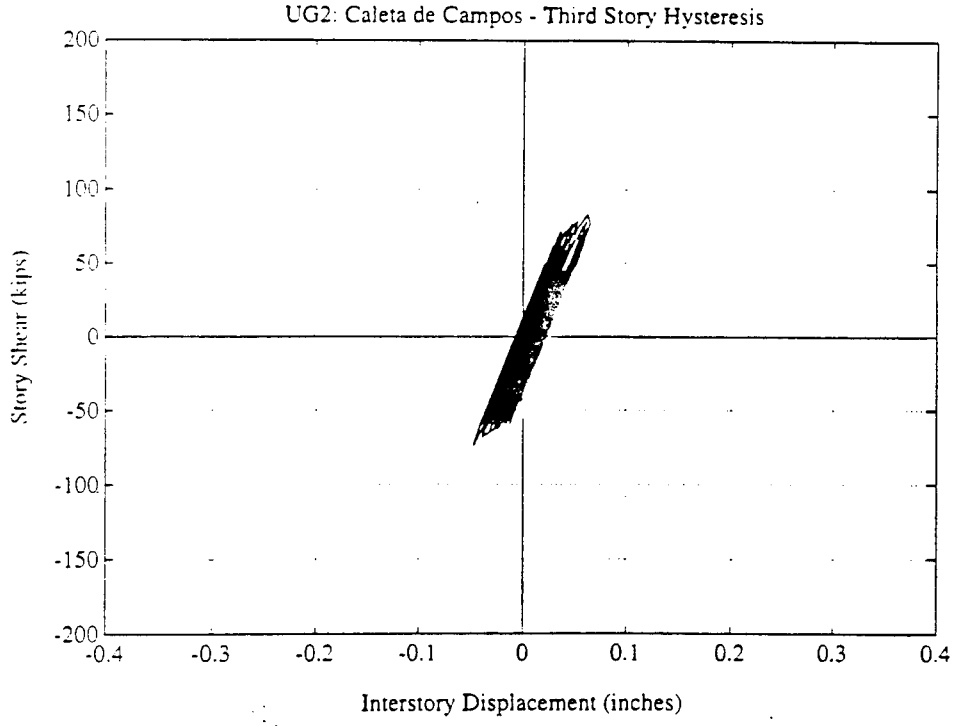

Figure 5.55 UG2: Caleta de Campos - Third Story Hysteresis

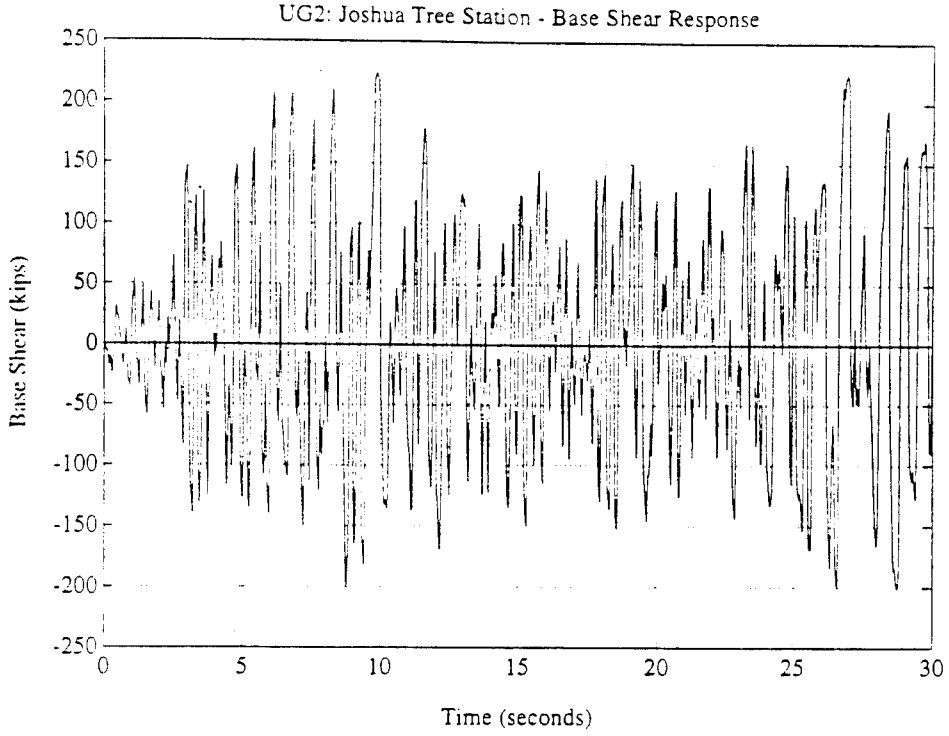

Figure 5.56 UG2: Joshua Tree Station - Base Shear Response

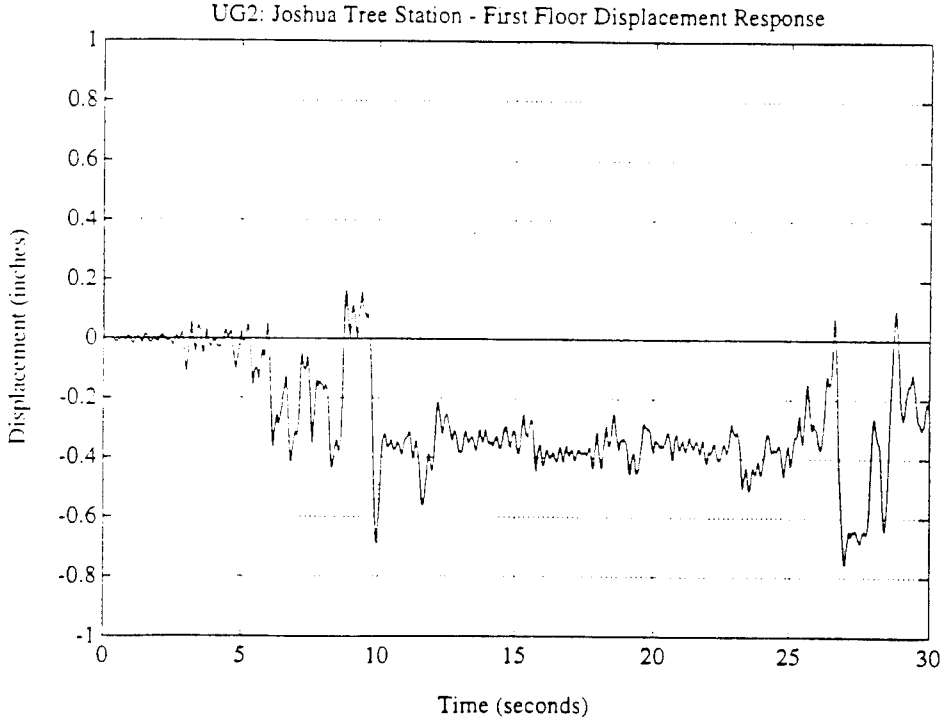

Figure 5.57 UG2: Joshua Tree Station - First Floor Displ. Response

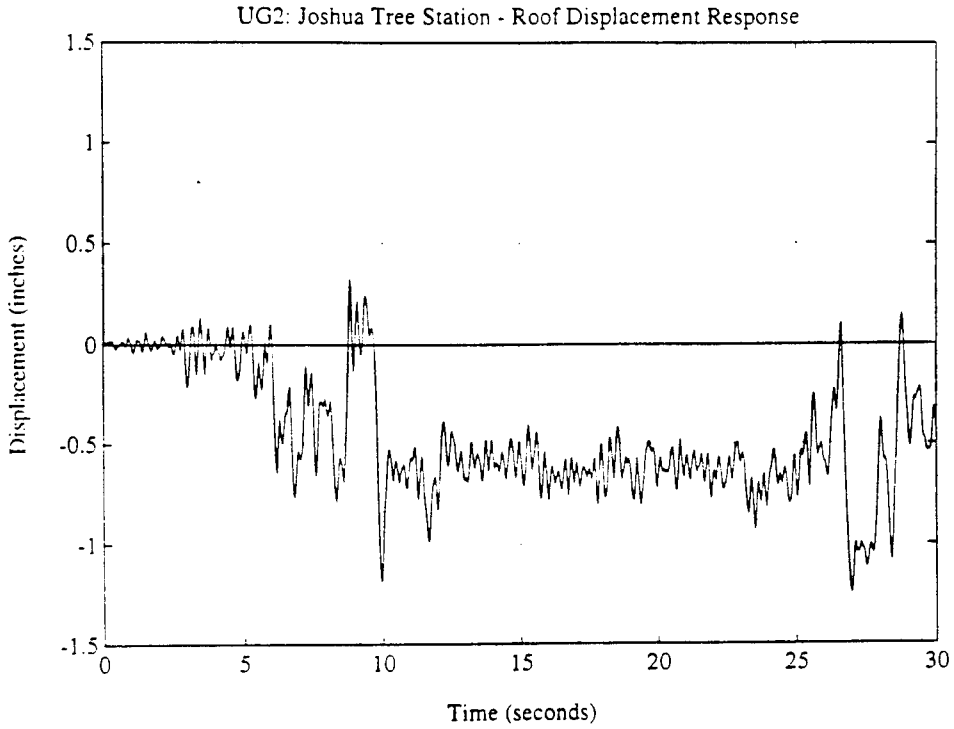

Figure 5.58 UG2: Joshua Tree Station - Roof Displacement Response

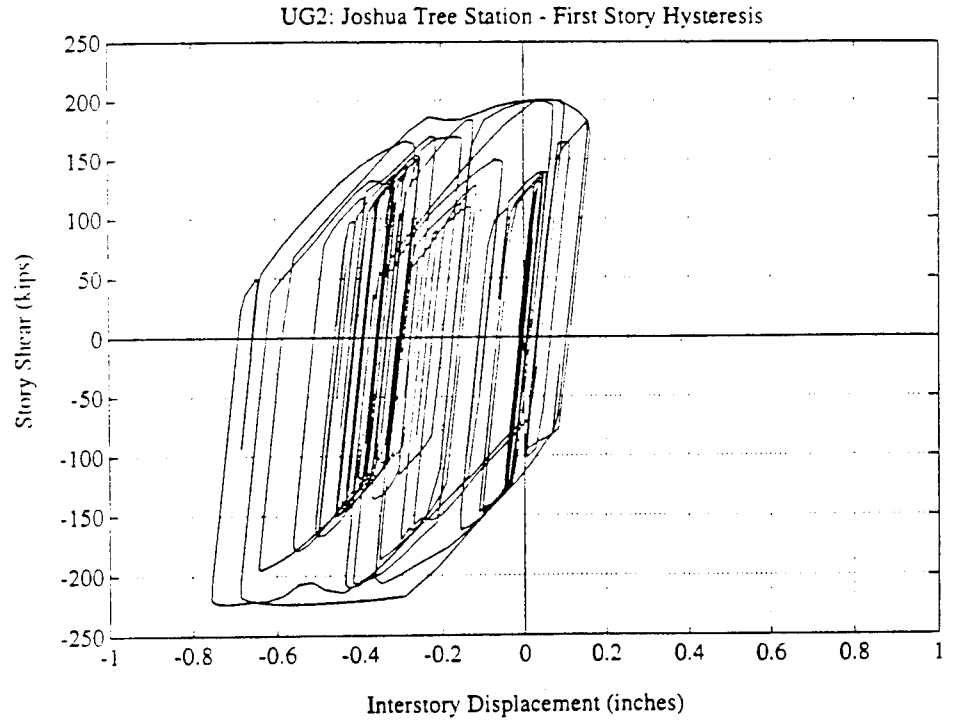

Figure 5.59 UG2: Joshua Tree Station - First Story Hysteresis

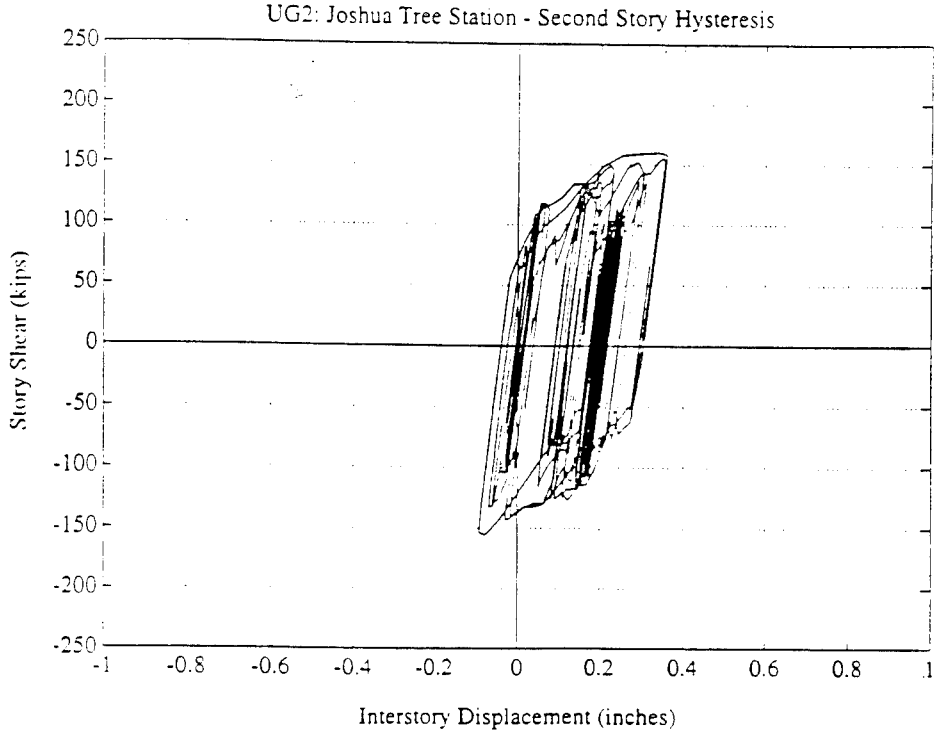

Figure 5.60 UG2: Joshua Tree Station - Second Story Hysteresis

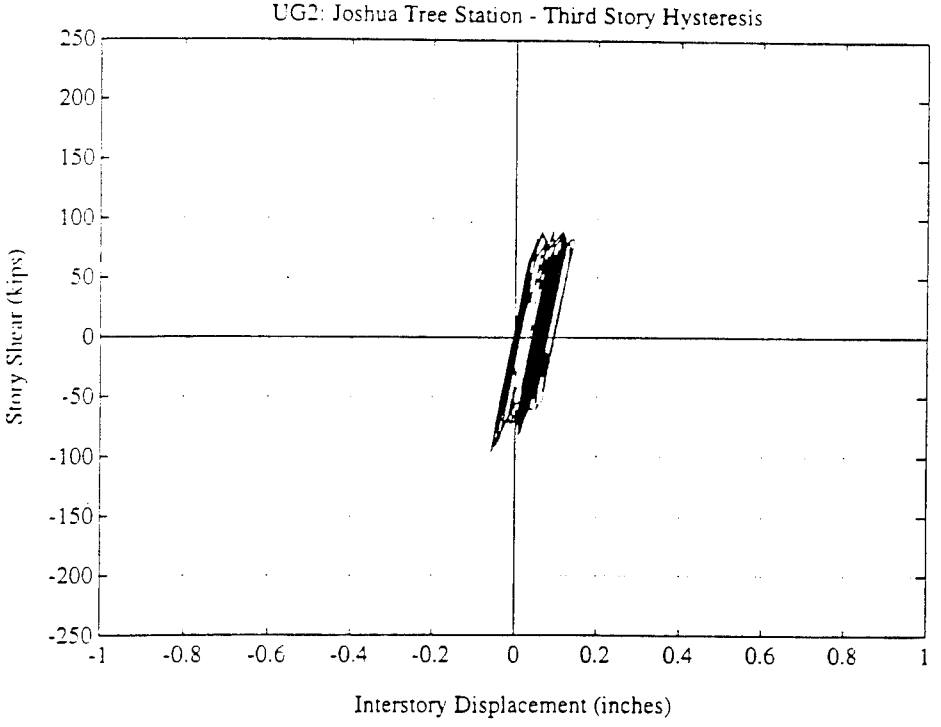

Figure 5.61 UG2: Joshua Tree Station - Third Story Hysteresis

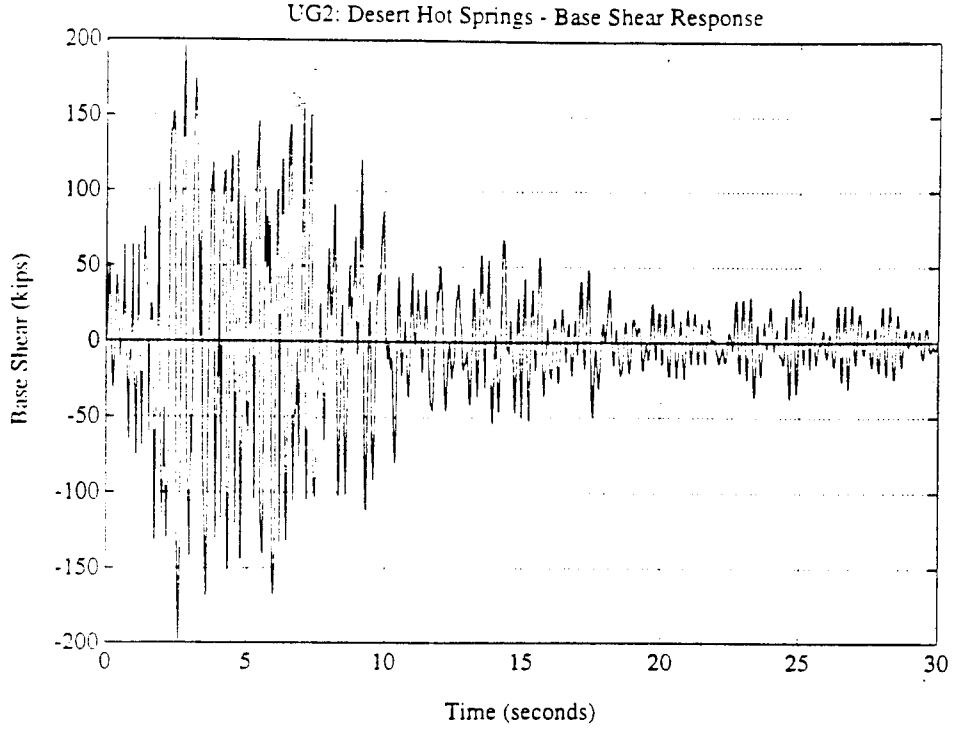

Figure 5.62 UG2: Desert Hot Springs - Base Shear Response

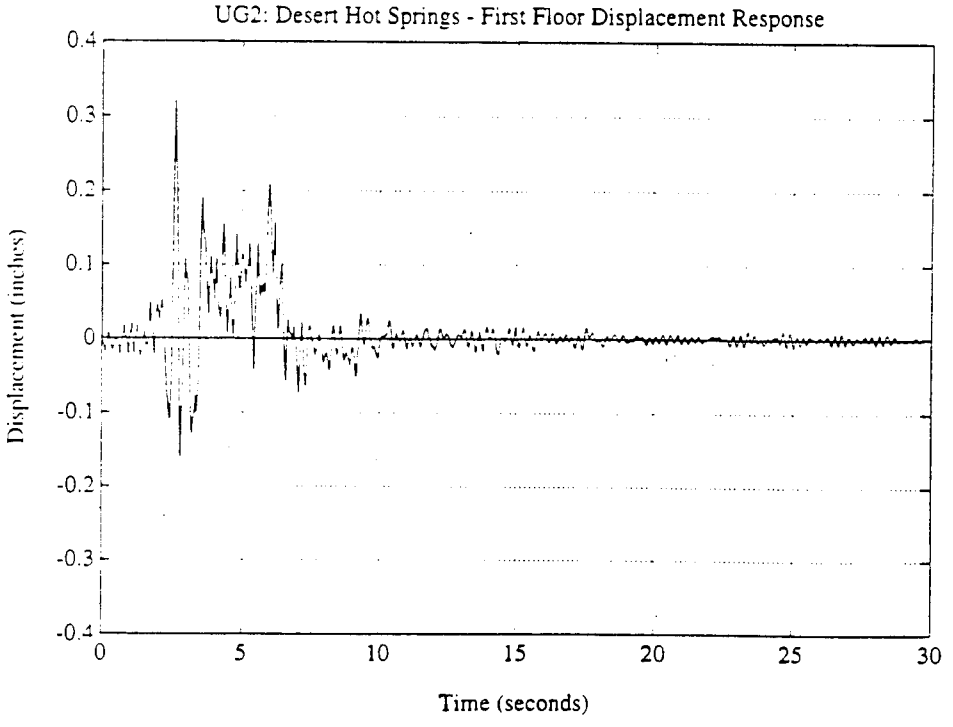

Figure 5.63 UG2: Desert Hot Springs - First Floor Displ. Response

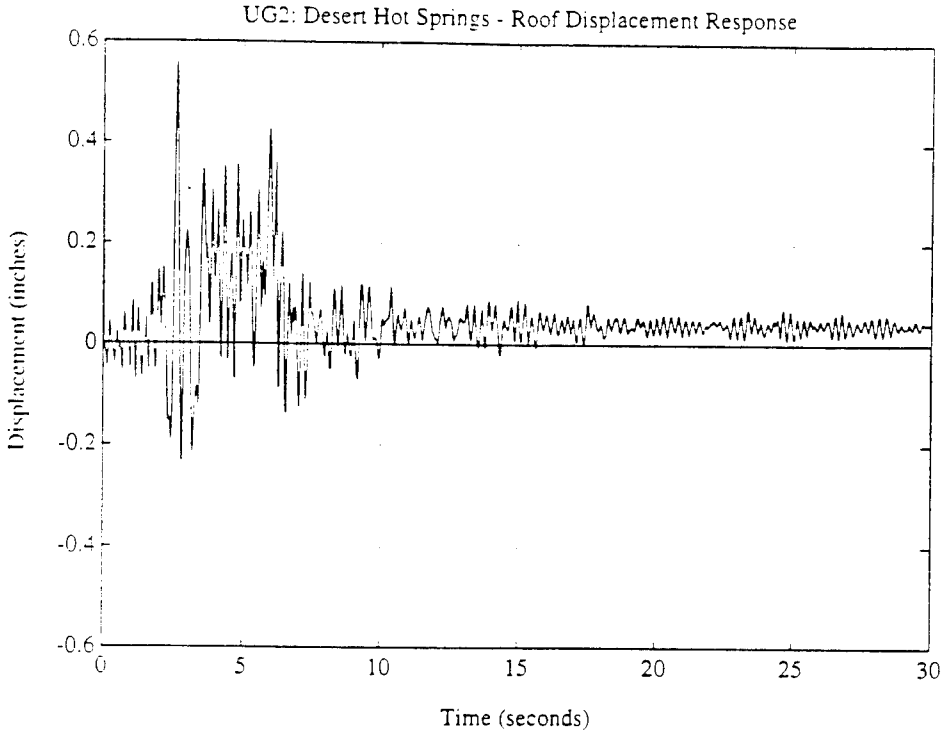

Figure 5.64 UG2: Desert Hot Springs - Roof Displacement Response

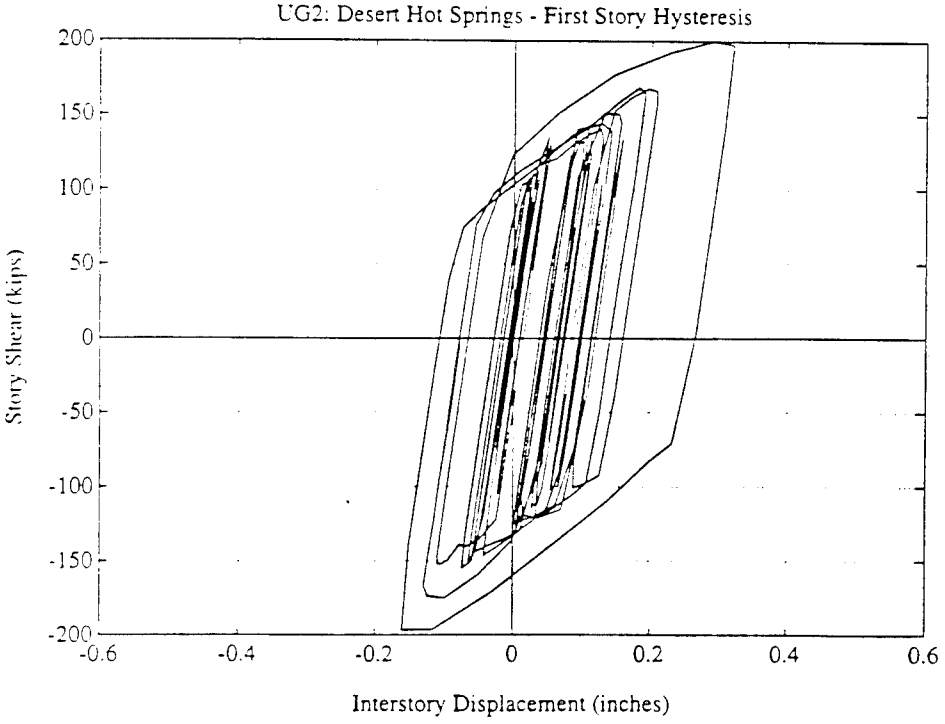

Figure 5.65 UG2: Desert Hot Springs - First Story Hysteresis

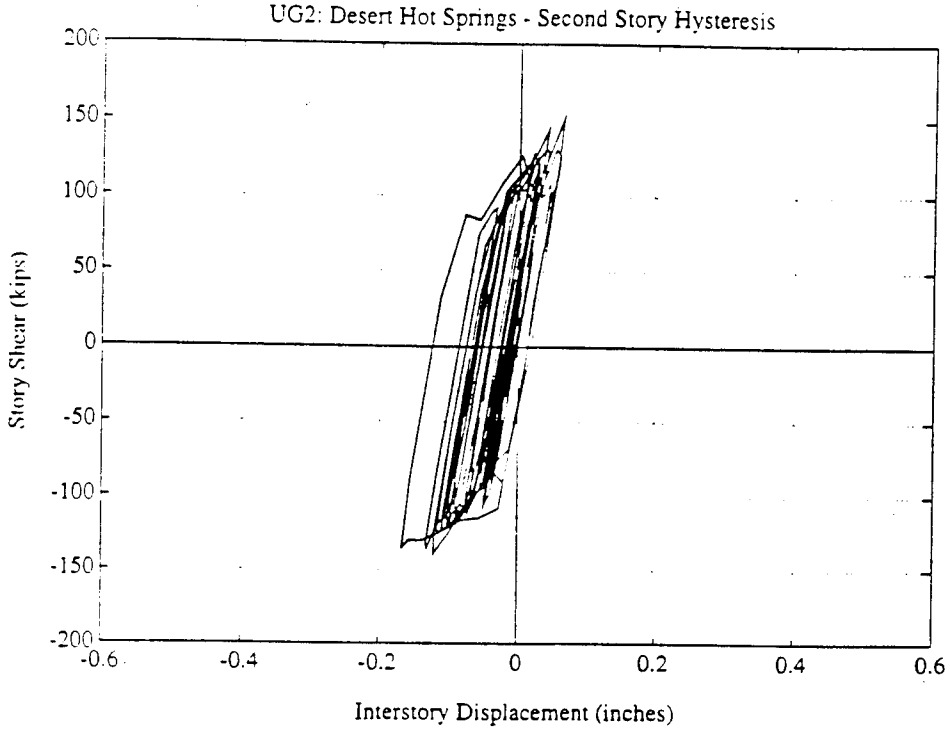

Figure 5.66 UG2: Desert Hot Springs - Second Story Hysteresis

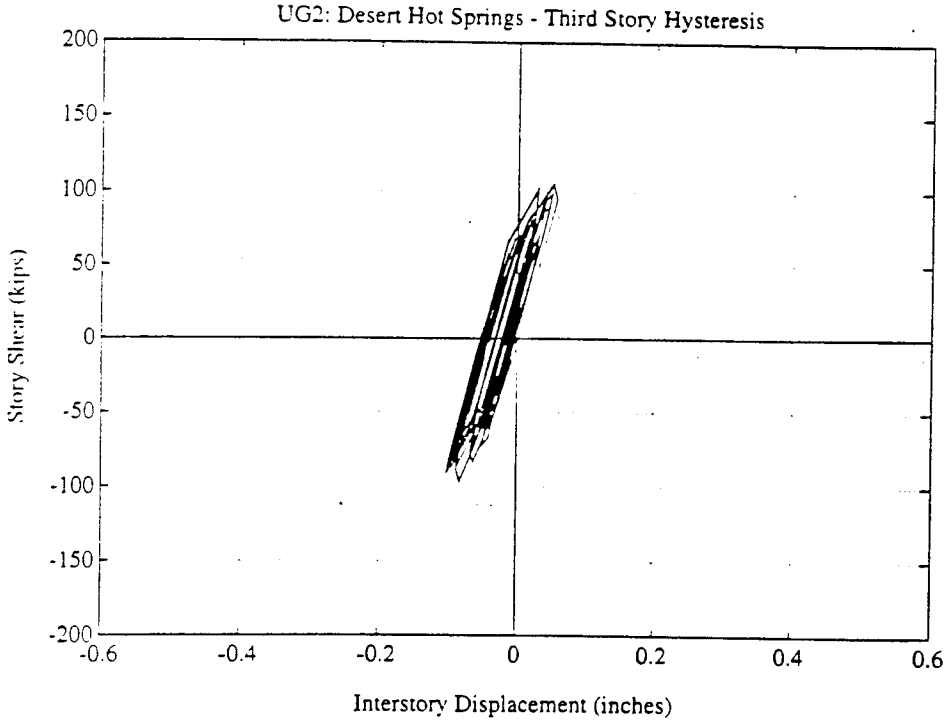

Figure 5.67 UG2: Desert Hot Springs - Third Story Hysteresis

6.0 MODELING SMA HYSTERESIS

6.1 Introduction

One limitation to the analysis of buildings incorporating SMA energy dissipators with DRAIN-2DX is the inability of DRAIN-2DX to model the triangular flag, rectangular flag, and bowtie hystereses illustrated in Figure 4.1. The intent of the research results presented in this chapter is to demonstrate that substantial reductions in the seismic response of buildings can be achieved with two of the three hystereses noted above: rectangular flag and triangular flag.

As part of the Phase I research effort, the rectangular and triangular flag hystereses were developed in the MATLAB environment and exported to a recently completed but as yet unpublished nonlinear computer program INADEL developed by Inaudi. The currently compiled version of INADEL can only accommodate lumped-mass stick-models of buildings. For this reason, the condensed mass and stiffness properties of the frame analyzed in Chapter 5 were extracted in Section 5.10.

The stick-model of the existing building is described in Figure 6.1 and consists of a lumped-mass model with three degrees of freedom. The strength-deformation relationship of each story is modeled by an elasto-plastic element. The floor masses are M_1 = 1.03 kip s^2/in, M_2 = 1.03 kip s^2/in, and M_3 = 0.87 kip s^2/ in. The story stiffnesses are 78 kip/in, 100 kip/in, and 80 kip/in; the story strengths are 67.5 kips, 120 kips, and 100 kips in the first, second, and third stories, respectively.

The response of this shear building to the Desert Hot Springs earthquake was computed using INADEL and compared with the results obtained using DRAIN-2DX in order to test the accuracy of INADEL. Figure 6.2 compares the first-story lateral displacement obtained using both programs using an integration step of 0.005s. It is apparent from the figure that comparable results are obtained using the two programs. In the following sections, the analysis of the seismic response of the structure with energy dissipating devices that can't be modeled in DRAIN-2DX is undertaken using INADEL.

6.2 Modeling SMA Hysteresis

Two force-deformation relations achievable with SMAs were studied. The first is a simplified model of the behavior of SMA material in tension while the second is a linear-friction model achievable using prestressed SMA wires loaded in the direction perpendicular to the wires. Figures 6.3 and 6.4 show the force-deformation relations used in the analyses. In the first force-deformation relation, denoted 'N' for Nitinol, the parameters are the initial stiffness K0, the force in the loading phase transformation

F1, and the force in the unloading phase transformation F2. In the second force-deformation relation, named 'T' for triangle, the parameters are the loading stiffness K1, the unloading stiffness K2, and the stiffness of the transition between loading and unloading, K3. Clearly, while the first model dissipated energy proportionally to the first power of the deformation amplitude, the second model dissipated energy proportionally to the square of the deformation amplitude.

6.3 MATLAB Modeling of SMA Hysteresis

The two force-deformation relationships ('N' and 'T') were programmed in the MATLAB environment as elements for INADEL. The element subroutines compute the force in the mechanical device as a function of the deformation history for a given set of element parameters (K0, F1, and F2 or K1, K2, and K3). A third element, an elastoplastic element, was available in INADEL and was used to model the mechanical characteristics of the reduced-order model of the building.

Two earthquake signals were used for the analyses: Desert Hot Springs and Caleta de Campos. The integration step was 0.005s for all the analyses.

Eight configurations of the energy dissipating devices were selected, and the responses of the mathematical model with and without the energy dissipating devices (EDDs) were computed. The configurations were named N1, N2, N3, N4, T1, T2, T3, and T4. The parameters of these configurations are described in the following tables.

NAME	FLOOR	K0 (kip/in)	F1 (kips)	F2 (kips)
N1	1	2000	600	300
	2	1333	400	200
	3	400	200	100
N2	1	6000	600	300
	2	4000	400	200
	3	2000	200	100
N3	1	3000	900	450
	2	2000	600	300
	3	600	300	150
N4	1	9000	900	450
	2	6000	600	300
	3	3000	300	150

Table 6.1 Configurations N1, N2, N3 and N4

NAME	FLOOR	K1 (kips/in)	K2 (kips/in)	K3 (kips/in)
T1	1	500	250	2000
	2	500	250	2000
	3	250	125	1250
T2	1	500	50	2000
	2	500	50	2000
	3	250	25	1250
T3	1	750	375	3000
	2	750	375	3000
	3	375	185	1850
T4	1	1000	100	4000
	2	1000	100	4000
	3	500	50	2500

Table 6.2 Configurations T1, T2, T3, and T4

6.4 Discussion of the Time History Analysis Results

The response of the model with and without energy dissipating devices was computed using INADEL. The maximum interstory drifts and maximum forces in the SMA energy dissipating devices obtained from the analyses are shown in the following tables for the Desert Hot Springs and Caleta de Campos earthquake records.

FLOOR	Interstory Drift (inches)								
	No EDD	N1	N2	N3	N4	T1	T2	T3	T4
1	3.15"	1.51"	0.45"	0.76"	0.45"	1.46"	1.43"	0.87"	0.75"
2	1.27"	1.09"	0.53"	1.04"	0.56"	1.03"	0.97"	0.72"	0.58"
3	1.16"	1.59"	1.32"	1.67"	1.77"	1.03"	0.99"	0.77"	0.67"

Table 6.3 Desert Hot Springs: Interstory Drifts

FLOOR	Maximum Axial Force (kips)							
	N1	N2	N3	N4	T1	T2	T3	T4
1	600k	600k	900k	900k	732k	714k	653k	753k
2	400k	400k	600k	600k	517k	487k	543k	580k
3	200k	200k	300k	300k	257k	249k	288k	339k

Table 6.4 Desert Hot Springs: Maximum Force In EDDs

FLOOR	Interstory Drift (inches)				
	No EDD	N1	N2	T1	T2
1	2.63"	0.57"	0.29"	1.23"	1.00"
2	0.88"	0.78"	0.46"	0.77"	0.67"
3	1.06"	1.15"	0.68"	0.76"	0.71"

Table 6.5 Caleta de Campos: Interstory Drifts

FLOOR	Maximum Axial Force (kips)			
	N1	N2	T1	T2
1	600k	600k	617k	501k
2	400k	400k	385k	337k
3	200k	200k	191k	177k

Table 6.6 Caleta de Campos: Maximum Forces In EDDs

From the results presented in Tables 6.3 through 6.6, it is apparent that significant improvements in the performance of the building can be achieved through the use of SMA energy dissipators. The interstory drifts can be substantially reduced by the increased stiffness and energy dissipation capability provided by the hysteretic SMA energy dissipators. Note that the distribution and characteristics of the energy dissipating devices used in configurations N1 to N4 and T1 to T4 were not optimized.

A comparison of the first interstory drift time history response for the building with and without energy dissipating devices is presented in Figures 6.5 for Configurations N1 and N2 and in Figure 6.6 for Configurations T1 and T2. The Desert Hot Springs earthquake record was used for this response comparison. Figure 6.7 shows the

force-deformation response of the first story of the building to the Desert Hot Springs earthquake record; no EDDs were included in the building for this analysis. Figures 6.8 and 6.9 illustrate the force-deformation response of the first-story building frame (dashed lines), and the force-deformation response in the EDD in the first story for Configurations N1 and T1 (solid lines), respectively.

The N1 and T1 energy dissipator configurations significantly improve the seismic response of the existing building (denoted EB in the figure titles) by reducing the displacements in the frame to a level that eliminates significant nonlinear response in the existing non-ductile concrete frame.

6.5 Summary and Conclusions

A preliminary study of the response of a non-ductile concrete frame upgraded with hysteretic energy dissipation devices has been undertaken.

Using a reduced-order model for the existing building and simple hysteretic models for the SMA energy dissipation devices, the seismic performance of the building with and without energy dissipators was computed and compared.

Although the selected configurations and parameters for the energy dissipators were not optimized, significant improvements in the response of the non-ductile frame were obtained using both the SMA alloy in tension (Configuration 'N') and a linear-friction SMA resistance scheme (Configuration 'T').

The results of this study using INADEL are essentially the same as those found from the DRAIN-2DX analysis presented in Chapter 5. INADEL offers modeling capabilities that do not currently exist in DRAIN-2DX. All four hystereses depicted in Figure 4.1 can be modeled with INADEL. Currently, of the four hystereses presented in Figure 4.1, only the rectangular hysteresis can be modeled in DRAIN 2DX.

The analytical work proposed for Phase II will involve the development of an SMA element for DRAIN-2DX whereby all of the hystereses presented in Figure 4.1 can be modeled in this commonly available nonlinear analysis program.

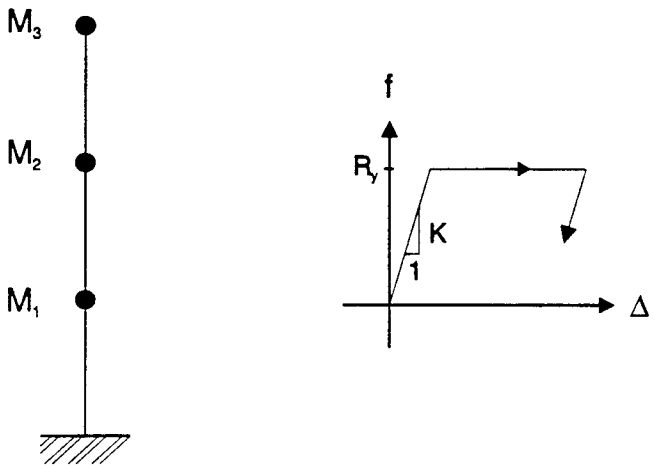

Figure 6.1 Mathematical Model For INADEL Analysis

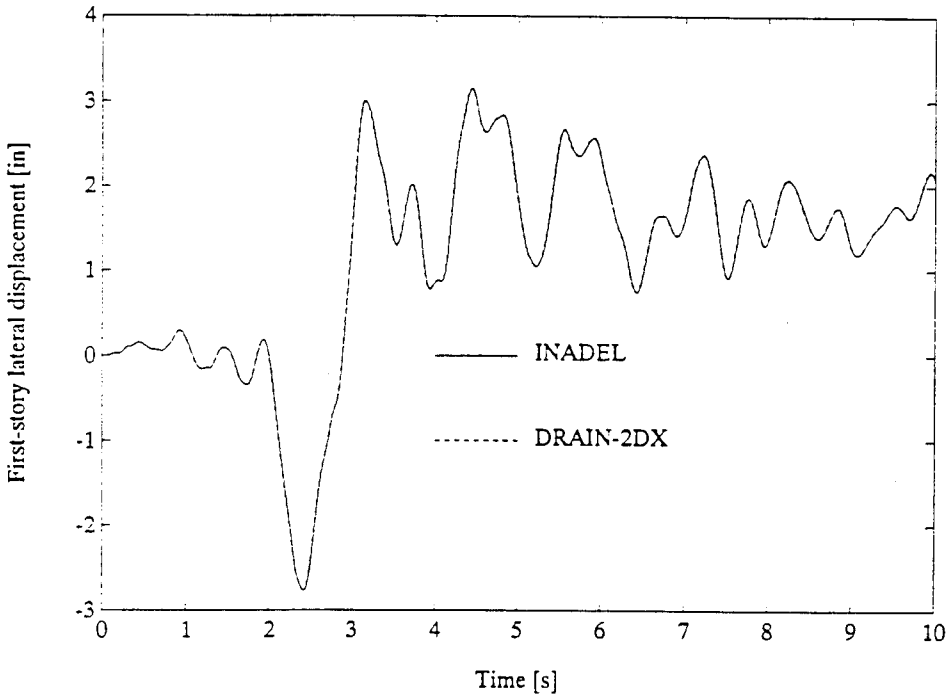

Figure 6.2 DRAIN-INADEL Response Comparison

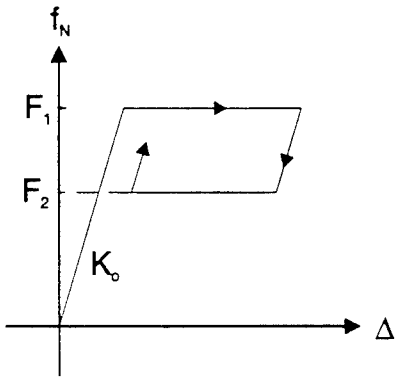

Figure 6.3 Configuration N Hysteresis

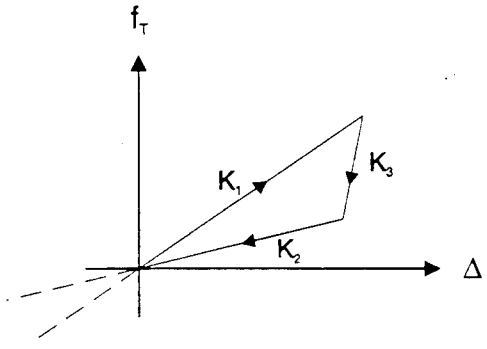

Figure 6.4 Configuration T Hysteresis

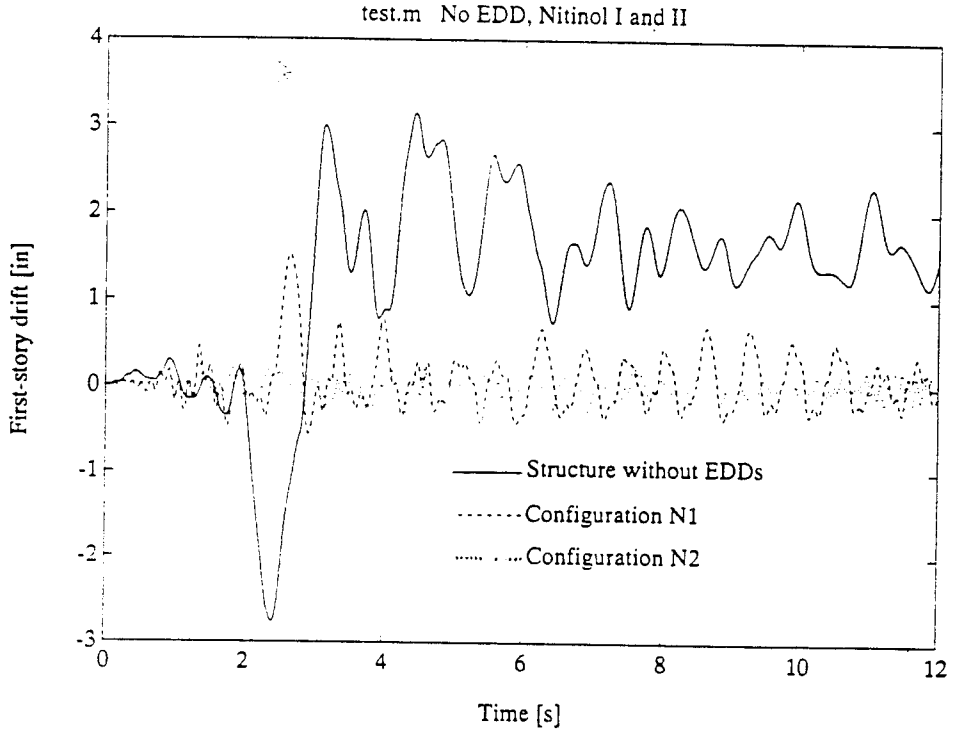

Figure 6.5 EB, N1, N2: Desert Hot Springs - First Floor Displ. Response

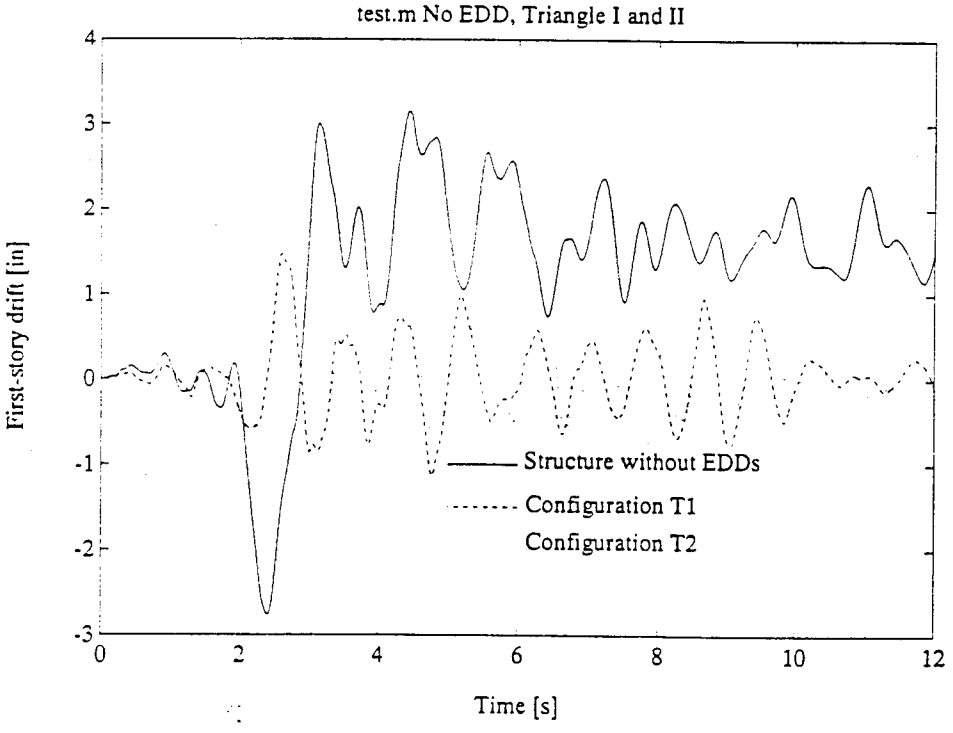

Figure 6.6 EB, T1, T2: Desert Hot Springs - First Floor Displ. Response

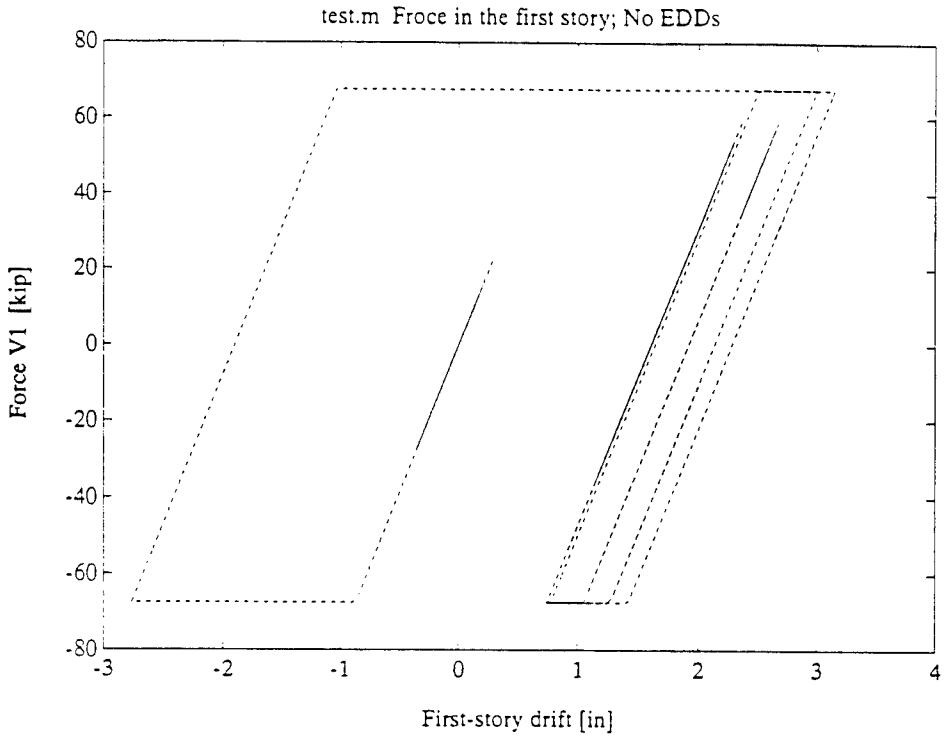

Figure 6.7 EB: Desert Hot Springs - First Story Hysteresis

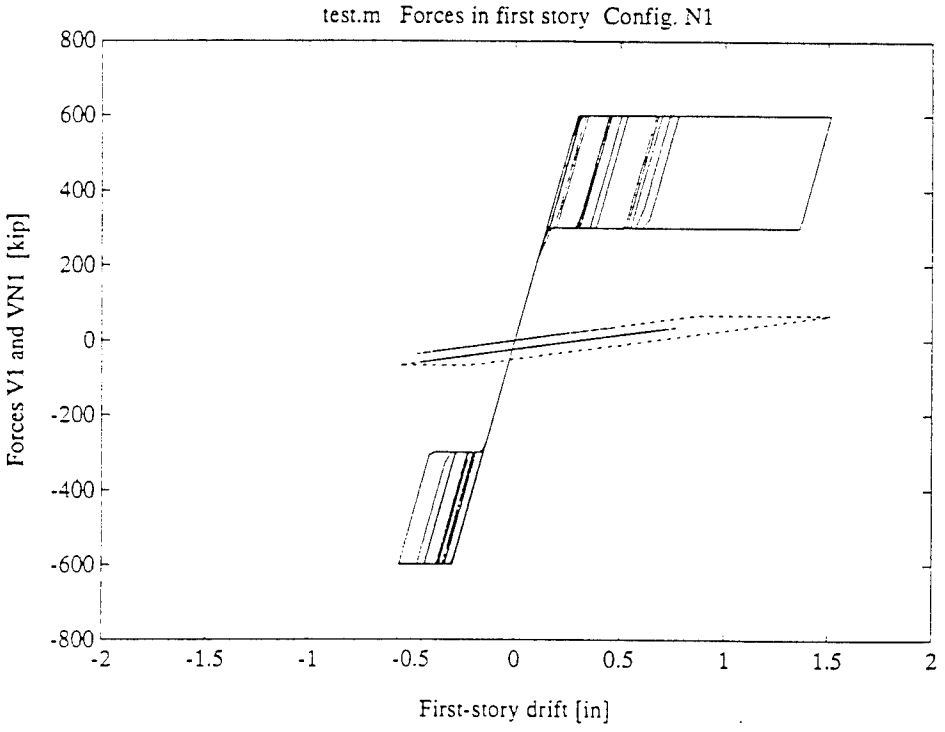

Figure 6.8 N1: Desert Hot Springs - First Story Hysteresis

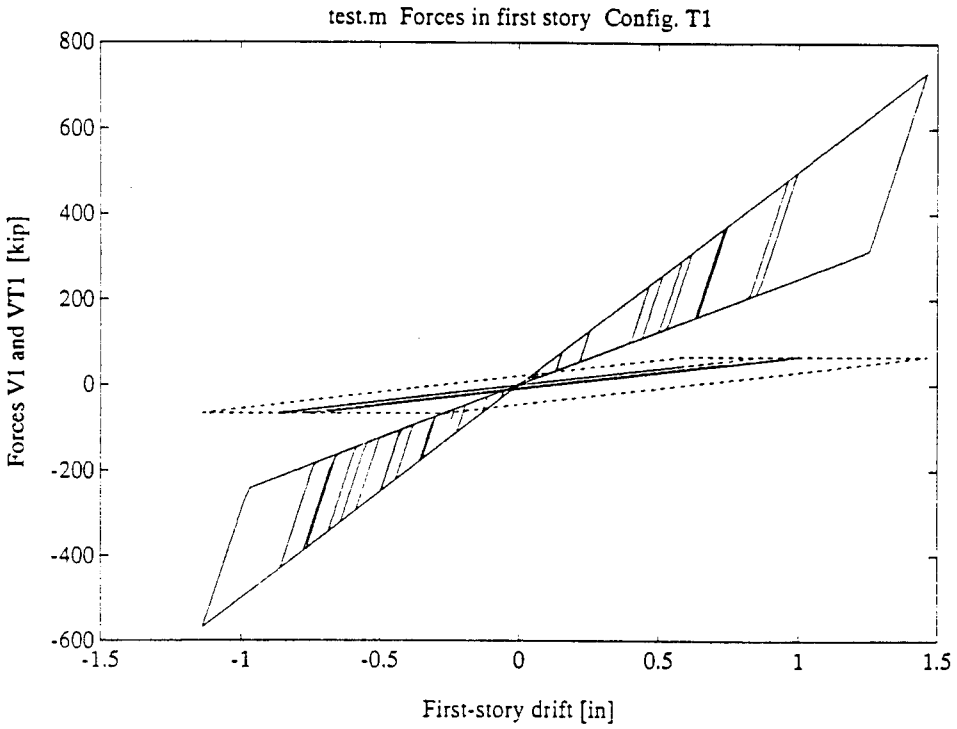

Figure 6.9 T1: Desert Hot Springs - First Story Hysteresis

7.0 SUMMARY, CONCLUSIONS, AND RECOMMENDATIONS

7.1 Summary of the Research Effort

The objective of the Phase I SBIR research effort was to develop the technical base required for the design of shape-memory alloy (SMA or SMM) energy dissipation devices for building structures. Although much of the information presented in this report has direct application to other civil, mechanical, and aerospace structures, only applications relevant to the retrofit of existing buildings and the construction of new buildings in regions of low, moderate, and high seismic risk are considered in this report.

The research effort was composed of four main tasks as described below:

Task 1. Characterization of the basic materials behavior in sufficient detail to provide a basis for the design of prototype energy dissipators.

Task 2. Development of a number of conceptual designs for structural damping devices and the characterization of their mechanical behavior.

Task 3. Detailed analysis of the seismic response of a pre-selected non-ductile concrete building, with and without SMM energy dissipators, under moderate earthquake shaking, to demonstrate the attributes of hysteretic damping.

Task 4. Parametric analyses of a reduced-order model of the pre-selected building (Task 3) upgraded with SMM energy dissipators possessing different hysteretic characteristics from those used in Task 3.

In addition to passive damping applications, SMMs have other important applications to the control of dynamic structural response, including semi-active and active control strategies. Active and semi-active control strategies using SMA alloys were not reviewed in detail in this report because the results of this Phase I research effort are intended to partly form the basis of retrofitting strategies for the DOD's large inventory of seismically hazardous buildings in the near future. A detailed evaluation of active control using shape-memory alloys will be conducted as part of the Phase II research effort.

An introduction to the seismic response of building structures, the mechanisms by which seismic energy is dissipated in conventional buildings, the advantages of supplemental damping devices, and the means by which these devices can be implemented (passive and active) are addressed in Chapter 2 of this report.

The characteristics of the mechanical behavior of NiTi SMMs (Task 1) was presented

in Chapter 3. A detailed testing program (Table 3.1) was developed to thoroughly investigate those mechanical characteristics of SMMs that could influence the design of both passive and active SMA energy dissipators. The two main features of SMAs, the shape-memory effect (SME) and the superelastic effect (SEE) were investigated in detail. The force-deformation characteristics of both the SME and SEE NiTI alloys as a function of temperature, thermomechanical processing, and alloy-prestress were investigated and described in this chapter. An annotated bibliography making reference to: material science; R-phase transitions; metallurgy, creep, and stress relaxation; temperature effects on superelasticity; SMM parametric models; temperature-related phenomena; thermomechanical processing; and engineering applications is also provided in Chapter 3.

Two conceptual designs of passive damping devices (Task 2) are described in Chapter 4: a truss link device and a truss joint device. Neither device was constructed as part of the Phase I research effort. SMA active control devices are described in Section 4.5. Details of such devices, based on direct actuation of the shape-memory effect; friction modulation; and stiffness modulation, are presented in this section. The design and construction of an SMA energy dissipator that can provide both passive and active control is described in Section 4.6. The response characteristics and operational feasibility of this device have been verified by simple test procedures. Comprehensive testing of this device using both active and passive control strategies will be performed as part of the Phase II research effort.

The results of a detailed analysis of a non-ductile reinforced concrete building, typical of many buildings in the DOD inventory, are presented in Chapter 5. The building analyzed in this study was selected by USACERL and is sited in Fort Lewis, Washington State. The building was constructed in 1956 using then-current seismic design procedures. The existing building was analyzed using the nonlinear static load-to-collapse and time-history analysis options in DRAIN-2DX. These analyses demonstrated that the existing building is a seismic hazard in the event of moderate or severe earthquake shaking. Two upgrade schemes were developed, based on the use of NiTi SMA energy dissipators (UG1 and UG2), to both increase the lateral stiffness of the building and to provide significant energy dissipation capacity at interstory drift levels low enough to protect the existing non-ductile frame. Only rectangular SMA hysteresis was assumed for the DRAIN-2DX analyses. Upgrade schemes UG1 and UG2 were analyzed using static load-to-collapse procedures and three recorded ground motion time histories. The results of these analyses are presented in Sections 5.12 and 5.13.

One attractive feature of SMAs is the option afforded to the structural designer in terms of hysteretic shape. Two hysteretic shapes, depicted by triangular and rectangular flags in Figure 4.1, both different from the rectangular shape used in Chapter 5, were implemented in INADEL for the nonlinear time-history analysis of a reduced-order model of the building. The results of these analyses are presented in

Chapter 6.

7.2 Conclusions of the Phase I Research Program

The Phase I research program has established the technical basis for the development, design, and construction of passive energy dissipation devices for the earthquake-resistant design and construction/retrofit of building structures. The mechanical characteristics of different shape-memory alloys were thoroughly investigated in a detailed testing program. SMAs can be configured to provide a shape-memory effect (SME) or a superelastic effect (SEE); energy dissipation devices based on both SME and SEE were shown to be technically viable.

Passive energy dissipation devices incorporating shape-memory alloys, in particular NiTi alloys, have a number of mechanical characteristics that are unavailable with other rate-independent supplemental damping systems currently in the marketplace, namely:

1. Environmental durability
2. Temperature independence of the hysteretic response
3. Excellent low- and high-cycle fatigue characteristics

In addition, SMA energy dissipators can be configured to provide a variety of hysteretic shapes, each of which might be optimal under certain circumstances.

Several prototype SMA energy dissipators were designed as part of the Phase I research effort. One energy dissipator was fabricated towards the end of the Phase I research program. Although preliminary testing of the device has been undertaken already, the results are currently unavailable. Detailed testing of this device is proposed as part of the Phase II SBIR research program.

Detailed analysis of one non-ductile reinforced concrete building (typical of many in the DOD inventory) in Washington State found the building to be vulnerable to collapse in the event of moderate or severe earthquake shaking. This assessment was based on the nonlinear time-history analysis of the building using three recorded earthquake ground motions consistent with moderate earthquake shaking at the building site. Two upgrade schemes developed for the building, based on the use of SMA energy dissipators installed in TS brace elements, were found to effectively mitigate the seismic hazard for the moderate level of earthquake shaking considered appropriate for the Fort Lewis site. The most cost-effective upgrade scheme for this particular building involved the addition of 6, 4, and 2 energy dissipators in each frame of the wing of the building considered, in the first, second, and third stories of the building, respectively. The use of 12 - 22 kip dissipators per building frame reduced the displacements in the building to a level whereby the existing frame suffered no

damage when subjected to three moderate earthquake ground motions.

As noted above, SMA energy dissipators can be configured to provide a variety of force-deformation profiles (see Figure 4.1). Two of these profiles (rectangular flag and triangular flag) were programmed in the MATLAB environment and exported to a newly-developed nonlinear program, INADEL. The results of these analyses demonstrated the attributes of these hysteretic shapes, namely substantial reductions in the response of the existing building. A large number of plausible hysteretic shapes make it possible to optimize the design of a supplemental damping system; such an optimization is impossible with most energy dissipation systems. Further development of the MATLAB:INADEL environment is planned for the Phase II research effort.

In summary, the materials characterization and device development reported in Chapters 2 and 3 of this report clearly demonstrate the technical viability of SMAs as passive energy dissipation devices for earthquake-resistant design applications in the building industry. The advantages of SMA-based energy dissipators over other hysteretic systems are outlined above. The vulnerability of one building typical of many in the DOD inventory was mitigated through the addition of SMA energy dissipators, clearly demonstrating the potential uses of passive energy dissipation technology.

7.3 Recommendations for Future Research

The next step in a co-ordinated, problem-focused research program involves the following work:

1. Additional development and testing of SMMs including copper- and iron-based shape-memory alloys as well as optimization of the NiTi family of alloys including CuNiTi.
2. Development of mathematical tools for the general nonlinear analysis of structural elements incorporating arbitrary hysteresis (see Figure 4.1) for inclusion into commercially available nonlinear packages such as DRAIN-2DX.
3. Schematic development of candidate SMA energy dissipators based on both shape-memory and superelastic hystereses.
4. Selection of a limited number of candidate dissipator designs.
5. Construction and testing of reduced-scale models of the candidate SMA energy dissipators selected in 4.
6. Rigorous 3-D analysis of a representative sample of the seismically-vulnerable buildings in the DOD inventory.
7. Evaluation of different SMA energy dissipator retrofit strategies for the buildings analyzed in 2.

8. Verification of the retrofit strategy to be achieved by the construction of a reduced-scale model of one of the DOD building types deemed hazardous by the E-SORB research team (in consultation with USACERL researchers) and the earthquake simulator testing of the building with and without SMA energy dissipators (as developed in Chapter 5).

REFERENCES

1. Aiken, I.D., Kelly., J.M., and Pall, A.S., "Seismic Response of a Nine-Story Steel Frame with Friction Damped Cross-Bracing," *Report No. UCB/EERC-88/17*, Earthquake Engineering Research Center, University of California at Berkeley, November 1988.

2. Aiken, I.D., Kelly., J.M., and Mahmoodi, P., "The Application of Viscoelastic Dampers to Seismically Resistant Structures," *Proceedings of the 4th U.S. National Conference on Earthquake Engineering*, Palm Springs, CA, 1990.

3. Aiken, I.D., and Kelly, J.M., "Earthquake Simulator Testing and Analytical Studies of Two Energy-Absorbing Systems For Multistory Structures," *Report No. UCB/EERC-90/03*, Earthquake Engineering Research Center, University of California at Berkeley, October 1990.

4. Aiken, I.D., Nims, D.K., and Kelly, J.M., "Comparative Study of Four Passive Energy Dissipation Systems," *Bulletin of the New Zealand National Society for Earthquake Engineering*, Vol. 25, No. 3, September 1992.

5. Aiken, I.D., Whittaker, A.S., Nims, D.K., and Kelly, J.M., "Testing of Passive Energy Dissipation Systems," to be published in *Earthquake Spectra*, Vol. 9, No. 3, EERI, Oakland, CA, August 1993.

6. Akbay, Z., and Aktan, H.M., "Intelligent Energy Dissipation," *Proceedings of the 4th U.S. National Conference on Earthquake Engineering*, Palm Springs, CA, 1990.

7. Arima, F., Miyazaki, M., Tanaka, H., and Yamazaki, Y., "A Study on Buildings With Large Damping Using Viscous Damping Walls," *Proceedings of the 9th World Conference on Earthquake Engineering*, Tokyo/Kyoto, Japan, August 1988.

8. Arista, A., and Gomez, R., "Influence of Energy Dissipation Devices on the Torsional Response of Single-Story Structures," *Proceedings of the Seminar on Seismic Isolation, Passive Energy Dissipation, and Active Control*, Applied Technology Council, ATC 17-1, March 1993.

9. Ashour, Samir A., "Elastic Seismic Response of Buildings With Supplemental Damping," Ph.D. Dissertation, Dept. of Civil Engineering, University of Michigan, January 1987.

10. Ashour, S.A., and Hanson, R.D., "Elastic Seismic Response of Buildings With Supplemental Damping," *Report UMCE 87-1*, Department of Civil Engineering, University of Michigan, 1987.

11. Baz, A.M., et al., "Active Control of Flexible Space Structures Using Nitinol Shape-Memory Actuators," *Final Report*, SDIO Contract #F49620-87-C-0035, 1987.

12. Bergman, D.M., and Hanson, R.D., "Characteristics of Viscoelastic Mechanical Damping Devices," *Proceedings of the ATC 17, Applied Technology Council*, 1986.

13. Bergman, D.M., and S.C. Goel, "Evaluation of Cyclic Testing of Steel-Plate Devices for Added Damping and Stiffness," *Report UMCE 87-10*, Civil Engineering Department, University of Michigan, November 1987.

14. Bertero, V.V., and Whittaker, A.S., "Seismic Upgrading of Buildings," *Proceedings of the 5th Chilean Conference on Seismology and Earthquake Engineering*, Chile, August 1989.

15. Blake, Ralph E., "Basic Vibration Theory," *Shock and Vibration Handbook*, Vol. 1, Ch. 2, C.M. Harris and C.E. Crede, Eds., McGraw-Hill, New York, N.Y., pp. 2-8, 1961.

16. Boardman, P.R., Wood. B.J., and Carr, A.J., "Union House—A Cross Braced Structure With Energy Dissipators," *Bulletin New Zealand National Society for Earthquake Engineering*, Vol. 16, No. 2, June 1993.

17. Bracci, J.M., Lobo, R.F., and Reinhorn, A.M., "Seismic Retrofit of Reinforced Concrete Structures Using Damping Devices" *Proceedings of the Seminar on Seismic Isolation, Passive Energy Dissipation, and Active Control*, Applied Technology Council, ATC 17-1, March 1993.

18. Buckle, I.G., "Future Directions in Seismic Isolation, Passive Energy Dissipation and Active Control" *Proceedings of the Seminar on Seismic Isolation, Passive Energy Dissipation, and Active Control*, Applied Technology Council, ATC 17-1, March 1993.

19. Chang, K.C., Soong, T.T., Lai, M.-L., and Nielsen, E.J., "Viscoelastic Dampers as Energy Dissipation Devices For Structural Applications," *International Workshop on Recent Developments in Base-Isolation Techniques for Buildings*, Tokyo, Japan, April 1992.

20. Chang, K.C., Soong, T.T., Lai, M.L., and Nielsen, E.J., "Development of a Design Procedure for Structures With Added Viscoelastic Dampers" *Proceedings of the Seminar on Seismic Isolation, Passive Energy Dissipation, and Active Control*, Applied Technology Council, ATC 17-1, March 1993.

21. Charleson, A.W., Wright, P.D., and Skinner, R.I., "Wellington Central Police Station, Base Isolation of an Essential Facility," *Proceedings of the Pacific Conference on Earthquake Engineering*, Vol. 2, Wairaki, New Zealand, August 1987.

22. Ciampi, V., "Use of Energy Dissipating Devices, Based on Yielding of Steel, for Earthquake Protection of Structures," *International Meeting on Earthquake Protection of Buildings*, pp. 41/D-58/D, Ancona, Italy, June 1991.

23. Cohen, J.M., "An Energy Dissipation Cladding System: Design Concepts and Feasibility of Seismic Retrofit" *Proceedings of the Seminar on Seismic Isolation, Passive Energy Dissipation, and Active Control*, Applied Technology Council, ATC 17-1, March 1993.

24. Constantinou, M.C., Symans, M.D, Tsopelas, P., and Taylor, D.P., "Fluid Viscous Dampers in Applications of Seismic Energy Dissipation and Seismic Isolation," *Proceedings of the Seminar on Seismic Isolation, Passive Energy Dissipation, and Active Control*, Applied Technology Council, ATC-17-1, March 1993.

25. Craig, J.I., Goodno, B.J., Pinelli, J.-P., and Moor, C., "Modeling and Evaluation of Ductile Cladding Connection Systems for Seismic Response Attenuation in Buildings," *Proceedings of the 10th World Conference on Earthquake Engineering*, Vol. 7, pp. 4183-4188, Madrid, Spain, July 1992.

26. Craig, J.I., Calisle, A.J., Goodno, B.J., Hsu, C.-C., and Sweriduk, G.D., Passive Damping for Structural Response Attenuation in Buildings Cladding," *Proceedings of the Seminar on Seismic Isolation, Passive Dissipation, and Active Control*, Applied Technology Council, ATC 17-1, March 1993.

27. Dieter Jr., G.E., "Mechanical Metallurgy," p. 467, McGraw-Hill, New York, 1961.

28. Duerig, T.W., and Melton, K.N., "Systematizing the Application of Shape Memory," *Proceedings of the Shape Memory Alloy, '86*, pp. 389-396, China Academic Publishers, Guilin, China, 1986.

29. Duerig, T.W., Melton, K.N., Stockel, D., and Wayman, C.M., "Engineering Aspects of Shape Memory Alloys," Butterworth-Heinemann Publishers, London, 1990.

30. Duerig, T.W., and Zadno, G.R., "An Engineer's Perspective of Pseudoelasticity," *Engineering Aspects of Shape Memory Alloys*, pp. 369-393, Butterworth-Heinemann Publishers, London, 1990.

31. Fariabi, S., et al., "The Effect of Cold Work and Heat Treatment on the Phase Transformations of Near Equiatomic NiTi Shape Memory Alloy," *Proceedings of the ICOMAT-89*, pp. 565-570, Trans Tech Publications, Sydney, Australia, 1990.

32. Fierro, E.A., and Perry, C.L., "San Francisco Retrofit Design Using Added Damping and Stiffness (ADAS) Elements" *Proceedings of the Seminar on Seismic Isolation, Passive Energy Dissipation, and Active Control*, Applied Technology Council, ATC 17-1, March 1993.

33. Fierro, E., Perry, C., Sedarat, H., and Scholl, R., "Seismic Retrofit in San Francisco Using Energy Dissipation Devices," submitted to *Earthquake Spectra*, Vol. 9, No. 3, EERI, Oakland, CA, August 1993.

34. Filiatrault, A., and Cherry, S., "Performance Evaluation of Friction Damped Braced Steel Frames Under Simulated Earthquake Loads," *Earthquake Spectra*, Vol. 3, No. 1, Earthquake Engineering Research Inst., Oakland, CA, 1987.

35. Filiatrault, A., and Cherry, S., "Seismic Design of Simple Friction Damped Braced Frames," *Proceedings of the 9th World Conference on Earthquake Engineering*, Tokyo/Kyoto, Japan, 1988.

36. Filiatrault, A., and Cherry, S., "A Simplified Design Procedure for Friction Damped Structures," *Proceedings of the 4USNCEE*, Palm Springs, CA, May 1990.

37. Filiatrault, A., and Cherry, S., "Seismic Design Spectra for Friction Damped Structures," *Journal of the Structural Division*, Vol. 116, No. ST5, American Society of Civil Engineers, New York, 1990.

38. Fitzgerald, T.F., Anagnos, T., Goodson, M., and Zsutty, T., "Slotted Bolted Connections in Aseismic Design for Concentrically Braced Connections," *Earthquake Spectra* Vol. 5, No. 2, pp. 383-391, Earthquake Engineering Research Inst., Oakland, CA, May 1989.

39. Foutch, D.A., Wood, S.L., and Brady, P.A., "Seismic Retrofit of Nonductile Reinforced Concrete Frames Using Viscoelastic Dampers" *Proceedings of the Seminar on Seismic Isolation, Passive Energy Dissipation, and Active Control*, Applied Technology Council, ATC 17-1, March 1993.

40. Fujita, S., Fujita, T., Morikawa, S., and Suizu, Y., "Seismic Response of Steel Framed Buildings Using Viscoelastic Damper," *Trans, 11th International Conference on Structural Mechanics in Reactor Technology*, Vol. K2, pp. 109-114, Tokyo, Japan, August 1991.

41. Funakubo, H., *Shape Memory Alloys*, Gordon and Breach Science Publishers, New York, 1987.

42. Giacchetti, R., Whittaker, A.S., Bertero, V.V., and Aktan, H.M., "Seismic Response of a DMRSF Retrofitted With Friction Slip Devices," *Proceedings of the First International Meeting on Base Isolation and Passive Energy Dissipation*, Assisi, Italy, 1989.

43. Graesser, E.J., and Cozzarelli, F.A., "Multidimensional Models of Hysteretic Material Behavior for Vibration Analysis of Shape Memory Energy Absorbing Devices," *Report NCEER-89-0018*, National Center for Earthquake Engineering Research, State University of New York at Buffalo, 1989.

44. Graesser, E.J., and Cozzarelli, F.A., "A Multidimensional Hysteretic Model for Plastically Deforming Metals in Energy Absorbing Devices," *Report NCEER-91-0006*, National Center for Earthquake Engineering Research, State University of New York at Buffalo, 1991.

45. Graesser, E.J., and Cozzarelli, F.A., "Shape Memory Alloys as New Materials for Aseismic Isolation," *Journal of Engineering Mechanics*, Vol. 117, No. 11, American Society of Civil Engineers, New York, 1991.

46. Grigorian, C.E., Yang, T.-S., and Popov, E.P., "Slotted Bolted Connection Energy Dissipators," *Report No. UCB/EERC-92/10*, Earthquake Engineering Research Center, University of California at Berkeley, July 1992.

47. Grigorian, C.E., and Popov, E.P., "Slotted Bolted Connections for Energy Dissipation" *Proceedings of the Seminar on Seismic Isolation, Passive Energy Dissipation, and Active Control*, Applied Technology Council, ATC 17-1, March 1993.

48. Hanson, R.D., "Basic Concepts and Potential Applications of Supplemental Mechanical Damping for Improved Earthquake Resistance," *Proceedings of the ATC 17, Applied Technology Council*, 1986.

49. Hanson, R.D., Wu, J.P., and Ashour, S.A., "Effect of Large Damping on Earthquake Response," *Proceedings of the 9th World Conference on Earthquake Engineering*, Tokyo/Kyoto, Japan, 1988.

50. Hanson, R. D., Aiken, I., Nims, D.K., Richter, P.J., and Bachman, R., "State-of-the-Art and State-of-the-Practice in Seismic Energy Dissipation" *Proceedings of the Seminar on Seismic Isolation, Passive Energy Dissipation, and Active Control*, Applied Technology Council, ATC 17-1, March 1993.

51. Hendsbee, D., "Retrofit of a Concrete Frame Building Using Added Damping" *Proceedings of the Seminar on Seismic Isolation, Passive Energy Dissipation, and Active Control*, Applied Technology Council, ATC 17-1, March 1993.

52. Hodgson, D.E., "Using Shape Memory Alloys," Shape Memory Applications, Inc., Sunnyvale, CA, 1988.

53. Hudson, D., "Response Spectrum Techniques in Engineering Seismology," *Proceedings of the First World Conference on Earthquake Engineering*, Berkeley, CA, 1956.

54. Hudson, D., "Equivalent Viscous Friction for Hysteretic Systems With Earthquake-Like Excitation, *Proceedings of the Third World Conference on Earthquake Engineering*, New Zealand, 1965.

55. Inaudi, J.A., and Kelly, J.M., "Active Isolation," *Proceedings of the U.S. National Workshop on Structural Control Research*, October 1990.

56. Inaudi, J.A., Kelly, J.M., and To, C.W.S., "Statistical Linearization Method in the Preliminary Design of Structures With Energy Dissipating Devices" *Proceedings of the Seminar on Seismic Isolation, Passive Energy Dissipation, and Active Control*, Applied Technology Council, ATC 17-1, March 1993.

57. International Conference of Building Officials, *Uniform Building Code*, Whittier, CA, 1991.

58. Jackson, C.M., Wagner, H.J., and Wasilewski, R.J., "55 Nitinol—The Alloy With a Memory," NASA Publication NASA-SP5110, Washington, DC, 1972.

59. Jacobsen, L, "Steady State Forced Vibration as Influence by Damping, " *Transactions*, ASME, Vol. 52, Part 1, pp. APM 169-181, 1930.

60. Japan Institute of Metals, *Proceedings of the ICOMAT-86*, Sendai, Japan, 1987.

61. Jara, J.M., Gomez-Soberon, C., Vargas, E., and Gonzalez, R., "Seismic Performance of Buildings With Energy Dissipating Systems" *Proceedings of the Seminar on Seismic Isolation, Passive Energy Dissipation, and Active Control*, Applied Technology Council, ATC 17-1, March 1993.

62. Jennings, Paul, C., "Periodic Response of a General Yielding Structure," *Journal of the Engineering Mechanics Division*, ASCE, Vol. 90, No. EM2, April 1964.

63. Jennings, Paul C., "Equivalent Viscous Damping for Yielding Structures," *Journal of the Engineering Mechanics Division*, ASCE, Vol. 94, No. EM1, February 1968.

64. Jennings, P.C., Housner, G.W., and Tsai, N.C., "Simulation Earthquake Motions," Earthquake Engineering Research Laboratory, California Institute of Technology, April 1968.

65. Kajima Corporation, "Honeycomb Damper Systems," 1991.

66. Kasai, K., Munshi, J.A., Lai, M.-L., and Maison, B.F., "Viscoelastic Damper Hysteretic Model: Theory, Experiment, and Application" *Proceedings of the Seminar on Seismic Isolation, Passive Energy Dissipation, and Active Control*, Applied Technology Council, ATC 17-1, March 1993.

67. Kawashima, K., and Aizawa, K., "Modification of Earthquake Response Spectra With Respect to Damping Ratio," *Proceedings of the 3rd U.S. National Conference on Earthquake Engineering*, Charleston, South Carolina, 1986.

68. Keel, C.J., and Mahmoodi, P., "Design of Viscoelastic Dampers for the Columbia Center Building," *Building Motion in Wind*, ASCE, New York, N.Y., 1986.

69. Kelly, J.M., Skinner, R.I., and Heine, A.J., "Mechanisms of Energy Absorption in Special Devices for Use in Earthquake-Resistant Structures," *Bulletin New Zealand National Society for Earthquake Engineering*, Vol. 5, No. 3, September 1972.

70. Kelly, J.M., and Tsztoo, D.F., "Earthquake Simulation Testing of a Stepping Frame With Energy-Absorbing Devices," *Bulletin of the New Zealand National Society for Earthquake Engineering*, Vol. 10, No. 4, 1977.

71. Kelly, J.M., and Skinner, M.S., "The Design of Steel Energy Absorbing Restrainers and Their Incorporation into Nuclear Power Plants for Enhanced Safety: Volume 4—Review of Current Uses of Energy Absorbing Devices," *Report UCB/EERC-79/10*, Earthquake Engineering Research Center, University of California, Berkeley, 1979.

72. Kelly, J.M., and Skinner, M.S., "Development and Testing of Restraints for Nuclear Piping Systems," *Report UCB/EERC-80/21*, Earthquake Engineering Research Center, University of California, Berkeley, 1980.

73. Kobori, T., Yamada, T., Takenaka, Y., Maeda, Y., and Nishimura, I., "Effect of Dynamic Tuned Connector on Reduction of Seismic Response—Application to Adjacent Office Buildings," *Proceedings of the 9th World Conference on Earthquake Engineering*, Vol. 5, Tokyo/Kyoto, Japan, August 1988.

74. Kobori, T., Sakamoto, M., Takahashi, M., Koshika, N., and Ishii, K., "Seismic Response Controlled Structure With Active Mass Driver Systems and Active Variable Stiffness System," *Proceedings of the U.S. National Workshop on Structural Control Research*, October 1990.

75. Kobori, T., Takahashi, M., Nasu, T., Niwa, N., and Kurata, N., "Shaking Table Experiment and Practical Application of Active Variable Stiffness (AVS) System," *Proceedings of the Second Conference on Tall Buildings in Seismic Regions*, Los Angeles, CA, May, 1991.

76. Kobori, T., and Kamagata, S., "Active Variable Stiffness System—Active Seismic Response Control," *Proceedings of the U.S.-Italy-Japan Workshop/Symposium on Structural Control and Intelligent Systems*, July 1992.

77. Lin, R.C., Liang, Z., Soong, T.T., and Zhang, R.H., "An Experimental Study of Seismic Structural Response With Added Viscoelastic Dampers," *Report NCEER-88-0018*, National Center for Earthquake Engineering Research, State University of New York at Buffalo, 1988.

78. MacDonald Schetky, L. *Proceedings, Engineering Aspects of Shape Memory Alloys*, Edited by T. Duerig, et al., Butterworth-Heinemann Publishers, London, 1990, pp. 170-177.

79. Maclean, B.J., "Shape Memory Material Actuator," Air Force Contract #F04611-88-C-0063, 1989.

80. Mahmoodi, P., "Structural Dampers," *Journal of the Structural Division*, Vol. 95, No. ST8, ASCE, New York, N.Y., 1969

81. Mahmoodi, P., Robertson, L.E., Yontar, M., Moy, C., and Feld, L., "Performance of Viscoelastic Dampers in World Trade Center Towers," *Proceedings of the 5th ASCE Structures Congress*, Orlando, FL, April 1987.

82. Mahmoodi, P., "Design of Viscoelastic Passive Dampers for Tall Structures," *Proceedings of the 7th Conference of Engineering Mechanics*, Los Angeles, CA, 1988.

83. Mahmoodi, P., and Keel, C.J., "Analysis and Design of Multi-Layer Viscoelastic Dampers for Tall Structures," *Proceedings of the 7th ASCE Structures Congress*, San Francisco, CA, May 1989.

84. Mahmoodi, P., and Keel, C.J., "Method of Damped Energy Calculation for Multi-Layer Viscoelastic Damper," *Proceedings of the 6th U.S. National Conference on Wind Engineering*, 1989.

85. Matthewson, C.D., and Davey, R.D, "Design of an Earthquake Resisting Building Using Precast Concrete Cross-Braced Panels and Incorporating Energy-Absorbing Devices," *Proceedings of the South Pacific Regional Conference on Earthquake Engineering*, Vol. 1, Wellington, New Zealand, May 1979.

86. Medeot, R., "Experimental Testing and Design of Aseismic Devices," *Proceedings of the International Meeting on Earthquake Protection of Buildings*, pp. 59/D-79/D, Ancona, Italy, 1991.

87. Miyazaki, M., and Mitsusaka, "Design of a Building With 20% or Greater Damping," *Proceedings of the 10th World Conference on Earthquake Engineering*, Madrid, Spain, July 1992.

88. Miyazaki, S., et al., "Transformation Pseudoelasticity and Deformation Behavior in a Ti-50, 6% Ni Alloy," *Scripts Metallurgica*, Vol. 15, pp. 287-292, 1981.

89. Miyazaki, S., Ohmi, Y., Otsuka, K., and Suzuki, Y., "Characteristics of Deformation and Transformation Pseudoelasticity in NiTi Alloys," *Proceedings of the ICOMAT-82*, p. C4-255, Leuven, Belgium, 1982.

90. Miyazaki, S., and Wayman, C.M., "The Shape Memory Mechanism Associated With the R-Phase Transition in Ti-Ni Single Crystals," *Proceedings of the ICOMAT-86*, p. 665, Japan Institute of Metals, Sendai, Japan, 1987.

91. Morin, M., et al. "Internal Friction of Cu-Zn-Aj," *Proceedings of the ICOMAT 1982*, Leuven, Belgium, 1982, pp. C4-685-689.

92. Murai, Y., Takase, Y., Sugimoto, H., and Nakashima, H., "Control of the Behavior of the SYP Building Under Wind Environment," *Proceedings of the Second Conference on Tall Buildings in Seismic Regions*, Los Angeles, CA, May, 1991.

93. Nashif, A., Jones, D.I.G., and Henderson, J.P., *Vibration Damping*, John Wiley and Sons, Inc., New York, 1985.

94. Newmark, N.M., and Hall, W.J., "Earthquake Spectra and Design," *EERI Monograph*, Earthquake Engineering Research Inst., Oakland, CA, 1982.

95. Nims, D.K., Inaudi, J.A., Richter, P.J., and Kelly, J.M., "Application of the Energy Dissipating Restraint to Buildings," *Proceedings of the Seminar on Seismic Isolation, Passive Energy Dissipation, and Active Control*, Applied Technology Council, ATC-17-1, March 1993.

96. Oiles Corporation, "General Catalogue of Earthquake Isolation and Vibration Damping," 1991.

97. Otsuka, K., and Shimizu, K. *Proceedings of the ICOMAT 1979*, Cambridge, Massachusetts, 1979, pp 607-618.

98. Otsuka, H., et al., "Shape Memory Effect in Fe-Mn-Si-Cr-Ni Polycrystalline Alloys," *Proceedings of the ICOMAT-89*, Trans Tech Publications, Sydney, Australia, 1990.

99. Pall, A.S., and Marsh, C., "Seismic Response of Friction Damped Braced Frames," *Journal of the Structural Division*, Vol. 108, No. ST6, American Society of Civil Engineers, New York, 1982.

100. Pall, A.S., Verganelakis, V., and Marsh, C., "Friction Dampers for Seismic Control of Concordia Library Building," *Proceedings of the 5th Canadian Conference on Earthquake Engineering*, Ottawa, Canada, 1987.

101. Pall, A.S., Ghorayeb, F., and Pall, R., "Friction Dampers for Rehabilitation of Ecole Polyvalente at Sorel, Quebec," *Proceedings of the 6th Canadian Conference on Earthquake Engineering*, pp. 389-396, Toronto, Canada, 1991.

102. Pall, A.S., Pall, R., "Friction-Dampers Used for Seismic Control of New and Existing Buildings in Canada," *Proceedings of the Seminar on Seismic Isolation, Passive Energy Dissipation, and Active Control*, Applied Technology Council, ATC 17-1, March 1993.

103. Perkins, J., Ed., "Shape Memory Effects in Alloys," Plenum Press, 1975.

104. Prakash, V., "Dynamic Response Analysis of Inelastic Building Structures: The DRAIN Series of Computer Programs" *Report No. UCB/SEMM-92/28*, University of California at Berkeley, 1992.

105. Prakash, V., Powell, G.H., Campbell, S.D., and Filippou, F.C., "DRAIN-2DX Preliminary Element User Guide," University of California at Berkeley, 1992.

106. Prakash, V., Powell, G.H., and Filippou, F.C., "DRAIN-2DX: Base Program User Guide," *Report No. UCB/SEMM-92/29*, University of California at Berkeley, 1992.

107. Proft, J.L, and Duerig, T.W., "The Mechanical Aspects of Constrained Recovery," *Engineering Aspects of Shape Memory Alloys*, pp. 115-129, Butterworth-Heinemann Publishers, London, 1990.

108. Quinn, M.P., "Nickel/Titanium/Vanadium Shape Memory Alloy," U.S. Patent No. 4,505,767, 1985.

109. Raychem Corporation Brochuse, "Shape Memory Metal," Menlo Park, CA, 1981.

110. Rea, Dixon, "Discussion of Jennings (1968)," *Journal of the Engineering Mechanics Division*, ASCE, Vol. 94, No EM6, December 1968.

111. Reinhorn, A.M., and Soong, T.T., "Full Scale Implementation of Active Bracing for Seismic Control of Structures," *Proceedings of the the U.S. National Workshop on Structural Control Research*, October 1990.

112. Richter, P.J., Nims, D.K., Kelly, J.M., and Kallenbach, R.M., "The EDR—Energy Dissipating Restraint, A New Device for Mitigation of Seismic Effects," *Proceedings of the the SEAOC 59th Annual Convention*, Lake Tahoe, September 1990.

113. Robinson, W.H., and Greenbank, L.R., "An Extrusion Energy Absorber Suitable for the Protection of Structures During an Earthquake," *International Journal of Earthquake Engineering and Structural Dynamics*, Vol. 4, 1976.

114. Robinson, W.H., and Cousins, W.J., "Recent Developments in Lead Dampers for Base Isolation," *Pacific Conference on Earthquake Engineering*, Vol. 2, Wairaki, New Zealand, August 1987.

115. Roik, K., Dorka, U., and Dechent, P., "Vibration Control of Structures Under Earthquake Loading by Three-Stage Friction-Grip Elements," *Earthquake Engineering and Structural Dynamics*, Vol. 16, No. 4, pp. 501-521, May 1988.

116. Rosenblueth, E., "Discussion of Hudson (1965)," *Proceedings of the the Third World Conference of Earthquake Engineering*, New Zealand, 1965.

117. Ruiz, P., and Penzien, J., "Pseudo Earthquake Generation," *Report No. UCB/EERC 69-3*, Earthquake Engineering Research Center, University of California at Berkeley, March 1969.

118. Sakamoto, H., et al., U.S. Patent No. 4,925,445, 1990.

119. Sakurai, T., Shibata, K., Watanabe, S., Endoh, A., Yamada, K., Tanaka, N., and Kobayashi, H., "Application of Joint Damper to Thermal Power Plant Buildings," *Proceedings of the the 10th World Conference on Earthquake Engineering*, Vol. 7, pp. 4149-4154, Madrid, Spain, July 1992.

120. Sasaki, K., "Experimental Evaluation of Nitinol for Energy Dissipating Devices," *Report UCB/SEMM-89/20*, Department of Civil Engineering, University of California, Berkeley, 1989.

121. Scholl, R.E., "Brace Dampers: An Alternative Structural System for Improving the Earthquake Performance of Buildings," *Proceedings of the the 8th World Conference on Earthquake Engineering*, San Francisco, CA, 1984.

122. Scholl, R.E., "Improve the Earthquake Performance of Structures With Added Damping and Stiffness Elements," *Proceedings of the the 4th U.S. National Conference on Earthquake Engineering*, Palm Springs, CA, 1990.

123. Scholl, R.E., "Design Criteria for Yielding and Friction Energy Dissipators," *Proceedings of the Seminar on Seismic Isolation, Passive Energy Dissipation, and Active Control*, Applied Technology Council, ATC 17-1, March 1993.

124. SEAONC Energy Dissipation Working Group, 1993, "Code Requirements of the Design and Implementation of Passive Energy Dissipation Systems," *Proceedings of the Seminar on Seismic Isolation, Passive Energy Dissipation, and Active Control*, Applied Technology Council, ATC 17-1, March 1993

125. Skinner, R.I., Kelly, J.M., and Heine, A.J., "Hysteretic Dampers for Earthquake-Resistant Structures," *International Journal of Earthquake Engineering and Structural Dynamics*, Vol. 3, pp. 287-296, 1975.

126. Skinner, R.I., Tyler, R.G., Heine, A.J., and Robinson, W.J., 1980, "Hysteretic Dampers for the Protection of Structures from Earthquakes," *Bulletin New Zealand National Society for Earthquake Engineering*, Vol. 13, No. 1, March 1980.

127. Soong, T.T., "Active Structural Control in Civil Engineering," *Technical Report NCEER-87-0023*, National Center for Earthquake Engineering Research, State University of New York at Buffalo, November 1987

128. Soong, T.T., *Active Structural Control: Theory and Practice*, Longman Scientific & Technical, New York, N.Y., 1989.

129. Soong, T.T., and Mahmoodi, P., "Seismic Behavior of Structures With Added Viscoelastic Dampers," *Proceedings of the the 4th U.S. National Conference on Earthquake Engineering*, Palm Springs, CA, 1990.

130. Steimer, S.F., and Godden, W.G., "Shaking Table Tests of Piping Systems With Energy-Absorbing Restrainers," *Report UCB/EERC-80/33*, Earthquake Engineering Research Center, University of California, Berkeley, 1980.

131. Steimer, S.F., and Chow, F.L., "Curved Plate Energy Absorbers for Earthquake Resistant Structures," *Proceedings of the the 8th World Conference on Earthquake Engineering*, San Francisco, CA, 1984.

132. Steimer, S.F., Godden, W.G., and Kelly, J.M., "Experimental Behavior of a Spatial Piping System With Steel Energy Absorbers Subjected to a Simulated Differential Seismic Input," *Report No. UCB/EERC-81/09*, Earthquake Engineering Research Center, University of California at Berkeley, July 1981.

133. Structural Engineers Association of CA, *Recommended Lateral Force Requirements and Commentary*, Sacramento, CA, 1990.

134. Su, Y.F., and Hanson, R.D., "Comparison of Effective Supplemental Damping: Equivalent Viscous and Hysteretic," *Proceedings of the the 4th U.S. National Conference on Earthquake Engineering*, Palm Springs, CA, 1990.

135. Su, Y.F., and Hanson, R.D., "Seismic Response of Building Structures With Mechanical Damping Devices," *Report UMCE 90-2*, Department of Civil Engineering, University of Michigan, 1990.

136. Tan, T.M.H., Ha, K.H., and Pall, R.D., "Simplified Analysis for Friction Damped Frames," *Proceedings of the the 9th World Conference on Earthquake Engineering*, Tokyo/Kyoto, Japan, 1988.

137. Tremblay, R., and Stiemer, S.F., "Energy Dissipation Through Friction Bolted Connections in Concentrically Braced Steel Frames," *Proceedings of the Seminar on Seismic Isolation, Passive Energy Dissipation, and Active Control*, Applied Technology Council, ATC 17-1, March 1993.

138. Tsai, K.-C., and Hong, C.-P., "Steel Triangular Plate Energy Absorber for Earthquake-Resistant Buildings," *Proceedings of the the First World Congress on Constructional Steel Design*, Mexico, 1992.

139. Tyler, R.G., "Tapered Steel Energy Dissipators for Earthquake Resistant Structures," *Bulletin of the New Zealand National Society for Earthquake Engineering*, Vol. 11, No. 4, December 1978.

140. Tyler, R.G., "Tapered Steel Cantilever Energy Absorbers," *Bulletin of the New Zealand National Society for Earthquake Engineering*, Vol. 11, No. 4, 1978.

141. Tyler, R.G., "Preliminary Tests on an Energy Absorbing Element for Braced Structures Under Earthquake Loading," *Bulletin of the New Zealand National Society for Earthquake Engineering*, Vol. 16, No. 3, 1983.

142. Tyler, R.G., "Further Notes on a Steel Energy-Absorbing Element for Braced Frameworks," *Bulletin New Zealand National Society for Earthquake Engineering*, Vol. 18, No. 3, September 1985.

143. Tyler, R. G., "Tests on a Brake Lining Damper for Structures," *Bulletin New Zealand National Society for Earthquake Engineering*, Vol. 18, No. 3, pp. 280-285, September 1985.

144. Uang, C.M., and Bertero, V.V., "Use of Energy as a Design Criterion in Earthquake-Resistant Design," *Report UCB/EERC-88/18*, Earthquake Engineering Research Center, University of California, Berkeley, 1988.

145. Uehara, K., Katano, Y., Ogino, N., Katoh, T., and Sakao, K., "Experimental Studies on a Vibration Control Wall With Viscoelastic Material," *Transactions of the 11th International Conference on Structural Mechanics in Reactor Technology*, Vol. K2: 115-120, Tokyo, August 1991.

146. Vezina, S., Proulx, P., Pall, R., and Pall, A.S., "Friction-Dampers for Aseismic Design of Canadian Space Agency," *Proceedings of the the 10th World Conference on Earthquake Engineering*, Madrid, Spain, 1992.

147. Wayman, C.M., "Phase Transformations in NiTi-Type Shape Memory Alloys," *Proceedings of the the ICOMAT-86*, p. 645, Japan Institute of Metals, Sendai, Japan, 1987.

148. Whittaker, A.S., Bertero, V.V., Alonso, J., and Thompson, C., "Earthquake Simulator Testing of Steel Plate Added Damping and Stiffness Elements," *Report UCB/EERC-89/02*, Earthquake Engineering Research Center, University of CA, Berkeley, 1989.

149. Whittaker, A.S., Bertero, V.V., Thompson, C.L., and Alonso, L.J., "Seismic Testing of Steel Plate Energy Dissipation Devices," *Earthquake Spectra*, Vol. 7, No. 4, pp. 563:604, Earthquake Engineering Research Inst., Oakland, CA, November 1991.

150. Whittaker, A., "Tentative General Requirements for the Design and Construction of Structures Incorporating Discrete Passive Energy Dissipation Devices," *Proceedings of the the Fifth U.S.-Japan Workshop on the Improvement of Building Structural Design and Construction Practices*, Applied Technology Council, ATC-15-5, September 1992.

151. Whittaker, A., Aiken, I., Bergman, D., Clark, P., Cohen, J., Kelly, J.M., and Scholl, R., "Code Requirements for the Design and Implementation of Passive Energy Dissipation Systems," *Proceedings of the Seminar on Seismic Isolation, Passive Energy Dissipation, and Active Control*, Applied Technology Council, ATC 17-1, March 1993.

152. Whittaker, A.S., and Aiken, I.D., "Passive Energy Dissipation Systems for Earthquake-Resistant Design," *Proceedings of the the 1993 ASCE Structures Congress*, Irvine, CA, April 1993.

153. Witting, P.R., and Cozzarelli, F.A., "Shape Memory Structural Dampers: Material Properties, Design and Seismic Testing," *Report No. NCEER-92-0013*, National Center for Earthquake Engineering Research, State University of New York at Buffalo, May 1992.

154. Wu, Jian-ping, 1987, "Statistical Study of the Inelastic Response of Structures With High Damping Subjected to Earthquakes," Ph.D. Dissertation, Dept. of Civil Engineering, University of Michigan, Ann Arbor, November 1987.

155. Wu, J., and Hanson, R.D., "Inelastic Response of Structures With High Damping Subjected to Earthquakes," *Report UMCE 87-9*, Department of Civil Engineering, University of Michigan, 1987.

156. Wu, J., and Hanson, R.D., "Study of Inelastic Spectra With High Damping," *Journal of the Structural Division*, Vol. 115, No. ST6, American Society of Civil Engineers, New York, 1989.

157. Wu, Jian-ping and Hanson, Robert D., "Inelastic Response Spectra With High Damping," *Journal of the Structural Division*, ASCE, Vol. 115, No. 6, June 1989, pp. 1412-1413.

158. Yao, J.T.P., and Asce, M., "Concept of Structural Control," *Journal of the Structural Division, Proceedings of the the American Society of Civil Engineers,* Vol. 98, No. ST7, July 1972

159. Yokota, H., Saruta, M., Nakamura., Y., Satake, N., and Okada, K., "Structural Control for Seismic Load Using Viscoelastic Dampers," *Proceedings of the the 10th World Conference on Earthquake Engineering*, Madrid, Spain, July 1992.

160. Youssef, N., and Guh, T.J., "Seismic Retrofit of Structures With Passive Energy Dissipation Devices," *Proceedings of the Seminar on Seismic Isolation, Passive Energy Dissipation, and Active Control*, Applied Technology Council, ATC 17-1, March 1993.

161. Zhang, R.H., Soong, T.T., and Mahmoodi, P., "Seismic Response of Steel Frame Structures With Added Viscoelastic Dampers, *Earthquake Engineering and Structural Dynamics*, Vol. 18, No. 3, 1975.

APPENDICES

A.1 Materials Test Data

TEST	MATERIAL	DIAMETER (in)	LOOPS	FREQUENCY (Hz)	TEMP. (°C)
1A	F4904-2-2	0.015	14	0.2	22
1B	F4903-2B	0.009	22	0.2	22
1C	F00642-1B	0.162	14	0.2	22
1D	F2234-2-2A	0.014	19	0.2	22
2A	F4904-2-2	0.015	14	0.3	22
2B	F4904-2-2	0.015	14	0.3	23
2C	F4904-2-2	0.015	14	1.0	23
2D	F4904-2-2	0.015	14	3.0	23
2E	F4904-2-2	0.015	14	10.0	23
2F	F4903-1B	0.035	5	3.0	23[a]
2G	F4903-1B	0.035	5	3.0	23
3A	F4904-2-2	0.015	14	0.2	40
3B	F4904-2-2	0.015	14	0.2	60
3C	F4904-2-2	0.015	14	0.2	80
3D	F4904-2-2	0.015	14	0.2	0
4A	F00642-1B	0.016	18	0.2	22[b]
4B	F00642-1B	0.016	18	0.1	23
4C	F4903-1B	0.035	6	0.1	23
5A	F4903-2B	0.009	15	0.2	23
6A	F4904-2-2	0.015	14[c]	0.2	23
6B	F4904-2-2	0.015	14[c]	0.2	22[b]
6C	F4904-2B	0.0091	16[d]	0.2	23
6D	F4904-2B	0.0091	16[d]	0.2	23

a. Sample came loose during testing
b. Servo gain too low
c. 6 of 14 loops slack to 2% strain
d. 7 of 14 wires slack to 4% strain
e. 8 of 16 loops slack to 4% strain

Details of the Testing Program

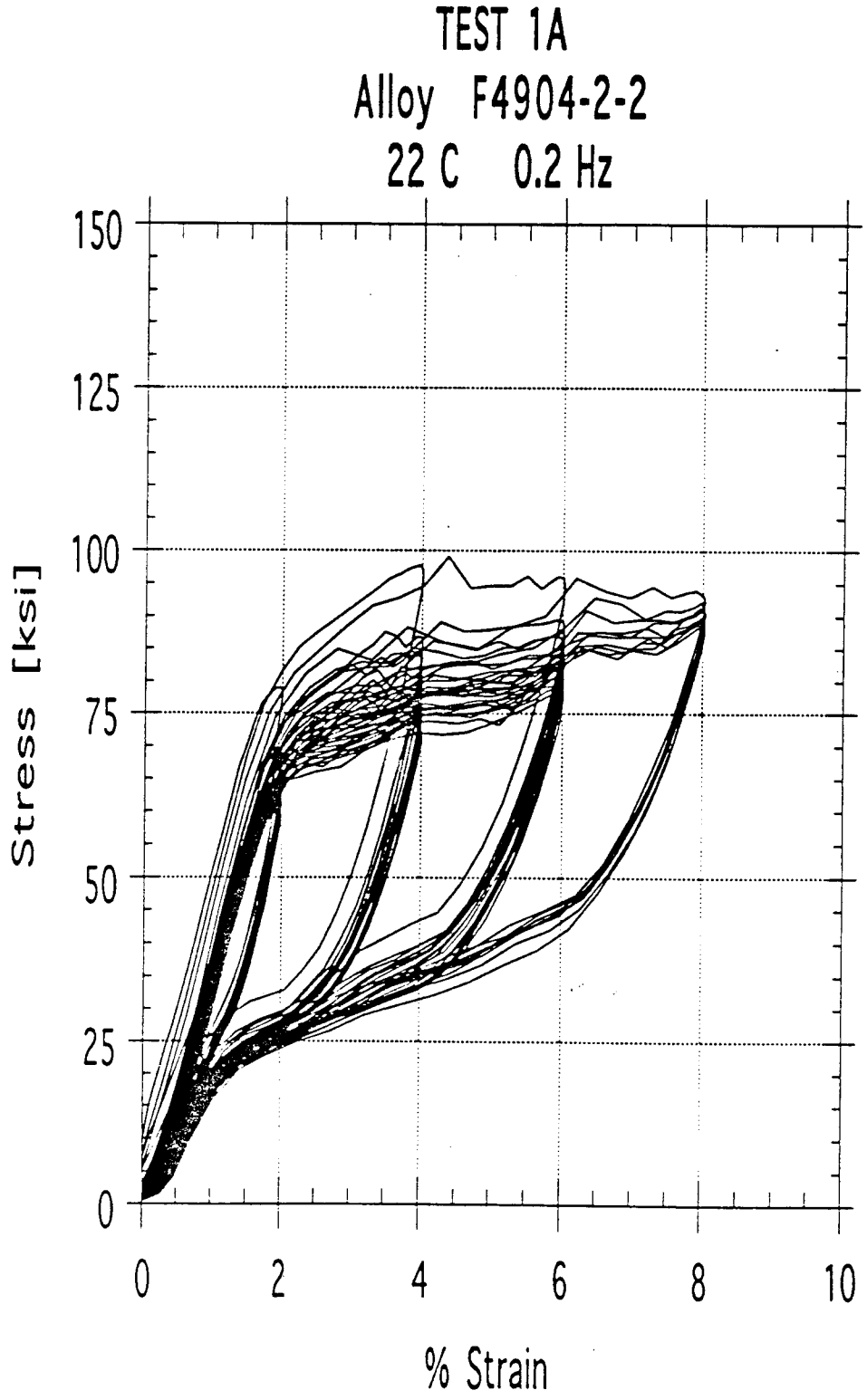
TEST 1A
Alloy F4904-2-2
22 C 0.2 Hz
150
125
100
75
50
25
0
Stress [ksi]
0
2
4
6
8
10
% Strain

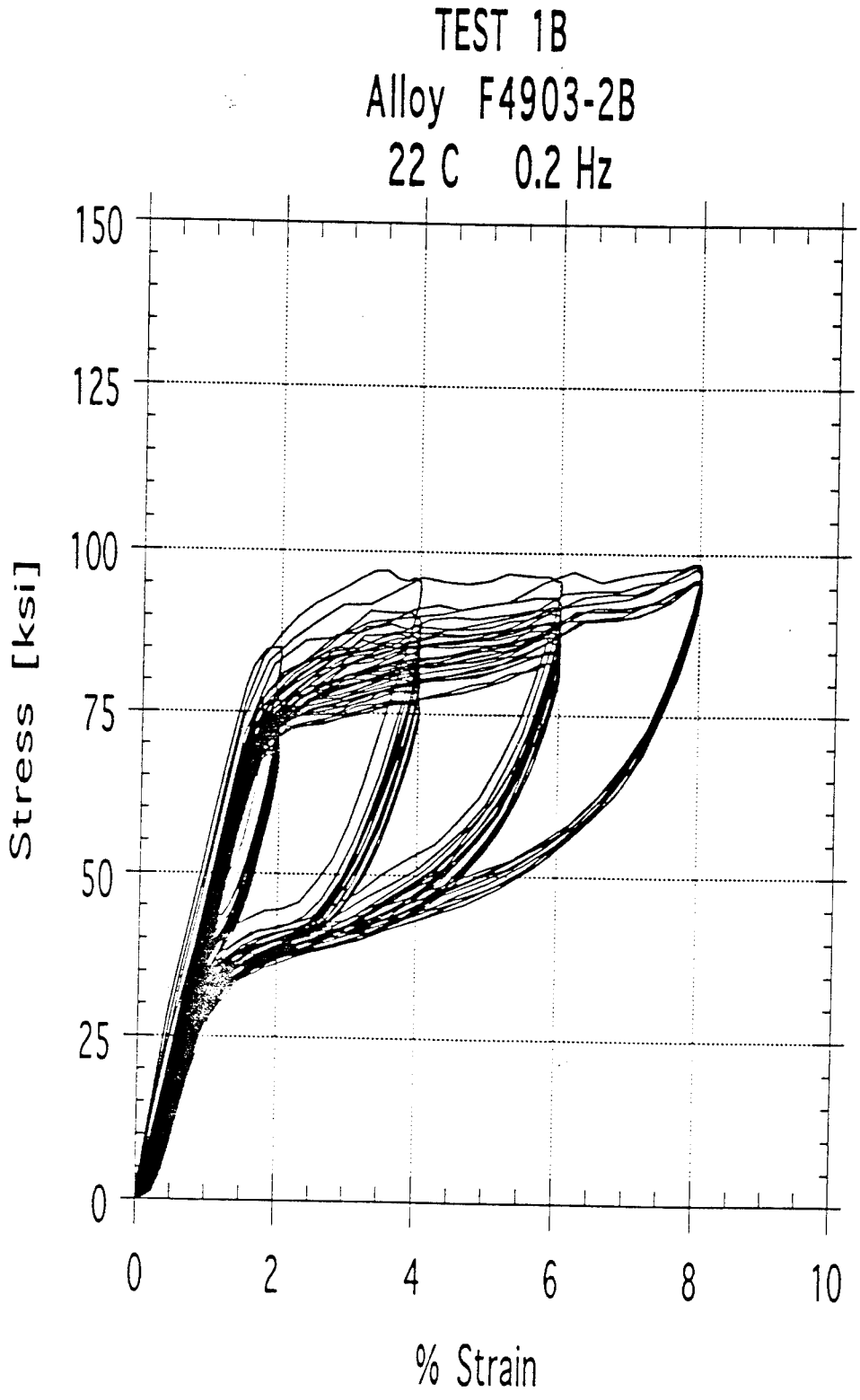
TEST 1B
Alloy F4903-2B
22 C 0.2 Hz
150
125
100
75
50
25
0
Stress [ksi]
0
2
4
6
8
10
% Strain

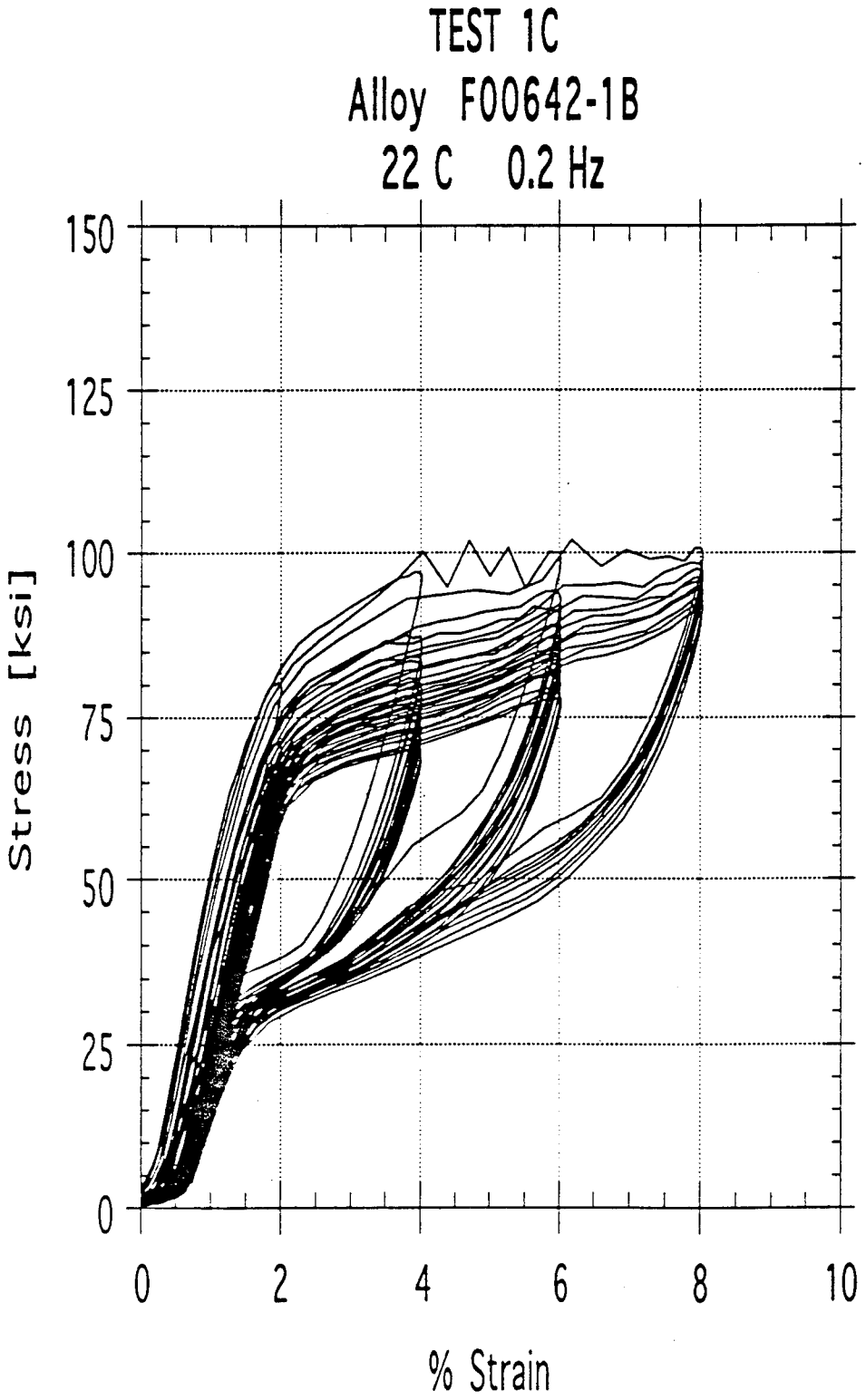
TEST 1C
Alloy F00642-1B
22 C 0.2 Hz
Stress [ksi]
150
125
100
75
50
25
0
0
2
4
6
8
10
% Strain

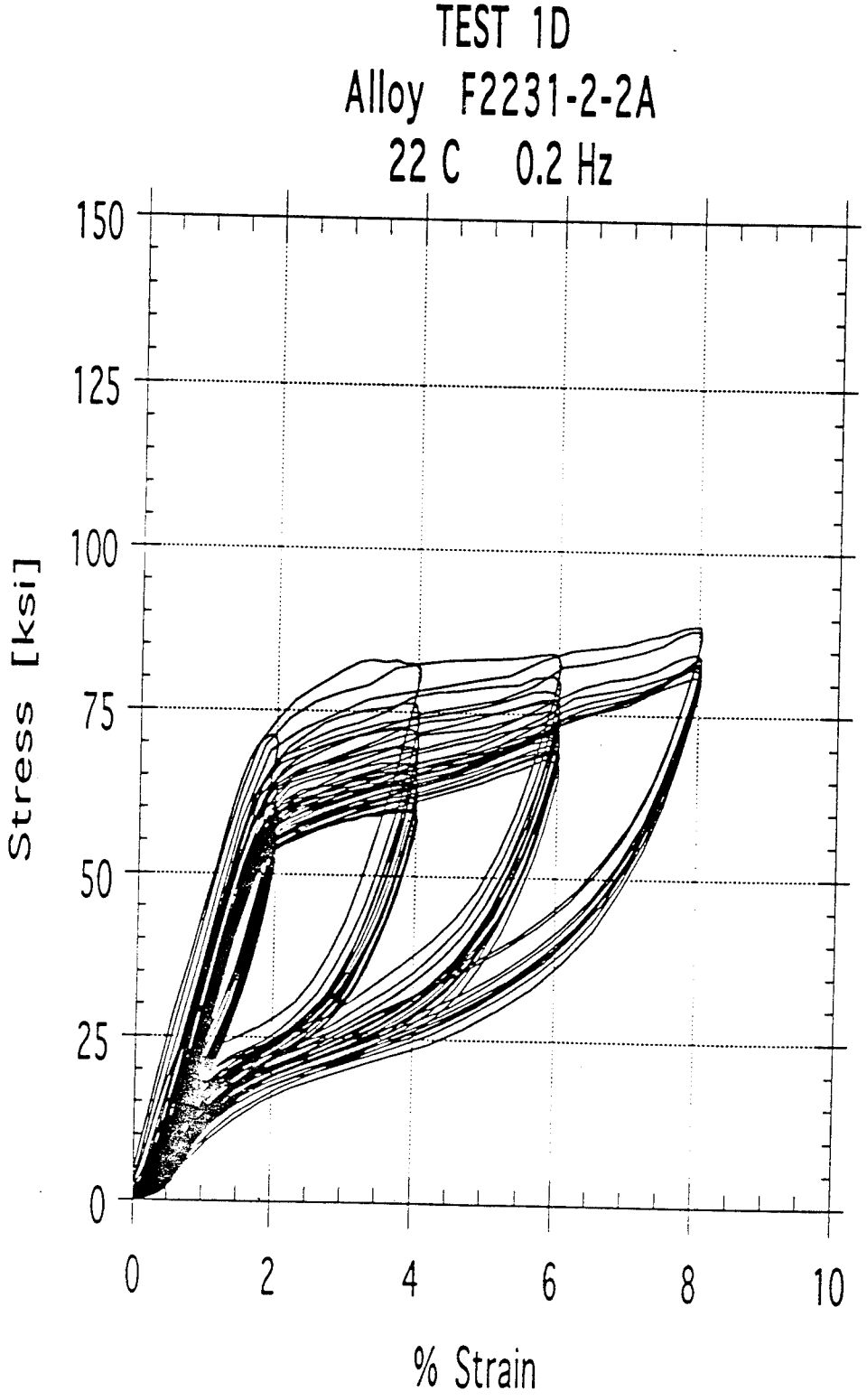
TEST 1D
Alloy F2231-2-2A
22 C 0.2 Hz
150
125
100
75
50
25
0
Stress [ksi]
0
2
4
6
8
10
% Strain

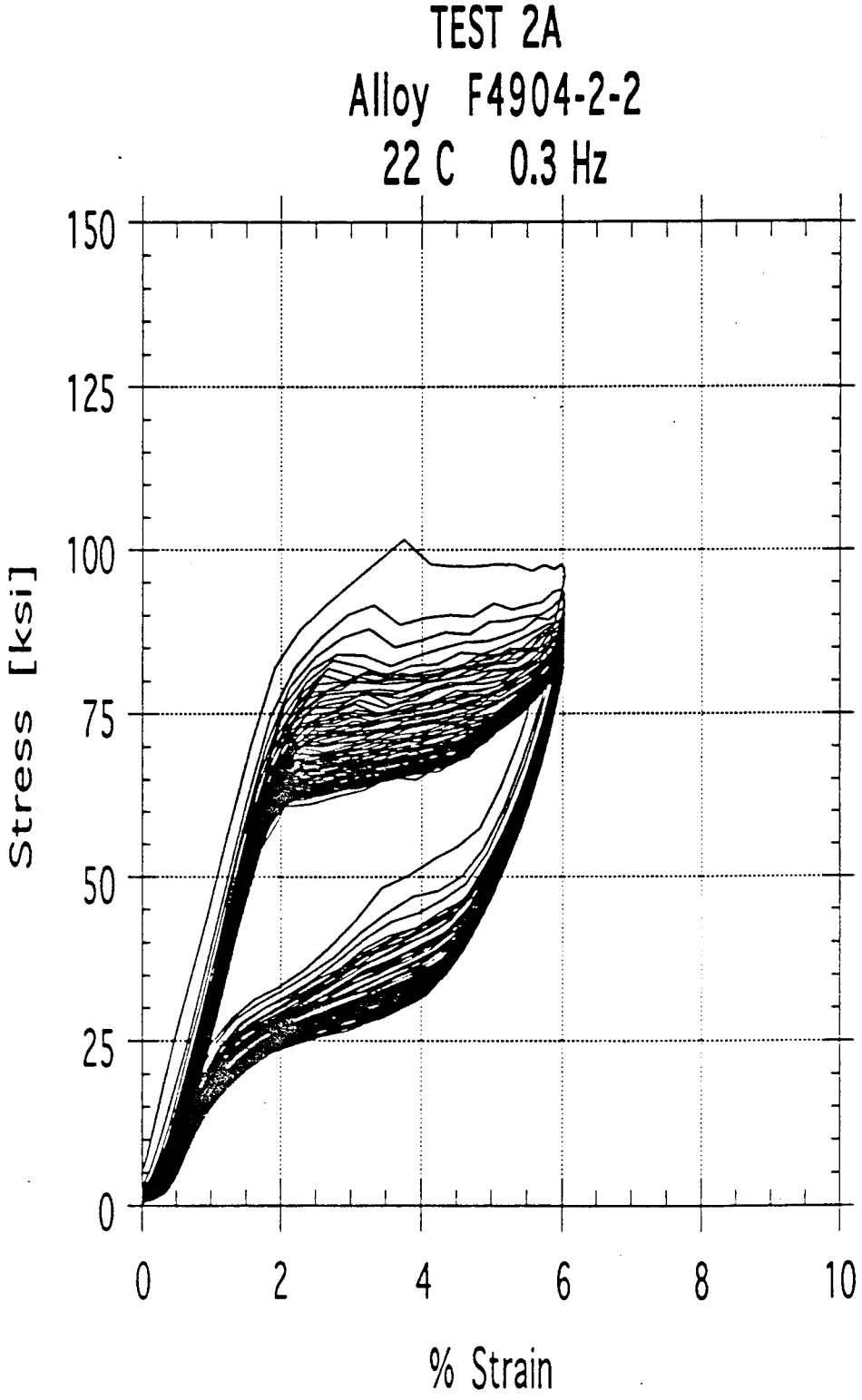
TEST 2A
Alloy F4904-2-2
22 C 0.3 Hz
Stress [ksi]
150
125
100
75
50
25
0
0
2
4
6
8
10
% Strain

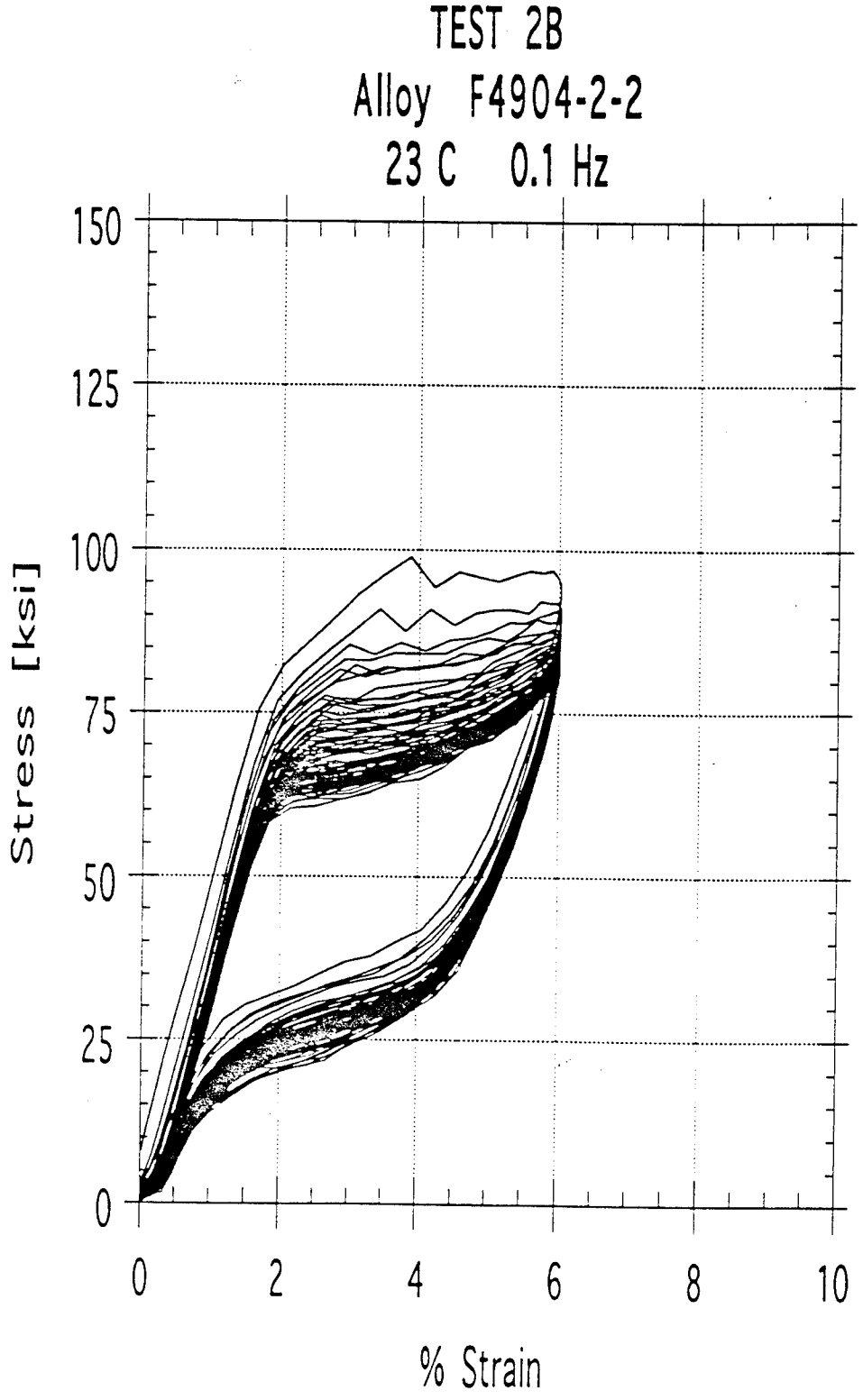
TEST 2B
Alloy F4904-2-2
23 C 0.1 Hz
150
125
100
75
50
25
0
Stress [ksi]
0
2
4
6
8
10
% Strain

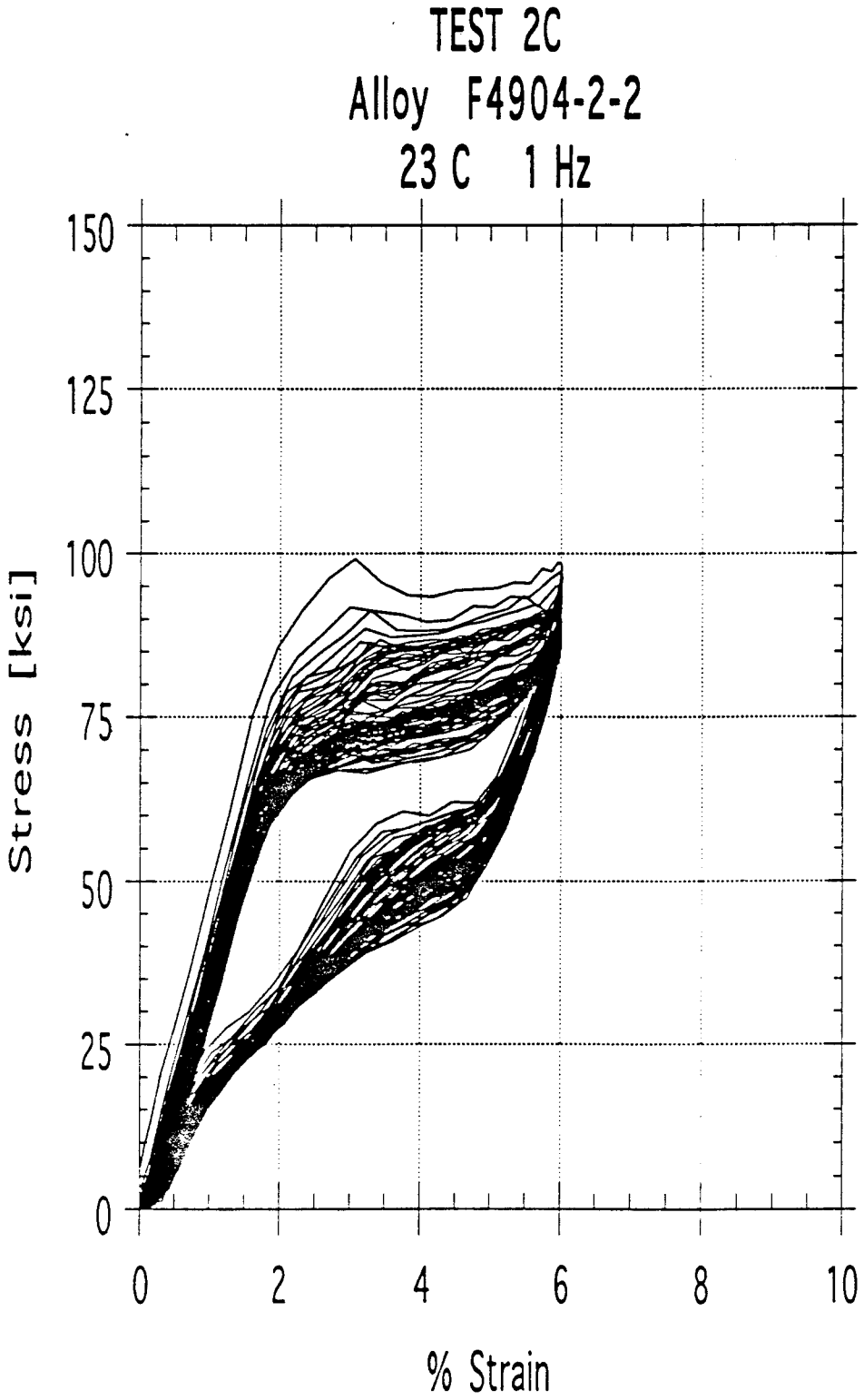
TEST 2C
Alloy F4904-2-2
23 C 1 Hz
150
125
100
75
50
25
0
Stress [ksi]
0
2
4
6
8
10
% Strain

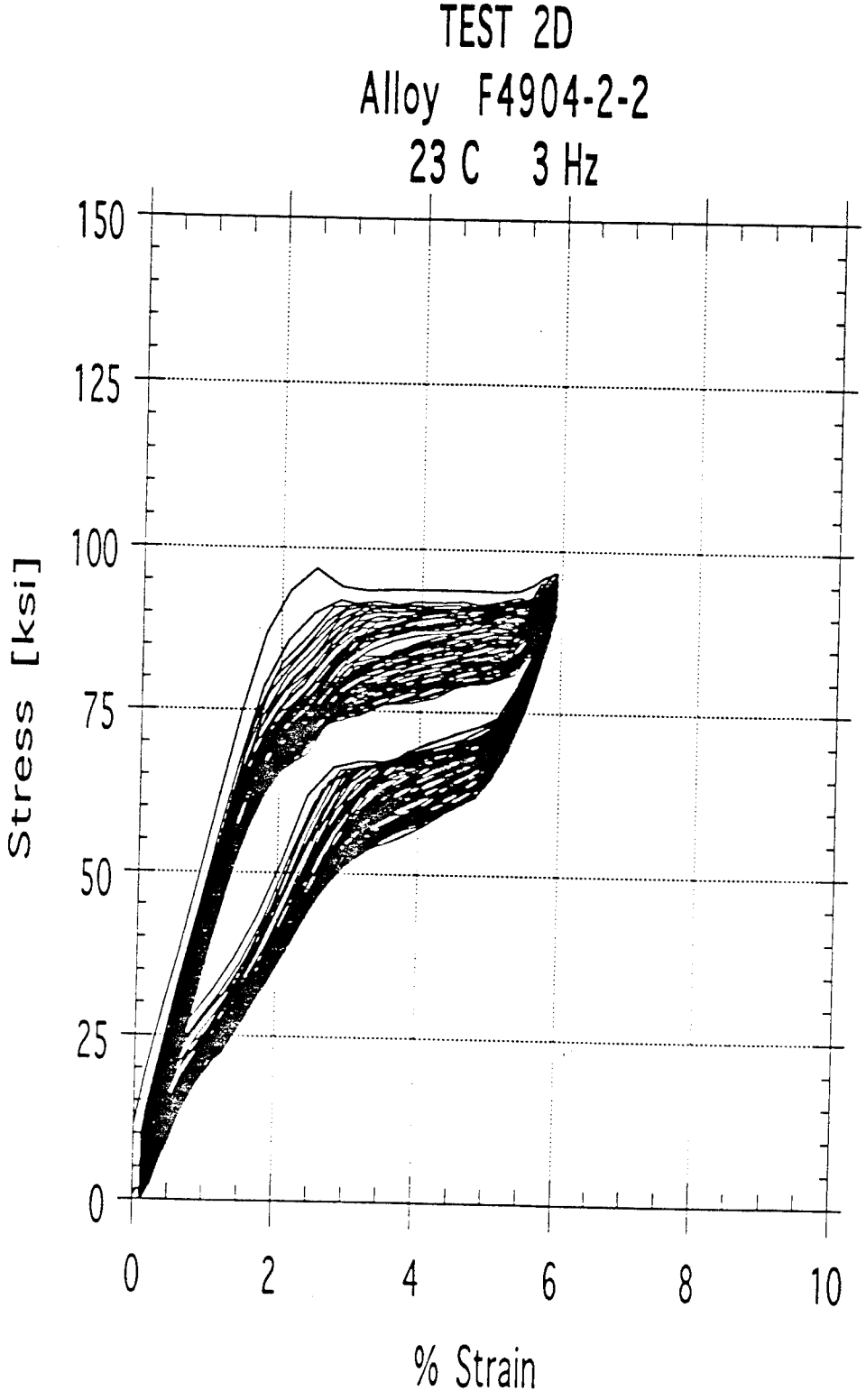
TEST 2D
Alloy F4904-2-2
23 C 3 Hz
150
125
100
75
50
25
0
Stress [ksi]
0
2
4
6
8
10
% Strain

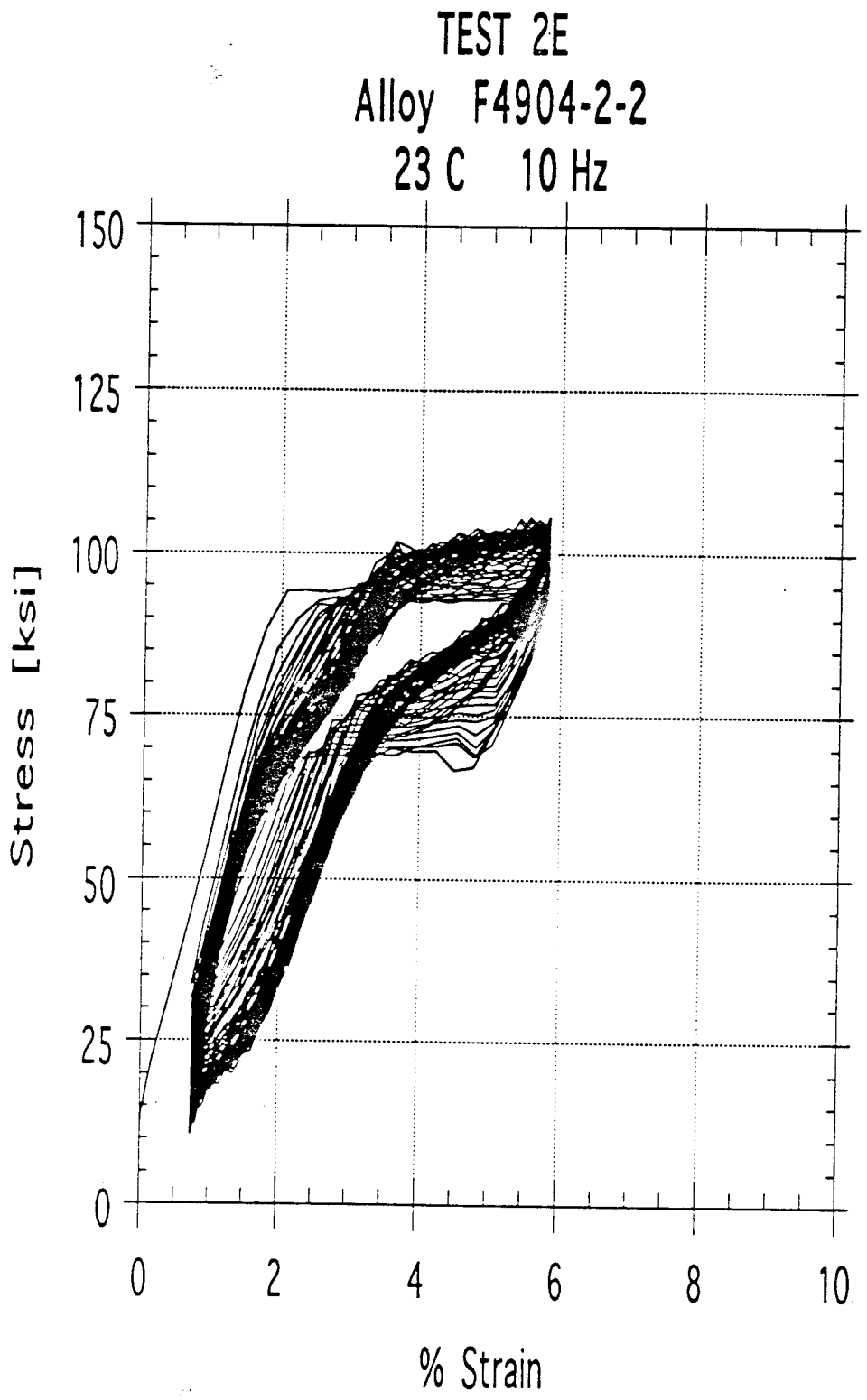
TEST 2E
Alloy F4904-2-2
23 C 10 Hz
Stress [ksi]
150
125
100
75
50
25
0
0
2
4
6
8
10
% Strain

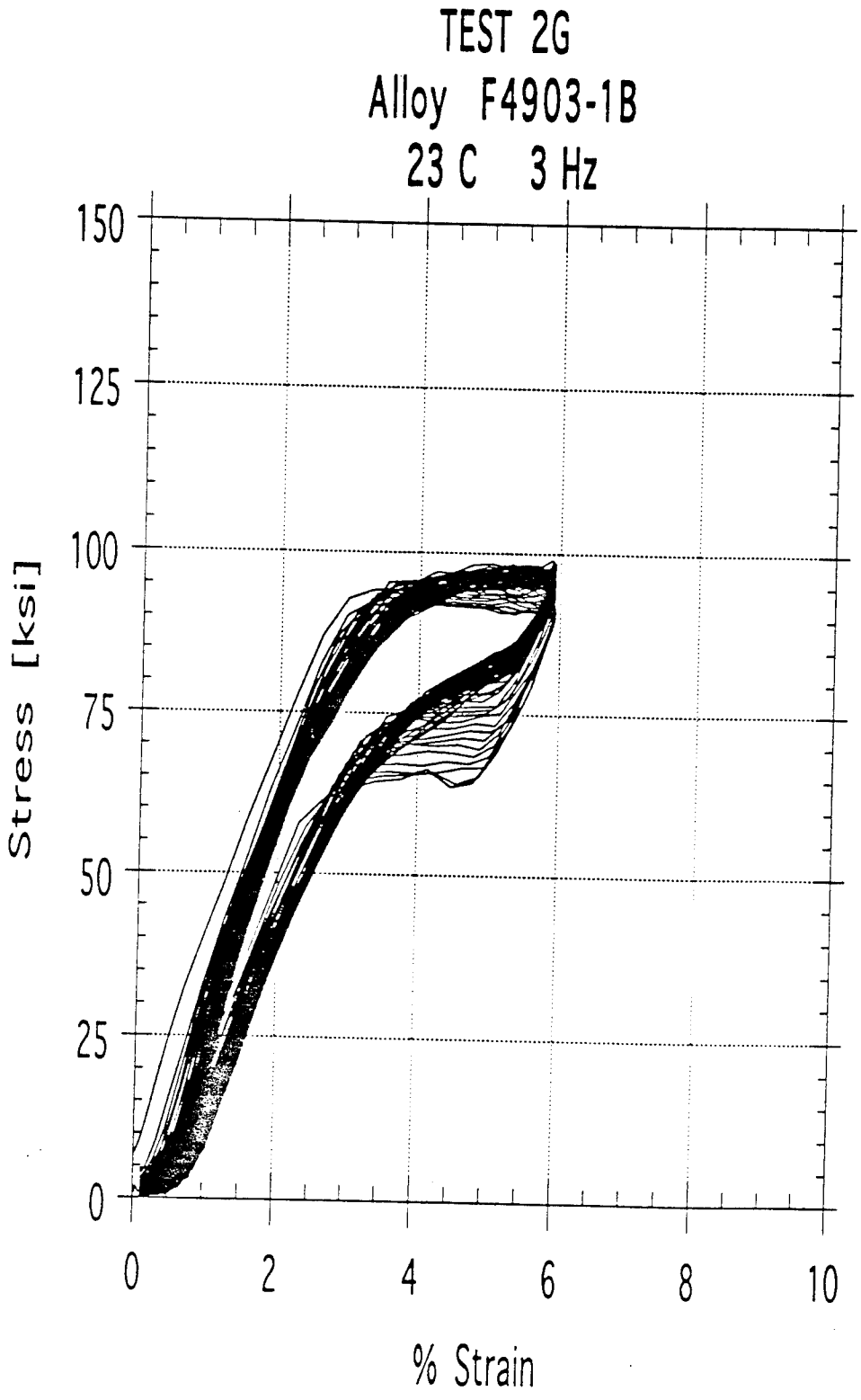
TEST 2G
Alloy F4903-1B
23 C 3 Hz
150
125
100
75
50
25
0
Stress [ksi]
0
2
4
6
8
10
% Strain

Alloy F4904-2-2
Cycle 50

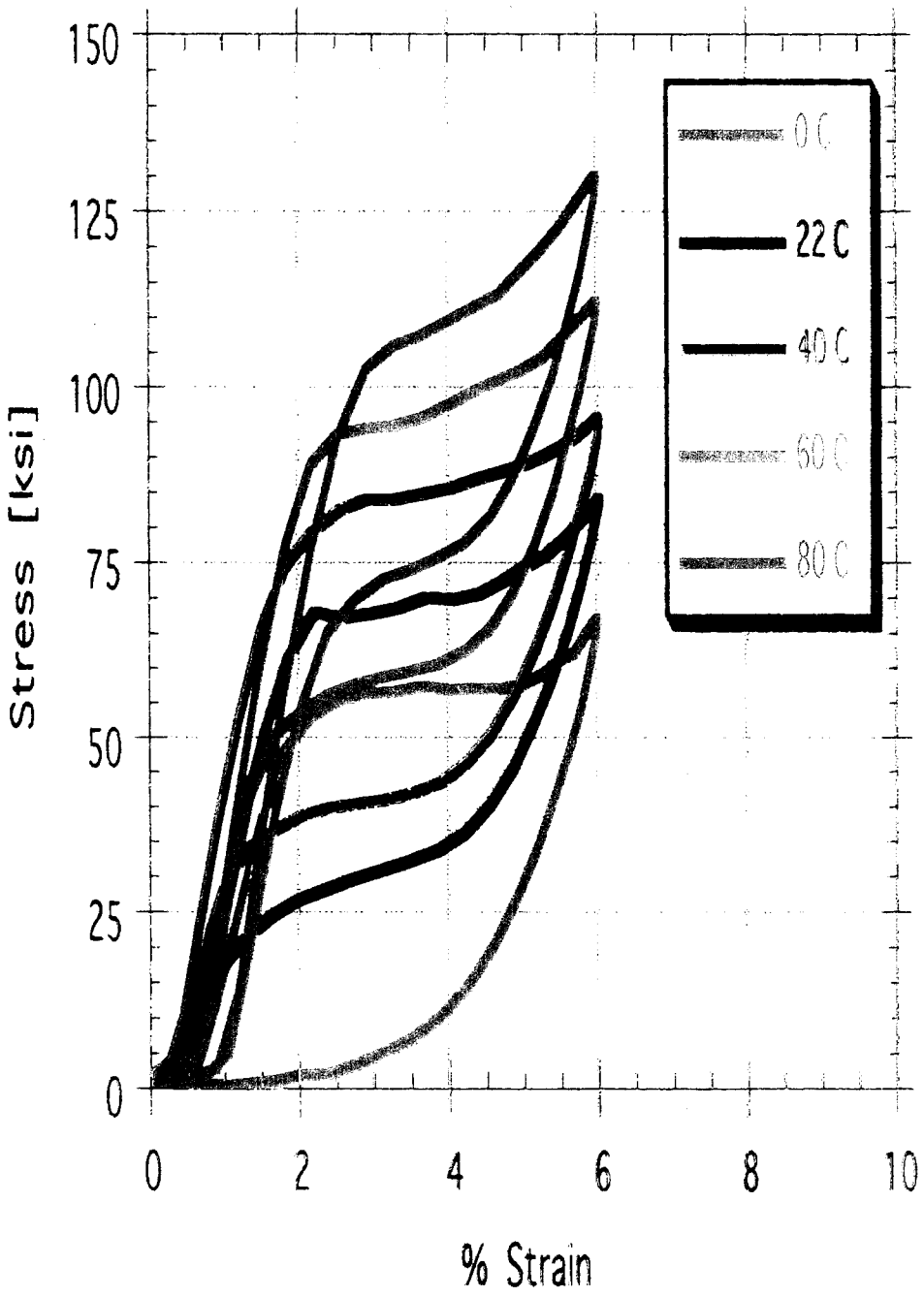

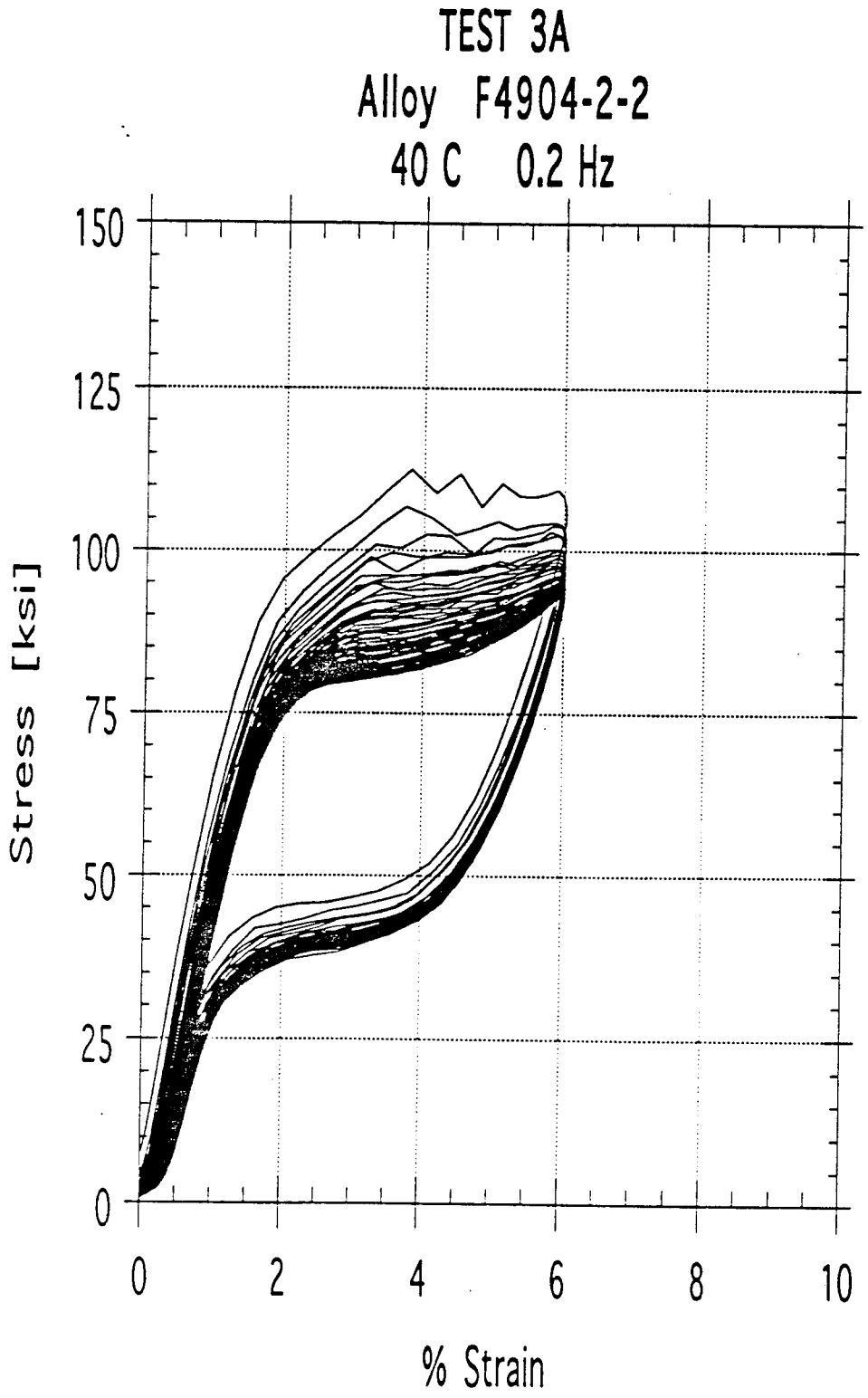
TEST 3A
Alloy F4904-2-2
40 C 0.2 Hz
Stress [ksi]
150
125
100
75
50
25
0
0
2
4
6
8
10
% Strain

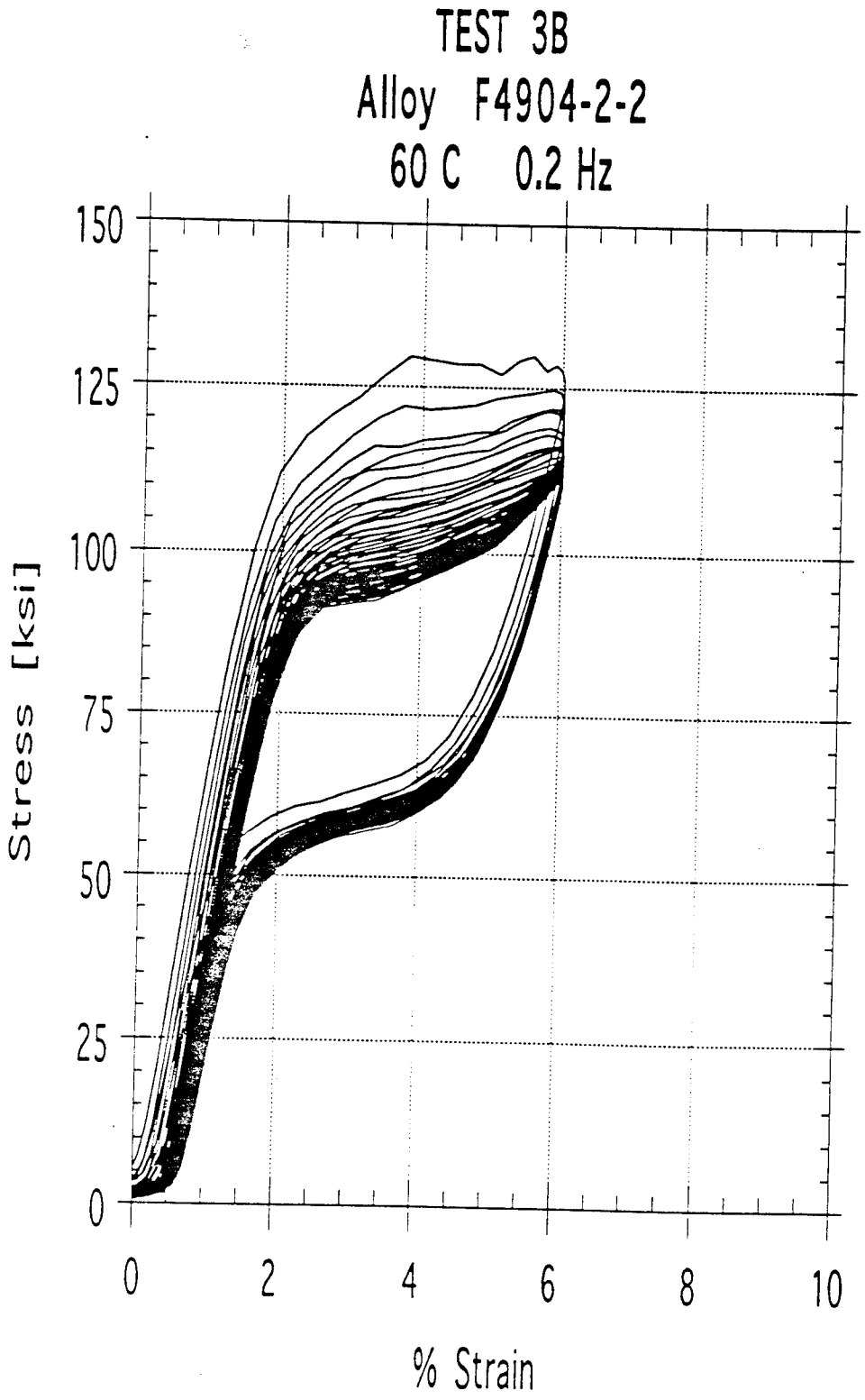
TEST 3B
Alloy F4904-2-2
60 C 0.2 Hz
150
125
100
75
50
25
0
Stress [ksi]
0
2
4
6
8
10
% Strain

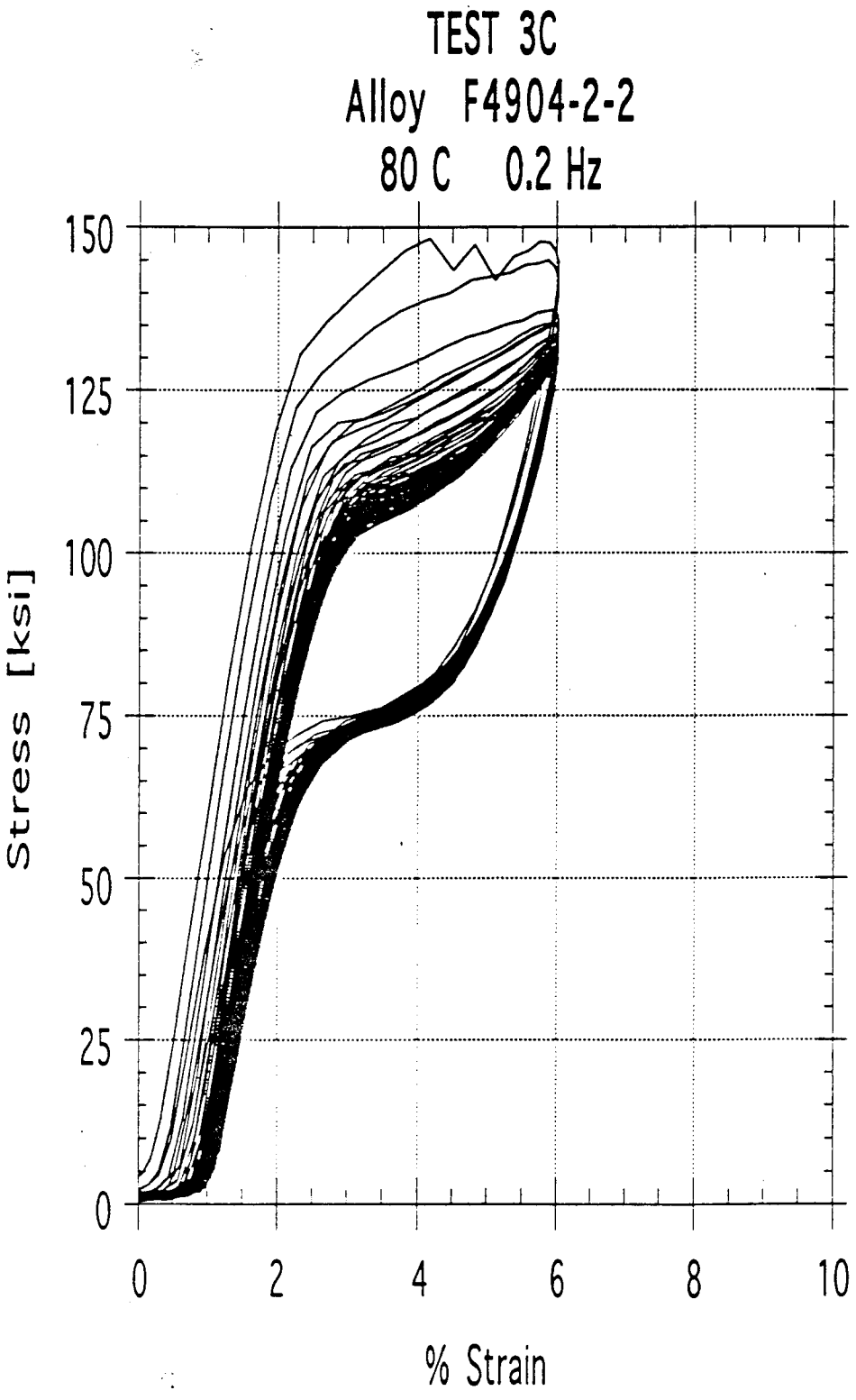
TEST 3C
Alloy F4904-2-2
80 C 0.2 Hz
Stress [ksi]
150
125
100
75
50
25
0
0
2
4
6
8
10
% Strain

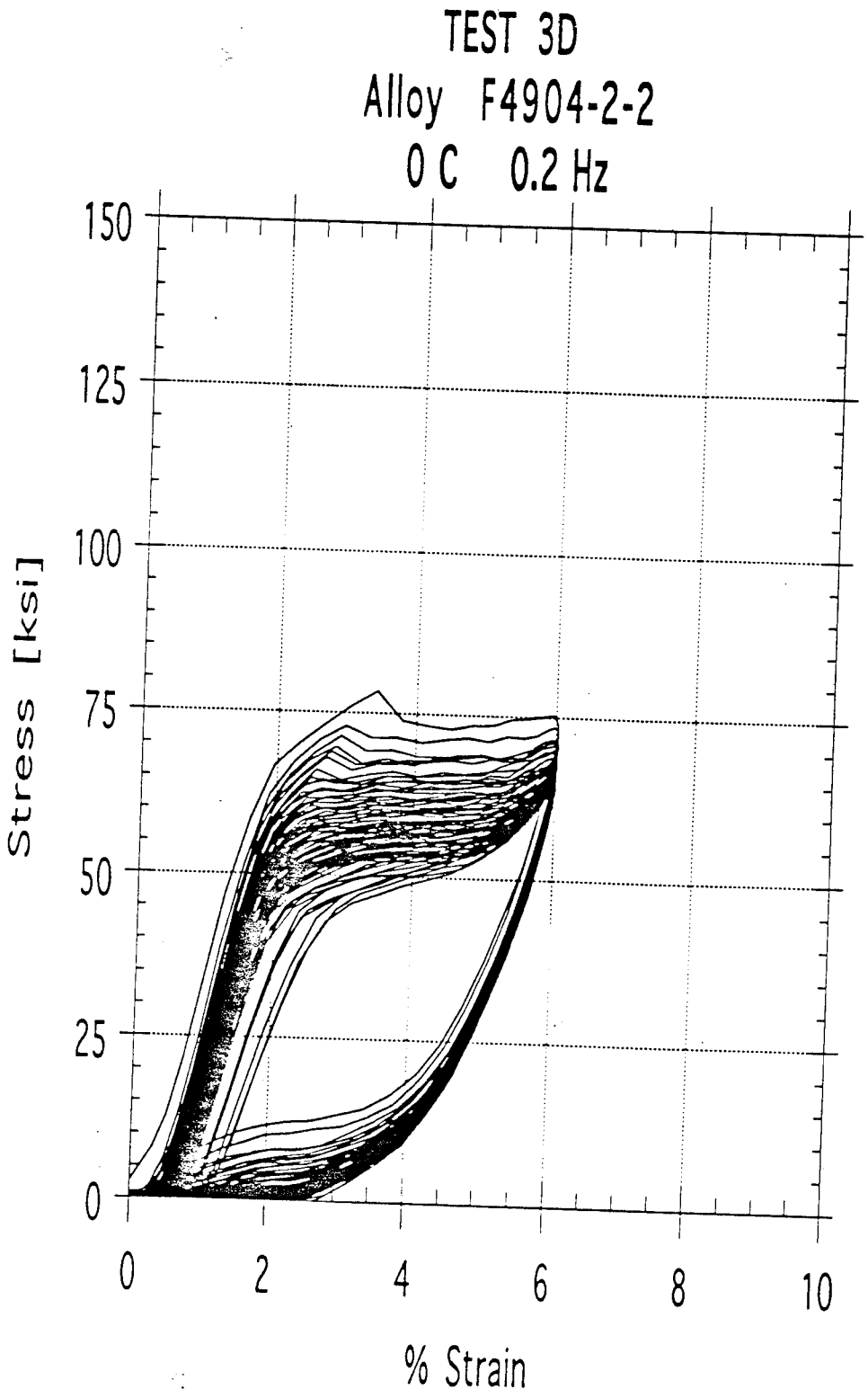
TEST 3D
Alloy F4904-2-2
0 C 0.2 Hz
150
125
100
75
50
25
0
Stress [ksi]
0
2
4
6
8
10
% Strain

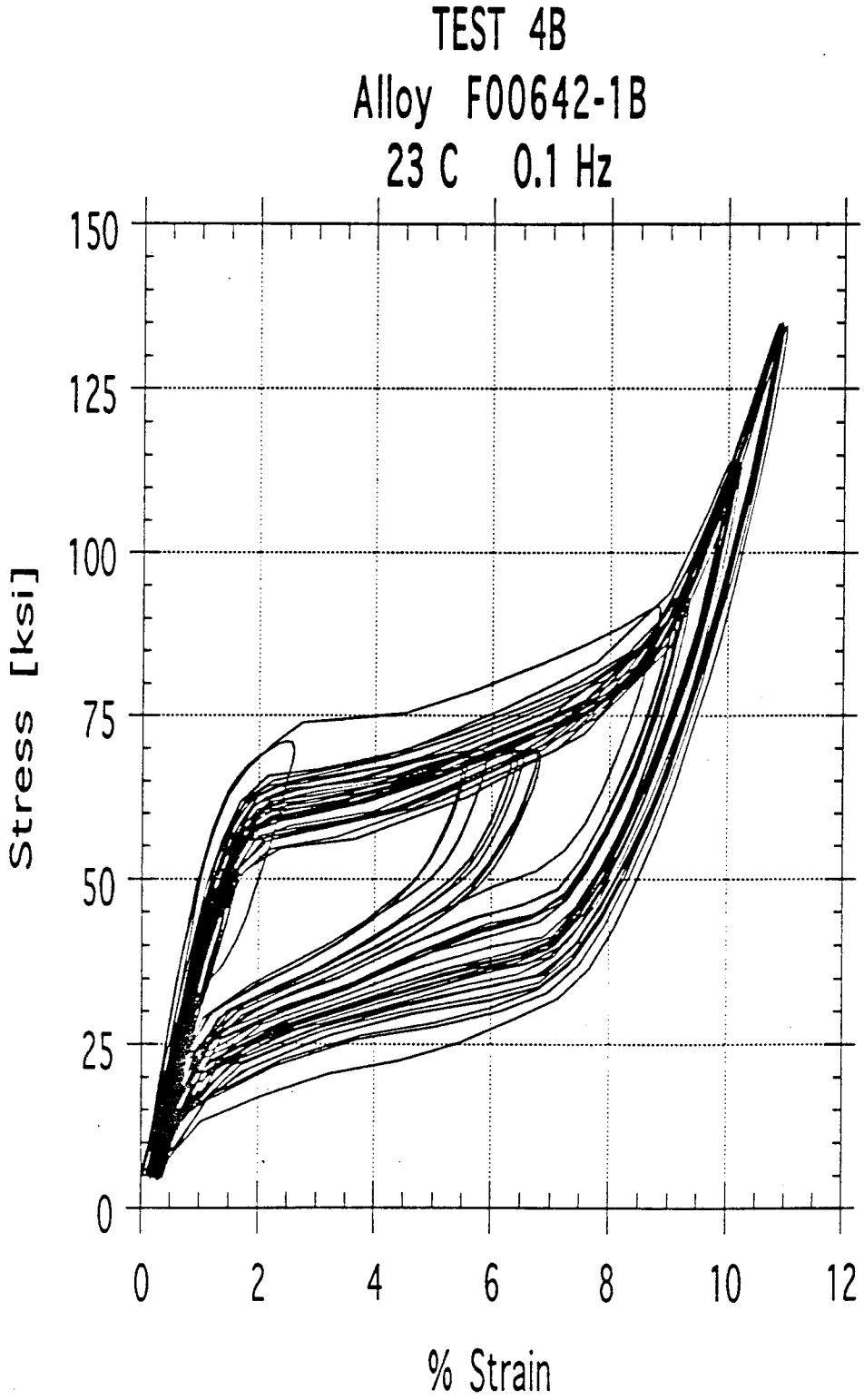
TEST 4B
Alloy F00642-1B
23 C 0.1 Hz
Stress [ksi]
150
125
100
75
50
25
0
0
2
4
6
8
10
12
% Strain

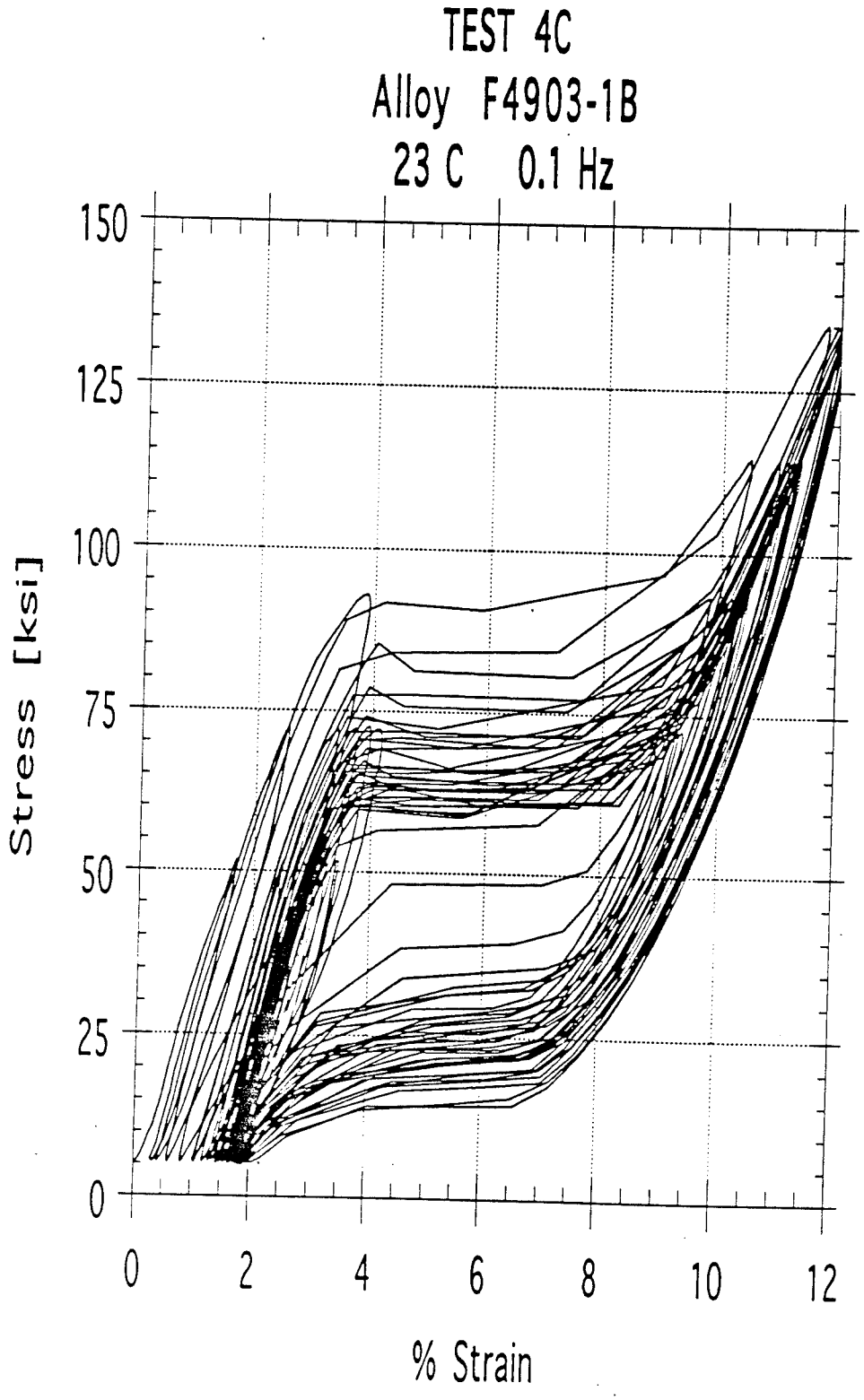
TEST 4C
Alloy F4903-1B
23 C 0.1 Hz
Stress [ksi]
150
125
100
75
50
25
0
0
2
4
6
8
10
12
% Strain

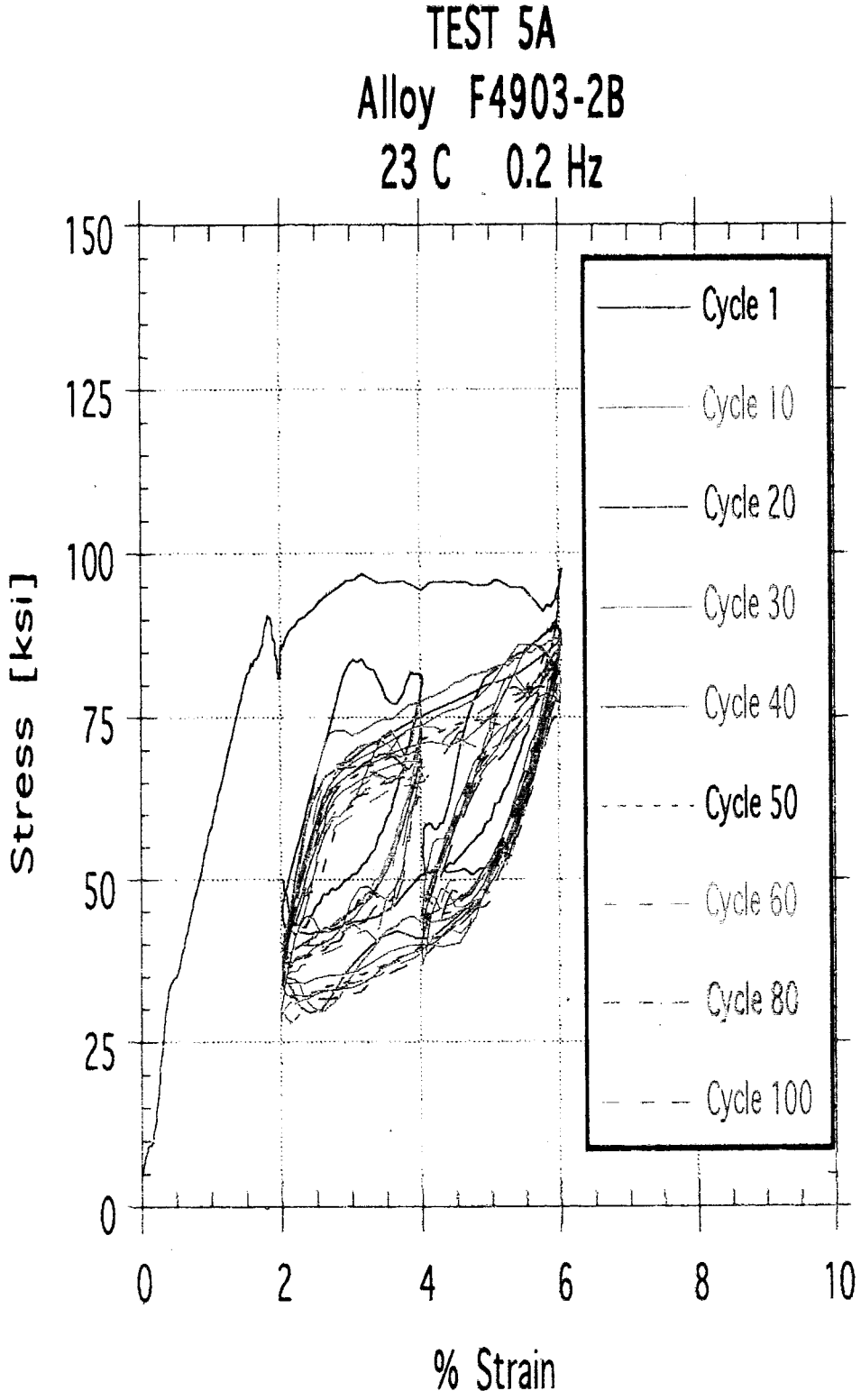
TEST 5A
Alloy F4903-2B
23 C 0.2 Hz
Stress [ksi]
150
125
100
75
50
25
0
0
2
4
6
8
10
% Strain
Cycle 1
Cycle 10
Cycle 20
Cycle 30
Cycle 40
Cycle 50
Cycle 60
Cycle 80
Cycle 100

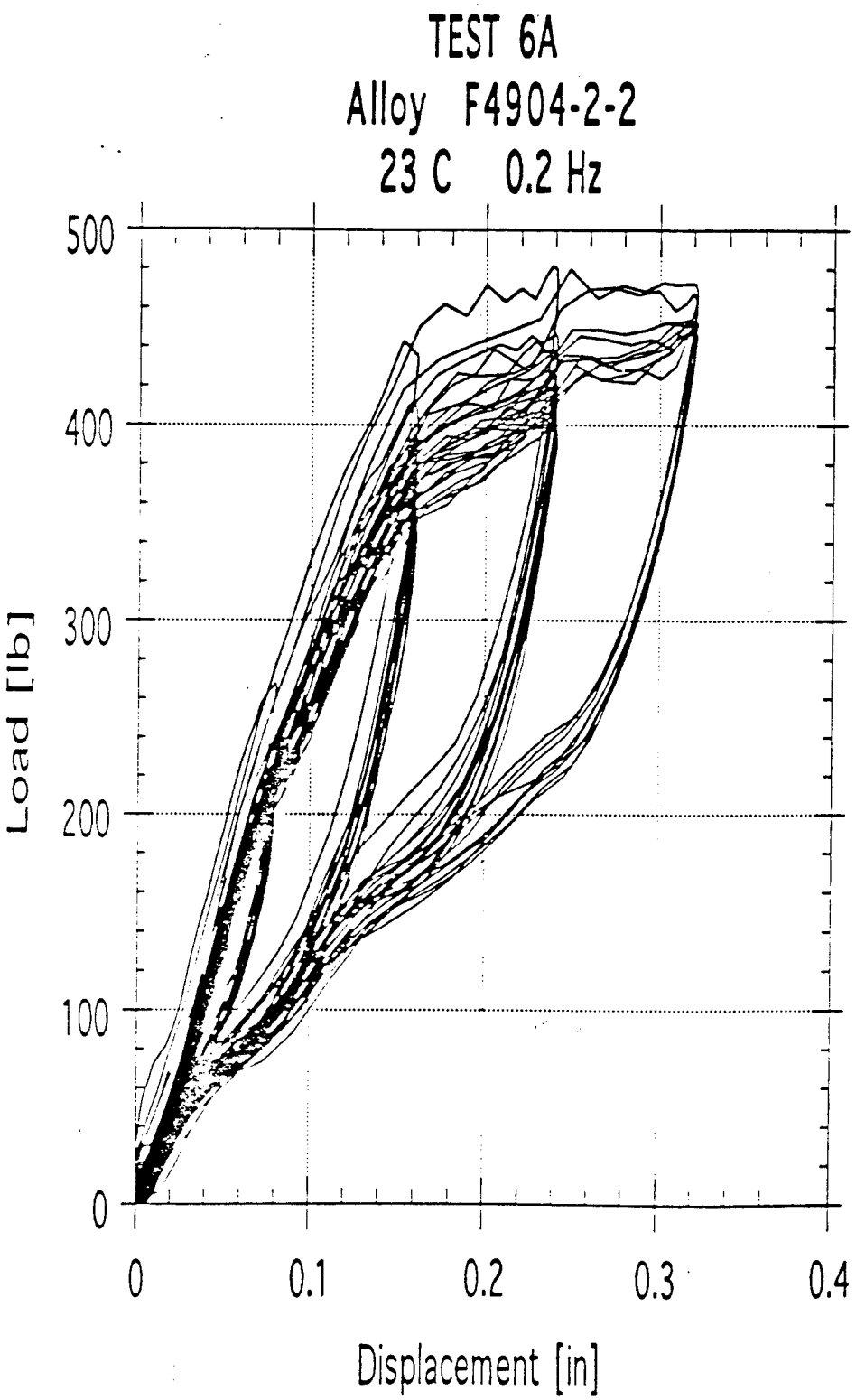
TEST 6A
Alloy F4904-2-2
23 C 0.2 Hz
Load [lb]
500
400
300
200
100
0
0
0.1
0.2
0.3
0.4
Displacement [in]

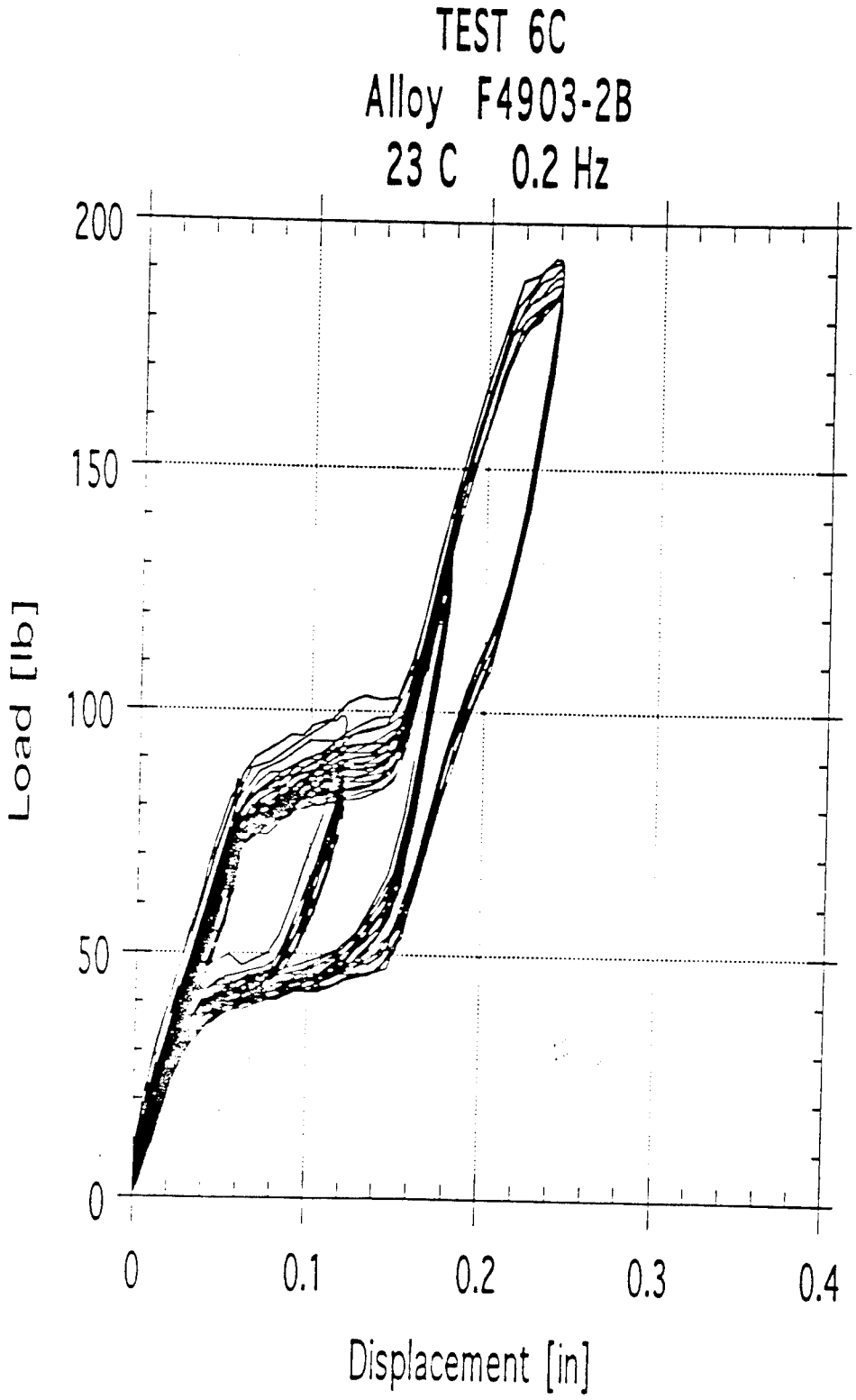
TEST 6C
Alloy F4903-2B
23 C 0.2 Hz
200
150
100
50
0
Load [lb]
0
0.1
0.2
0.3
0.4
Displacement [in]

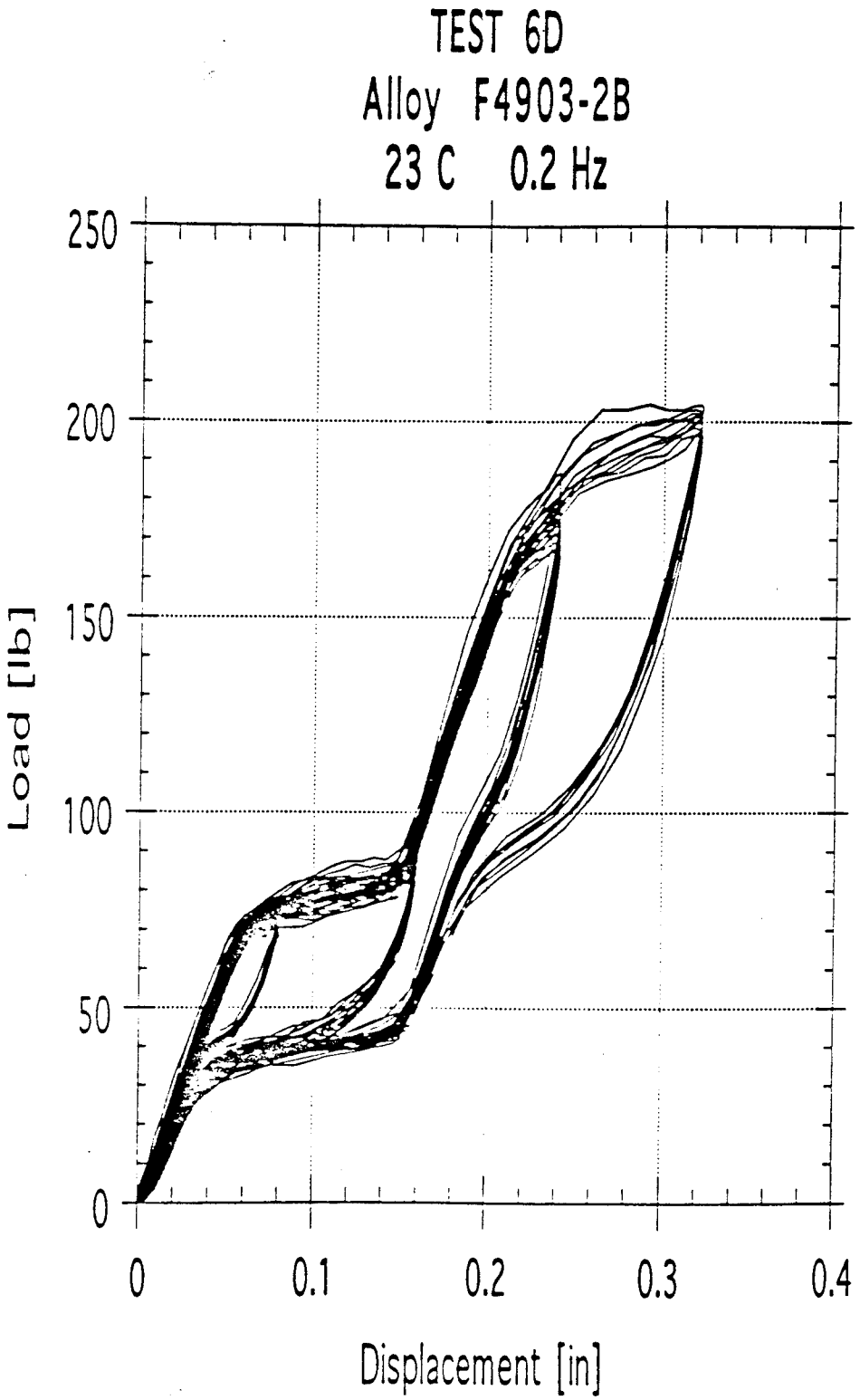
TEST 6D
Alloy F4903-2B
23 C 0.2 Hz
250
200
150
100
50
0
Load [lb]
0
0.1
0.2
0.3
0.4
Displacement [in]

A.2 Design Calculations

BUILDING ANALYSIS

PLAN DETAILS

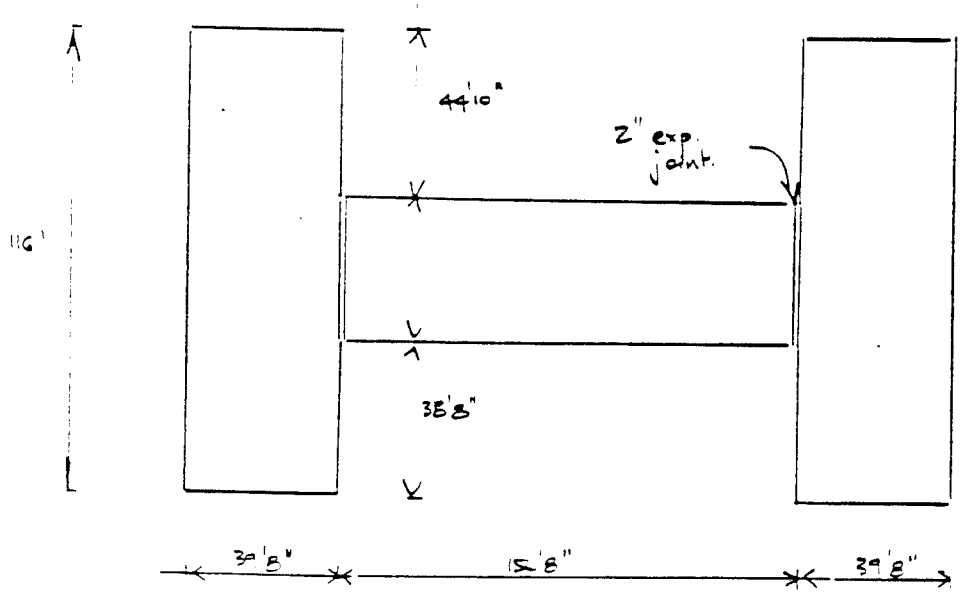

PLAN

ELEVATION DETAILS

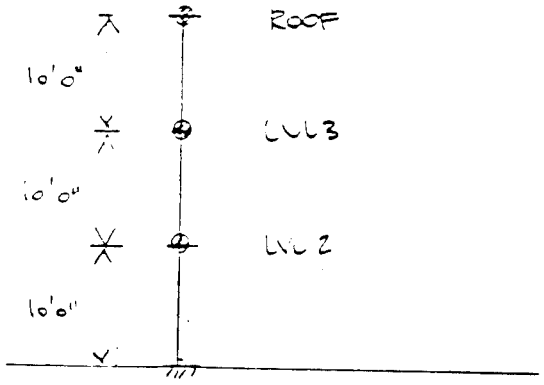

CONSTRUCTION DETAILS

Designed in 1956

Located in Fort Irwin, WA

Seismic zone 3 (1956)

REACTIVE WEIGHT CALCULATION

2ND FLOOR (3RD FLOOR SIM.)

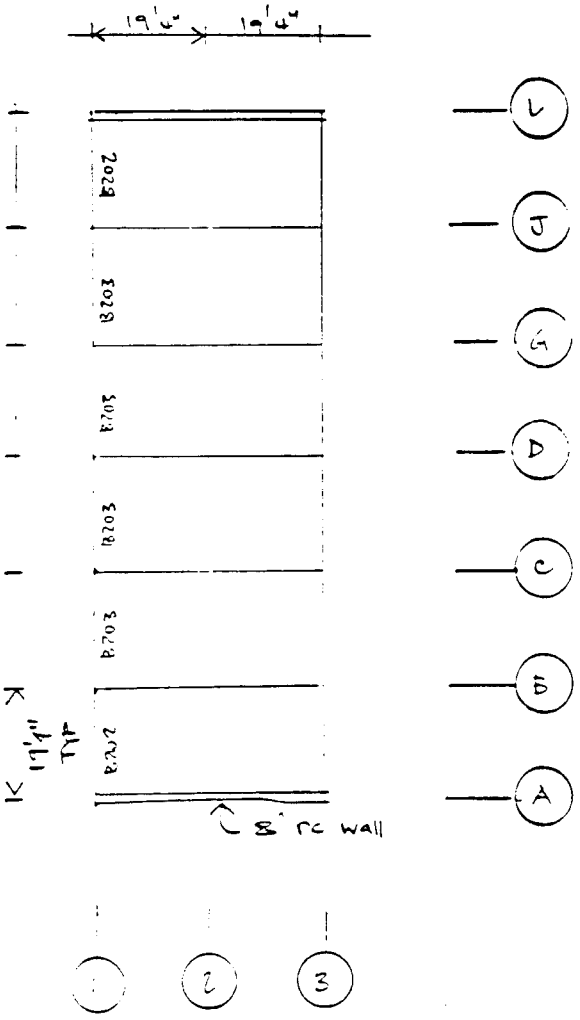

B202 : 10" x 18'8"
B203 : 10" x 18'8"

A1, L1 : ≈ 18" x 18"
B1→J1 : 12" x 23¾"
B2→J2 : 14" x 14"

FLOOR LOADS

DL	7" slab	=	= 88 #/□'
	C+S	=	= 15 #/□'
	Finishes	=	= 2 #/□'
LL	Permanent	=	= 10 #/□'
			115 #/□'

∴ Reactive wt to frame on (1) = 115 x 19.3 x 116

= 257 kips

COLUMN WEIGHTS

18" x 18" : w = 0.34 k/'
12" x 24" : w = 0.30 k/'
14" x 14" : w = 0.20 k/'

∴ Reactive wt to frame on (1) = $0.34 \times 9' \times 2$ (clear) $+ 0.3 \times 9' \times 5 + 0.20 \times 9' \times \frac{5}{2}$

= 24.1 k

WALL WEIGHT

DL : 8" rc wall = $\frac{8}{12} \times 150$ = 100 ± /b'
: Finishes = 6 ± /b'

110 ± /b'

Reactive wt to frame on (1) = $0.110 \times 10' \times 39'8" \times \frac{2}{2}$

= 43.8 k

BEAMS FINISHES ON (1)

DL : Beam B202, 203 = 0.19 k/'
8" rc block = $\frac{8}{12} \times 120 \times 2'6"$ = 0.20 k/'
Overhang = $2' \times \frac{4}{12} \times 150$ = 0.10 k/'
Precast sill = $\frac{7}{12} \times \frac{10}{12} \times 150$ = 0.07 k/'
Glass etc = 0.05 k/'

0.61 k/'

∴ Reactive wt to frame on (1) = 0.61 x 116 = 70.8 k

SUMMARY

∴ Reactive wt to frame on 1 = 257 + 24 + 44 + 71

= 397 k

Roof

∴ Same floor plate as LVL 2

FLOOR LOADS

DL	7" slab	=	88 #/□'
	C-S	=	15 #/□'
	Roofing	=	15 #/□'
LL	Permanent	=	—
			118 #/□'

∴ Reactive wt to frame on (1) = 118 x 193 x 116

= 264 kips

COLUMN WEIGHTS

Reactive wt to frame on (1) = $\frac{24 \cdot 1}{2}$

= 12 kips

SUMMARY

∴ Reactive wt to frame on 1 = 257 + 24 + 44 + 71

= 397 k

ROOF

· Same floor plate as LVL 2

FLOOR LOADS

DL	7" slab	=	= 88 #/0'
	C-S	=	15 #/0'
	Roofing	=	15 #/0'
LL	Permanent	=	—
			118 #/0'

∴ Reactive wt to frame on (1) = 118 x 19.3 x 116

= 264 kips

COLUMN WEIGHTS

Reactive wt to frame on (1) = $\frac{24.1}{2}$

= 12 kips

WALL WEIGHT

Reactive weight to frame on (1) = $\frac{438}{2}$

= 219 kips

BEAMS, FINISHES ON (1)

DL : Beam B402, 403 = = 0.23 k/'
Overhang = 1' x $\frac{4}{12}$ x 150 = 0.05 k/'

0.30 k/' say

∴ Reactive wt to frame on (1) = 0.3 x 116

= 34.8 k

SUMMARY

Reactive wt to frame on (1) = 204 + 12 + 24 + 35

= 335 kips ←

COLUMNS

(a) : 18" × 18"

(b) : 12" × 24"

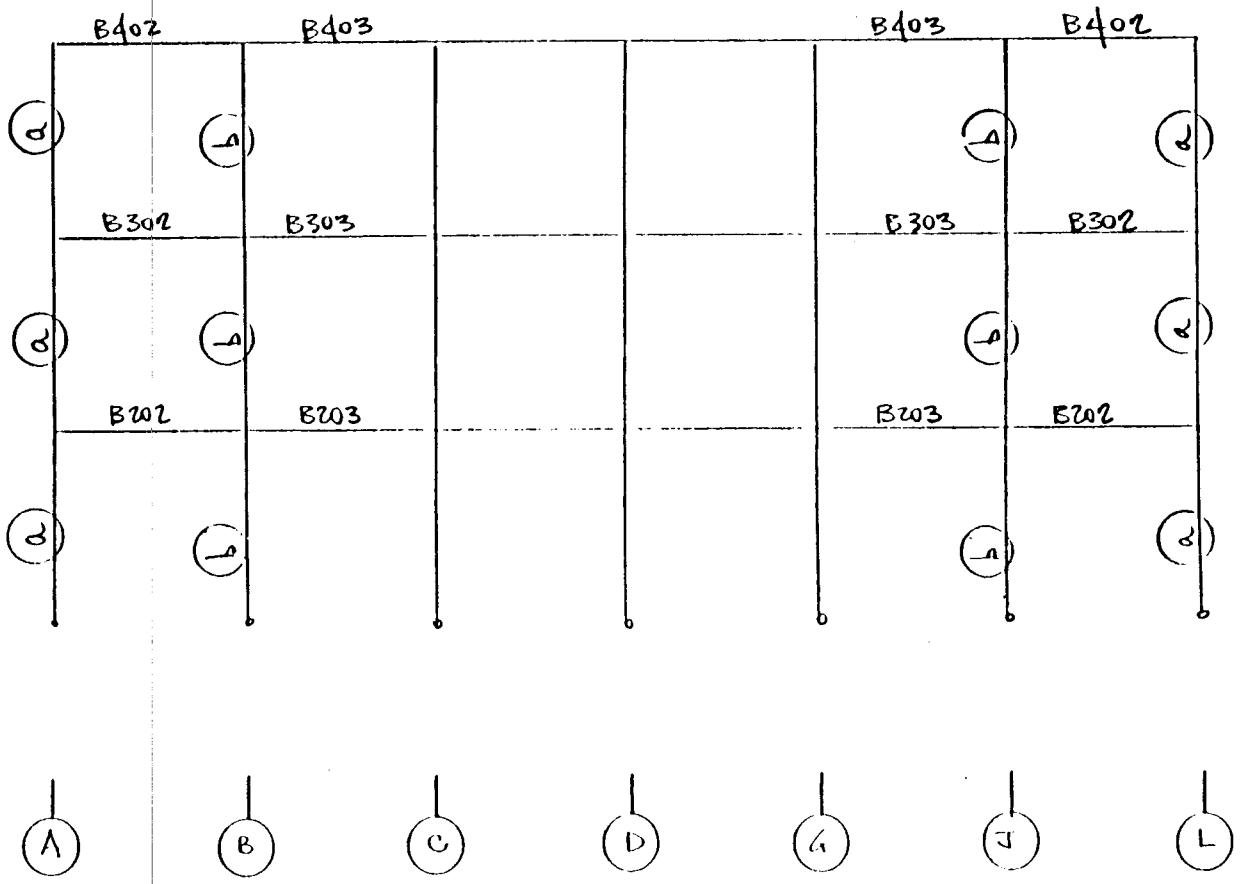

(1) COLUMN & BEAM MARKS

NODAL LAYOUT & GEOMETRY

NOMENCLATURE

○ ELEMENT #

< > STIFFNESS TYPE
YIELD SURFACE

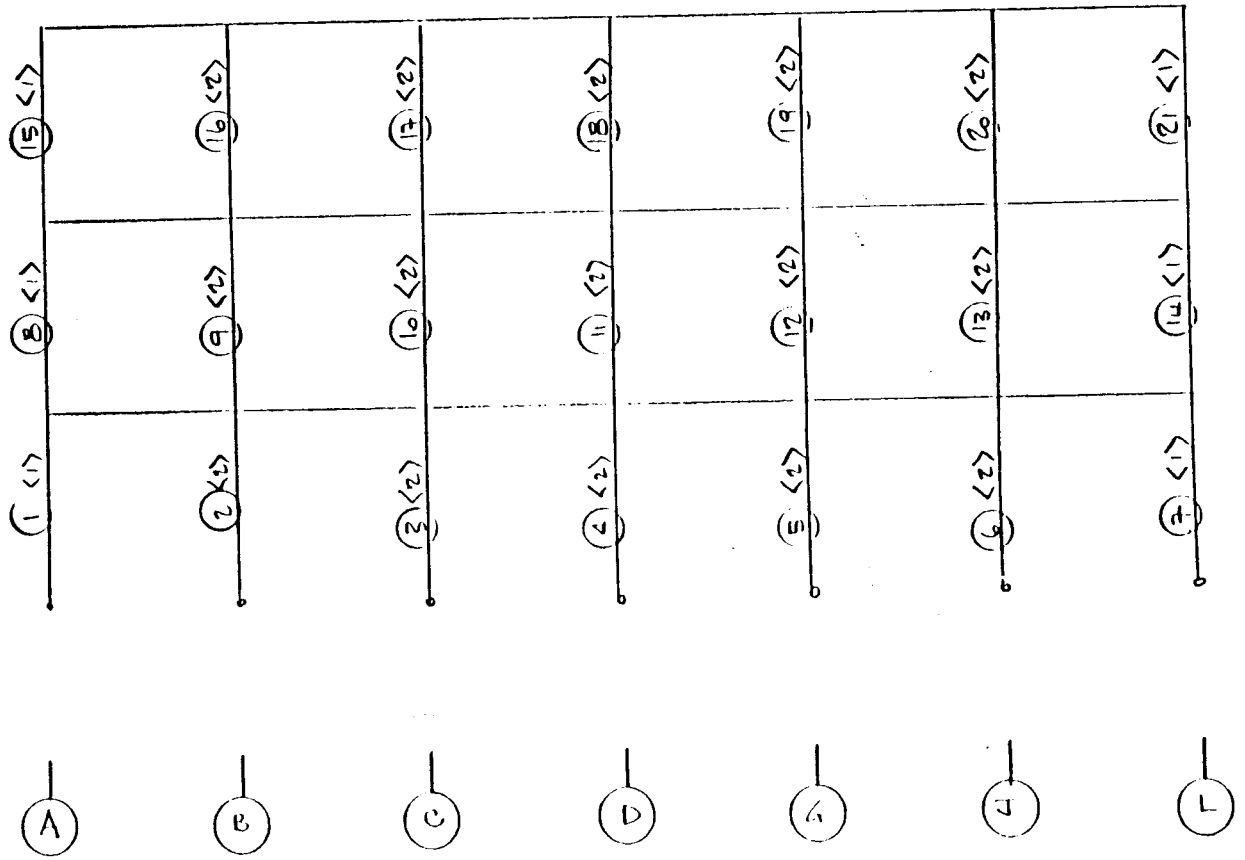

ELEMENT GROUP 1

COLUMNS

NOMENCLATURE

○ ELEMENT #

< > STIFF TYPE

\ Yield Surface

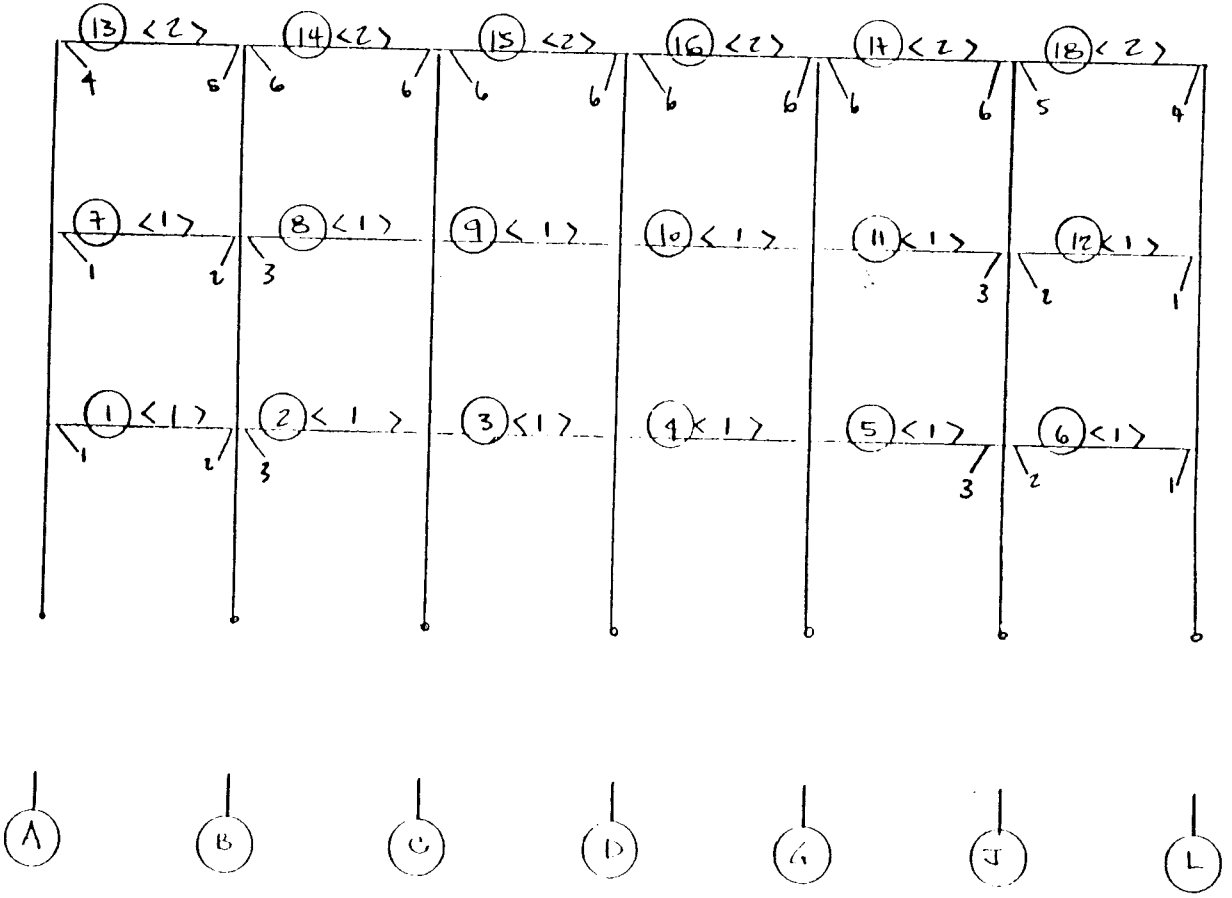

COLUMN GROUP 2

BEAMS

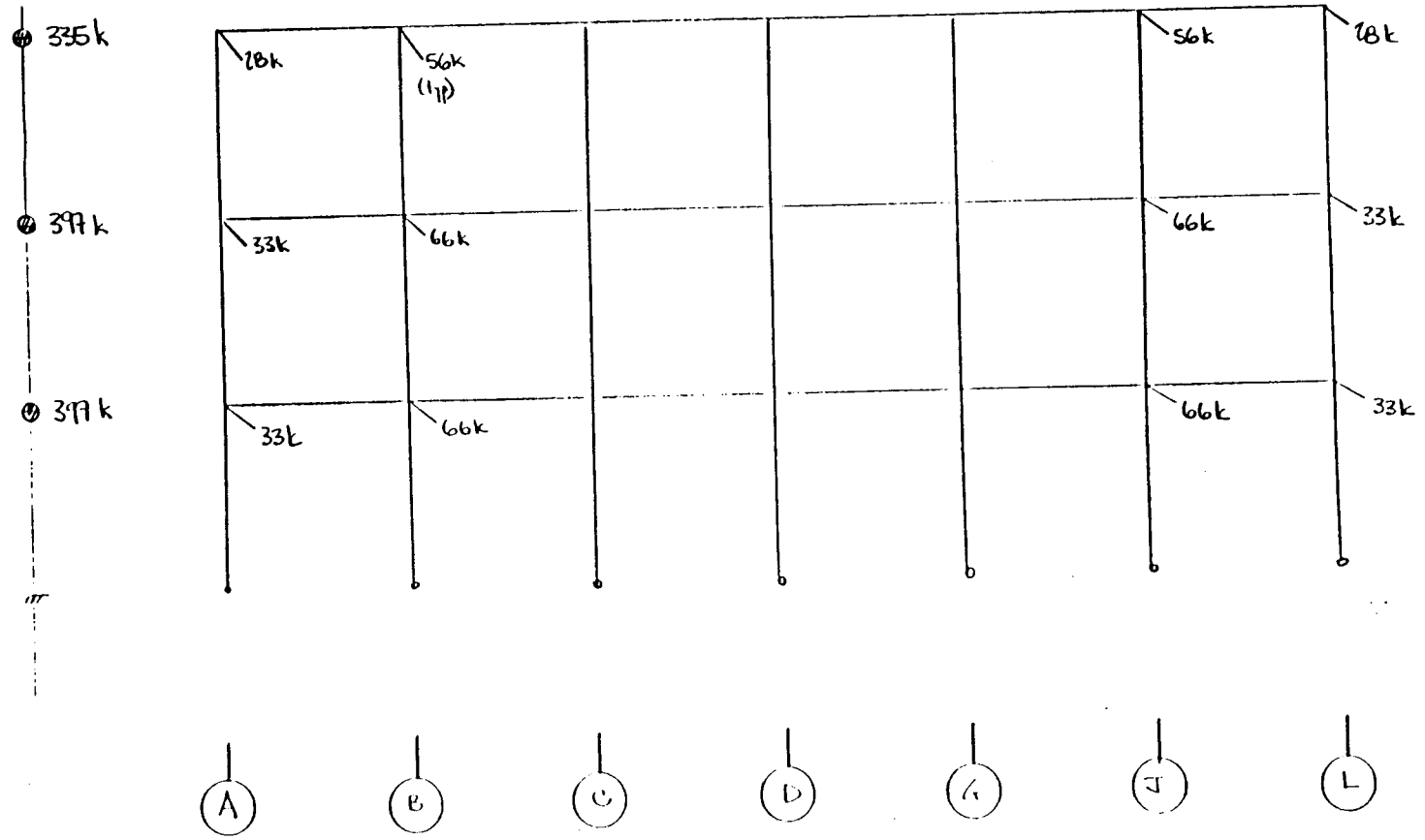

NODAL MASSES (×g)

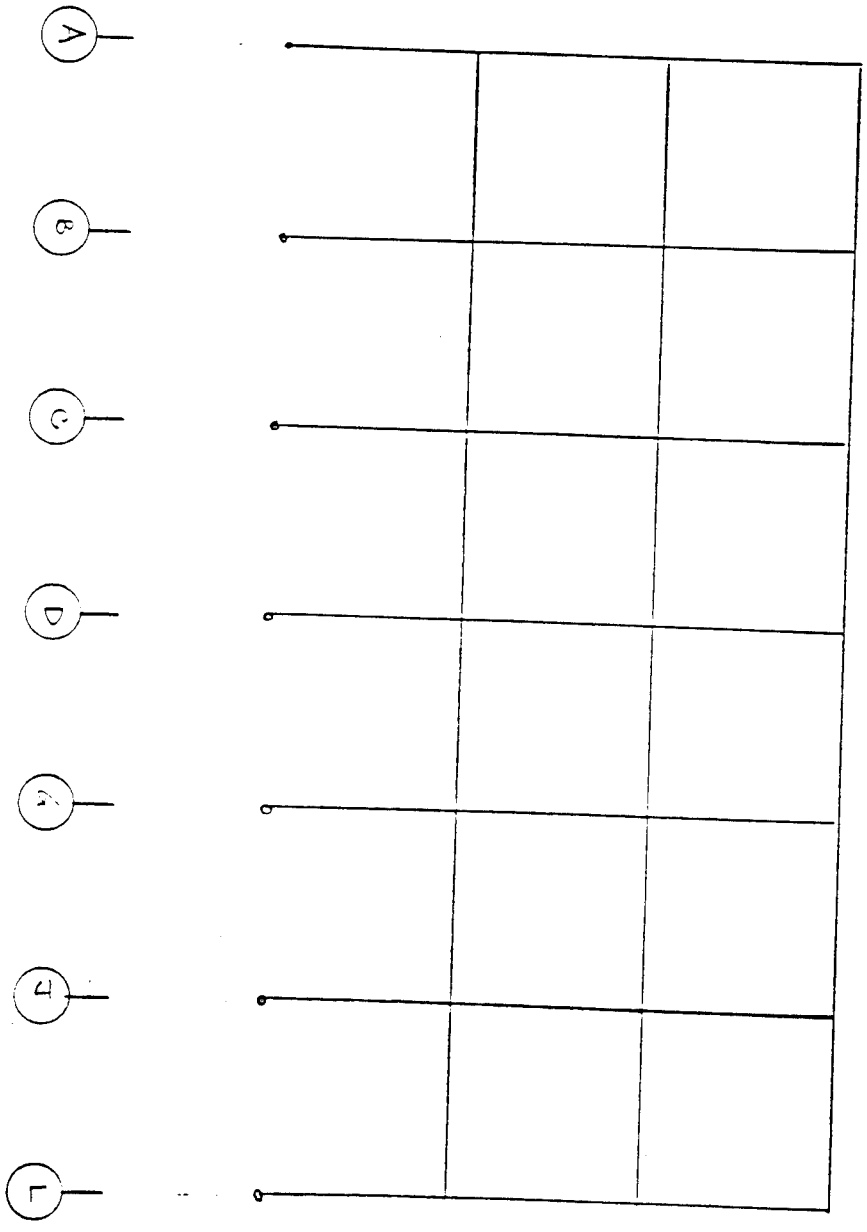
A
B
C
D
E
F

COLUMN PROPERTIES

a) TYPE (a)

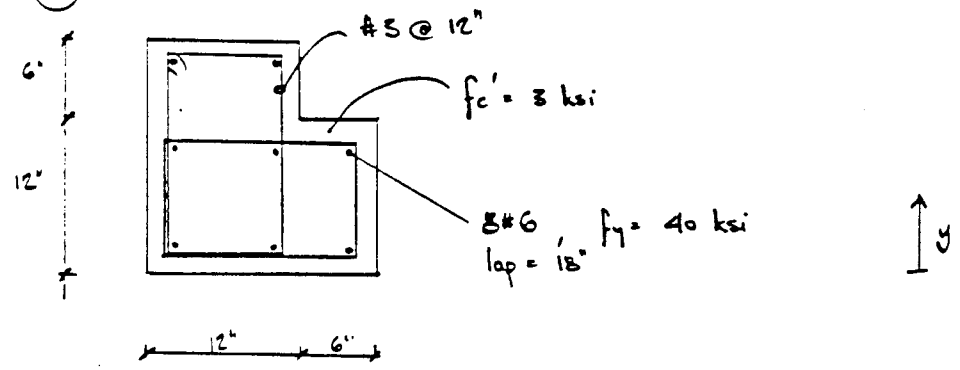

A_g = 288 in²

A_{st} = 0.44 0" × 8 = 3.53 0"

$\bar{y}$ = 8.25" , I_{xx} = 7182 in⁴

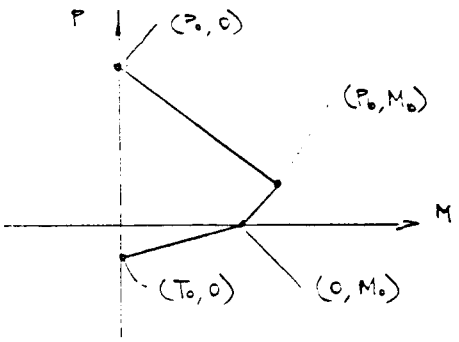

Note: l_d (#6, f_y = 40 ksi) = 13"

Tension splice length = 1.3 l_d

= 17"

< 18" lap ✓

∴ $T_o = A_{st} f_y$ = 141 k = 140 k say

∴ $P_o = (0.85 f_c')(A_g - A_{st}) + f_y A_{st}$ = 866 k = 870 k say

P_b, M_b 410 k, 2300 k"

∴ 0, M_o : 0 k, 540 k"

b) TYPE (b)

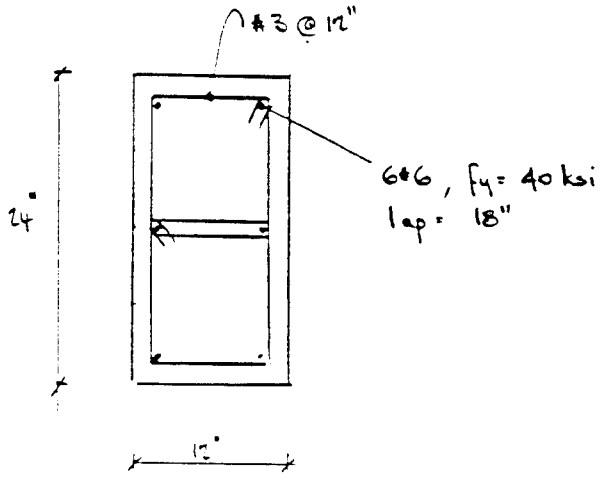

A_g = 288 in² A_{st} = 2.64 in²

I_{xx} = 13824 in⁴

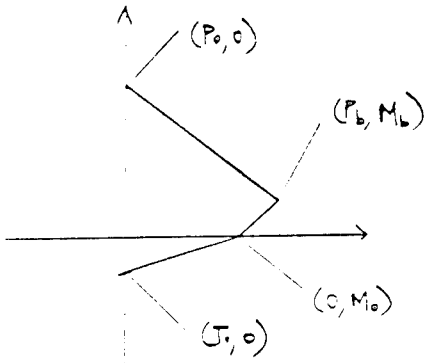

∴ $T_0 = A_{st} f_y = 2.64 \times 40 = 106$ k say 105 k

∴ $P_0 = 0.85 f'_c (A_g - A_{st}) + f_y A_{st}$ = 833 k say 830 k

∴ P_b, M_b = 380 k, 2840 k"

∴ 0, M_0 = 0, 740 k"

BEAM PROPERTIES

VERTICAL SECTION

@ (1)

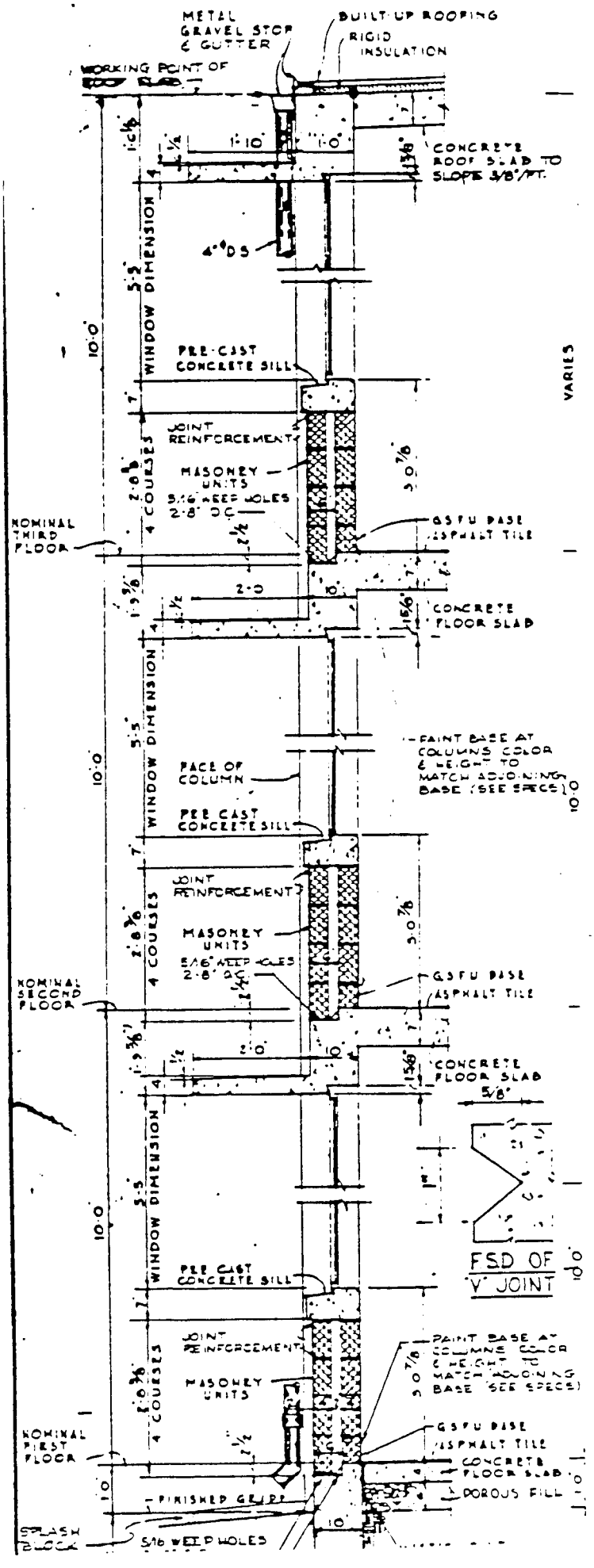

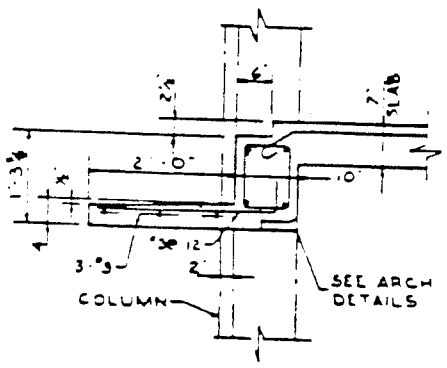

SECT 32/3J 32/3J

SCALE 1/4"=1'-0"

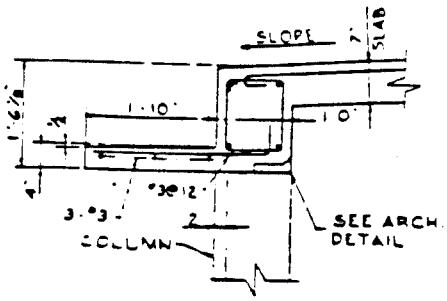

SECT 30/3J 30/3J

SCALE 1/4"=1'-0"

SECTION @ FLOOR

SECTION @ ROOF

BEAM PROPERTIES

B102, B203, B302, B303

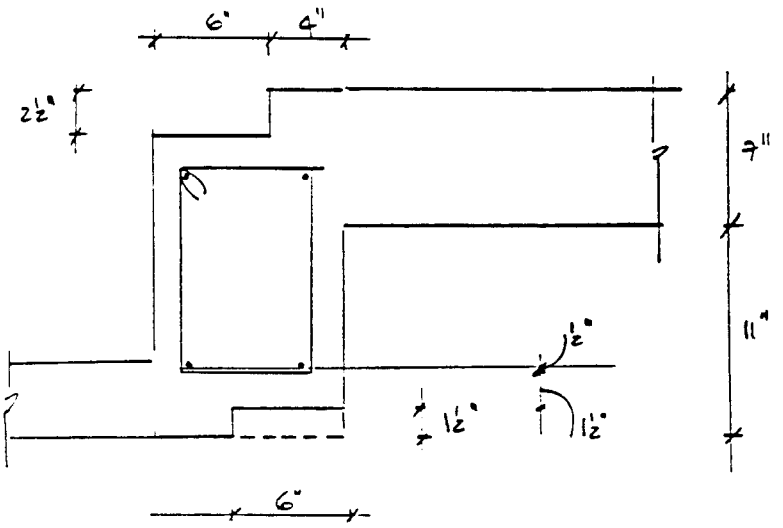

- Slab width : 19'4"/12 = 20" ⟩ use 24"
  6x t = 42" ⟩
- Idealized section :

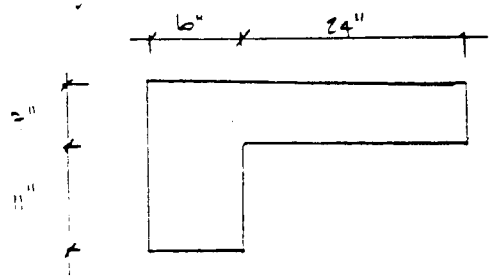

A = 348 in²

$\bar{y}$ = 11.6"

I_{xx} = 8622 in⁴

- M - ϕ relation

$d^+ = 18 - 1\frac{1}{2} - 1\frac{1}{2} - \frac{1}{2}" = 14\frac{1}{2}"$

$d^- = 15\frac{1}{2}" - 1\frac{1}{2}" - 1\frac{1}{2}" - \frac{1}{2}" = 12\frac{1}{2}"$

For B302

@ (A) , cliscont. end , 2#6 T , anchored @ face of col
2#8 B

For M_u^- : $a = 1.38"$ ~ same level as comp^n rebar

$\therefore M_n^- = 2 \times 0.44 \times 40 \left(12.5" - \frac{1.38}{2}\right) = \underline{415\ k"}$

For M_u^+ : $a = 0.73"$ ∴ ignore the comp^n steel

$\therefore M_n^+ = 2 \times 0.79 \times 40 \times (14.5 - 0.37) = \underline{893\ k"}$

@ (B) , continuous end ; 2#6T, 1#10T
2#8B

For M_u^- : $A_{st} = 2.10\ in^2$, $a = 3.29"$

$d' = 2.5"$ $\epsilon_s = 0.0007 = 0.5\epsilon_y$

$\therefore M_n^- = 2.10 \times 40 \left(12.5 - \frac{3.29}{2}\right) = \underline{911\ k"}$

For M_u^+ : $2 \times 0.79 \times 40 \times (14.5 - 0.37) \times \frac{l}{l_d}$ → anchorage
l_d --> 24"

$= 893 \times \frac{11}{24} = \underline{410\ k"}$

For B303

@ (C) : 2#6, 2#7 T
3#6 B

For M_u^- : $A_{st} = 2.08\ in^2$; $a = 3.26"$

$d = 2.5"$, $\epsilon_s > 0.5\epsilon_y$ ∴

$\therefore M_n^- = 2.08 \times 40 \times (12.5 - 1.63) = \underline{904\ k"}$

For M_u^+ : $3 \times 0.44 \times 40 \times (14.5 - 1.03) \times \frac{l}{l_d}$ → 11"
--> 13"

$= 511 \times 11" = \underline{601\ k"}$

B402, B403

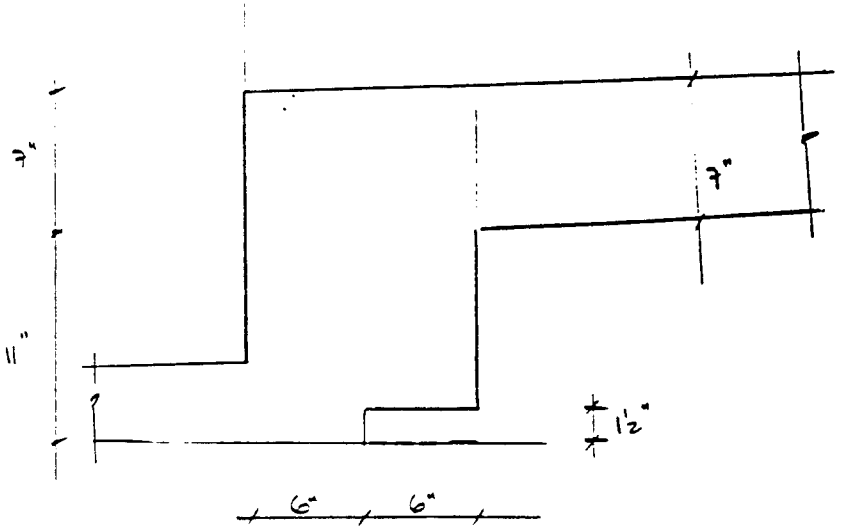

- Slab width . 24"

- Idealized section

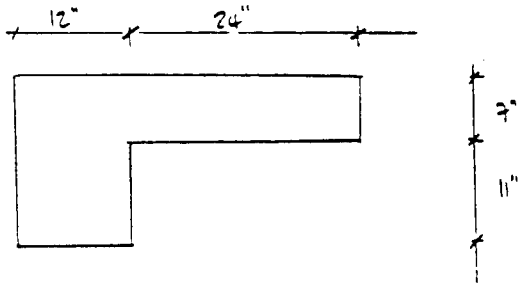

A = 384 in²

$\bar{y}$ = 11.40"

I_{xx} = 9431 in⁴

- M- ψ relation

d^+ = 14.5"

d^- = 14.5"

For B4C2

@ (A) ; discont. end ; 2#6 T, 2#6 B, anchored @ face of col.

For M_u^- : $a = 1.15"$ $\therefore \epsilon_y = 0$

$\therefore M_u^- = 2 \times 0.44 \times 40 \times (14.5 - 0.58) = \underline{490 \text{ k"}}$

For M_u^+ : $a = 0.38"$ $\therefore \epsilon_y = 0$

$\therefore M_u^+ = 2 \times 0.44 \times 40 \times (14.5 - 0.19) = \underline{503 \text{ k"}}$

@ (E) : cont. end ; 2#6, 1#5 T, 2#6 B

For M_u^- : $a = 1.54"$ $\therefore \epsilon_y = 0$

$\therefore M_u^- = 1.18 \times 40 \times (14.5 - 0.77) = \underline{648 \text{ k"}}$

For M_u^+ : $a = 0.38"$ $\therefore \epsilon_y = 0$

$M_u^+ = 503 \times \frac{l}{l_1} = 503 \times \frac{11}{13} = \underline{425 \text{ k"}}$

For B4C3

@ (C) : cont. ; 2#6, 1#5 T, 2#6 B

$M_u^- = \underline{648 \text{ k"}}$

$M_u^+ = \underline{425 \text{ k"}}$

GRAVITY ACTIONS ON (E) FRAMING

2ND FLOOR, 3ED FLOOR

Floor = 0.115 x 9.67 = 1.11

Beams etc = 0.61 k/' = 0.61

1.72 k/'

$M^- = \frac{wl^2}{12} = \frac{1.72 \times (19.3-2)^2}{12} = 514\ k''$

$V = \frac{wl}{2} = \frac{1.72 \times 19.3}{2}$ (for correct axial load in col.)

= 16.6 k

P = 0 k

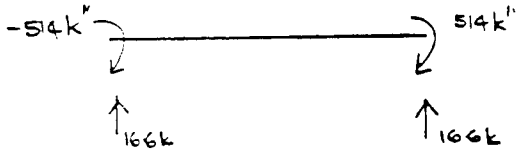

ROOF

Floor = 0.118 x 9.67 = 1.14 k/'

Beams etc = 0.30 = 0.30 k/'

1.44 k/'

$M^- = \frac{1.44 \times 17.3^2}{12} = 432\ k''$

$V = \frac{1.44 \times 19.3}{2} = 13.9\ k.$

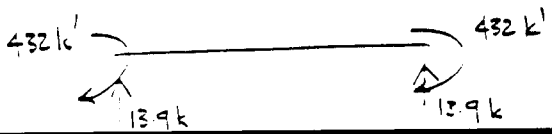

COLLAPSE ANALYSIS

- Assume that hinge stability is assured
- Ignore DL moments
- Use kinematic method

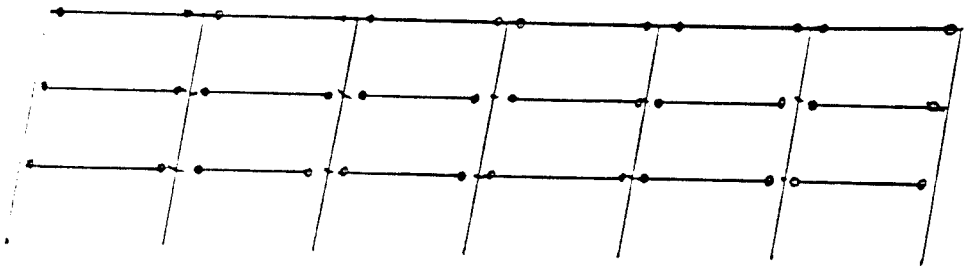

B2C2 $M_u^+ = 893$ k" ; $M_u^- = 415$ k" @ discont. end

$M_u^+ = 410$ k" , $M_u^- = 911$ k" @ cont. end

B2C3 $M_u^+ = 601$ k" ; $M_u^- = 904$ k"

B402 $M_u^+ = 503$ k" ; $M_u^- = 490$ k" @ discont end

B403/2 $M_u^+ = 425$ k" ; $M_u^- = 648$ k" @ cont. end

Internal work

$$W_I = \sum M_{ui}\theta_i = \theta(893+415)\times 2 + (410+911)\times 2\theta + \theta(601+904)\times 4\times 2 + \theta(490+503) + \theta(425+648) + \theta(425+648)\times 4 = 23656\,\theta$$

} LVL 2/3

External work

$W_E = \sum P_i h_i \delta_i$ $\langle h = 120" \rangle$

$= P(120\theta + 240\theta + 360\theta)$ for 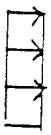

$= 720\,P\theta$

$\therefore \quad P = \frac{23656}{7100} = 3.28\ k$

Now $Y_b = 3P$ for rectangular dist^n

$= 98.5\ k$

$W_E = P(120\theta) + 2P(240\theta) + 3P(360\theta)$ for 

$= 1680\ P\theta$

$\therefore \quad P = \frac{23656}{1680} = 14.1\ k$

Now $Y_b = 6P$ for triangular dist^n

$= 84.4\ k$

SUMMARY

Considering both rect. and tri. force distributions,

$$84\ k < V_{max} < 98\ k$$

or

$$0.14\ W < V_{max} < 0.17\ W$$

Note that 1/ hinge stability not assured

2/ only 1 mechanism considered

3/ kinematic method provides an upper bound on the collapse load.

: pedro Mon Feb 8 10:03:47 1993
e: Mon, 8 Feb 93 10:03:46 PST
n: pedro (Peter Clark)
asw
ject: Re: acceleration files
tent-Length: 937

ave these on the UNIX system - they are easily transferable to diskette.

ummary:

eta de Campos:
---
noacan EQ, 9-19-85, 4886 pts. @ 0.01 sec, M=8.1, dist.=21 km, acc. in g

component -> range=(-0.131,0.141) g
component -> range=(-0.100,0.140) g

red in ~pedro/eqsignals.d/cale.000 and cale.090, single column data

nua Tree Fire Station:
---
iers EQ, 6-28-92, 4000 pts. @ 0.02 sec., M=7.6, dist.=9 km, acc. in g

component -> range=(-0.176,0.273) g
component -> range=(-0.255,0.284) g

red in ~pedro/eqsignals.d/josh.360 and josh.090, single column data

ert Hot Springs:
---
n Springs EQ, 7-8-86, 3000 pts. @ 0.02 sec, M=5.9, dist.=12 km, acc. in g

component -> range=(-0.286,0.300) g
component -> range=(-0.247,0.269) g

red in ~pedro/eqsignals.d/deshot.000 and deshot.090, single column data

e this helps, Pedro

CERL EBIR

Hinge rotation capacity :

B203 2#6 T ; 2#7 T ; 3#6 B
#3 □ @ 12" o.c.

$c^+ = 2.06"$; $c^- = 3.26"$

$M_u^+ = 601$ k" ; $M_u^- = 904$ k"

$\bar{\rho}_{s_1} = \dfrac{2.08 \square" \times 12 + 2(8 + 10) \times 0.11}{8 \times 10 \times 12} = 0.030$

$\rho_{s_2} = \dfrac{3 \times 0.44 \times 12 + 2 \times 18 \times 0.11}{8 \times 10 \times 12} = 0.021$

$b = 10"$

$z = 16"$

$\dfrac{\bar{\rho}_s f_y}{2\omega} = 0.06$, 0.042

$\epsilon_c^{\circ} = 0.003 + 0.02 \times \dfrac{10}{116} + 0.06^2 = 0.0083$

$\epsilon_c^{\circ} = .003 + 0.0017 + 0.042^2 = 0.0065$

$\phi_u^{\circ} = \dfrac{.0083}{2.06} = 0.0040$ ——— 1

$\phi_u^{2} = \dfrac{.0065}{3.26} = 0.0020$ ——— 2

For elastic behaviour, $k \triangleq 0.3$ say

$d(1-k) \triangleq 8.8"$ say

$\phi_Y = \dfrac{0.0014}{8.8} = 0.0002$

Using Corley : $l_p = 0.5d + 0.2\sqrt{d} \cdot \dfrac{z}{d}$

$= 0.5 \times 12.5 + 0.2\sqrt{12.5} \times \dfrac{16}{12.5}$

$\therefore \quad l_p = 12"$

$\therefore \quad \theta_p = l_p (\phi_u - \phi_y) = 12" \times (0.0018)$

$= 0.02$ radians

$\therefore$ For the purposes of these analyses, failure could be assumed once beam hinge rotations exceed 0.02 radians.

OR

If the ultimate concrete strain is assumed to be 0.004 ($= \epsilon_c$), the following hinge rotations are possible

$\epsilon_c = 0.004$

$\phi_u = \frac{0.004}{2.06} ; \frac{0.004}{3.26} = 0.0019 ; 0.0013$

Noting that gravity and seismic moments could be additive, a more conservative estimate of θ would be $1/4$ or $58°$:

$l_p = 1.5 \times 12.5 - 0.2\sqrt{12} \times \frac{58}{12.5} \approx 9.5"$

$\therefore \quad \theta_p^{max} = l_p (\phi_u - \phi_y) = 9.5 (0.0013 - 0.0002)$

$= 0.01$ radians

$\therefore$ For the purposes of these analyses, failure will be assumed to have occurred once θ_p exceeds 0.01 radians

APPENDIX : Calculation of (P_b, M_b) for columns

a) TYPE (a)

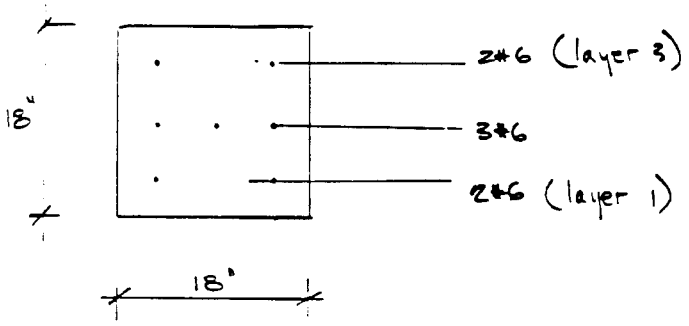

$\epsilon_Y = 0.0014$ for $f_Y = 40$

$$c = \frac{0.003}{.003 - (-0.0014)} d_1 = 0.68 \times 15.5 = 10.5"$$

$$a = 1.85 \times 10.5 = 8.95"$$

$$\epsilon_{s_1} = 0.0014$$

$$\epsilon_{s_2} = \left(\frac{c - \hat{d}}{c}\right) .003 = 0.0004 \triangleq 0$$

$$\epsilon_{s_3} = \left(\frac{c - d_2}{c}\right) .003 = 0.0023 > \epsilon_Y$$

$$\therefore C_c = 1.85 \times 3 \times 8.95 \times 18 = 410 \text{ k.}$$

$$F_{s_1} = 0.88 \times -40 = -352 \text{ k}$$

$$F_{s_3} = (40 - .85 \times 3) \times 0.88 = 32.9 \text{ k.}$$

$$\therefore P_b = 410 + 32.9 - 352 = 407 \text{ k.}$$

$$M_b = 1845 + 213 + 228 = 2286$$

Use $P_b = 410 \text{ k}$

$M_b = 2300 \text{ k}"$

5) TYPE (5)

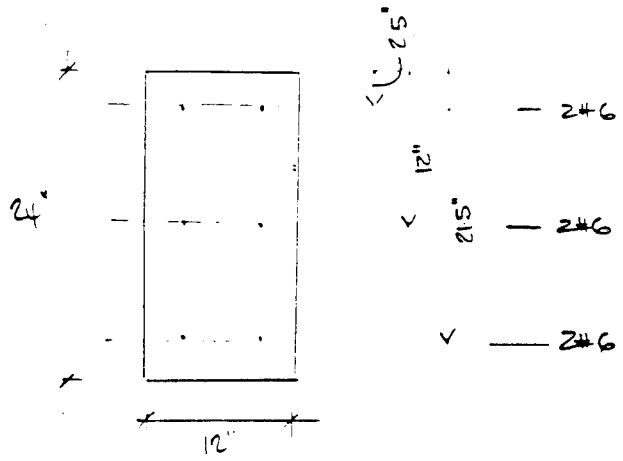

$$c = \frac{0.003}{0.0014} \times 21.5 = 14.7"$$

$$a = 12.5"$$

$$\epsilon_{s1} = 0.0014$$

$$\epsilon_{s2} = 0$$

$$\epsilon_{s3} = \frac{14.7 - 2.5}{14.7} \times .003 = 0.0025 > \epsilon_y$$

$$C_c = 0.85 \times 3 \times 12.5 \times 12 = 382\ k$$

$$F_{s1} = -40 \times .88 = -352\ k$$

$$F_{s3} = (40 - .85 \times 3)\ 0.88 = 32.9\ k.$$

$$\therefore P_b = 382 - 352 + 32.9 = 379\ k"$$

$$\therefore M_b = 2196 + 334 + 312 = 2842\ k"$$

$$\therefore \text{Use} \quad P_b = 380\ k$$

$$\underline{M_b = 2840\ k"}$$

CERL

Damping For Time-History Analysis

- Provide $\xi = 5\%$ in modes 1 & 2

- For existing building $T_1 = 1.55$ sec ; $w_1 = 4.05$ r/s
  $T_2 = 0.18$ " $w_2 = 34.89$ r/s

$$\therefore \underline{\xi} = 0.5 \begin{bmatrix} 1/w_1 & w_1 \\ 1/w_2 & w_2 \end{bmatrix} \langle \alpha \ \beta \rangle^T = 0.5 \begin{bmatrix} 0.247 & 4.05 \\ 0.0287 & 34.89 \end{bmatrix} \langle \alpha \ \beta \rangle^T$$

$$\therefore \langle \alpha \ \beta \rangle^T = A^{-1} \underline{\xi} = \frac{1}{2.11} \begin{bmatrix} 17.450 & -2.010 \\ -0.0144 & 0.123 \end{bmatrix} \langle 0.05 \ \ 0.05 \rangle^T$$

$$\therefore \begin{bmatrix} \alpha \\ \beta \end{bmatrix} = \begin{bmatrix} 0.3656 \\ 0.0026 \end{bmatrix} \quad \text{——— (1)}$$

- For upgraded building $T_1 = 0.20$ sec ; $w_1 = 31.40$ r/s
  $T_2 = 0.079$ sec ; $w_2 = 79.49$ r/s

$$\therefore \underline{\xi} = 0.5 \begin{bmatrix} 0.0318 & 31.40 \\ 0.0125 & 79.49 \end{bmatrix} \langle \alpha \ \beta \rangle^T$$

$$= \begin{bmatrix} 0.0159 & 15.70 \\ 0.0062 & 39.75 \end{bmatrix} \langle \alpha \ \beta \rangle^T$$

$$\therefore \langle \alpha \ \beta \rangle^T = \frac{1}{0.5346} \begin{bmatrix} 39.75 & -15.70 \\ -0.0031 & 0.00795 \end{bmatrix} \langle 0.05 \ \ 0.05 \rangle^T$$

$$\therefore \begin{bmatrix} \alpha \\ \beta \end{bmatrix} = \begin{bmatrix} 2.2489 \\ 0.00091 \end{bmatrix} \quad \text{——— (2)}$$

A.3 Code Requirements for Energy Dissipation Devices

TENTATIVE

SEISMIC DESIGN REQUIREMENTS FOR PASSIVE ENERGY DISSIPATION SYSTEMS

ENERGY DISSIPATION WORKING GROUP OF THE
BASE ISOLATION SUBCOMMITTEE
OF THE SEISMOLOGY COMMITTEE

STRUCTURAL ENGINEERS ASSOCIATION
OF NORTHERN CALIFORNIA

DRAFT

15 April 1993

DRAFT

TENTATIVE SEISMIC DESIGN REQUIREMENTS FOR PASSIVE ENERGY DISSIPATION SYSTEMS

Base Isolation Subcommittee
of the Seismology Committee
Structural Engineers Association of
Northern California

APRIL 1993

SUBCOMMITTEE MEMBERS

Andrew Whittaker - Chair
Ian Aiken
Peter Clark
Julie Cohen
José Inaudi
James Kelly
Roger Scholl

CORRESPONDING MEMBERS

Robert Bachman
Vitelmo Bertero
Michel Bruneau
Michael Constantinou
Ron Hamburger
Robert Hanson
Charles Kircher
Robert Krumme
David Lee
Douglas Nims
Egor Popov
Richard Sause
Chris Thompson

PREFACE

This document has been prepared by the Energy Dissipation Working Group of the Base Isolation Subcommittee of the Seismology Committee of the Structural Engineers Association of Northern California (SEAONC) with the intent of supplementing the Structural Engineers Association of California's (SEAOC) "Tentative Lateral Force Requirements, October, 1990" (1990 Blue Book) with additional design requirements developed specifically for buildings incorporating discrete passive energy dissipating devices. The format and nomenclature is consistent to facilitate formal integration into the *Uniform Building Code* (UBC) in the event such requirements are adopted.

The SEAOC Seismology Committee has not had the opportunity to review and approve these tentative requirements. This document is published in its tentative form to allow broad review. By publishing the tentative requirements, SEAONC is neither advocating nor opposing use of passive energy dissipation devices in lieu of other structural seismic resisting systems.

This document has been prepared in keeping with the most current information and practice of the present state-of-the-art of engineering design. However, the authors, editors and all organizations and individuals who have contributed to this publication are not responsible for any errors, omissions, negligence or any other deficiencies that may results from the use of this publication.

INTRODUCTION

Acceptable performance of a building during earthquake shaking is predicated on the building's ability to absorb and dissipate energy. For severe, long-duration earthquake shaking, a building must be capable of absorbing and dissipating energy in a stable manner for a large number of loading cycles. In conventional earthquake-resistant buildings, energy dissipation (damage) occurs in plastic hinge zones in members that typically form part of the gravity load resisting system; such damage may be irreparable.

The function of an energy dissipation unit (EDU) in an energy dissipation system (EDS) is to dissipate earthquake-induced energy. Since the EDUs do not form part of the gravity load-resisting system, they are easily replaceable after an earthquake. The general philosophy of these guidelines is to confine the inelastic activity in the EDS primarily to the EDUs and for the gravity load-resisting system to remain elastic for the Design Basis Earthquake (DBE).

The potential advantages of energy dissipation systems (EDS) and the recent advancements in EDU products have already led to the design and construction of buildings and bridges incorporating EDUs in Canada, Japan, Mexico, New Zealand, and the United States. This activity and concerted research efforts in the United States has in turn identified a need to supplement existing building codes with design requirements developed specifically for such buildings. This need is shared by the public which requires assurance that such buildings are "safe" and by the engineering profession which requires a minimum standard upon which design and construction can be based.

This document was prepared in keeping with the most current information and the present state-of-the-practice of energy dissipation. However, seismic energy dissipation is a relatively new technology and there are many design-related issues that require additional research. In establishing the design requirements in this document, the Energy Dissipation Working Group recognized these limitations and chose a conservative approach in resolving conflicting points of view. It is anticipated that as experience with these types of structures increases and as the results of related research become available, the design requirements for energy dissipation systems can be refined accordingly.

Rather than addressing a specific method of energy dissipation this document provides general design requirements applicable to a wide range of possible systems. In remaining general, the design requirements rely on mandatory testing of system hardware to confirm the engineering parameters used in the design and to verify the overall adequacy of the energy dissipation system. Some systems may not be capable of demonstrating acceptability by test and, consequently, would not be permitted. In general, acceptable systems will:

- remain stable for required design displacements;
- provide non-decreasing resistance with increasing displacement (for rate-independent systems);
- not degrade under-repeated cyclic load; and
- have quantifiable engineering parameters (e.g., force-deflection and energy dissipation characteristics).

In order to provide a sufficient level of lateral and torsional redundancy in a building incorporating EDUs, a minimum of two vertical lines of EDUs must be provided in each of the building's principal directions and the lines must be continuous

from the base of the building; the lines of EDUs do not have to extend to the top of the building.

These requirements prescribe the use of dynamic analysis procedures to determine maximum responses. Dynamic analysis procedures include both response spectrum analysis and linear and nonlinear time history analysis. These analysis procedures output forces and displacements at the ultimate (strength) level.

The spectral demands of the DBE correspond to a level of ground motion that has a 10 percent probability of being exceeded in a 50 year time period. For building design not using a site-specific hazard analysis, the design basis spectra are defined by the ground motion spectra specified by the UBC for dynamic analysis of buildings.

Minimum base shear coefficients at the ultimate (strength) level are specified for EDSs. The minimum base shear coefficient is calculated as ZC/R_w per the method specified in the UBC, and scaled to the ultimate (strength) level, via a material-dependent conversion factor (α), for comparison with the results of the dynamic analysis. The minimum base shear coefficient is dependent on the type of lateral load resisting system: for EDSs with no supplemental moment frame (non-dual system), the minimum base shear coefficient is computed sing an R_w of 10; for dual system EDSs, the minimum base shear coefficient is computed using an R_w of 12. The R_w values of 10 and 12 are consistent with those specified for a steel EBF in a building frame system ($R_w = 10$), and a steel EBF with a supplemental steel SMRF in a dual system ($R_w = 12$).

A. GENERAL

1. Every structure incorporating energy dissipators and every portion thereof shall be designed and constructed in accordance with the requirements of this document and the applicable sections of Chapter 23 of the UBC.

   a. The Lateral Force Resisting System shall be designed to resist the deformations and stresses produced by the effects of seismic ground motions as provided in this document.

   b. Where the prescribed wind forces produce greater deformations or stresses than the seismic forces, such loads shall be used for design in lieu of the deformations and stresses resulting from earthquake forces.

   c. A minimum of two vertical lines of EDUs must be provided in each of the building's principal directions. These lines must be continuous from the base of the building if the EDUs are rate-independent.

   d. An EDS may be designed as a dual system. The supplemental moment frame must be a SMRF if it experiences inelastic deformations for the DBE.

   e. The general intent of this document is that the EDS, excluding the EDUs, remain essentially elastic for the DBE. All elements in the EDS, excluding the EDUs, that experience substantial inelastic deformations, shall be detailed in

Commentary to A.1.

The requirements of this section provide design displacements, design forces and other specific requirements for structures incorporating discrete passive energy dissipation (PED) devices. all other design requirement including:

a) loads (other than seismic)
b) load combinations
c) allowable forces and stresses
d) horizontal shear distribution
e) compatibility, and
f) material detailing

are covered by the applicable chapters and sections of the UBC.

Conceptually there are two types of energy dissipation devices: rate dependent and rate independent devices. That is, the hysteric response of the device is either dependent or independent of the frequency of the loading, respectively.

In this document, the only type of rate dependent devices explicitly recognized is the viscous, or viscoelastic, PED device. Linear procedures can be used for the earthquake resistant design of structures incorporating viscous, or viscoelastic energy dissipation, provided that the structural elements, excluding the EDUs, remain elastic for the design-basis earthquake.

A number of rate-independent PED devices are implicitly recognized in this document:

a) friction - slip devices
b) metallic yielding devices

accordance with the relevant provisions of the UBC, to respond in a ductile manner.

f. If EDUs do not provide increasing resistance with increasing displacement, the EDS must comply with the dual system requirements of the UBC, as modified in Section A(1)d.

c) shape-memory alloy devices

Equivalent linear procedures for the design of EDSs incorporating rate-independent EDUs have not yet been developed; they are the subject of a research effort by the EDWG and the University of California at Berkeley and The University of Michigan at Ann Arbor. Consequently, nonlinear dynamic analysis is mandated for EDSs incorporating rate-independent EDUs.

If the member actions resulting from the application of the design wind forces exceed the seismic member actions calculated in Section E of this document, the wind-induced member actions shall be used in the design.

In order to improve the torsional response and redundancy in a structure, a minimum of two vertical lines of EDUs must be provided in each principal direction of the building. If the EDUs are rate-independent, these lines must be continuous from the base of the building. EDUs do not have to be installed in every story of the building.

The use of dual lateral force resisting systems is promoted in this document as prudent earthquake-resistant design. If a supplemental moment frame is used as part of, or in parallel with an EDS, the moment frame must be detailed as a special moment-resisting frame if the seismic analysis predicts that the moment frame will experience inelastic actions during the design-basis earthquake.

The general intent of this document is to constrain the inelastic activity to the EDUs, thereby precluding damage to the remainder of the structural frame during the design-basis earthquake. However, if the seismic analysis predicts that structural elements other than the EDUs will experience

inelastic deformations during the design-basis earthquake, these elements must be detailed to respond in a ductile manner in accordance with the relevant chapters and sections in the UBC.

EDUs that do not provide increasing resistance with increasing displacement, such as certain friction-slip devices, must be used as part of a dual system in order to provide each story of the building with post-yield stiffness in order to reduce the potential for the concentration of inelastic deformation at any one location within the building.

B. DEFINITIONS

The definitions of Chapter 23 of the UBC and following definitions apply to the provisions in this document:

1. **DESIGN-BASIS EARTHQUAKE (DBE):** the level of earthquake ground shaking which has a 10 percent probability of being exceeded in a 50 year time period.

2. **DESIGN EDU DISPLACEMENT:** the displacement in the EDU corresponding to the DBE.

3. **DESIGN INTER-STORY DISPLACEMENT:** the inter-story displacement in the EDA corresponding to the DBE.

4. **EFFECTIVE EDU STIFFNESS:** the value of the lateral force in the EDU divided by the lateral displacement in the EDU.

5. **ENERGY DISSIPATION ASSEMBLY (EDA):** the one-bay assembly composed of the EDU('s) and its (their) lateral and gravity support frame(s).

6. **ENERGY DISSIPATION SYSTEM (EDS):** the complete collection of lateral force resisting elements including all individual EDUs and all structural elements which transfer force between elements of the EDS.

7. **ENERGY DISSIPATION UNIT (EDU):** the element in the EDA designed to dissipate energy. The primary attribute of the EDU is its ability to dissipate energy in a stable manner. The EDU shall not be used as an essential part of the gravity load resisting system in a building.

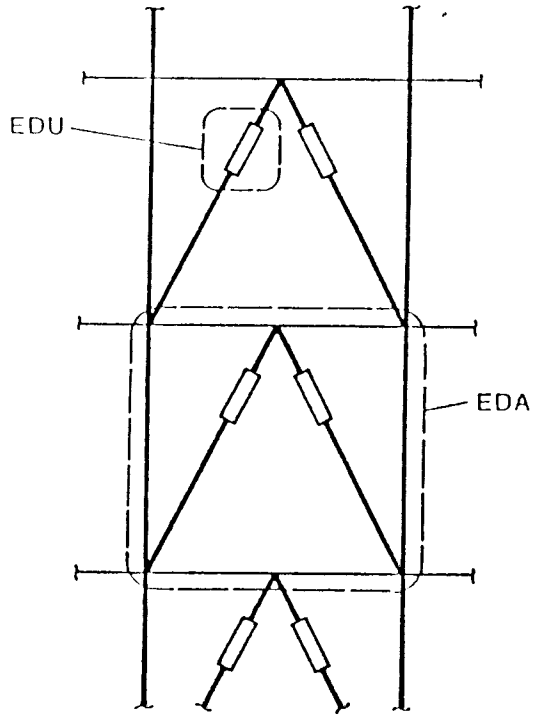

8. **GRAVITY LOAD RESISTING SYSTEM:** the load path by which gravity loads are transferred into the foundation system.

9. **INTER-STORY DISPLACEMENT:** the difference in the computed horizontal displacements of two adjacent floor levels in the direction under consideration.

10. **LATERAL LOAD RESISTING SYSTEM:** the load path by which lateral forces (induced by earthquake, wind or blast loading) are transferred into the foundation system.

11. **RATE-DEPENDENT EDU's:** have mechanical characteristics that are dependent on the frequency of the applied loading or deformation.

12. **VISCOUS DAMPING (VD):** the value corresponding to energy dissipated during cyclic response of the rate-dependent EDS's.

C. SYMBOLS AND NOTATIONS

The symbols and notations of Chapter 23 of the UBC and the following symbols and notations apply to the provisions of this document:

b_1 = The shortest plan dimension of the structure, in feet, measured perpendicular to b_2.

b_2 = The longest plan dimension of the structure, in feet, measured perpendicular to b_1.

d^+ = Maximum positive displacement of an EDU during each cycle of prototype testing.

d^- = Maximum negative displacement of an EDU during each cycle of prototype testing.

e = The actual eccentricity, in feet, measured in plan between the center of mass of the structure and the center of rigidity of the EDS, plus accidental eccentricity, in feet, taken as the most disadvantageous position of a [rectangle or ellipse] with major and minor dimensions of $0.1b_1$ and $0.1b_2$ about the calculated center of mass.

F^- = Maximum negative force in an EDU during a single cycle of prototype testing at a displacement amplitude of d^-.

F^-_{max} = Maximum negative force in an EDU for all cycles of prototype testing at a constant displacement amplitude of d^-.

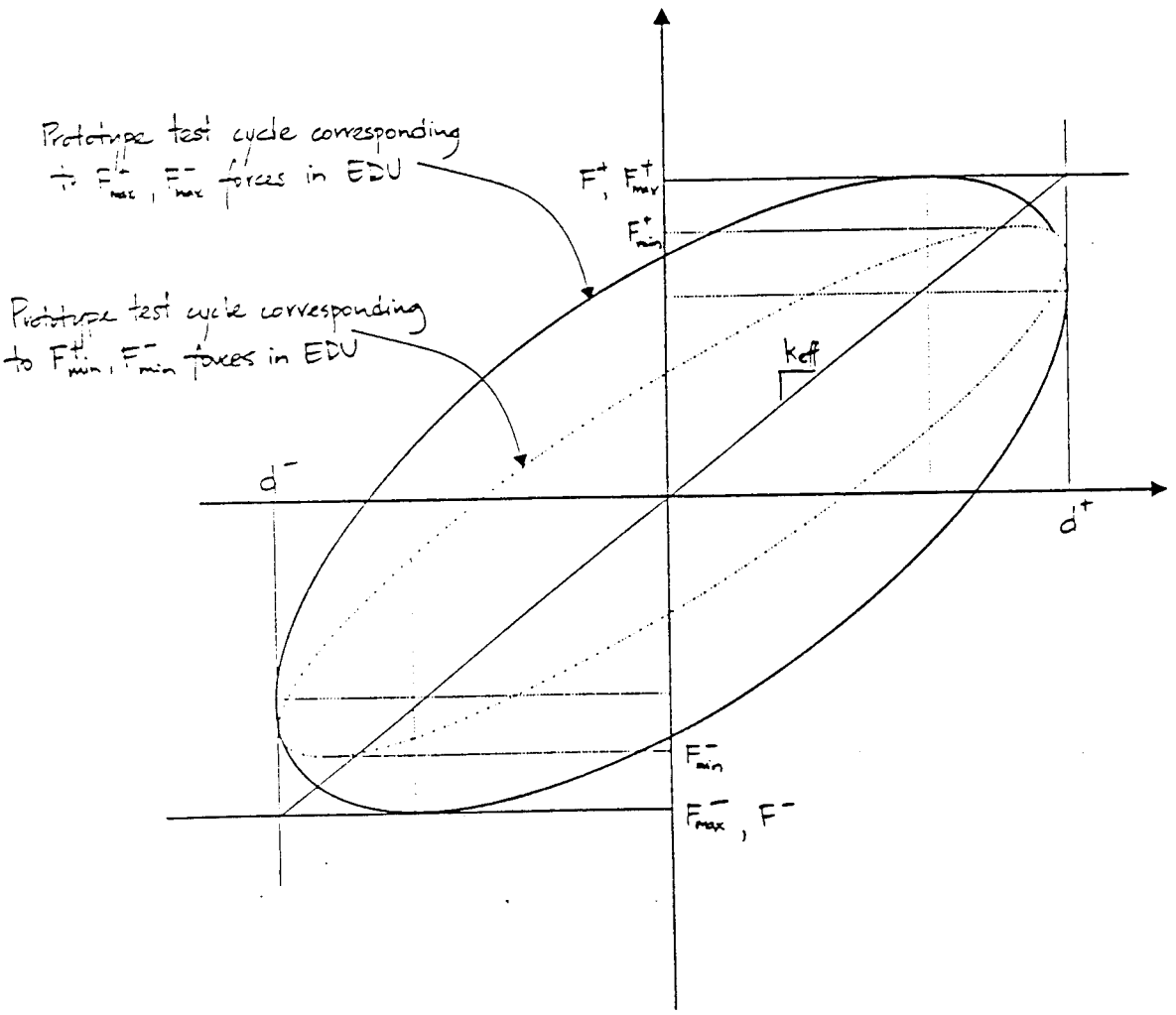

$$\text{EDU } K_{eff} = \frac{F^+ + F^-}{d^+ + d^-}$$

F^-_{min} = Minimum negative force in an EDU for all cycles of prototype testing at a constant displacement amplitude of d^-.

F^+ = Maximum positive force in an EDU during a single cycle of prototype testing at a displacement amplitude of d^+.

F^+_{max} = Maximum positive force in an EDU for all cycles of prototype testing at a constant displacement amplitude of d^+.

F^+_{min} = Minimum positive force in an EDU for all cycles of prototype testing at a constant displacement amplitude of d^+.

k_{eff} = Effective Stiffness of an EDU, as prescribed by Formula J-1.

R_w = Response reduction factor; defined in Table 1.

V = The total lateral seismic design force or shear at the base.

W = The total seismic dead load defined in Section 2334(a) of the UBC.

α = A material-dependent conversion factor to scale forces from the working stress (UBC Chapter 23) level to the ultimate (strength) level; defined in Table 2.

D. CRITERIA SELECTION

1. **Basis for Design.** The procedures and limitations of the design of structures incorporating EDUs shall be determined considering zoning, site characteristics, occupancy, configuration and structural system.

2. **Stability of the EDS.** The stability of the load carrying elements of the EDS shall be verified by analysis and test, for a lateral seismic displacement equal to the Maximum Inter-Story Displacement.

3. **Selection of Lateral Response Procedure.** Any structure incorporating an EDS must be designed using the dynamic lateral response procedure of Section E.

   a. **Dynamic Analysis.** The dynamic lateral response procedure of Section E shall be used for the design of structures incorporating an EDS as specified below:

      1. **Response Spectrum Analysis.** Response spectrum analysis may be used for the design of a rate-dependent EDS provided the EDS (excluding the EDUs) remains elastic. The analysis shall use either the spectra (compatible with the soil type at the site) provided in the UBC for regular structures as defined in Section 2312(d)B of the UBC, or site-specific spectra as defined in Section D3(a)3.

      2. **Time-History Analysis.** Nonlinear time history analysis must be used for design of any structure incorporating an rate-

Commentary to D.2.

The acceptable performance of a building incorporating a passive energy dissipation system during the design earthquake is predicated on the EDUs exhibiting stable nonlinear behavior. As such, the response of the EDUs must be verified by both analysis **and** testing (see Commentary to Section J).

Commentary to D.3.

a. Two analysis procedures are currently used for the design of conventional buildings in accordance with Chapter 23 of the UBC: static lateral force and dynamic analysis. Static lateral force procedures may be unable to adequately capture the response of highly nonlinear hysteretic systems; this is a subject of research by the EDWG. The rigorous method of analysis on nonlinear building systems makes use of dynamic analysis, either linear or nonlinear. Until research on the use of static lateral response procedures for designing nonlinear systems incorporating passive energy dissipators is completed, and the results reviewed by the SEAONC membership, only dynamic analysis procedures can be used for designing structures incorporating EDUs.

a.1. The response spectrum method can be used for the design of EDUs incorporating rate-dependent (viscous or viscoelastic) EDUs because the viscous damping afforded to the EDSs by the EDUs can be adequately quantified. Yielding of the structural frame will result in energy being dissipated by non-viscous means and as such its effects cannot be adequately evaluated using an assumed equivalent viscous damping ratio and an elastic design response spectrum. The use of the response spectrum method is therefore limited to EDSs that both incorporate rate-dependent EDUs and in which the

independent EDS and for all rate-dependent EDSs not satisfying D3(a)1.

3. **Site-Specific Design Spectra.** Site-specific ground motion spectra of the Design-Basis Earthquake developed in accordance with Section E.2 may be used for the design and analysis of all structures incorporating an EDS and shall be used for all EDSs sited on Soil Type 4.

structural frame outside the EDUs remains elastic for the design-basis earthquake.

a.2 Nonlinear time history analysis is required for the design of all lateral load-resisting elements in an EDS, including the EDUs, unless the EDS satisfies the requirements that permit response spectrum analysis.

a.3 Site-specific motion spectra may be used in lieu of the UBC spectra to characterize the seismic demands of the design-basis earthquake.

E. DYNAMIC LATERAL RESPONSE PROCEDURE

1. **General.** As required by Section D3(a), every structure incorporating an EDS, or portion thereof, shall be designed and constructed to resist earthquake forces as specified in this section and the applicable requirements of Section F, G and H of these Recommendations.

2. **Ground Motion.**

   a. **Design Spectra.** Properly substantiated, site-specific spectra may be used for design of all EDSs.

      1. A design spectrum shall be constructed for the Design-Basis Earthquake (DBE) and shall include near-fault effects as appropriate. This design spectrum shall not be taken as less than the normalized response spectrum given in Figure No. 23-3 of Chapter 23, Part III of the UBC, for the appropriate soil type, scaled by the seismic zone coefficient.

         EXCEPTION: If a site-specific spectrum is calculated for the Design-Basis Earthquake, then the 5% damped design spectrum may be taken as less than 100 percent, but not less than 80 percent of the normalized response spectrum given in Figure 23-3 of Chapter 23-3, Part III of the UBC, for the appropriate soil type, scaled by the seismic zone coefficient.

Commentary to E.

1. The procedure in this section has been developed because of the need to explicitly model the deformational characteristics of the EDS. This is especially important for EDSs that have damping characteristics which are amplitude-, rather than velocity-, dependent since it is difficult to define an appropriate value of equivalent viscous damping for these systems.

2. If a site-specific spectrum is not developed, buildings incorporating EDSs shall be designed using the elastic spectra adopted for the design of conventional buildings as specified in Chapter 23 of the UBC.

The requirement for three time histories is a minimum. The scaling requirement ensures that each selected time history is reasonably compatible with the design spectrum and contains significant energy in the period range of interest. It is recommended that recorded time histories be used for scaling because of the more realistic phase relationships between the frequency components of the earthquake.

3. The requirements in this section ensure that the three-dimensional response of the building, including the contribution of the EDUs, will be captured accurately. The mathematical model should properly represent structures which have a non-uniform or unsymmetric distribution of EDUs.

The distinction between different types of models used for EDUs is necessary because different analysis procedures are required depending on the mechanism of energy absorption in a particular EDS.

4. Rational analysis procedures appropriate for the type(s) of EDS(s) in the building should be used which incorporate

b. **Time Histories.** Pairs of horizontal ground motion time-history components shall be selected from not less than three recorded events. These motions shall be scaled such that the square root sum of the squares (SRSS) of the 5 percent-damped spectrum of the scaled horizontal components does not fall below 1.3 times the 5 percent-damped spectrum of the Design-Basis Earthquake by more than 10 percent in the period range of the fundamental structural period (T_1) for periods from T_1 minus 0.5 second to T_1 plus 1.0 second.

1. The strong motion duration of the time histories shall be consistent with the magnitude and source characteristics of the DBE.

2. Time histories developed for sites within 15 km of a major active fault shall incorporate near-fault phenomena.

3. **Mathematical Model.**

a. **General.** The mathematical model of the EDS, including the EDUs, shall conform to Chapter 23 of the UBC and to the requirements of Section E3(b).

b. **Modeling.** The EDS shall be modeled with sufficient detail to:

1. account for the spatial (plan and elevation) distribution of the EDUs;
2. calculate the translational and torsional responses of the structure considering the realistic earthquake input and fully account for the presence of EDSs.

4.d. The requirement of the three time histories is a minimum and as such the maximum response value derived from the three time histories shall be used.

4.e. The minimum design base shear as specified by equation 34-1 in Section 2334 of the UBC is required to guard against the use of unrealistically low design base shear forces that might result from the use of just three elastic spectrum-compatible ground motions.

5. This drift limit is the same as that required in Chapter 23 of the UBC and as such ensures performance equivalency between structures incorporating EDSs and conventional buildings designed according to the UBC.

most disadvantageous location of mass eccentricity, and

3. account for the effects of vertical load, bilateral load, and/or the rate of loading, if the force-deflection properties of the EDS are dependent on one or more of these parameters.

The mathematical model of the EDS shall be classified as either a Type 1 or Type 2 model. Type 1 models may be used for rate-dependent EDUs in an EDS in which the elements other that the EDUs remain elastic during the DBE. Type 2 models shall be used for all other EDSs.

c. Energy Dissipation System - Type 1:

1. The EDUs shall be modeled using the Effective EDU Stiffness characteristics developed and verified by test in accordance with the requirements of Section J.
2. The modal viscous damping ratios afforded to the EDS by the EDUs are computed using rational analysis procedures.

d. Energy Dissipation System - Type 2:

1. The EDUs shall be modeled using deformational characteristics developed and verified by test in accordance with the requirements of Section J.
2. The EDS, excluding the EDUs, shall be modeled using nominal material properties in the elastic range, and appropriate post-yield characteristics.

4. Description of Analysis Procedures

a. **General.** A response spectrum analysis and/or a time-history analysis shall be performed in accordance with Section 2335, Sections D3(a)1 and E2(a) of these Recommendations and the following requirements. The minimum design base shear force shall be calculated in accordance with Section E4(e). When the lateral shear force on structural elements, determined using either response spectrum or time-history analysis, is less than the minimum level prescribed in Section E4(e), then all response parameters, including member forces and moments, shall be adjusted upward proportionally.

b. **Input Earthquake.** The Design Basis Earthquake shall be used to calculate the Design Inter-Story Displacements in the EDS.

c. **Response Spectrum Analysis.**

1. Response spectrum analysis shall be performed using modal analysis techniques and modal damping values computed for that number of modes so that at least 90 percent of the participating mass of the structure is included in the calculation of response for each principal horizontal direction.
2. Response spectrum analysis used to determine the Design Inter-Story Displacements shall include simultaneous excitation of the model by 100 percent of the most critical direction of ground motion and 30 percent of the ground motion on the orthogonal axis.

d. **Time-History Analysis.**

1. Time-history analysis shall be performed with at least three appropriate pairs of horizontal time-history components, as defined in Section E2(b).
2. Each pair of time histories shall be applied simultaneously to the model, considering the most disadvantageous location of mass eccentricity.
3. The maximum response of the parameter of interest calculated by the three time-history analyses shall be used for design.

e. **Minimum Design Base Shear**

1. The minimum design base shear shall not be less than the design base shear calculated from Equation 34-1 in Section 2334 of the UBC, multiplied by the conversion factor α. The value of R_w to be used in Equation 34-1 is specified in Table 1; values for α are specified in Table 2.

5. **Drift Limits.** The maximum inter-story displacement corresponding to the DBE shall not exceed 0.015 times the story height.

F. LATERAL LOAD ELEMENTS OF STRUCTURES AND NON-STRUCTURAL COMPONENTS.

1. **General.** Parts or portions of a structure, permanent non-structural components and the attachments to them, and the attachments for permanent equipment supported by a structure shall be designed to resist seismic forces and displacements as prescribed by this section and the applicable requirements of Section 2336 of the UBC.

2. **Forces and Displacements.**

   a. **Structural Components.** The elements in the EDA shall be designed using capacity design procedures based on at least 1.2 times the forces in the EDUs at their respective Design EDU Displacements.

   b. **Non-Structural Components.** Non-structural components, or portions thereof shall be designed to resist a total lateral seismic force equal to either the maximum dynamic response of the component or that required by Section 2336.

   c. **Components Which Cross An EDU Interface.** Structural and Non-Structural Components, or portions thereof, which cross and EDU interface shall be designed to withstand the appropriate Design Inter-Story Displacement.

Commentary to F.

1. The intent of these requirements is to ensure that structural components in the EDA will remain essentially elastic during the Design-Basis Earthquake (DBE) while nonstructural components and attachments shall perform to the levels required by Section 2336 of the UBC.

2.a. The purpose of the 1.2 factor is to ensure that the EDA will yield before the surrounding elements during the DBE. Otherwise, damage to elements adjacent to an EDU may prevent the EDU from achieving its desired performance. It is important when incorporating EDUs within a structure to establish a hierarchy of actions in which it is understood that the EDU will be activated first.

2.b. This requirement is designed to ensure that the performance of nonstructural components and attachments be at least equal to that specified by Section 2336 of the UBC in lieu of additional analyses. However, it is recommended that where possible additional dynamic analyses be undertaken to more reliably predict the response of nonstructural components. The design forces should then be taken as the minimum of those specified by Section 2336 or those calculated in the dynamic analysis.

2.c. All components which cross an EDU interface should be appropriately detailed to accommodate the movement expected across the interface.

G. DETAILED SYSTEM DESIGN REQUIREMENTS.

1. **General.** The EDS and the remainder of the structural system shall comply with the requirements of these Recommendations and the material requirements of Chapters 24 through 28 of the UBC. In addition, the EDS shall comply with the detailed system requirements of this section and the applicable portions of Section 2337 of the UBC.

2. **Energy Dissipation System.**

   a. **Environmental Conditions.** In addition to the requirements for vertical and lateral loads induced by wind and earthquake, the EDS shall be designed with consideration given to other environmental conditions including aging effects, creep, fatigue, operating temperature and exposure to moisture and damaging substances.

   b. **Wind Forces.** Structures incorporating rate-independent EDUs shall resist the prescribed wind loads in the elastic range.

   c. **Inspection and Replacement.** Access for inspection and replacement of the EDUs shall be provided.

   d. **Quality Control.** A quality control testing program for EDUs shall be established by the engineer-of-record for the structural design.

Commentary on G.1.

The design of the structural elements in both the EDS (excluding the EDUs) and in the gravity load-resisting frame shall conform with the requirements of the relevant chapters of the UBC.

The UBC (1991) mandates *Allowable Stress Design* (ASD) for steel structures; the member actions output by nonlinear time history analysis and response spectrum analysis are at the **strength** level. The member actions output by these analyses may be divided by 1.6 in order to compute design forces at the ASD level.

The UBC (1991) mandates *Ultimate Strength Design* (USD) for reinforced concrete structures; the member actions output by nonlinear time history analysis and response spectrum analysis are **likewise** at the strength level. These member actions need not be increased by load factors to compute design forces.

Commentary on G.2.

a. Exposure of EDUs to aggressive environmental conditions **may** lead to degradation of their mechanical characteristics. Due consideration must be given to the operating conditions into which the EDUs will be placed. Potential changes in the mechanical characteristics of the EDU over its design life should be considered in the design process.

b. Rate-independent EDUs based on metallic yielding are susceptible to failure by low-cycle fatigue. EDUs subject to such failure must be designed to remain elastic for the design wind forces to guard against such a failure. Friction-slip devices and EDUs incorporating certain shape-memory alloys

3. **Structural System.**

a. **Building Separations.** Minimum separations between the building and surrounding walls and/or buildings shall be calculated using rational procedures based on DBE demands.

are not susceptible to such failure and are thus exempt from this requirement.

c. Reasonable access to the EDUs for inspection and replacement shall be provided.

d. A quality control program is necessary for both the fabrication and installation of EDUs. Since energy dissipation is an emerging technology, reference standards for the fabrication and installation of EDUs may be unavailable. The engineer-of-record shall prepare such standards covering materials, tolerances, and workmanship if reference standards are unavailable.

H. FOUNDATIONS

1. **General.** Foundations shall be designed and constructed in accordance with the applicable requirements of the UBC using design gravity forces calculated in accordance with Sections 2303 through 2306; design wind forces calculated in accordance with Sections 2311 through 2329, and seismic forces calculated in Section E divided by the conversion factor α.

Commentary on H.1.

The foundation design provisions in the UBC (1991) are based on the use of allowable, or working, stress loads. The seismic forces calculated in Section E. are at the *strength* level. In order to reduce these strength-level forces to working stress-level forces, the forces in Section E. are divided by the factor α. This results in the working stress-level forces being used for gravity, wind, and seismic loads.

I. DESIGN AND CONSTRUCTION REVIEW

1. **General.** Design and construction review of all structures incorporating EDUs shall be performed in accordance with the following requirements.

   a. Design review of the EDS and related test programs shall be performed by an independent engineering review panel including persons licensed in the appropriate disciplines, and experienced in seismic analysis including the theory and application of energy dissipation methods.

2. **Energy Dissipation System.** EDS design review shall include, but should not necessarily be limited to, the following:

   a. Review of the preliminary design, including the determination of the Design Inter-Story Displacements and design lateral force level.

   b. Overview and observation of prototype testing (Section J).

   c. Review of the final design of the EDS and supporting analyses.

   d. Review of the EDS quality control testing program (Section J).

Commentary on I.

1. The general objective of the design review process is to ensure that general and sound concepts are adhered to in the application of EDSs to structures. The process is not intended to replace or be a substitute for licensing agency review and approval.

Appropriate overview of the aspects of construction related to the EDS shall be performed by the design engineer. This shall include observation of the EDU installation process and post-installation inspection.

2. It is not required that the independent review panel observe the EDU prototype or production testing. However, the panel shall be responsible for a review of the results of the prototype tests.

The extent of the review of the final EDS design shall be limited to a general overview. It is not intended that the review panel be responsible for performing a comprehensive and detailed check of the design analyses.

The EDU quality control/production testing program shall be approved by the review panel.

J. REQUIRED TESTS OF THE ENERGY DISSIPATION SYSTEM

1. General.

a. The deformation characteristics of the EDUs used in the design and analysis of structures incorporating an EDS shall be based on the following tests of a selected sample of the components prior to construction.

b. The tests specified in this section are for establishing and validating the design properties of the EDUs.

2. Prototype Tests.

a. Prototype tests shall be performed separately on full-size specimens of the EDUs in the EDS. The number of EDUs to be tested shall be determined by the engineer-of-record and the chairperson of the review panel. Specimens tested shall not be used for construction.

b. Prototype tests are not required if an EDU of similar size and of the same type and material as the prototype EDU has been previously tested using the specified sequence of tests, and the test results have been properly documented by ICBO.

c. For each test cycle the hysteretic behavior of the test specimen shall be recorded.

d. The following sequence of tests shall be performed on the EDU for the prescribed number of cycles at

a vertical load equal to the average dead load on the EDU as installed in the building.

1. Two hundred (200) fully-reversed cycles of loading at a lateral force corresponding to the wind design force.

2. Fifty (50) fully-reversed cycles of loading at each of the following increments of the Design EDU Displacement; 0.50 and 1.0.

3. Ten (10) fully-reversed cycles of loading at the Maximum EDU Displacement.

e. If the force-deflection properties of the EDUs are dependent on the rate of loading, then each set of tests specified in Section J2(d) shall be performed dynamically at three different rates of loading. The frequency of loading shall correspond to ½, 1, and 2 times the fundamental structural frequency.

The force deflection properties of an EDU shall be considered to be dependent on the rate of loading if there is greater than a plus or minus 10 percent change in the Effective EDU Stiffness at the Design EDU Displacement for either a factor of two increase or a factor of two decrease in the rate of loading, where the frequency of loading is taken as the fundamental structural frequency.

f. If the EDUs are subjected to bilateral load, and if the force-deflection properties of the EDUs are dependent on bilateral load, then the tests specified in Sections J2(d) and J2(e) shall be augmented to

include the maximum bilateral load at the Design EDU Displacement.

The force-deflection properties of an EDU shall be considered to be dependent on bilateral load, when the bilateral and unilateral force-deflection properties have greater than a 10 percent difference in the Effective EDU Stiffness at the Design EDU Displacement.

3. Determination of Force-Deflection Characteristics.

a. The force-deflection characteristics of the EDU shall be based on the cyclic load test results for each fully reversed cycle of loading.

b. The Effective EDU Stiffness shall be calculated for each cycle of loading as follows:

$$k_{eff} = \frac{F^+ - F^-}{d^+ - d^-} \qquad \text{(J-1)}$$

4. System Adequacy.

a. The performance of the test specimens shall be assessed as adequate if the following conditions are satisfied:

1. The force-deflection plots of all tests specified in Section J2 have a non-negative incremental force-carrying capacity.

2. For each test sequence specified in Section J2(d), each test specimen shall exhibit no greater than a 10 percent difference between the Effective EDU Stiffness for each test

cycle and the average value of Effective EDU Stiffness for that test sequence.

3. For the test sequence specified in Section J2(d), each specimen shall exhibit no greater than a 20 percent decrease in the average energy dissipated during one cycle of loading as calculated from the first three cycles of loading.

TABLE 1

RESPONSE REDUCTION FACTOR (R_w)

BASIC STRUCTURAL SYSTEM	R_w
A. Bearing Wall System	N.A.
B. Building Frame System	10
C. Moment-Resisting Frame System	10
D. Dual System	12

TABLE 2

CONVERSION FACTOR (α)

MATERIAL	α
A. Structural Steel	1.7
B. Reinforced Concrete	1.4

USACERL DISTRIBUTION

Chief of Engineers
ATTN: CEHEC-IM-LH (2)
ATTN: CEHEC-IM-LP (2)
ATTN: CECC-R
ATTN: CECW-ED
ATTN: CEMP-ET
ATTN: CERD-L
ATTN: CERD-M

CECPW 22310-3862
ATTN: CECPW-EB-S

US Army Engr Divisions
ATTN: Library (12)
North Pacific Division 97208-2870
ATTN: CENPD-PE-TE

US Army Engr District
ATTN: Library (9)
Alaska 99506
Charleston 29402
Los Angeles 90012
Louisville 40201
Memphis 38103
Sacramento 95814
San Francisco 94105
Seattle 98124
St. Louis 63101

CEWES 39180
ATTN: Library

Tyndall AFB 32403
ATTN: HQAFCESA Program Ofc

Naval Facilities Engr Command
ATTN: OOCE 20374-5063
ATTN: Pacific Division
ATTN: Naval Facilities Engr Service Center 93043-4328

Langley AFB, VA 23665
ATTN: HQ AMC/CEE

Scott AFB, IL 62225
ATTN: HQ AMC CEE

Wright-Patterson AFB, OH 45433
ATTN: HQ AFMC CEE

Brooks AFB, TX 76901
ATTN: AFOMS-Health Facilities Division

Fort Sam Houston, TX 78234-6000
ATTN: US Army Medical Command-MCFA

National Science Foundation 22230
Earthquake Hazards Mitigation Directorate

National Center for Earthquake Engineering Research 14260-2200
ATTN: Science and Engineering Library

Earthquake Engineering Research Center 94804-4698
ATTN: University of California at Berkeley

University of Illinois at Urbana-Champaign 61801
ATTN: Engineering Library
ATTN: Civil Engineering Department

National Institute of Standards and Technology 20899
ATTN: Earthquake and Engineering Group

Department of Veteran Affairs 20420
ATTN: 087C

Department of Energy 20585
ATTN: Office of Risk Assessment and Technology

General Services Administration 20405
ATTN: Office of Design and Construction (PQSB)

Federal Emergency Management Agency 20472
ATTN: Mitigation Directorate

Department of the Interior 80225
ATTN: Bureau of Reclamation, D-3130

Nuclear Regulatory Commission 20555
ATTN: Mailstop NL/S-217A

US Postal Service 20260-6434
ATTN: 475 L'Enfant Plaza, SW

Department of State 22219
ATTN: Office of Foreign Buildings

Tennessee Valley Authority 37902
ATTN: WT 9C-K

Defense Tech Info Center 22304
ATTN: DTIC-FAB (2)

59
6/95